FACULTEIT LANDBOUWKUNDIGE

EN TOEGEPASTE BIOLOGISCHE

WETENSCHAPPEN

Academiejaar 2002 – 2003

MODELLING ISOTHERMAL COCOA BUTTER CRYSTALLIZATION: INFLUENCE OF TEMPERATURE AND CHEMICAL COMPOSITION

MODELBOUW VAN DE ISOTHERME CACAOBOTERKRISTALLISATIE: INVLOED VAN TEMPERATUUR EN CHEMISCHE SAMENSTELLING

door

ir. Imogen FOUBERT

Thesis submitted in fulfilment of the requirements for the degree

of Doctor (Ph.D.) in Applied Biological Sciences: Chemistry

Proefschrift voorgedragen tot het bekomen van de graad van

Doctor in de Toegepaste Biologische Wetenschappen: Scheikunde

op gezag van

Rector: **Prof. dr. Andreas DE LEENHEER**

copyright.pdf	chapter 6.pdf
dankwoord.pdf	chapter 7.pdf
table of contents.pdf	general conclusions.pdf
samenvatting.pdf	references.pdf
summary.pdf	annex I.pdf
chapter 1.pdf	annex II.pdf
chapter 2.pdf	annex III.pdf
chapter 3.pdf	annex IV.pdf
chapter 4.pdf	annex V.pdf
chapter 5.pdf	curriculum vitae.pdf

Decaan: Promotoren:

Prof. dr. ir. Herman VAN LANGENHOVE **Prof. dr. ir. Koen DEWETTINCK**

Prof. dr. ir. André HUYGHEBAERT

Gent, mei 2003

de auteur
the author

Ir. Imogen Foubert

de promotoren
the promotors

Prof. dr. ir. Koen Dewettinck

Prof. dr. ir. André Huyghebaert

EEN WOORD VAN DANK

Na een jaar dat in het kader van mijn ingenieursthesis volledig rond kaas draaide, schakelde ik midden 1999, kwestie van andere smaakpapillen te oefenen, over op chocolade en meer bepaald op zijn belangrijkste ingrediënt cacaoboter. Na drie en een half jaar lagen er 250 pagina's op tafel, maar dat was onmogelijk geweest zonder de hulp en steun van een aantal mensen die ik hierbij in de bloemetjes - of moet het zijn in de chocolade - wil zetten.

Eerst en vooral ben ik Prof. dr. ir. André Huyghebaert erkentelijk voor de mogelijkheid die hij me geboden heeft om binnen zijn vakgroep te doctoreren en voor de interesse die hij gedurende de jaren steeds betoonde. Prof. dr. ir. Koen Dewettinck zorgde voor de meer dagdagelijkse opvolging. Ook hem wil ik bedanken voor het vertrouwen en de steun, vooral op het einde van de rit toen ik soms meermaals per dag op zijn bureau stond om weer eens een nieuw inzicht te toetsen of weer eens een vraag voor te leggen die bij het schrijven gerezen was.

Een heel speciaal woord van dank wil ik richten aan Prof. dr. ir. Peter Vanrolleghem, eigenlijk mijn derde promotor. Zonder hem zou dit doctoraatswerk er allicht totaal anders hebben uitgezien: met minder, misschien voor sommigen saaie of overbodige wiskunde. Voor mij gaf het modelleerwerk echter een zeer interessante extra dimensie aan het onderzoek. Ik waardeer de tijd die hij, ondanks zijn uiterst drukke agenda, aan dit werk heeft gespendeerd. Hjärtligt tack för det trevliga og lärorika samarbete.

Het Fonds voor Wetenschappelijk Onderzoek Vlaanderen wens ik te bedanken voor de financiële steun.

De leden van de lees- en examencommissie (Prof. dr. ir. R. Verhé, Prof. dr. ir. P. Van der Meeren, Prof. dr. ir. P. Vanrolleghem, Prof. dr. ir. M. Hendrickx, Dr. ir. M. Kellens en Dr. W. Meeussen) wens ik te bedanken voor hun waardevolle commentaren waarmee zeker ook in de toekomst, bij het schrijven van artikels en in verder onderzoek, zal rekening gehouden worden.

Ik houd eraan ook een woord van dank te richten aan dr. ir. Olivier Thas voor de statistische hulp en aan ir. Dirk De Pauw en ir. Ingmar Nopens voor de hulp bij het modelleerwerk in WEST.

Ook de volgende bedrijven ben ik dank verschuldigd voor het leveren van stalen en de hulp bij het uitvoeren van sommige experimenten: Barry Callebaut België (ir. Herwig Bernaert), De Smet Engineering (dr. ir. Wim De Greyt en Jose Vila Ayala), ADM Cocoa en Barry Callebaut Nederland.

Ik bedank ook de thesisstudenten Thijs Keersebilck en Willem Basten voor hun bijdrage aan dit doctoraat. I would also like to thank the thesis students Curtis Mbulanyumba Kalua and Cristina Villegas Alvarez for their contribution to this PhD.

Lof ook voor Dr. ir. Bart Goderis en Monika Basiura van het Laboratorium voor Macromoleculaire Structuurchemie van de KULeuven. Zij leverden uitstekend werk bij het verwerken en interpreteren van de synchrotron resultaten. Zonder hun hulp hadden er allicht geen synchrotron resultaten in dit werk gestaan.

Alle vroegere en huidige medewerkers van onze dienst ben ik dank verschuldigd voor de collegialiteit, de goede raad, de hulp en het creëren van een goede sfeer. Met de collega's op het bureau, en dat zijn er mede door het verhuizen van het afgelopen jaar veel, beleefde ik ook tijdens het werk een leuke tijd. Er werd inderdaad al eens wat gebabbeld en gelachen over niet-wetenschappelijke onderwerpen. Ik wil hen ook bedanken voor de steun, vooral tijdens de laatste schrijfweken. Een speciale vermelding verdienen ook de mensen in het labo die experimenten voor mij hebben uitgevoerd of thesisstudenten hebben opgeleid. Eén, nu eigenlijk ex-collega, verdient een afzonderlijke vermelding. Met dr. ir. Bert Vanhoutte voerde ik, mede door de sterke verwantschap tussen onze onderwerpen, veel wetenschappelijke discussies, op het bureau maar ook bijvoorbeeld op de trap of in de gang. We waren het niet altijd met elkaar eens en onze benaderingen waren weliswaar verschillend, maar de discussies zorgden steeds voor stof tot nadenken.

Mijn echtgenoot Aldo wil ik bedanken voor de vele uren die hij naar mijn kristallisatie- en modelleerverhalen heeft geluisterd, voor de steun op de moeilijke momenten, voor het volledig nalezen van alle 250 pagina's en voor het verzorgen van de figuren. Mijn papa doorworstelde eveneens alle 250 pagina's op zoek naar taalkundige fouten. Ik bewonder zijn doorzettingsvermogen om te zoeken naar fouten in een tekst waarvan hij niet altijd begreep waar het over ging. Ook mama, oma en mijn vrienden en vriendinnen bedank ik voor hun steun en interesse gedurende de jaren en voor het tolereren van mijn niet altijd even opgewekt humeur.

Imogen Foubert
Gent, 30 april 2003

TABLE OF CONTENTS

SAMENVATTING

Veel levensmiddelen bestaan voor een belangrijk gedeelte uit vet, waarvan een substantieel gedeelte in gekristalliseerde vorm voorkomt. De chemische samenstelling en de procescondities beïnvloeden het primair kristallisatiegedrag van een vet. Dit gedrag omvat niet enkel wanneer en in welke mate het vet uitkristalliseert, maar ook het polymorfisme (het bestaan van verschillende kristallijne fasen met dezelfde chemische samenstelling die van elkaar verschillen in structuur maar dezelfde vloeibare fase opleveren na afsmelten) en de morfologie van de kristallen en de mogelijke polymorfe transities. De procescondities beïnvloeden ook de verdere aggregatie van de primaire kristallen tot clusters en verder tot een driedimensionaal netwerk. Elk van deze structuurniveaus bepaalt de macroscopische eigenschappen van het levensmiddel. Dit onderzoek behandelde het primair kristallisatiegedrag van cacaoboter. Het kristallisatiegedrag van dit geel vet, dat geëxtraheerd wordt uit cacaobonen, is van uitzonderlijk belang voor de chocoladeindustrie.

De literatuurstudie over vetkristallisatie (hoofdstuk 1) behandelde enerzijds de basisbeginselen van nucleatie en kristalgroei en anderzijds het polymorfisme van vetten. De meeste aandacht werd echter besteed aan het modelleren van de kristallisatiekinetiek van vetten. Een overzicht werd gegeven van de verschillende experimentele technieken die gebruikt worden om kristallisatiedata te verzamelen en van de verschillende modellen die gebruikt worden om de kristallisatiekinetiek te beschrijven. Het Avrami model en in mindere mate het Gompertz model bleken de meest gebruikte. Het Avrami model heeft zijn theoretische basis als voordeel maar er werd aangetoond dat de fit verre van perfect is. Dit is mogelijk het gevolg van de veronderstellingen die gemaakt werden om de theorie te ontwikkelen, en waaraan in het geval van vetkristallisatie niet noodzakelijkerwijze voldaan is. Er werd aangetoond dat het Gompertz model reeds een betere fit toelaat dan het Avrami model maar dat ook die nog niet toereikend is. Een voordeel van het Gompertz model is de heldere fysische interpretatie van de parameters, een nadeel is zijn zwakke theoretische achtergrond. Deze literatuurstudie leidde bijgevolg tot de conclusie dat er nog ruimte is voor een ander model dat de kristallisatiekinetiek van vetten beter kan beschrijven.

De literatuurstudie over cacaoboter (hoofdstuk 2) toonde aan dat cacaoboter voor het belangrijkste gedeelte uit triacylglycerolen bestaat. Minorcomponenten zijn echter ook

aanwezig. De chemische samenstelling van cacaoboter kan lichtjes variëren afhankelijk van enerzijds de groeiomstandigheden en de ouderdom van de boom, en anderzijds van het productieproces uit de cacaobonen en de eventuele opzuivering van de cacaoboter. Deze kleine verschillen in chemische samenstelling brengen ook kleine verschillen in de fysische eigenschappen, zoals de kristallisatiekinetiek, met zich.

Het experimentele gedeelte van deze studie begon met de ontwikkeling van een verbeterde methode om de isotherme cacaoboterkristallisatie te volgen met behulp van differentiële scanning calorimetrie (hoofdstuk 3). De invloed op de isotherme kristallisatiekinetiek van cacaoboter van de staalnameprocedure, het protocol om de stalen af te smelten voorafgaand aan de kristallisatie, en de koelsnelheid naar de kristallisatietemperatuur werden onderzocht. Een smeltprotocol van 65°C gedurende 15 minuten en een koelsnelheid van 8°C min^{-1} werden gekozen voor gebruik in de verdere experimenten. Er werd eveneens aangetoond dat een wijziging in de staalnameprocedure de kristallisatie kan beïnvloeden. Speciale aandacht ging uit naar de integratie van de bekomen kristallisatiepieken. Deze integratie is noodzakelijk om een (in de meeste gevallen sigmoïdale) kristallisatiecurve te bekomen die de hoeveelheid vrijgestelde kristallisatiewarmte als functie van de tijd weergeeft. Er werd aangetoond dat wanneer de integratielimieten visueel bepaald worden, het resultaat in sterke mate afhangt van de uitvoerder en bovendien verschilt wanneer dezelfde uitvoerder de integratie verscheidene malen herhaalt. Om de hierdoor veroorzaakte hoge variabiliteit te elimineren, werd een objectief berekeningsalgoritme ontwikkeld om de integratiegrenzen vast te leggen.

In het tweede gedeelte van dit onderzoek werd een nieuw model ontwikkeld om de kristallisatiekinetiek van vetten te beschrijven (hoofdstuk 4). Dit model beschrijft het kristallisatieproces als een eerste orde voorwaartse reactie en een terugwaartse reactie met orde *n*. Deze terugwaartse reactie wordt mogelijk veroorzaakt door een lokaal herafsmelten en / of een heroplossen van kristallen. Er werd aangetoond dat het voorgestelde model steeds een betere fit vertoont dan het Avrami model en ook beter presteert dan het Gompertz model, voor de beschrijving van de meerderheid van de datasets. Bij de resterende datasets presteert het voorgestelde model slechts iets slechter dan het Gompertz model. Een belangrijke eigenschap van het voorgestelde model in vergelijking met het Gompertz model is de mogelijkheid om kristallisatiecurves met een verschillende graad van asymmetrie te beschrijven. De universaliteit van het voorgestelde model werd aangetoond door het te fitten aan datasets die de kristallisatie

beschrijven van twee totaal verschillende vetten (cacaoboter en melkvet) bij verschillende temperaturen en gemeten met behulp van verschillende experimentele technieken. Een belangrijk voordeel van het voorgestelde model is zijn ontwikkeling in de vorm van een differentiaalvergelijking. Dit laat toe om het model ook te gebruiken onder tijdsafhankelijke omstandigheden, zoals bijvoorbeeld bij niet-isotherme kristallisatie. Om de parameterschatting te vereenvoudigen werd eveneens de algebraïsche oplossing onder isotherme omstandigheden bepaald.

In het derde gedeelte van dit onderzoek (hoofdstuk 5) werden verschillende analysetechnieken (differentiële scanning calorimetrie, puls nucleair magnetische resonantie, microscopie met behulp van gepolariseerd licht en tijdsopgeloste X-stralen diffractie gebruik makend van synchrotronstraling) gebruikt om de isotherme cacaoboterkristallisatie te bestuderen bij temperaturen tussen 17°C en 23°C. Er werd aangetoond dat de kristallisatie binnen dit temperatuursbereik een tweestapsproces is. Een mechanisme voor de twee stappen werd voorgesteld. In de eerste stap kristalliseert een gedeelte van de smelt in de α polymorf, terwijl de tweede stap α gemedieerde β' kristallisatie omvat. Dit laatste betekent dat de reeds gevormde α kristallen omkristalliseren naar β' wat aanleiding geeft tot kristallisatie van bijkomende α kristallen, die dan op hun beurt omkristalliseren naar β'. Dit zou betekenen dat er geen β' kristallen rechtstreeks uit de smelt gevormd worden. In de laatste fase van de tweede kristallisatiestap vindt enkel een omkristallisatie van α naar β' plaats, wat aanleiding geeft tot de aanwezigheid van een isosbestisch punt in de X-stralendiffractiepatronen opgemeten bij kleine hoeken.

Het volgende gedeelte van dit onderzoek (hoofdstuk 6) bestudeerde de invloed van de temperatuur (19°C – 23°C) op de isotherme cacaoboterkristallisatie. De inductietijd van de eerste kristallisatiestap, namelijk de kristallisatie van een gedeelte van de smelt in de α polymorf, werd gemeten met behulp van een lichtverstrooiingstechniek. In het bestudeerde temperatuursbereik bleek het mogelijk de Turnbull-Fisher vergelijking aan deze data te fitten. Met differentiële scanning calorimetrie en puls nucleair magnetische resonantie werd verder aangetoond dat de hoeveelheid vast vet, afkomstig van de α kristallisatie in de eerste kristallisatiestap, daalt als functie van de temperatuur. De hoeveelheid warmte die vrijgesteld wordt in de tweede kristallisatiestap, begint echter slechts te dalen bij hogere temperaturen. De inductietijd van de tweede kristallisatiestap, dus de inductietijd voor de omkristallisatie van α naar β', neemt toe bij toenemende

temperatuur. Het is echter mogelijk dat de inductietijd van de tweede kristallisatiestap ook beïnvloed wordt door de snelheid van kristalgroei. De snelheidsconstante *K* daalt als functie van de temperatuur en dit vooral bij hogere temperaturen. De orde van de terugwaartse reactie daalt tot een bepaalde temperatuur en blijft dan constant.

De invloed van de chemische samenstelling op de isotherme cacaoboterkristallisatie werd bestudeerd in het laatste gedeelte van dit onderzoek (hoofdstuk 7). Naast het vetzuur- en triacylglycerolprofiel werd ook de hoeveelheid van een aantal minorcomponenten (diacylglycerolen, vrije vetzuren, fosfolipiden, zeep, onverzeepbare stoffen, ijzer en primaire oxidatieproducten) bepaald. Er werd aangetoond dat er significante verschillen zijn in de chemische karakteristieken en in de kristallisatieparameters tussen de bestudeerde cacaoboters. Met behulp van voorwaartse meervoudige lineaire regressie werd nagegaan welke chemische karakteristieken de kristallisatieparameters beïnvloeden. De verhouding van de verzadigde tot de onverzadigde vetzuren en de mono-onverzadigde tot de di-onverzadigde triacylglycerolen heeft de belangrijkste invloed op de hoeveelheid kristallisatie, de inductietijd van de tweede kristallisatiestap en de orde van de terugwaartse reactie. De hoeveelheid diacylglycerolen heeft de belangrijkste invloed op de snelheidsconstante. Andere minorcomponenten met een aanzienlijke impact op verschillende kristallisatieparameters zijn vrije vetzuren, fosfolipiden en zepen.

SUMMARY

An important constituent of many food products is fat, of which a substantial part is present in the crystallized form. The chemical composition and processing conditions determine the primary crystallization behaviour of fat. This involves not only when and to what extent the fat crystallizes, but also the polymorphism (i.e. the existence of several crystalline phases of the same chemical composition that differ mutually in structure but yield identical liquid phases upon melting) and the morphology of the crystals and the possible polymorphic transitions. The processing conditions also influence the further aggregation of the primary crystals to clusters and further to a three-dimensional network. Each of these levels of structure determines the macroscopic properties of the food product. This research focused on the primary crystallization behaviour of cocoa butter. The crystallization behaviour of this yellow fat extracted from cacao-beans, is very important in chocolate manufacturing.

The literature review on fat crystallization (chapter 1) covered the fundamentals of nucleation and crystal growth, and polymorphism. However, the main emphasis was on the modelling of the crystallization kinetics of fats. An overview of the different experimental techniques used to obtain crystallization data and of the different models used to describe the kinetics, was given. The Avrami model and to a lesser extent the Gompertz model, are mostly used. The Avrami model has the advantage of a theoretical basis but its fit is far from being perfect, as was demonstrated. This may be due to the underlying assumptions, which are often not satisfied in the case of fat crystallization. It was revealed that the Gompertz model provides a better fit than the Avrami model but it is not satisfactorily yet. An advantage of the Gompertz model is the straightforward physical interpretation of the parameters, a disadvantage its weak theoretical basis. This literature review reached to the conclusion that there was room for another model able to better describe the crystallization kinetics of fats.

The literature review on cocoa butter (chapter 2) showed that triacylglycerols constitute the main part of cocoa butter, though some minor components are also present. The chemical composition of cocoa butter can vary slightly depending on the growth conditions and the age of the tree on the one hand, and on the production process of the cocoa butter from the cacao-beans and any refining of the cocoa butter on the other

hand. These slight differences in chemical composition also lead to small differences in the physical properties, such as the crystallization kinetics.

The experimental part of this research started with the development of an improved method to study the isothermal cocoa butter crystallization by means of differential scanning calorimetry (chapter 3). The influence on the isothermal crystallization kinetics of cocoa butter of the sample preparation procedure, the protocol to melt the samples prior to crystallization and the cooling rate to the crystallization temperature, were studied. A melting protocol of 65°C for 15 minutes and a cooling rate of 8°C min^{-1} were chosen for use in further experiments. It was also demonstrated that a change in the procedure to prepare the samples can influence the crystallization. Special attention was given to the integration of the obtained crystallization peaks. This integration is necessary to get a (mostly sigmoid) crystallization curve representing the amount of heat released as function of time. It was shown that when the integration limits are determined visually, the result strongly depends on the operator and also differs when the same operator performs the integration several times. To eliminate the high variability introduced by such a visual determination of the integration limits, an objective calculation algorithm to determine these limits was developed.

In the second part of this research a new model to describe the crystallization kinetics of fats was developed (chapter 4). This model describes the crystallization process as a first order forward reaction and a reverse reaction of order *n*. This reverse reaction may be related to local remelting of crystals and / or redissolving of crystals. It was demonstrated that the proposed model has a better quality of fit than the Avrami model under all conditions studied and also performs better than the Gompertz model for the majority of the data series. For the other data series it only performs slightly worse. An important feature of the proposed model when compared to the Gompertz model is its ability to fit crystallization curves with different degrees of asymmetry. The universality of the proposed model was shown by fitting the model to data series obtained by crystallizing two completely different fats (cocoa butter and milk fat) at different temperatures and using different analytical techniques. An important advantage of the proposed model is also the fact that it was built in the form of a differential equation. This allows the model also to be used under time-varying conditions, as e.g. in non-isothermal crystallization. To facilitate parameter estimation, the algebraic solution under isothermal conditions was also determined.

In the third part of this research (chapter 5) different analytical techniques (differential scanning calorimetry, pulsed nuclear magnetic resonance, polarized light microscopy and real-time X-ray diffraction using synchrotron radiation) were used to study the isothermal cocoa butter crystallization at temperatures between 17°C and 23°C. In this temperature range the crystallization was shown to be a two-step process. A mechanism for these two steps was proposed. In the first step part of the melt crystallizes in the α polymorph, while the second step consists of α mediated β' crystallization. The latter means that α crystals that are already formed transform to β' crystals, leading to the formation of extra α crystals, which in turn transform to β'. This would mean that no β' crystals are formed directly from the melt. In the later stages of the second step only a polymorphic transition from α to β' takes place, leading to the existence of an isosbestic point in the short angle X-ray scattering patterns.

The next part of this research (chapter 6) dealt with the influence of temperature (19°C-23°C) on the isothermal cocoa butter crystallization. The induction time of the first crystallization step, i.e. the crystallization of part of the melt in the α polymorph, was determined by scanning diffusive light scattering. It was shown that in the studied temperature range, the Turnbull-Fisher equation could be fitted to these data. Using differential scanning calorimetry and pulsed nuclear magnetic resonance it was demonstrated that the amount of solid fat from α crystallization in the first step of the process decreases with temperature. The amount of heat released during the second crystallization step, only starts to decrease at higher temperatures. The induction time of the second part of the crystallization process, i.e. the induction time for the polymorphic transition from α to β' increases with temperature. Probably, however, the induction time of the second part of the crystallization process is also influenced by the crystal growth rate. The rate constant K decreases as the temperature increases, especially at higher temperatures. The order of the reverse reaction decreases up to a certain temperature and then remains constant.

The influence of chemical composition on the isothermal cocoa butter crystallization was studied in the last part of this research (chapter 7). Apart from the fatty acid and triacylglycerol profile, the amounts of some minor components (diacylglycerols, free fatty acids, phospholipids, soap, unsaponifiable matter, iron and primary oxidation products) were determined. It was revealed that there is a significant difference in all the chemical characteristics as well as in the crystallization parameters between the

investigated cocoa butters. With forward multiple linear regression it was investigated which chemical characteristics influence the different crystallization parameters. The ratios of saturated to unsaturated fatty acids and mono-unsaturated to di-unsaturated triacylglycerols have the most important effect on the amount of crystallization, the induction time of the second step of the crystallization process and the order of the reverse reaction. The amount of diacylglycerols has the most important influence on the rate constant. Other minor components with a rather pronounced influence on different crystallization parameters are the free fatty acids, phospholipids and traces of soap.

INTRODUCTION

A considerable number of food products contains an important amount of fat, of which a substantial amount is present in the crystallized form. Examples of such food products are butter, margarine, chocolate, ice cream and spreads like cream cheese. The macroscopic properties of these products, such as the appearance and the mouth feel are of primary importance for the consumers' perception of the product. These properties, however, also influence the processing of the products and their application possibilities. The ultimate goal of many studies is to be able to truly understand and eventually predict these macroscopic properties. This would allow the manufacturer to optimize the quality of the products and to maintain a good quality under all circumstances. To reach this goal, it is necessary to characterize and define the different levels of structure present in the material and their respective relation to the macroscopic properties. Figure 1 outlines the structural hierarchy in fatty materials.

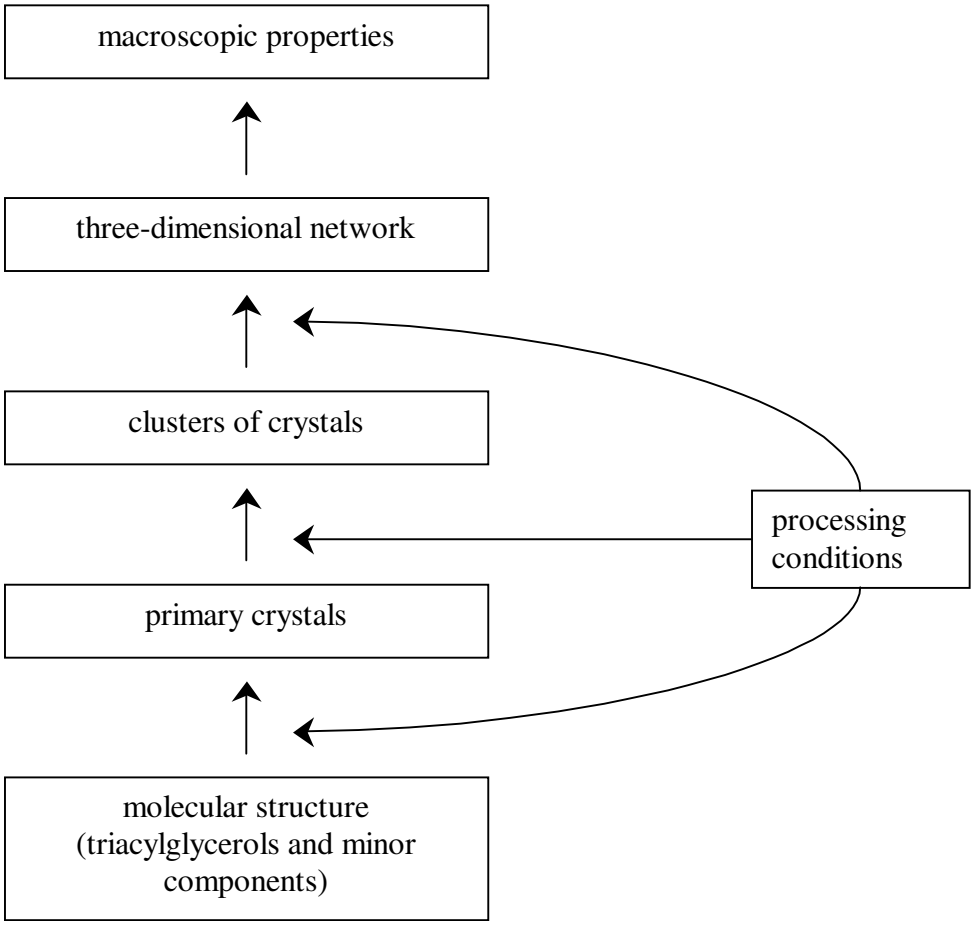

Figure 1 Structural hierarchy in fatty materials (after Narine & Marangoni, 1999)

When fats, containing triacylglycerols and minor components, are cooled from the melt to a temperature below their melting point, i.e. when they are supercooled, they undergo a liquid-solid transformation to form primary crystals with specific shapes and sizes and with a characteristic polymorphism. Polymorphism is defined as the existence of several crystalline phases of the same chemical composition that differ mutually in structure but yield identical liquid phases upon melting. The primary crystals aggregate or grow into each other, to form clusters, which interact further, resulting in the formation of a continuous three-dimensional network. The liquid phase of the fat is trapped within this solid network. The macroscopic properties of a fat can be influenced by all these structure levels; however, most directly by the structure level that is closest to the macroscopic world. Each step in this structural hierarchy is influenced by the processing conditions (Narine & Marangoni, 1999).

This research deals with the first step in this structural hierarchy, the primary crystallization behaviour. This behaviour depends on the chemical composition of the fat (triacylglycerols and minor components) and on the processing conditions (characterized by a specific combination of time, temperature and shear). The crystallization behaviour involves the crystallization kinetics of the fat, i.e. when and to what extent the fat crystallizes but also the polymorph in which the fat crystallizes, the morphology of the crystals and the transitions from one polymorph to another.

Cocoa butter was used as the substrate for this research. It is a yellow fat, extracted from fermented beans of the cacao tree, *Theobroma cacao*. The Aztecs already cultivated these trees long before the arrival of the Europeans. In these times the beans were praised both for their use as a currency and for the production of a spiced drink called ‘chocolatl’. Nowadays, cocoa butter is mainly used in chocolate and confectionery production. During chocolate manufacturing, the crystallization behaviour is important in the unit operations of tempering and cooling. The objective of tempering is the production of the right amount of crystal seeds of the appropriate size and in the proper polymorph. During subsequent cooling, the bulk of the cocoa butter is deposited on the seeds, forming a fat crystal network. The crystallization is, however, not finished after cooling but continues during storage. Furthermore, recrystallization occurs during storage and distribution, often resulting in the quality defect known as fat bloom, which is characterized by a lack of gloss and the presence of white areas on the surface of the chocolate.

It is the general objective of this research to develop a mathematical model, which is able to describe the isothermal, static (i.e. without agitation) crystallization kinetics of fats better than the models generally used in literature, and which can be adapted for use under different processing conditions (e.g. non-isothermal crystallization). This model is then used to quantify the influence of temperature and chemical composition on the isothermal, static crystallization kinetics of cocoa butter.

The first two chapters of this PhD thesis provide a literature review of fat crystallization and of the substrate cocoa butter. In the third chapter an improved method is developed to study the isothermal cocoa butter crystallization using differential scanning calorimetry. The numerical integration of the crystallization peaks is emphasized. The fourth chapter presents the new model to describe the isothermal crystallization kinetics of fats. The qualities of the proposed model are compared to those of the Avrami and Gompertz models, two models generally used in literature to describe the isothermal crystallization kinetics of fats. In the fifth chapter different analytical techniques (differential scanning calorimetry, pulsed nuclear magnetic resonance, polarized light microscopy and real-time X-ray diffraction using synchrotron radiation) are used to gain more insight into the specific processes taking place during the isothermal cocoa butter crystallization. It is investigated in which polymorph the cocoa butter crystallizes and whether this polymorph is formed directly from the melt or via a polymorphic transition from a less stable polymorph. Finally, the model developed in chapter 4 is applied to study the effect of the isothermal crystallization temperature (chapter 6) and the chemical composition of the cocoa butter (chapter 7) on the crystallization kinetics.

1 FAT CRYSTALLIZATION

1.1 Introduction

Food products in which fat crystallization is important include chocolates and confectionery coatings, dairy products such as butter and cream and vegetable spreads. An understanding of fat crystallization processes in these products plays a critical role in determining the overall product quality. Fat crystallization may affect several properties of a food: the consistency, the mouth feel and the emulsion stability. Fat crystallization is also important in fractionation, where products with varying melting and physical properties are made (Hartel, 1992 and Walstra, 1987).

The first part of this chapter deals with the fundamentals of crystallization. The two main steps, nucleation and crystal growth are discussed. The second part deals with polymorphism. These first two parts are rather brief since good reviews exist in literature: Aquilano and Sgualdino (2001), Boistelle (1988) and Garside (1987) for the fundamentals of nucleation and crystal growth and Chapman (1961), Hagemann (1988), Hernqvist (1990), Larsson and Dejmek (1990) and Sato et al. (1999) for polymorphism. The third part of this chapter deals with the modelling of the crystallization kinetics of fats and provides an overview of the experimental techniques used to obtain crystallization data and the models different authors use.

1.2 Fundamentals of nucleation and crystal growth

Crystallization can take place from the vapour, the melt or the solution phase. Special theories have not been developed to treat each of these different phase changes but general theories have been adapted to apply to specific cases (Garside, 1987).

Crystallization can be separated into several steps. The first is the generation of sufficient thermodynamic driving force. Once this has been attained, nucleation occurs, a process in which crystals are generated by bringing growth units together in order to form a crystal lattice. From then on, further crystal growth can occur (Hartel, 1992).

1.2.1 Nucleation

1.2.1.1 Types of nucleation

Three types of nucleation can be distinguished: primary (homogeneous and heterogeneous) and secondary nucleation.

If nucleation is not catalysed by the presence of fat crystals or foreign solid surfaces, it is called primary, homogeneous nucleation. In this case, supercooling up to 30 K should be applied before crystallization can occur (Kloek, 1998).

If the presence of foreign surfaces catalyses the nucleation process, this gives rise to primary, heterogeneous nucleation occurring at lower levels of supersaturation (1–3 K) than homogeneous nucleation (Garside, 1987). Most natural fats contain enough catalytic impurities for heterogeneous nucleation to take place (Walstra, 1987).

Secondary nucleation occurs in the presence of crystals of the material being crystallized and can therefore only occur after primary homogeneous or heterogeneous nucleation and subsequent crystal growth (Kloek, 1998). Tiny crystallites, exceeding the critical size, are removed from the surface of the existing crystals and serve as secondary nuclei for further growth (Kellens, 1991). Secondary nucleation is especially observed when crystallization takes place in solution or in industrial crystallizers (Boistelle, 1988).

1.2.1.2 Classical nucleation theory for homogeneous nucleation (Boistelle, 1988 and Garside, 1987)

The driving force for crystallization is the difference in chemical potential $\Delta\mu$ [J mole^{-1}] (or partial molar Gibbs free energy) between the liquid and the solid. The larger the chemical potential difference, the larger the driving force for crystallization.

To obtain nucleation from a solution, it is necessary to supersaturate the system by achieving a concentration C [m^{-3} or equivalent] higher than the concentration at saturation C_s [m^{-3} or equivalent]. The difference in chemical potential then is:

$$\Delta\mu = R_g \times T_K \times \ln(C / Cs) \qquad \textbf{[1.1]}$$

where R_g is the universal gas constant [8.314 J mole^{-1} K^{-1}] and T_K the absolute temperature [K]. The term $ln(C/C_s)$ is called the supersaturation, $ln(\sigma)$ [-], while C/C_s is

the supersaturation ratio σ [-]. For ideal solutions, the concentration at saturation C_s is given by the Hildebrand equation:

$$\ln C_s = \frac{\Delta H_m}{R_g}\left(\frac{1}{T_{Km}} - \frac{1}{T_K}\right) \quad \textbf{[1.2]}$$

where T_{Km} and ΔH_m are respectively the absolute melting temperature [K] and the molar enthalpy variation in the system during the transition [J mole^{-1}]. It has to be noted that the values of T_{Km} and ΔH_m for the specific polymorph have to be taken into account.

At low values, the supersaturation is often approximated by expanding the ln-term in equation [1.1] by a Taylor series and using only the first term. This results in:

$$\ln(\sigma) \approx \frac{C - C_s}{C_s} = \frac{\Delta C}{C_s} = \sigma_r = \sigma - 1 \quad \textbf{[1.3]}$$

The term $\frac{\Delta C}{C_s}$ is called the relative supersaturation σ_r [-].

For crystallization from the melt, supercooling should be achieved and the difference in chemical potential can be written as:

$$\Delta\mu = \Delta H_m \frac{T_{Km} - T_K}{T_{Km}} \quad \textbf{[1.4]}$$

The difference $T_{Km} - T_K = \Delta T$ is named supercooling [K]. In this case the relative supersaturation can be written as:

$$\sigma_r = \frac{\Delta T}{T_{Km}} \quad \textbf{[1.5]}$$

Nucleation occurs when growth units meet giving rise to a distribution of clusters, called embryos. The Gibbs free energy change ΔG [J] for formation of such an embryo is determined by a positive surface term ΔG_s [J] due to surface tension and a negative volume term ΔG_v [J]. This Gibbs free energy change ΔG is also called the activation free energy. For a spherical embryo with radius r [m] ΔG is:

$$\Delta G = 4\pi r^2 \gamma - \frac{4\pi r^3 \Delta\mu}{3V_m} \quad \textbf{[1.6]}$$

where γ is the surface free energy per unit surface area [J m^{-2}] and V_m is the molar volume [m^3 $mole^{-1}$]. Figure 1.1 illustrates the dependence of ΔG on the embryo radius. A critical radius r^* [m] exists for which ΔG is maximum:

$$r^* = \frac{2\gamma V_m}{\Delta\mu} \qquad \textbf{[1.7]}$$

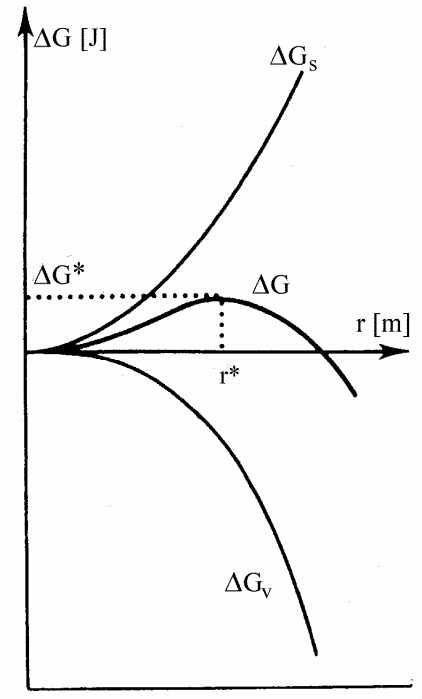

Figure 1.1 Variation of the Gibbs free energy change ΔG [J] for three-dimensional nucleation as function of nucleus size r [m] (Boistelle, 1988)

Since growth of the embryo only leads to a decrease of ΔG once the embryo radius is higher than the critical radius, the embryo is stable above the critical nucleus and unstable below it.

Inserting equation [1.7] into equation [1.6] yields the critical activation free energy for nucleation ΔG^* [J]:

$$\Delta G^* = \frac{16\pi {V_m}^2 \gamma^3}{3(\Delta\mu)^2} \qquad \textbf{[1.8]}$$

The factor $\frac{16\pi}{3}$ results from the spherical shape attributed to the nucleus and may in general be replaced by a dimensionless shape factor.

The nucleation rate J [s^{-1} m^{-3}] at which new nuclei are formed is a problem of kinetics and is determined by the rate at which embryos surmount the maximum in the free energy curve. Supposing the embryos follow a Boltzmann distribution as function of their free energy, the nucleation rate can be written as:

$$J = A_J \times e^{\frac{-\Delta G^*}{k_B T_K}} \quad \textbf{[1.9]}$$

where A_J represents the global kinetic coefficient [s^{-1} m^{-3}] and k_B is the Boltzmann constant [1.380 10^{-23} J K^{-1}]. A_J can also be written as:

$$A_J = \frac{N_m \times k_B \times T_K}{h_P} \quad \textbf{[1.10]}$$

with N_m the number of molecules per m^3 [m^{-3}] and h_P Planck's constant [6.626 10^{-34} J s].

When nucleation occurs from the melt or a high viscosity solution it is necessary to take into account the difficulty encountered by a molecule to cross the interface between the liquid and solid phases. Therefore, in that case an additional critical activation free energy for volume diffusion ΔG^*_{vd} [J] is added to equation [1.9] which is rewritten as:

$$J = A_J \times e^{\frac{-\Delta G^*}{k_B T_K}} \times e^{\frac{-\Delta G^*_{vd}}{k_B T_K}} \quad \textbf{[1.11]}$$

Equation [1.11] is generally known as the Turnbull – Fisher equation. When the temperature decreases the volume diffusion term may become rate-determining causing the nucleation rate to drop off at these lower temperatures.

1.2.1.3 Heterogeneous nucleation (Boistelle, 1988, Garside, 1987 and Hartel, 1992)

In heterogeneous nucleation, the process of molecular orientation is enhanced by the presence of a foreign surface, e.g. a dust particle or a microscopic structure in the vessel wall, which orients molecules preferentially so that a crystal lattice is more easily formed.

To derive the critical activation free energy for heterogeneous nucleation, ΔG^*_{het} [J], it is convenient to consider a cap-shaped nucleus realizing a contact angle ω with the foreign surface (Figure 1.2). The value of ω depends on the way the foreign surface is wetted by the nucleus. The surface free energies involved in this process are γ_0 [J m^{-2}]

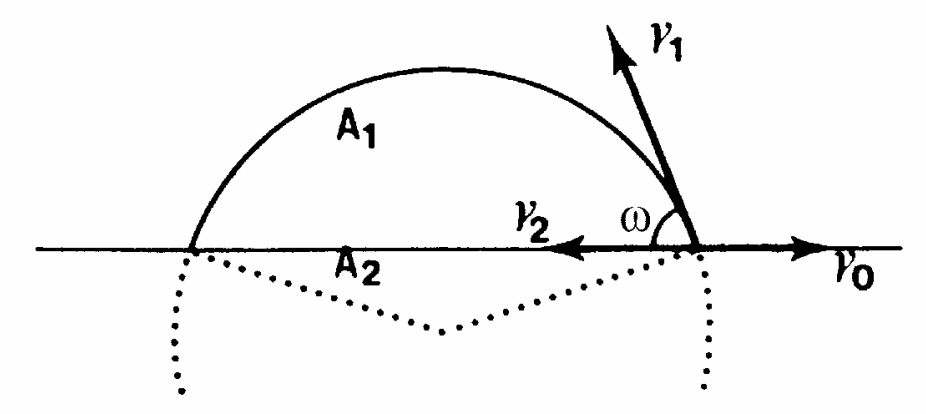

Figure 1.2 Cap-shaped nucleus forming by heterogeneous nucleation on a foreign substrate. The arrows represent the different surface free energies between foreign surface, mother phase and nucleus (Boistelle, 1988).

between foreign surface and mother phase, γ_1 [J m^{-2}] between nucleus and mother phase and γ_2 [J m^{-2}] between nucleus and foreign surface. When the nucleus is onto the foreign surface, two excess energies have been expended for creating the new surfaces, whereas one has been gained in losing a fraction of the area of the foreign surface. The Gibbs free energy change for heterogeneous nucleation ΔG_{het} [J] is therefore the sum:

$$\Delta G_{het} = -\Delta G_v + A_1\gamma_1 + A_2\gamma_2 - A_2\gamma_0 \qquad \textbf{[1.12]}$$

By calculating the volume of the cap and the surfaces and taking into account that the different surface free energies are related by:

$$\gamma_0 = \gamma_2 + \gamma_1 \cos\omega \qquad \textbf{[1.13]}$$

ΔG_{het} can be written as:

$$\Delta G_{het} = \frac{-\pi r^3 \Delta\mu(2 - 3\cos\omega + \cos^3\omega)}{3V_m} + 2\pi r^2(1-\cos\omega)\gamma_1 - \pi r^2(1-\cos^2\omega)\gamma_1\cos\omega \qquad \textbf{[1.14]}$$

in which r [m] is the radius of the underlying sphere.

Then it can be calculated that the critical radius r^* for which ΔG_{het} is maximum, is the same as for homogeneous nucleation:

$$r^* = \frac{2\gamma_1 V_m}{\Delta\mu} \qquad \textbf{[1.15]}$$

However, since the spherical cap contains fewer molecules than the full sphere, the energy barrier is less for heterogeneous than for homogeneous nucleation. Inserting

equation [1.15] in equation [1.14] yields the critical activation free energy for heterogeneous nucleation:

$$\Delta G^*_{het} = \Delta G^* \times \left(\frac{1}{2} - \frac{3}{4}\cos\omega + \frac{1}{4}\cos^3\omega \right) \quad \textbf{[1.16]}$$

which is the product of ΔG^* for homogeneous nucleation and a term depending on the value of the contact angle ω. For $\omega = 90°$ (the contact is limited to a geometrical point) ΔG^*_{het} equals $\Delta G^* / 2$ and for ω tending towards zero (perfect wetting of the substrate), ΔG^*_{het} also tends towards zero, which means that in the limiting case, no activation free energy at all is required for nucleation.

1.2.2 Crystal growth

Once nuclei are formed and exceed the critical size, they become crystallites of which the growth depends not only on external factors (supersaturation, solvent, temperature, impurities) but also on internal factors (structure, bonds, defects) (Boistelle, 1988).

The mechanism by which a crystal surface grows is determined by the nature of the interface between the crystal and the liquid (Garside, 1987). There are three types of faces: kinked (K), stepped (S) and flat (F) faces (Figure 1.3) (Boistelle, 1988).

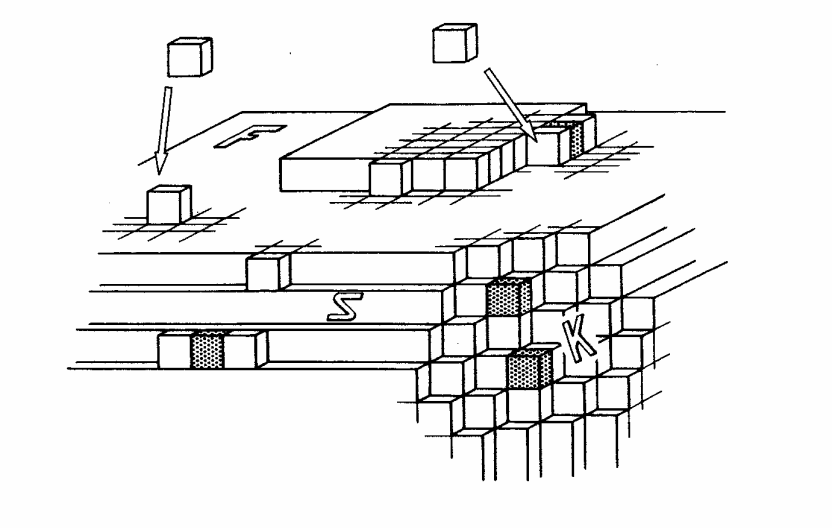

Figure 1.3 Schematic picture of different growth faces. Each small cube represents a growth unit (Aquilano & Sgualdino, 2001).

1.2.2.1 Growth of a kinked (K) face

A kinked (K) face looks like an infinite population of kink sites. Continuous growth will occur since no thermodynamic barriers to the growth process exist: each growth unit in

a supersaturated state reaching the surface will be incorporated in the crystal. As a consequence the growth rate of a K face is proportional to the relative supersaturation σ_r (Aquilano & Sgualdino, 2001 and Garside, 1987).

However, when growth occurs from the melt, the activation free energy for self-diffusion of the molecules in the melt plays an essential role in the growth kinetics. Because of this the growth rate is also inversely proportional to the viscosity. If the viscosity increases drastically with decreasing temperature, it may happen that at a given temperature the growth rate passes through a maximum and begins to decrease with increasing supercooling (Boistelle, 1988).

1.2.2.2 Growth of a stepped (S) face

From a kinetic viewpoint a stepped (S) face is similar to a K face. However, the number of kink sites per unit area is lower compared to a K face. As for a K face, the growth rate for an S face is proportional to the relative supersaturation, but due to the lower number of kink sites the growth rate of an S face will be lower than that of a K face (Aquilano & Sgualdino, 2001).

1.2.2.3 Growth of a flat (F) face

Flat (F) faces grow layer after layer, either by a two-dimensional nucleation mechanism or by a spiral growth mechanism (Boistelle, 1988).

When the crystal surface is without any defect, growth takes place by two-dimensional nucleation. The growth units that adsorb on the surface must diffuse, encounter and coalesce to form a stable two-dimensional nucleus (Boistelle, 1988). Once a surface nucleus is formed, the new crystal layer can be filled by attachment of growth units near the kink or by repeated surface nucleation and subsequent surface diffusion to existing surface nuclei (Kloek, 1998). As a result the growth rate of a perfect flat face is proportional to the two-dimensional nucleation rate and hence its expression contains the exponential term depending on the Gibbs free energy of formation of critical two-dimensional nuclei. The growth rate is near zero below a certain critical value of the relative supersaturation and increases dramatically above this value (Aquilano & Sgualdino, 2001). This type of growth mechanism is rather rare (Boistelle, 1988).

The second layer growth mechanism is the spiral growth mechanism, which occurs much more frequently than the previous one. When a screw dislocation emerges on a

face, it provides a step. When the growth units adsorb on the face they first diffuse towards and along the step. As soon as they encounter a kink, they are trapped into the surface. The step advances by rotating around the emergence point of the dislocation. After a complete rotation, one or several layers of growth units have been added to the crystal. There are several theoretical expressions for the growth rate and the general growth rate equation is very complex. It can, however, be said that at low supersaturation the growth rate of the face is a quadratic function of supersaturation, whereas at high supersaturation it turns into a linear function of supersaturation (Boistelle, 1988).

1.3 Polymorphism

Polymorphism is defined as the existence of several crystalline phases of the same chemical composition that differ mutually in structure but yield identical liquid phases when melting. Two crystalline forms are monotropic if one is stable and the other metastable under all conditions. Transition will only take place in the direction of the more stable form. Two crystalline forms are enantiotropic when each has a definite range of stability. Either modification may be the stable one and transition can go in either direction depending on the conditions (Nawar, 1996).

1.3.1 The three basic polymorphs

The polymorphs of simple saturated triacylglycerols can be classified into three crystallographic types (α (alpha), β' (beta prime) and β (beta)) according to their hydrocarbon subcell packing (Hagemann, 1988). A subcell is the smallest spatial unit of repetition along the chain axis (Nawar, 1996). The α polymorph is associated with the hexagonal subcell packing in which the fatty acid chains are perpendicular to the methyl end group plane and are assumed to be oscillating with a high degree of molecular freedom. The β' polymorph is associated with the orthorhombic subcell packing in which the fatty acid chains are tilted with respect to the methyl end group plane and where adjacent zigzag fatty acid chains are in different planes. The β polymorph is associated with the triclinic subcell packing where in contrast to the orthorhombic subcell packing, all zigzag fatty acid chains are in the same plane (Timms, 1984). Figure 1.4 shows schematic diagrams of these three basic polymorphs.

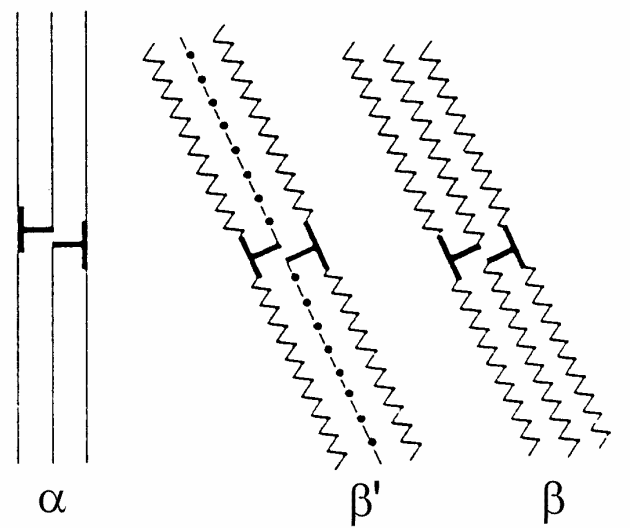

Figure 1.4 Schematic diagrams comparing the polymorphs α, β' and β as exemplified by tristearin (Timms, 1984)

Because each of the subcell packings is characterized by a unique set of X-ray diffraction lines in the wide angle region between 3.5 and 5.5 Å (the short spacings), the three basic polymorphs can be unambiguously identified on the basis of wide angle X-ray diffraction (WAXD). The hexagonal subcell packing of the α polymorph is easy to identify as it exhibits one strong diffraction line around 4.15 Å. The orthorhombic subcell packing of the β' polymorph is characterized by two strong diffraction lines around 3.7 and 4.2 Å. The triclinic subcell packing of the β polymorph gives a whole series of diffraction lines with one prominent line at 4.6 Å and two other less intense lines around 3.6 and 3.8 Å. (Kellens, 1991).

The polymorphs differ in stability, melting point, melting enthalpy and density. The α polymorph is the least stable and has the lowest melting point, melting enthalpy and density. The β polymorph is the most stable and has the highest melting point, melting enthalpy and density. The β' polymorph has intermediate properties (Walstra, 1987).

According to equation [1.9] the polymorph with the lowest critical activation free energy for nucleation ΔG^* has the highest nucleation rate. The surface free energy γ in the equation for ΔG^* [1.8] will vary a lot between the most unstable polymorph which has a structure close to that of the liquid phase and the most stable polymorph with a structure very much different from that of the liquid phase. This leads to a lower critical activation free energy and thus a higher nucleation rate for the α polymorph despite the fact that the difference in chemical potential $\Delta\mu$ is larger for the β form (Rousset, 1997).

According to Loisel (1996) the crystal growth rate increases with the stability of the polymorph, while Kellens (1991) stated that the growth rate of the unstable polymorph is higher than that of the stable polymorph. This order, however, reverses at higher driving forces.

1.3.2 Other polymorphs

Polymorphism has become more complicated by the presence of multiple sub modifications of the basic polymorphs. For the saturated monoacid triacylglycerols, it is accepted that at least two β' polymorphs exist. Different sub modifications are even more prevalent in mixed acid triacylglycerols (Kellens, 1991 and Sato et al., 1999).

Low-temperature XRD experiments showed the existence of a fourth polymorph, the sub-α polymorph. This polymorph is sometimes called the γ polymorph. The XRD pattern of this polymorph is similar to that of the β' form (Hagemann, 1988 and Kellens, 1991).

1.3.3 Phase transitions

Most triacylglycerol transitions are monotropic or irreversible and are characterized by first-order kinetics. Only the sub-α to α transition is assumed to be reversible and of the second order type. Second-order transitions occur over a wide temperature range and do not involve heat exchange. Large changes in crystal structures do not occur in second-order transitions, which merely involve an increase in molecular movement (Hagemann, 1988 and Kellens, 1991). Loisel et al. (1998a), however, stated that the sub-α to α transition, at least in cocoa butter, is also irreversible. They deduced this from the observation that cooling of the α polymorph, obtained by transition of the sub-α polymorph on heating, did not restore the latter even after one day at a low temperature.

A metastable crystal can change into a stable one via rearrangements of its structural unities until a complete transformation occurs (solid-state phase transition) or via melting and recrystallization (melt-mediated phase transition). If a suitable solvent is involved, the metastable phase dissolves and a new stable phase is allowed to form from its supersaturated solution (solvent-mediated phase transition). When a number of phase transitions from a less stable state to more and more stable states are possible, usually the closest more stable modification is formed and not the most stable one (Aquilano & Sgualdino, 2001).

Phase transition kinetics can be quite different, ranging from almost instantaneous to extremely slow for some solid-state transitions (Aquilano & Sgualdino, 2001).

1.3.4 Arrangement of triacylglycerol molecules in the crystalline phase

The X-ray scattering patterns at small angles (SAXS) of the different polymorphs also reflect a series of lines related to the thickness of the layers formed by the side-by-side arrangement of the chains (the long spacings). The layer thickness depends on the length of the molecule and on the angle of tilt between the chain axis and the methyl end group plane. The triacylglycerols are arranged head to tail and form a chair shaped structure with the fatty acid at the 2-position forming the back of the chair. Two packing modes are possible, resulting in pairs of two (2L packing) or three (3L packing) fatty acid chains long (Figure 1.5) (Kellens, 1991). Pairs of three fatty acid chains are formed when the fatty acid chains are mixed: i.e. when large differences exist in the number of carbon atoms of the different chains and when saturated and unsaturated fatty acids are mixed in the same triacylglycerol (Sato, 1987).

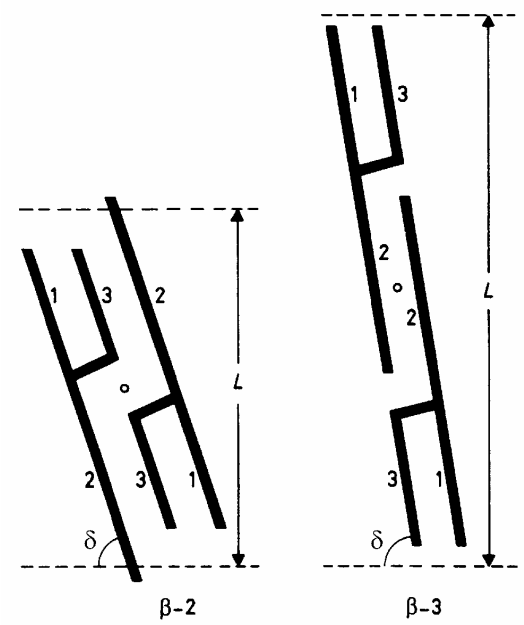

Figure 1.5 Arrangement of the triacylglycerol molecules in the crystalline phase: double and triple chair arrangements of the β form. L is the layer thickness and δ is the angle of tilt (Walstra, 1987).

1.4 Modelling of the crystallization kinetics of fats

1.4.1 Introduction

The crystallization kinetics of fats (particularly the rate of crystallization and the rate of change from one polymorph to another) are as important as the equilibrium behaviour of fats and their mixtures since they are relevant to real systems of fat production. After all, understanding when and to what extent fat components crystallize under certain conditions is the basis for controlling operations in which (re)crystallization is important (Hartel, 1992).

Equations such as described in section 1.2 find their basis in thermodynamics. The disadvantage of these equations is that they are not always easy to use in practice because a lot of the thermodynamic properties are often not known.

From the late 1970s onwards, but especially in the last few years, quite some articles have been published in which the isothermal crystallization of fats is mathematically modelled to enable quantification of differences in the crystallization behaviour between different products and crystallization conditions. A model is fitted directly to the experimental data sets and parameters with a physical meaning are extracted. Models to describe the non-isothermal crystallization kinetics of fats were not found. In the field of polymer crystallization, the majority of the proposed theoretical formulations to predict non-isothermal crystallization kinetics are based on modifications of the Avrami model (Di Lorenzo & Silvestre, 1999).

1.4.2 Investigated substrates

Table 1.1 provides an overview of the substrates investigated. The aim of the different studies was to quantify differences in crystallization behaviour between different substrates and / or different crystallization conditions (e.g. different isothermal crystallization temperature). As Metin & Hartel (1998) mentioned, very often the crystallization behaviour of a particular substrate has been extensively studied but very little quantitative data are available. Quantification was thus the main merit of these studies.

1.4.3 Experimental techniques to obtain crystallization data

Several experimental techniques can be used to follow the isothermal crystallization of fats as function of time. However, here only the methods used in modelling studies are

considered: differential scanning calorimetry (Kawamura, 1979, Kerti, 1998, Metin & Hartel, 1998, Toro-Vazquez et al., 2000, Vanhoutte, 2002 and Ziegleder, 1990), pulsed nuclear magnetic resonance (pNMR) (Herrera et al., 1999a, Herrera et al., 1999b, Kloek et al., 2000, Ng & Oh, 1994, Vanhoutte, 2002 and Wright et al., 2000) and transmittance / turbidity measurements (Dibildox-Alvarado & Toro-Vazquez, 1997).

Table 1.1 Substrates used to study the isothermal crystallization kinetics of fats

Substrate	**Author(s)**
cocoa butter	Kerti (1998), Metin & Hartel (1998) and Ziegleder (1990)
cocoa butter alternatives	Kerti (1998)
milk fat	Herrera et al. (1999a), Vanhoutte (2002) and Wright et al. (2000)
blends of cocoa butter and milk fat (fractions)	Metin & Hartel (1998)
sunflower seed oil	Herrera et al. (1999b)
palm oil	Kawamura (1979), Ng & Oh (1994)
solutions of fully hydrogenated palm oil in sunflower oil	Kloek et al. (2000)
tripalmitin in sesame oil	Dibildox-Alvarado & Toro-Vazquez (1997)
palm stearin in sesame oil	Toro-Vazquez et al. (2000)

1.4.3.1 DSC

In a DSC experiment the sample to be examined and a reference substance are subjected to a controlled time-temperature program. The difference in energy input into the sample and the reference is measured. No phase transition should occur in the reference in the considered temperature range. When analyzing fat samples, air is mostly used as a reference material. When a fat sample is heated and starts melting, extra latent heat has to be added to the sample. Consequently, the difference in energy input into sample and reference changes. This difference in energy is measured and used to follow the melting process. For a crystallization process the reverse is valid. Consequently, DSC

can be used to study phase transitions, such as crystallization, melting and polymorphic transitions, in fat samples.

In an isothermal DSC crystallization experiment, the sample is melted first and then rapidly cooled to the crystallization temperature. Subsequently, the exothermal heat flow induced by the crystallization process is measured as function of time (Simon & Süverkrup, 1995). The exact conditions used to melt the sample and the cooling rate can change depending on samples and studies.

The relative amount of material crystallized as function of time is calculated by integration of the isothermal DSC curves. The area enclosed by a baseline and the exothermal peak corresponds to the heat of crystallization, ΔH [J g^{-1}]. The relative amount of crystallized material F [-] at a given time t [any time unit] is approximated by the ratio of the integration of the exothermal rate to the total area in accordance with equation [1.17] (Kawamura, 1979):

$$F = \frac{\int_{t=0}^{t} \frac{d\Delta H(t)}{dt} dt}{\Delta H} \qquad \textbf{[1.17]}$$

The advantages of DSC, as mentioned by Ziegleder (1990) are: (i) the ability to strictly control temperature, (ii) the small sample size which makes the presence of foreign nuclei so seldom that they hardly influence the crystallization and (iii) the ability to measure free from mechanical effects. Disadvantages are the rather low sensitivity and the calculation necessary to obtain F.

More information about the principles of DSC and recent developments is given in section 3.1.1.

1.4.3.2 pNMR

With pNMR the fraction solid fat is measured directly. Its principle is summarized as follows: the sample is placed in a magnetic field and subjected to a short (5 μs) pulse of radio frequency. All protons within the sample are excited by the pulse in such a way that, once the pulse is terminated, a decaying signal appears at a receiver coil wound around the sample. The rate of decay is strikingly different for protons in the liquid (decaying in about 1 ms) and in the solid phase (decaying in a few tens of μs). By measuring the signal amplitude at two different moments in time (immediately after the

end of the pulse and about 70 to 150 μs after the end of the pulse) the solid/liquid ratio can be determined (Brosio et al., 1980).

In a pNMR experiment the samples are melted first to destroy any memory effect (the exact conditions can vary depending on samples and studies) and then transferred to a thermostatic water bath at the crystallization temperature. Then readings of the amount of solid fat are taken at appropriate time intervals.

Wright et al. (2001) compared different techniques used in fat crystallization studies and concluded that pNMR was the best method to characterize the overall crystallization process. The other techniques, turbidity and light-scattering measurements, tend to get saturated prior to the completion of the crystallization process and therefore it is not possible to obtain reliable data at later stages of crystallization. Isothermal DSC was also attempted in this study, but abandoned. As additional advantages of pNMR the authors mentioned the rapid cooling and accurate temperature control of the water bath-based cooling.

1.4.3.3 Transmittance / turbidity

In a study by Dibildox-Alvarado & Toro-Vazquez (1997) isothermal crystallization curves were obtained by measuring the transmittance (600 nm) of tripalmitin in sesame oil solutions as function of time. A double-beam spectrophotometer with data acquisition system and temperature control was utilized. The fractional crystallization F [-] as function of time t [any time unit] was calculated as:

$$F = \frac{(Tr_i - Tr)}{(Tr_i - Tr_f)} \qquad \textbf{[1.18]}$$

where Tr_i [-] is the transmittance of the oil solution at time zero, Tr [-] is the transmittance at time t and Tr_f [-] is the minimum transmittance obtained during the crystallization process. However, a few years later the same research group (Toro-Vazquez et al., 2000) also started to use DSC, indicating that crystal birefringence might have affected the transmittance values, modifying the crystallization curve in comparison with the one obtained by DSC. From the photographs obtained by transmitted polarized light microscopy it could indeed be seen that the intrinsic birefringence of crystals is not constant in time, probably due to events like heterogeneous nucleation and secondary crystallization.

Marangoni (1998) stated that turbidity measurements, which are closely related to transmittance measurements, are not suitable for the kinetic characterization of crystallization processes because: (i) the maximal turbidity does not correspond to the end of crystallization or to the maximal volume or mass of crystallized material achieved, but simply represents the point at which the crystallizing material becomes too opaque and the amount of transmitted light becomes negligible, (ii) zero angle scattering is only proportional to the amount of crystals provided that no multiple scattering occurs, an assumption which does not apply when the particles become larger than the wavelength divided by 20 and (iii) an observed decrease in transmitted light can be due to light refraction.

1.4.4 Models used to describe the isothermal crystallization

The Avrami model is most frequently used to describe the isothermal crystallization kinetics of fats (Dibildox-Alvarado & Toro-Vazquez, 1997, Kawamura, 1979, Kerti, 1998, Metin & Hartel, 1998, Toro-Vazquez et al., 2000, Vanhoutte, 2002, Wright et al., 2000 and Ziegleder, 1990). Some authors use a modified Avrami equation, also called the Avrami-Erofeev equation (Herrera et al., 1999a, Herrera et al., 1999b, Ng & Oh., 1994 and Toro-Vazquez & Dibildox-Alvarado, 1997). Recently, Kloek et al. (2000) and Vanhoutte (2002) used a reparameterized Gompertz equation to describe their crystallization curves. Berg & Brimberg (1983) proved that empirical equations used for aggregation and flocculation can also be used to describe fat crystallization.

In the following sections more details about these models are given.

1.4.4.1 Avrami model

The Avrami model is the most widely used approach for the description of isothermal phase transition kinetics. In the 1940s various authors independently developed this kinetic formulation, sometimes called the Johnson-Mehl-Avrami-Kolmogorov equation (Wright et al., 2000). The theory was initially developed for low molecular weight materials such as metals. Later it was extended to the crystallization of high polymers (Kawamura, 1979).

Avrami (1939 and 1940) stated there is an overwhelming amount of evidence pointing to the conclusion that a phase is nucleated by tiny germ nuclei which already exist in the liquid phase and whose effective number is $\bar{N}_0$ [m^{-3}] per unit nucleation region. The

number of germ nuclei per unit region at time t (N [m^{-3}]) decreases from $\bar{N}_0$ in two ways: (i) some of them become active growth nuclei as a result of free energy fluctuations with probability p per unit time [s^{-1}] and (ii) some of them get swallowed by growing grains of the new phase. The number of growth nuclei can increase linearly in time (sporadic nucleation) or the large majority of the growth nuclei can be formed near the beginning of the transition (instantaneous nucleation). V represents the volume of the crystalline phase per unit volume of space. Avrami also introduced a characteristic time scale, defined as $pdt = d\tau$. This characteristic time scale is in fact a rescaled time taking into account the value of p.

Further, Avrami made the assumption that when one grain impinges upon another, growth ceases. The volume at rescaled time τ of any grain which began growth from a nucleus at rescaled time z is denoted as $v(\tau,z)$ [m^3]. The number of such grains is given by $N(z)$ [m^{-3}]. The total extended volume V_{ext} [-] (the term 'extended' refers to the volume the grains would have had, provided that the growth had remained unimpeded) is thus:

$$V_{ext} = \int_0^{\tau} v(\tau, z) N(z) dz \qquad \textbf{[1.19]}$$

Let r [m], the 'radius', be a one-dimensional measure of the size of a grain and R [m s^{-1}] the direction averaged rate of growth of r, then r, at time t, of a grain which began growth at time y is:

$$r(t, y) = \int_y^t R dx \qquad \textbf{[1.20]}$$

or, if the rescaled time τ is introduced:

$$r(\tau, z) = \int_z^{\tau} \frac{R}{p} du \qquad \textbf{[1.21]}$$

Then the grain volume will be:

$$v(\tau, z) = \chi r^3 = \chi \left[\int_z^{\tau} \frac{R}{p} du \right]^3 \qquad \textbf{[1.22]}$$

where χ [-] is a shape factor, equal to $4\pi/3$ for a sphere.

Since the factors governing the tendency of the growth nuclei to grow out of the germ nuclei are similar to those governing further growth, Avrami assumed that *p* and *R* are approximately proportional throughout a considerable temperature and concentration range called the isokinetic range. Thus, if *R/p* is constant for a given substance in the isokinetic range, equation [1.19] can be integrated:

$$V_{ext} = \chi \frac{R}{p}^{3} \int_{0}^{\tau} (\tau - z)^3 N(z) dz \qquad \textbf{[1.23]}$$

In any region, selected arbitrarily, the part of the volume still without crystallized matter is designated as the 'nonoverlapped' volume. Then, on average, the ratio of the nonoverlapped volume *v'* to the extended volume v_{ext} of a randomly selected region is equal to the density of untransformed matter *1-V* at that time, i.e.

$$\frac{v'}{v_{ext}} = 1 - V \qquad \textbf{[1.24]}$$

The same reasoning may be applied, not to the volumes of the single grains, but to the nonoverlapped and extended portions of the increments of these grains in an element of time. Equation [1.25] is then obtained for the average grain:

$$\frac{dv}{dv_{ext}} = 1 - V \qquad \textbf{[1.25]}$$

since the nonoverlapped decrease of a grain is nothing more than the increment in transformed volume of that grain.

For the unit volume this leads to:

$$\frac{dV}{dV_{ext}} = 1 - V \qquad \textbf{[1.26]}$$

Integrating and rearranging, this gives:

$$V = 1 - e^{-V_{ext}} \qquad \textbf{[1.27]}$$

In this way the entire problem of determining the kinetics of the crystallization has been reduced to finding V_{ext} in any particular case. To find the value for V_{ext} equation [1.23] is integrated taking into account equations [1.28] and [1.29]. Equation [1.30] is obtained after the introduction of the parameter β defined in equation [1.31].

$$N(z) = \bar{N}_0 \, e^{-z} \qquad \textbf{[1.28]}$$

$$E_q(-x) = \frac{1}{q!}\int_0^x (x-z)^q e^{-z} dz = (-1)^{q+1}\left[e^{-x} - 1 + x ... (-1)^{q+1} \frac{x^q}{q!} \right] \qquad \textbf{[1.29]}$$

$$V_{ext} = \frac{6\chi R^3 \bar{N}_0}{p^3}\left[e^{-\tau} - 1 + \tau - \frac{\tau^2}{2!} + \frac{\tau^3}{3!} \right] = \beta E_3(-\tau) \qquad \textbf{[1.30]}$$

$$\beta = \frac{6\chi R^3 \bar{N}_0}{p^3} \qquad \textbf{[1.31]}$$

This equation is valid up to $\tau = \bar{\tau}$, the time corresponding to the exhaustion of germ nuclei. Beyond $\tau = \bar{\tau}$, the upper limit of the integral in equation [1.23] should be replaced by $\bar{\tau}$ and the result of integration may be expressed as:

$$V_{ext} = \beta\left\{ E_3(-\tau) - e^{-\bar{\tau}} E_3\left[-(\tau - \bar{\tau}) \right] \right\} \qquad \textbf{[1.32]}$$

When $\bar{N}_0$ is very large, i.e. exhaustion of the germ nuclei does not occur until the end of crystallization, two limiting cases can be considered. When τ is very small, i.e. when *p* is very small (and *t* is not too large), thus in the case of sporadic nucleation, the first four terms of the series development of the exponential term $e^{-\tau}$ in equation [1.30] cancel against the other terms between the square brackets. Hence, only the term of the fourth power in τ is of importance as the first term, which does not cancel. By inserting the thus obtained equation for V_{ext} in equation [1.27] the following equation is obtained:

$$V = 1 - e^{(-\beta\tau^4/4!)} = 1 - e^{(-\chi R^3 \bar{N}_0 \, pt^4)/4} \qquad \textbf{[1.33]}$$

Note that a not too large value for *p* and a very small value for *t* lead to similar values of τ and therefore support the same reasoning. However, Avrami did not take this case into account.

On the other hand, for τ very large, i.e. for *p* very large and *t* not too small, thus for instantaneous nucleation, the exponential term $e^{-\tau}$ and the terms up to the order of τ^2 in equation [1.30] can be disregarded compared to the last term between square brackets and the following equation for *V* is obtained:

$$V = 1 - e^{(-\beta\tau^3/3!)} = 1 - e^{-\chi R^3 \bar{N}_0 t^3} \quad \textbf{[1.34]}$$

Again, τ can also be very large in the opposite case (*t* very large and *p* not too small), a case that Avrami again did not take into account.

For intermediate values of *p* the dependence of *V* upon *t* will lie between equations [1.33] and [1.34].

In general, equations [1.33] and [1.34] can be written as:

$$V = 1 - e^{-kt^m} \quad \textbf{[1.35]}$$

the equation generally known as the Avrami equation.

For plate-like and linear growth an analysis similar to the previous one leads to other values for *k* and *m* (Table 1.2).

Table 1.2 Summary of the values obtainable for *k* and *m* in the Avrami model

Growth morphology	**Sporadic nucleation**		**Instantaneous nucleation**	
	***k* [s^{-m}]**	***m* [-]**	***k* [s^{-m}]**	***m* [-]**
Linear	$\frac{\chi' \times R \times \bar{N}_0 \times p}{2}$	2	$\chi' \times R \times \bar{N}_0$	1
Plate-like	$\frac{\chi' \times R^2 \times \bar{N}_0 \times p}{3}$	3	$\chi' \times R^2 \times \bar{N}_0$	2
Spherical	$\frac{\chi \times R^3 \times \bar{N}_0 \times p}{4}$	4	$\chi \times R^3 \times \bar{N}_0$	3

Table 1.2 shows that the rate constant *k* is dependent on the nucleation (amount of germ nuclei $\bar{N}_0$ for instantaneous nucleation and rate of nucleation $p\bar{N}_0$ for sporadic nucleation) and on the growth rate. The exact relationship depends on the specific case. The Avrami exponent *m* depends on the nucleation type (sporadic or instantaneous) and the growth morphology of the crystallizing particles. The meaning of the *m* value is, however, not straightforward since an *m* value of 2 and 3 can have two different meanings.

Theoretically, integer values should be obtained for *m*. However, it is frequently found by analysis of experimental data that the Avrami exponent is a non-integer value. Several causes have been suggested: (i) discrepancies in the assumptions used in the derivation of the model, (ii) the true nucleation rate varies during the process, (iii) the growth rate changes during the process, (iv) the growth morphology changes during the process and (v) crystalline aggregates grow concurrently from both instantaneous and sporadic nuclei (Long et al., 1995 and Supaphol & Spruiell, 2000).

Evans (1945), obviously without knowledge of the prior work of Avrami, obtained the same model based on the problem of expanding waves created by raindrops on a pond.

1.4.4.2 Modified Avrami model

Apart from the original Avrami model as derived in section 1.4.4.1, some authors also use a so-called modified Avrami model, also called the Avrami-Erofeev model. This modified equation is:

$$V = 1 - e^{-(k't)^{m'}} \qquad \textbf{[1.36]}$$

This equation differs from the original Avrami equation in this way that the rate constant *k'* is also raised to the power *m',* which is not the case in the original Avrami equation.

The origin of this modified model can be found, on the one hand, in the work of Ng (1975) who described the development of the Erofeev model and, on the other hand, in the work of Khanna & Taylor (1988) who modified the Avrami model to eliminate the dependence of *k* on *m*.

Ng (1975) described the development of the Erofeev model in a work on the thermal decomposition in the solid state. The development was based on the Avrami theory. From equations [1.27] and [1.30] it can be deduced that for three-dimensional growth

$$-\ln(1-V) = const\left[e^{-\tau} - 1 + \tau - \frac{\tau^2}{2!} + \frac{\tau^3}{3!}\right] \qquad \textbf{[1.37]}$$

and when returning to the original time scale ($\tau = p*t$):

$$-\ln(1-V) = const\left[e^{-pt} - 1 + pt - \frac{p^2t^2}{2!} + \frac{p^3t^3}{3!}\right] \qquad \textbf{[1.38]}$$

Equation [1.38] can be transformed into a simplified form in two limiting cases (see also the deduction of equations [1.33] and [1.34]): when $p \times t$ is much smaller than 1, equation [1.38] turns into:

$$-\ln(1-V) = const(\frac{p^4 t^4}{4!}) \quad \textbf{[1.39]}$$

or

$$\left[-\ln(1-V)\right]^{1/4} = \frac{const}{24} p \times t = const' \times t \quad \textbf{[1.40]}$$

and when $p \times t$ is much larger than 1, equation [1.38] turns into:

$$-\ln(1-V) = const(\frac{p^3 t^3}{3!}) \quad \textbf{[1.41]}$$

or

$$\left[-\ln(1-V)\right]^{1/3} = \frac{const}{6} p \times t = const' \times t \quad \textbf{[1.42]}$$

These equations can be represented by the generalized Erofeev equation:

$$\left[-\ln(1-V)\right]^{1/m'} = k' \times t \quad \textbf{[1.43]}$$

which equals equation [1.36].

Khanna et al. (1988) claimed that the value of k obtained from the original Avrami model may not be correct, since k is strongly correlated to m. According to the authors, this problem may be eliminated by using a modified equation such as [1.36]. What they did, was transform the Avrami constant k from a complex constant of an m^{th} order process to a first order rate constant, despite the fact that crystallization is not a first order process. It can be calculated that the k' value of the modified Avrami model is the m^{th} root of the k value of the original model (Marangoni, 1998):

$$k' = k^{1/m} \quad \textbf{[1.44]}$$

The modified Avrami model thus simply is a reparameterized Avrami model.

Khanna et al. (1988) showed that by modifying the Avrami model more meaningful values for the rate constant could be obtained. They, for example, compared the overall crystallization rates of virgin nylon 6 and extruded nylon 6. By means of programmed rate DSC, isothermal DSC experiments and optical microscopy they proved that the

crystallization rate of virgin nylon 6 is dramatically lower. Consequently, if k is an overall rate constant, it should always have a higher value for the extruded nylon 6 resin compared to the virgin material. When calculating k through linear regression it appeared that the value was higher for the extruded nylon 6 at temperatures below 200°C but lower at temperatures above 200°C. When calculating k' from the modified Avrami model the value was always higher for the extruded nylon 6, as expected. The authors also cite other work where the original Avrami model has yielded rate constants, which did not coincide with the expected values.

Khanna et al. (1988) further claim that despite the modification the model retains its original correspondence to nucleation and crystal growth processes. The presented modification simply corrects the value of k by eliminating the influence of m.

The authors thus conclude that attempts to obtain k values through the original Avrami model may lead to erroneous results, especially when comparing processes with different values of m.

Marangoni (1998) did not agree with this modified Avrami model. According to him, Khanna et al. (1988) arbitrarily suggested a modification of the Avrami model without providing any theoretical justification. The only justification the authors provided was their opinion that k and m were correlated and that the transformation would solve this problem. However, they gave no proof.

1.4.4.3 Gompertz model

Kloek et al. (2000) and Vanhoutte (2002) fitted their crystallization curves to a reparameterized Gompertz equation as deduced by Zwietering et al. (1990). The latter authors compared the ability of several sigmoid functions to describe a bacterial growth curve. Most of the equations contain mathematical fitting parameters rather than parameters with a biological meaning making it difficult to provide initial guesses for the parameters. Therefore, the growth models were rewritten to substitute the mathematical fitting parameters with biologically meaningful parameters such as a_G [% solid fat or equivalent depending on the measuring technique used] (the maximal value reached), μ_G [% solid fat s^{-1} or equivalent depending on the measuring technique used] (the maximum specific growth rate which is defined as the tangent in the inflection point) and λ_G [s] (the lag time, which is defined as the x-axis intercept of that tangent) (Figure 1.6).

This reparameterization was performed by deriving an expression for the biologically meaningful parameters as function of the mathematical fitting parameters of the basic function.

The unmodified Gompertz equation is written as:

$$Y = A \times \exp\left[-\exp\left(B - D \times t\right)\right] \quad \textbf{[1.45]}$$

with Y [-] being the logarithm of the relative population size.

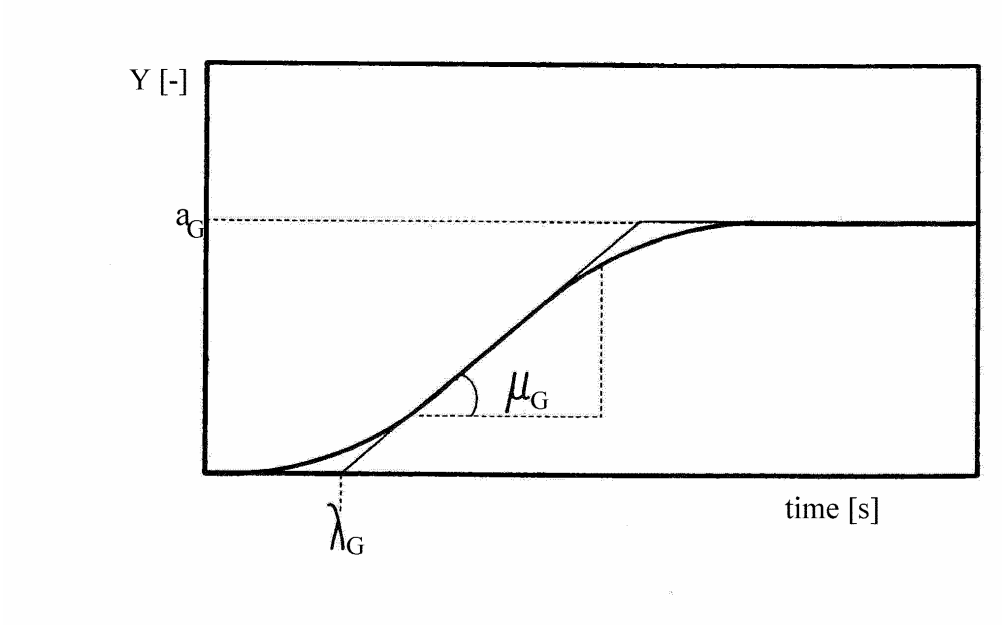

Figure 1.6 Visual representation of the Gompertz parameters

To obtain the inflection point (at $t = t_i$) of the curve, the second derivative of the function with respect to t is set to zero. This leads to:

$$t_i = B / D \quad \textbf{[1.46]}$$

An expression for the maximum specific growth rate can be derived by calculating the first derivative at this inflection point:

$$\mu_G = \frac{A - D}{e} \quad \textbf{[1.47]}$$

with e being the Euler number (2.718281…).

The parameter D in the unmodified Gompertz equation can thus be substituted by:

$$D = \frac{\mu_G \times e}{A} \quad \textbf{[1.48]}$$

To obtain an expression for the lag-time, the tangent line through the inflection point is calculated and the intercept with the t-axis deduced:

$$\lambda_G = \frac{(B-1)}{D} \quad \textbf{[1.49]}$$

The parameter *B* can thus be substituted by:

$$B = \frac{\mu_G \times e}{A}\lambda_G + 1 \quad \textbf{[1.50]}$$

The a_G value equals the *A* value since *Y* approaches *A* when *t* approaches infinity. The parameter *A* in the unmodified Gompertz equation can thus be substituted by a_G, yielding the reparameterized Gompertz equation:

$$Y = a_G \times \exp\left\{-\exp\left[\frac{\mu_G \times e}{a_G} \times (\lambda_G - t) + 1\right]\right\} \quad \textbf{[1.51]}$$

Kloek et al. (2000) and Vanhoutte (2002) used this reparameterized Gompertz equation but replaced *Y* by *f* [% solid fat or J g^{-1} depending on the measuring technique], the amount of crystallization at time *t*. Then a_G is the maximum amount of crystallization [% solid fat or J g^{-1} depending on the measuring technique used]. Kloek et al. (2000) used this model because they claimed several analogies between the crystallization of fats and bacterial growth: production of bacteria is comparable with nucleation and growth of crystals and consumption of nutrients is comparable with decrease of supersaturation.

1.4.4.4 Aggregation and flocculation model

Berg & Brimberg (1983) noticed that the course of fat crystallization is similar to that of aggregation and flocculation of colloids. The authors had previously derived empirical rate formulae for aggregation (equation [1.52]) and flocculation (equation [1.53]) from experimental data:

$$C - C_0 = -k_2\sqrt{t - t_0} \quad \textbf{[1.52]}$$

$$\ln\frac{C}{C_0} = -k_4\sqrt{t - t_0} \quad \textbf{[1.53]}$$

Prior to the main phase, an induction period exists where equations [1.54] and [1.55] apply to aggregation and flocculation respectively.

$$C - C_0 = -k_1 \times (t - t_0)^2 \quad \textbf{[1.54]}$$

$$\ln \frac{C}{C_0} = -k_3 \times (t - t_0)^2 \quad \textbf{[1.55]}$$

C [m^{-3}] is the concentration of particles in the liquid phase at time t [s], C_0 and t_0 are the initial values of C and t and the k_i constants are rate constants for each phase.

In their study the authors examined whether the kinetics of fat crystallization could indeed be described by equations [1.52] to [1.55]. They used experimental results on palm oil and hardened soy oil obtained from literature.

Since C-C_0 is the decrease of the concentration of dispersed particles, this value equals the amount of solid fat and the aggregation equations [1.52] and [1.54] can be used. For the flocculation equations [1.53] and [1.55], however, the value of C_0 has to be known. The amount of solid fat at equilibrium was taken as an estimate for C_0.

Equations [1.52] to [1.55] fitted the literature data well and the authors thus concluded that fat crystallization matches the mechanism of aggregation and flocculation: solid fat is formed by aggregation of dispersed particles and fat crystals also grow by aggregation. It was suggested that the particles are the unit cells of the crystals, which are dispersed in the liquid and that the solid phase grows by addition of unit cells.

1.4.5 Parameter estimation

The aim of parameter estimation is to obtain the values of the parameters that give the best fit to a given set of data.

No clear information on parameter estimation for the aggregation and flocculation model of Berg & Brimberg was given.

Kloek et al. (2000) and Vanhoutte (2002) estimated the parameters of the reparameterized Gompertz model by non-linear regression. An additional advantage of the reparameterized model when compared to the original model is that it is straightforward to calculate 95% confidence intervals for the biologically meaningful parameters, which is not the case when these parameters are not estimated directly from the equation but are calculated from mathematical fitting parameters.

Herrera et al. (1999a), Herrera et al. (1999b) and Wright et al. (2000) also used non-linear regression to estimate the parameters of the modified Avrami and original Avrami model respectively. Others (Kawamura, 1979, Metin & Hartel, 1998, Toro-

Vazquez et al., 2000 and Ziegleder, 1990), however, linearize the Avrami equation by a logarithmic transformation:

$$\ln(-\ln(1-V)) = \ln k + m \ln t \quad \textbf{[1.56]}$$

Toro-Vazquez & Dibildox-Alvarado (1997) also linearized the modified Avrami equation. This linearization procedure, which makes it possible to estimate the parameters by linear regression using standard spreadsheet programs, is, however, statistically questionable (see Annex III.1 for more details).

Moreover, some authors do not use all collected data to estimate the parameters. For instance, Ziegleder (1990) stated that because of the insecurity in determining the starting- and end point of the integration, only the data points between V = 0.1 and V = 0.9 are taken into account. Kawamura (1979) followed the same reasoning, whereas Toro-Vazquez & Dibildox-Alvarado (1997) even limited the data to the values obtained between 0.25 and 0.75.

Ziegleder (1990) introduced yet another correction. In theory V equals zero at the starting-point of the integration, but in reality it seemed that already some solid fat had been formed at t = 0. Based on pNMR results V was put equal to 0.03 at t = 0 and therefore, the values of V were corrected as follows:

$$V' = \frac{V + 0.03}{1.03} \quad \textbf{[1.57]}$$

It can be noticed, however, that the value of 0.03 is rather arbitrary and may change depending on samples and studies.

1.4.6 Comparison of the models

No clear information on how to apply the aggregation and flocculation model could be extracted from Berg & Brimberg (1983) ‘s article and this model is thus not taken into account in this comparison.

The modified Avrami model is a reparameterization of the original Avrami model possibly leading to better parameter estimations but it does not differ from the original model from a curve-fitting point of view.

Figure 1.7 compares the quality of fit of the Avrami and Gompertz models for an isothermal cocoa butter crystallization. It can be seen that the Gompertz model provides a better fit than the Avrami model but that neither model fits the data satisfactorily.

The Avrami model has the advantage that it was especially developed to describe crystallization processes, that it was developed from a theoretical basis and that it has often been used in the field of fat crystallization. A disadvantage is that the theory is developed on the basis of some assumptions that are often not satisfied in the case of fat crystallization. This may raise questions about the applicability of the model.

A benefit of the Gompertz model is that its parameters have a very straightforward physical interpretation. The theoretical basis for using the Gompertz model for fat crystallization is, however, rather weak. Bacterial growth can intuitively be compared with fat crystallization, but this provides no real theoretical justification.

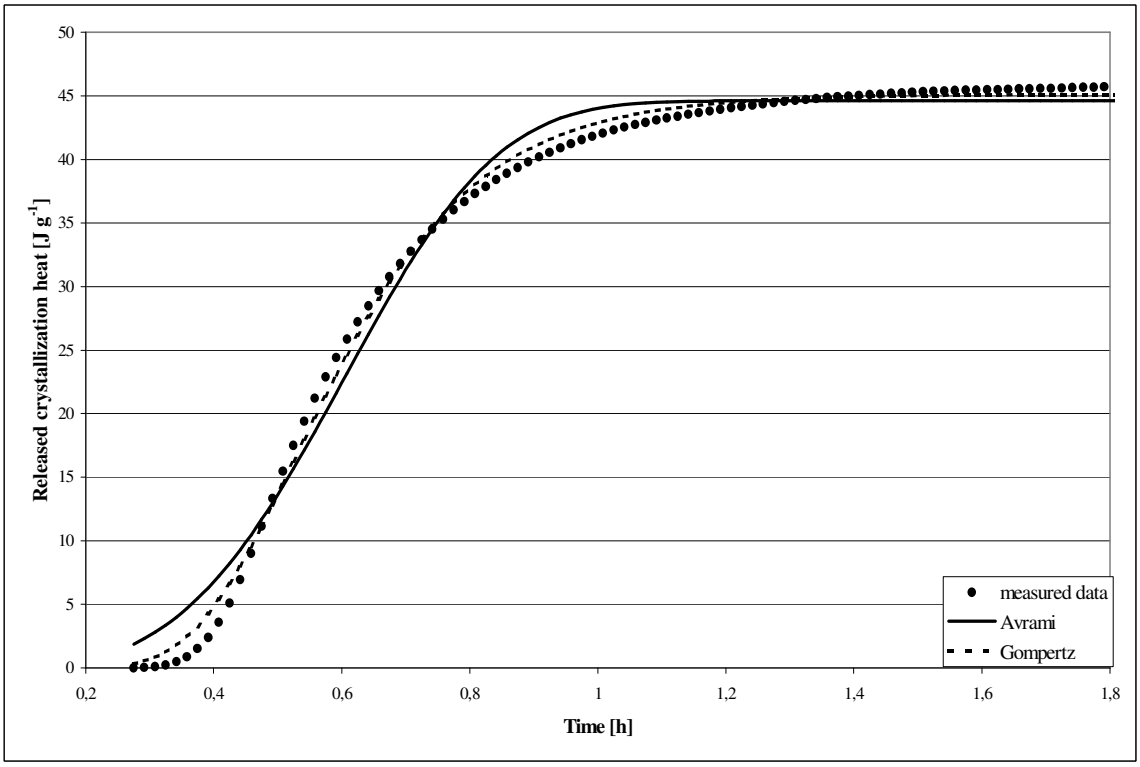

Figure 1.7 Comparison of the quality of fit of the Avrami and Gompertz models

1.5 Conclusions

In quite some food products fat crystallization is important. Insight in the crystallization kinetics of fats, i.e. when and to what extent fat components crystallize under certain conditions, is necessary for controlling the operations in the manufacturing process which are based on fat crystallization. It is thus not surprising that quite some articles have been published in which the isothermal crystallization of fats is mathematically modelled to enable quantification of differences in the crystallization behaviour between different products and crystallization conditions. The (modified) Avrami and

the Gompertz model have been used, both have advantages and disadvantages and neither model fits the data satisfactorily. Models to describe the non-isothermal crystallization kinetics of fats were not found in literature despite the fact that quite some industrial processes are based on non-isothermal crystallization. There is thus room for an improved model which is able to describe the isothermal crystallization kinetics of fats better and which can be adapted for use under non-isothermal conditions. To be able to develop such a model high quality experimental data are necessary. Possible experimental techniques to obtain these crystallization data are DSC and pNMR, each having its advantages and disadvantages.

2 COCOA BUTTER

2.1 Introduction

The properties of cocoa butter have drawn the attention of many investigators, owing to the significance of cocoa butter in the confectionary industry. The first section of this chapter describes the process from cacao-bean to cocoa butter. Sections 2.3 and 2.4 deal with the chemical and physical properties respectively. In the latter section special emphasis is given to the polymorphism of cocoa butter. Finally the use of cocoa butter, mainly for chocolate manufacturing is discussed.

2.2 Production

Cocoa butter is extracted from the seeds of a small tree botanically known as *Theobroma cacao*. The tree is grown in all wet tropical forest regions, mostly within 20 degrees of latitude of the equator. The three main growing areas are West Africa, South East Asia and South America. World production of cacao-beans in 1999/2000 was estimated at little over three million tonnes. The top five producing countries are Ivory Coast, Brazil, Ghana, Indonesia and Malaysia (Hancock & Fowler, 1994 and ICCO, 2000).

Cacao is usually classified into three types: Forastero, Criollo and Trinitario. About 95% of the world's cacao is now derived from Forastero trees and this cacao is termed bulk cacao in trade. Criollo has white cotyledons and is the original cultivated type. The origin of the Trinitarios is usually stated as the result of hybridisation between Forastero and Criollo trees. The Trinitario and Criollo varieties produce mainly the 'fine' or 'flavour' cacaos (Hancock & Fowler, 1994).

The different steps needed to produce cocoa butter from the cacao pod are discussed in the following sections and summarized in Figure 2.1.

2.2.1 **From cacao pod to cacao-beans** (Hancock & Fowler, 1994, Hanneman, 2000 and ICCO, 2002)

Cacao-beans are embedded in a sweet mucilaginous pulp in the cacao pod. These pods are usually oval in shape, measure between 15 and 30 cm and contain some 30 to 60 beans. Each bean consists of two cotyledons (the nib) and a small germ, all enclosed in a skin (the shell). The cotyledons serve both as the storage organs containing the food

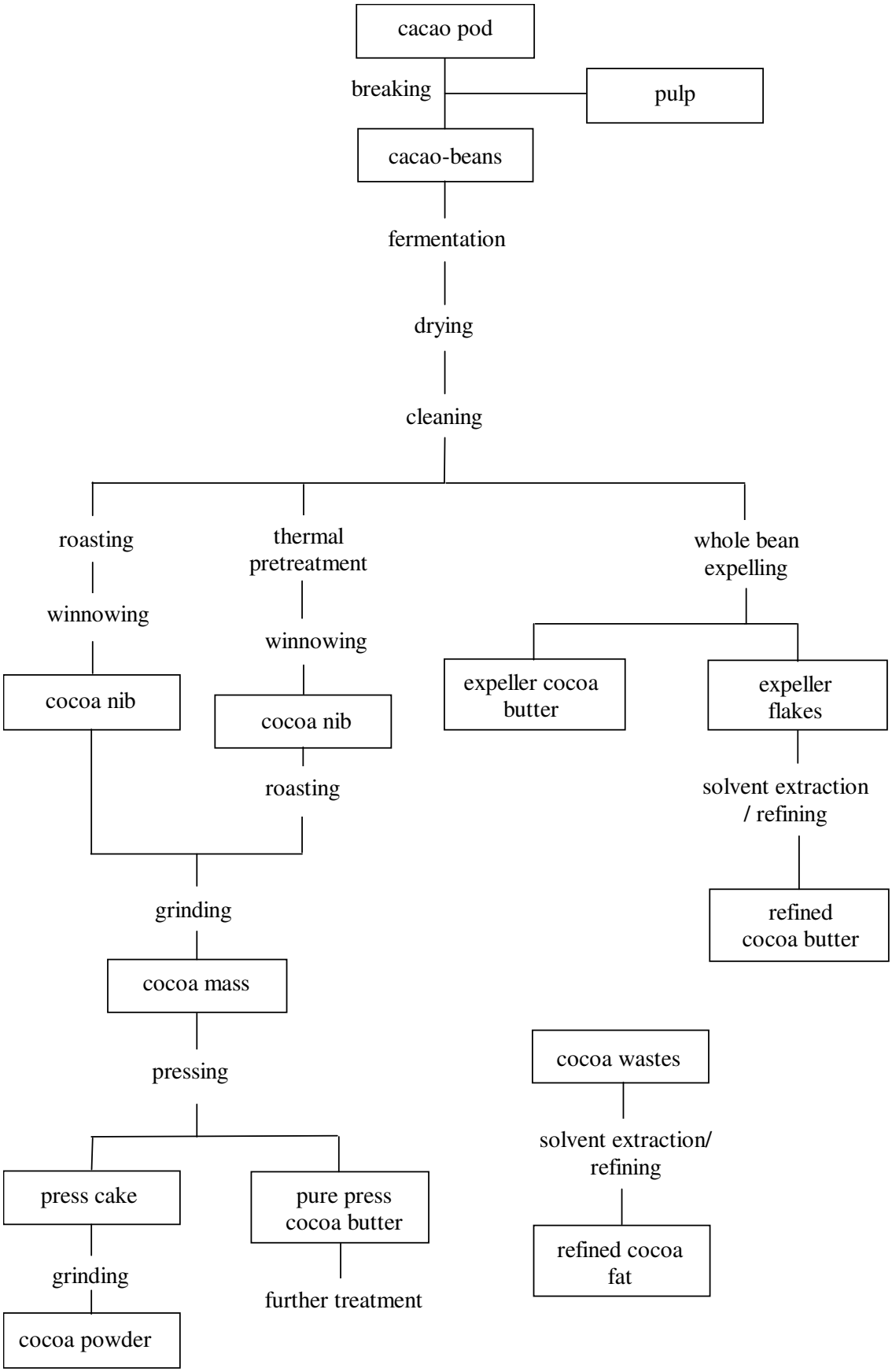

Figure 2.1 Overview of the different steps in the production of cocoa butter (after Meursing, 1994)

for the development of the seedling, and as the first two leaves of the plant when the seed germinates. The food store consists of fat (cocoa butter), which amounts to about half the weight of the dry seed.

After being harvested from the tree, the pods are broken open and emptied of its beans. A lot of the pulp drains away as a liquid.

2.2.2 **Fermentation** (Hancock & Fowler, 1994 and Hoskin & Dimick, 1994)

Fermentation, which takes from four to seven days, can be carried out in a variety of ways, but all consist of heaping a quantity of fresh beans together and allowing micro-organisms to develop. Fermentation begins with yeasts converting the sugars in the remaining pulp to ethanol. Then, bacteria start to oxidize the ethanol to acetic acid and further to carbon dioxide and water, producing heat and raising the temperature during the first 24 hours to 40°C. As the pulp starts to break down and drain away during the second day, the amount of bacteria further increases, lactic acid is produced and the acetic acid bacteria more actively oxidize ethanol to acetic acid. By this time the temperature has reached 45°C. In the remaining days of fermentation, bacterial activity continues under conditions of increasingly good aeration as the remains of the pulp drain away allowing air to diffuse between the beans.

The chemical changes within the bean depend on the dying of the cotyledon cells, which causes the cellular membranes to break down and consequently allows the different constituents to come into contact with each other. Bean death is primarily caused by acetic acid, but the high temperature is also contributory. The antocyanins and other polyphenolic compounds in the pigment cells diffuse in the main storage cells where they meet various enzymes bringing about hydrolytic reactions. These include the breakdown of the coloured anthocyanins of the Forastero beans so that there is some bleaching of the cotyledons. As more air reaches and enters the beans, oxidative and browning reactions take place and the tissue darkens. The details of the chemical changes essential for the development of chocolate flavour are not fully understood. A reaction of particular importance, however, is the oxidation of protein-polyphenol complexes formed during the early stages of fermentation. This reaction reduces the astringency and bitterness, as the oxidized polyphenols form a complex with proteins and peptides, modifying further protein degradation reactions.

When the fermentation is completed the beans are reasonably free from adherent pulp, but still have a high moisture content.

2.2.3 **Drying** (cocoa butter quality, 2002, Hancock & Fowler, 1994 and Hoskin & Dimick, 1994)

In regions where the weather is dry at harvest time, the beans can be sun dried. It usually takes about a week of sunny weather to dry the beans to the desired 7% moisture content. Where the weather is less dry and sunny, drying is done artificially. This can introduce two problems. On the one hand the beans can be dried too quickly, which does not allow for an adequate loss of volatile acids such as acetic acid and thus leads to very acidic beans. On the other hand the smoke (if a wood fire is used) may find its way onto the beans producing an unpleasant taste, which cannot be removed by further processing.

Insufficient drying results in too high moisture contents in the bean and this can lead to a microbiologically initiated breakdown of the fatty components. This causes high free fatty acid and diacylglycerol contents degrading both flavour and physical characteristics.

2.2.4 **Cleaning** (Kleinert, 1994)

Fermented and dried cocoa-beans always contain a wide variety of foreign materials. It is essential to remove them completely to maintain the quality of the product, as well as to protect the processing machines. Cleaners use a series of techniques, such as sieving, vibration, aspiration and magnetic attraction, to remove the different types of impurities.

2.2.5 **Roasting, winnowing, grinding and alkalizing to obtain cocoa mass**

The roasting process consists of heating the beans to 110 - 220°C, depending on the bean type, and is needed for the reduction of the moisture content and for the development of chocolate flavour. One of the most important and complex reactions involving flavour during the roasting process is the non-enzymatic browning or Maillard browning. However, not only the sugars and amino acids but also other compounds such as peptides, proteins, vitamins and fats and their oxidation products will enter reactions and influence the final product flavour. With the many compounds found in chocolate, it is virtually impossible to identify all reactions and pathways needed to produce chocolate flavour (Hoskin & Dimick, 1994).

Winnowing is the process in which the shell is separated from the nib. Traditionally winnowing is performed after roasting, since the latter loosens the shell and thus enhances its removal. However, the main disadvantage of this whole bean roasting is

that fat migrates from the nib to the shell thus reducing the fat content of the obtained cocoa mass. Additional disadvantages are that during the roasting process the shell is also heated, which may cause combustion gases from any remaining foreign materials on the shell to affect the flavour of the cocoa mass and that energy is required to heat the shell which is then thrown away. Furthermore, the whole bean roasting process is never optimal for all beans because of their different sizes. Due to all these disadvantages this traditional process of whole bean roasting gradually disappears in favour of nib roasting. In this case the shell is removed before roasting. To facilitate this, a thermal pre-treatment is applied before winnowing (De Ginestel, 1998b and Kleinert, 1994).

After roasting and winnowing the cocoa nib is grinded to cocoa mass. After this grinding process, the fineness of the mass should be so that no grittiness is felt in the mouth when eating chocolate or drinking products containing cocoa powder obtained from that cocoa mass (see 2.2.6). Grinding is normally carried out by a series of mills (Meursing, 1994). Sometimes roasting is performed after grinding in a process called mass roasting (Kleinert, 1994).

The cocoa mass that will be used in the pressing industry is usually obtained from alkalized cocoa nib. In the alkalizing process, cocoa nib is treated with an alkaline solution. The main aim is to give the cocoa powder (see 2.2.6) a more pronounced chocolate colour. It also leads to a neutralization of the natural acidity. The alkalizing process has to be performed carefully to prevent saponification and interesterification of the cocoa butter (Cros & Bianchi, 1998 and Meursing, 1994).

2.2.6 **Extraction of cocoa butter** (EG, 2000, Hanneman, 2000, Meursing, 1994 and Pontillon, 1998a)

The fat of the cacao-bean can be extracted from various raw materials, giving rise to different qualities of butter.

The best quality, pure press butter, is extracted from the cocoa mass with hydraulic presses. These are impressive machines: a modern press is 7.15 metres long, weighs 33 tonnes and can be loaded with 220 kg of cocoa mass. Pressing is carried out at 100 MPa and 100°C. The cocoa butter that flows from the press is filtered to remove remaining cocoa particles. The press cake is grinded to obtain cocoa powder.

Cacao-beans of inferior quality are often pressed without previous deshelling in continuous expeller presses. This leads to expeller cocoa butter.

The expeller cake and various cocoa waste materials are completely defatted by solvent extraction, giving rise to refined cocoa butter on the one hand and refined cocoa fat on the other hand.

The different types of cocoa butter must meet some quality criteria: pure press cocoa butter must not contain more than 1.75% free fatty acids and not more than 0.35% unsaponifiable matter. For expeller and refined cocoa butter, the threshold value for free fatty acids is the same but it is increased to 0.50% for unsaponifiable matter. This higher threshold for unsaponifiable matter in expeller and refined cocoa butter is due to the fact that fat obtained from the shell contains a lot of unsaponifiable matter, as was demonstrated by Rossi et al. (1994).

2.2.7 Further treatment of cocoa butter

As stated in section 2.2.5 cocoa butter obtained from alkalized mass can have a higher soap content, which affects the crystallization characteristics of the butter. Washing permits to reduce this soap content (De Ginestel, 1998b).

Because of its strong flavour, natural cocoa butter is seldom used in milk chocolate, but will first be deodorized. Deodorization is also used to minimize the variability of the flavour components. It strips these components from the natural cocoa butter by means of high temperatures, high vacuum and steam injection. The resulting cocoa butter is milder in flavour and has lower levels of flavour volatiles, free fatty acids, phospholipids, diacylglycerols and tocopherols (Hanneman, 2000).

2.3 Chemical properties

Triacylglycerols are the main components of cocoa butter, as they represent about 97%. The remaining 3% are minor components, such as free fatty acids, mono- and diacylglycerols, phospholipids, glycolipids, unsaponifiable matter, etc. (Pontillon, 1998a).

The chemical composition of a vegetable fat constituting the energy storage of a plant, such as cocoa butter, varies slightly according to the growing conditions (e.g. climate) and age of the plant. For this reason the numerous analyses of different authors on

different samples of cocoa butter show small differences (Schlichter-Aronhime & Garti, 1988a).

The first section discusses the different fatty acids making up the triacylglycerols, the second section deals with the triacylglycerol profile while the last section covers the minor components. In every section attention is given to the potential influence of the country of origin.

2.3.1 Fatty acid composition

In terms of its fatty acid composition, cocoa butter is a relatively simple fat. Palmitic, stearic and oleic acid, generally account for over 95% of the fatty acids. Of the remaining acids, linoleic and arachidic acid are present at the highest level (Talbot, 1994b). Table 2.1 gives an overview of the fatty acid composition of cocoa butters from different countries of origin. This table also indicates the abbreviations that will be used for the different fatty acids.

The total amount of unsaturated fatty acids is higher in Brazilian cocoa butter. Values higher than 40% are reported, while for the other cocoa butters values between 36 and 38% are found (Klagge & Sen Gupta, 1990 and Shukla, 1995).

Table 2.1 Fatty acid composition (weight %) of cocoa butters from different countries of origin (Klagge & Sen Gupta, 1990 and Shukla, 1995)

Country of origin	Palmitic acid (P) (16:0)	Stearic acid (S) (18:0)	Oleic acid (O) (18:1)	Linoleic acid (L) (18:2)	Arachidic acid (A) (20:0)
Ecuador	25.6	36.1	34.7	2.6	1.0
Brazil	23.9-25.2	33.2-33.4	36.6-37.8	3.5-4.1	1-1.3
Ghana	25.1-25.4	37.6-37.8	32.8-33.6	2.6-2.8	1.1-1.2
India	25.6	36.6	33.9	2.8	1.1
Nigeria	25.8	36.3	33.6	3.2	1.1
Ivory Coast	25.7-25.9	35.4-37	33-34.5	2.9-3.4	1.1-1.2
Indonesia	24.2	37.4	34.4	2.8	1.2
Malaysia	25-25.1	37.6	33.6	2.6	1.1-1.2

2.3.2 Triacylglycerol composition

Triacylglycerols are composed of one glycerol molecule and three fatty acids. The fatty acids present are denoted with the abbreviations as introduced in Table 2.1. For example, SOS is a triacylglycerol with a stearic acid molecule at the 1- and 3-positions and an oleic acid molecule at the 2-position.

Taking into account the fatty acid composition as presented in section 2.3.1 and following the statistical rule of even distribution of fatty acids within the triacylglycerols applicable to natural fats, it is expected that most of the triacylglycerols are mono-unsaturated containing one oleic acid molecule (Schlichter-Aronhime & Garti, 1988a). Table 2.2 shows that this is true indeed. Apart from these mono-unsaturated triacylglycerols some di-unsaturated triacylglycerols and a very small amount of tri-saturated and tri-unsaturated triacylglycerols are present. The three major triacylglycerols, accounting for 70 to 85%, are POP, POS and SOS (Schlichter-Aronhime & Garti, 1988a). Approximately 20% of the triacylglycerols are liquid at room temperature (Shukla, 1995).

Table 2.2 Triacylglycerol composition (mole %) of cocoa butters from different countries of origin (Shukla, 1995)

Country of origin	PSS	POP	POS	SOS	SOA	POO	SOO	PLP	PLS	SLS	PLO
Ghana	0.4	15.3	40.1	27.5	1.1	2.1	3.8	2.5	3.6	2.0	0.6
India	0.5	15.2	39.4	29.3	1.3	1.9	3.3	2.0	3.1	1.7	0.5
Brazil	trace	13.6	33.7	23.8	0.8	6.2	9.5	2.8	3.8	1.8	1.5
Ivory Coast	0.3	15.2	39.0	27.1	1.3	2.7	4.1	2.7	3.6	1.9	0.8
Malaysia	0.5	15.1	40.4	31	1	1.5	2.7	1.8	3.0	1.4	0.3
Sri Lanka	1.9	14.8	40.2	31.2	1.0	2.3	3.9	2.5	1.4	0	0.8
Nigeria	0.5	15.5	40.5	28.8	1.0	1.7	3.0	2.2	3.5	1.8	0.4

Note: Small amounts of PPS, OOO and SLO can also be present

The main difference between cocoa butters from different countries of origin is the ratio of mono-unsaturated (mainly POP, POS and SOS) to di-unsaturated (mainly POO and SOO) triacylglycerols (see Table 2.2). In general, especially Brazilian but also other

South American cocoa butters contain the highest amount of di-unsaturated triacylglycerols (around 15%) while Asian cocoa butters contain the lowest amount of these triacylglycerols (around 5%). African cocoa butters contain intermediate amounts (Chaiseri & Dimick, 1989 and Schlichter-Aronhime & Garti, 1988a). This coincides with the higher amounts of unsaturated fatty acids found in Brazilian cocoa butters (see section 2.3.1).

Lehrian et al. (1980) tried to explain these findings by performing a controlled microclimate temperature study. They focused heat lamps or resistance heaters on selected pods on trees to raise the environmental temperature during the later stages of growth and ripening and observed a clear correlation between growing temperature and degree of unsaturation of the fatty acids. Since Bahia, the main cacao-producing region in Brazil, is farther from the equator than most other cacao growing regions, it shows lower temperatures. The result is cocoa butter with higher amounts of unsaturated fatty acids and di-unsaturated triacylglycerols. Other countries in South America such as Columbia, Ecuador and Peru also have a period when the temperatures are below 20°C at night, resulting in high amounts of unsaturated fatty acids. Average minimum temperatures in West Africa are fairly constant at 20-22°C but the average maximum can fall to 27-29°C in the wet season. In Asia, on the other hand, the maximum temperature is uniform at 30-33°C. This explains the slightly lower amounts of di-unsaturated triacylglycerols in Asian cocoa butters when compared to West African.

In addition to the climate other factors such as the cacao variety can influence the fatty acid and triacylglycerol composition of the cocoa butter (Chaiseri & Dimick, 1989).

2.3.3 Minor components

As well as triacylglycerols, cocoa butter contains some other components in much smaller amounts. These so-called minor components include free fatty acids, mono- and diacylglycerols, phospho- and glycolipids and unsaponifiable matter.

Depending on the study free fatty acid contents differ but are generally between 0.4 and 3%. Most of the obtained values are below the legal limit of 1.75% (see section 2.2.6). Chaiseri & Dimick (1989) found three samples above this limit, originating from Ecuador, Malaysia and Peru, while Shukla (1995) found two samples above the limit, originating from Nigeria and Ivory Coast. These high values can be due to hydrolysis by lipase from mould contamination because of insufficient drying, extended fermentation or prolonged storage of fresh beans (Chaiseri & Dimick, 1989 and Pontillon, 1998a).

Chaiseri & Dimick (1989) concluded that South American, African and Asian cocoa butters were similar in free fatty acid content (mean values of 1.25, 1.27 and 1.44% respectively) but that North and Central American cocoa butters contained significantly lower amounts with an average of 0.79%. The explanation is probably the lower degree of fermentation commonly applied in these regions. As expected, palmitic acid, stearic acid and oleic acid are the major free fatty acids found (Chaiseri & Dimick, 1995a).

Shukla (1995) observed diacylglycerol contents between 1.1 and 2.8% for cocoa butters from different countries of origin, but did not observe any correlation between the amount of diacylglycerols and the production region. Pontillon (1998a) stated a mean value of 1%. Only traces of monoacylglycerols are present (Pontillon, 1998a).

Reported phospholipid levels vary between 0.1-0.2% (Chaiseri & Dimick, 1995a), 0.34% (Arruda & Dimick, 1991), 0.37% (Davis & Dimick, 1989), 0.8-0.9% (Savage & Dimick, 1995) and 0.72-0.94% (Shukla, 1995). Parsons et al. (1969) found values between 0.28 and 0.45% in raw cacao-beans from different countries of origin. They also found a tendency for African beans to have a lower concentration of phospholipids than beans of American origin. The number of samples was, however, too small to allow any definite conclusions. For the amount of glycolipids, Pontillon (1998) reported a value of 0.3% while Chaiseri & Dimick (1995a) reported values between 0.3 and 0.8%.

The amount of unsaponifiable matter depends on the author cited: values range from 0.3 to 1.5% (Schlichter-Aronhime & Garti, 1988a).

2.4 Physical properties

Cocoa butter is a special fat because of its typical physical properties that are, of course, determined by its typical chemical composition. The most remarkable physical characteristic is the narrow melting range, between 32 and 35°C, i.e. just below body temperature. This property is determined by the relatively simple triacylglycerol composition (see section 0) when compared to e.g. milk fat which has a much broader melting range caused by a much broader triacylglycerol distribution. Another special quality of cocoa butter is the quick meltdown in a narrow range of temperatures, which produces a cool sensation and is responsible for the pleasurable release of flavour (Hanneman, 2000 and Schlichter-Aronhime & Garti, 1988a). Due to its relatively

simple chemical composition, cocoa butter is a strongly polymorphous fat. The polymorphism of cocoa butter is discussed in section 2.4.3.

2.4.1 Solid fat content curve

To quantify the physical properties of cocoa butter a chart displaying the solid fat content (SFC) as function of temperature is used.

Figure 2.2 is an idealized example of such a curve.

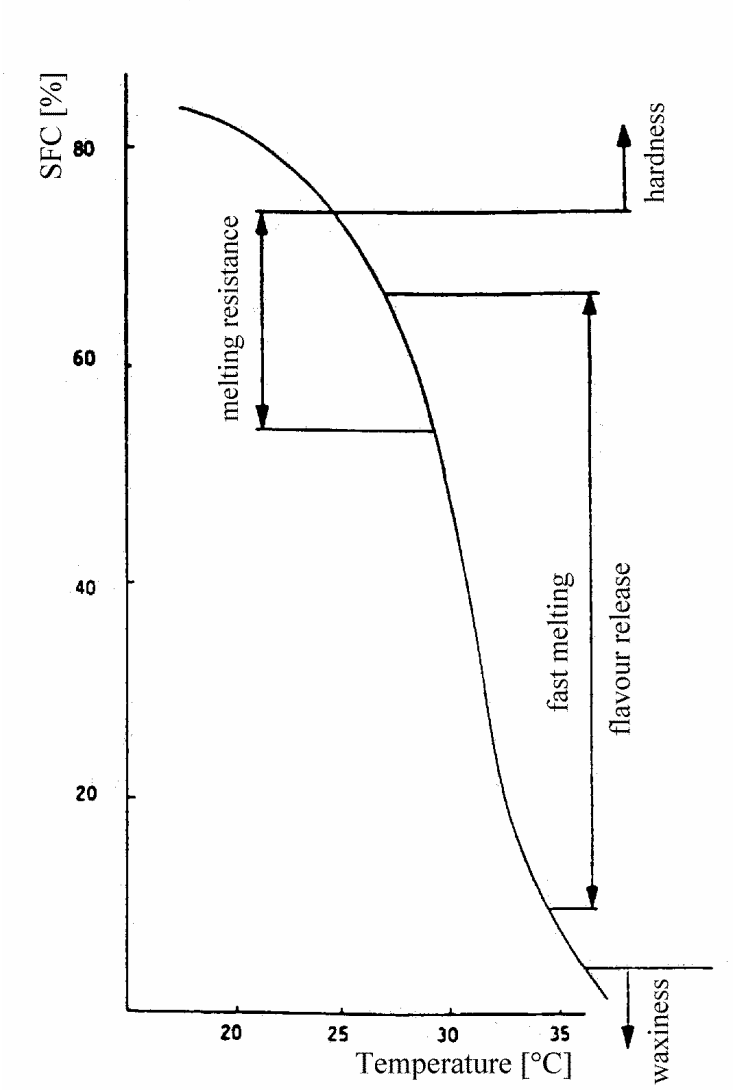

Figure 2.2 Idealized SFC curve of chocolate indicating the importance of the different zones (Klagge & Sen Gupta, 1990)

On inspection the SFC curve gives an indication of the performance of a fat for a given application. The curve can be divided into different zones and each zone is related to a specific property of the chocolate made on the basis of the cocoa butter. In zone 1 (less than 25°C) cocoa butter is hard due to high SFC values. At 25°C, the SFC value should

be at least 75%, or the chocolate will not snap when it is broken but it will bend like rubber. Zone 2 (between 25 and 30°C) gives an indication of the melting resistance of the chocolate, especially at higher environmental temperatures occurring in summer. If at 30°C, the SFC value is lower than 48%, the chocolate will easily melt in summer and will stick to the fingers. In zone 3 (between 25 and 35°C) the cocoa butter melts rapidly, releasing flavours, giving a pleasant fluidity in the mouth and a slight cooling sensation. The absence of a zone 4 (more than 37°C) means that cocoa butter is completely melted at body temperature and there is thus no waxy sensation after eating (Hanneman, 2000 and Klagge & Sen Gupta, 1990).

2.4.2 Influence of country of origin

As the chemical composition of cocoa butter varies slightly with the country of origin of the beans (see section 2.3), so do the physical properties. Generally, Malaysian cocoa butter is hard whereas Brazilian is soft. The hardness of cocoa butter is correlated with its triacylglycerol composition: Malaysian cocoa butter contains low amounts of di-unsaturated triacylglycerols whereas Brazilian contains high amounts (see section 0) (Shukla, 1995).

The SFC curves as described above also have a different course for cocoa butters from different countries of origin. Figure 2.3 shows the SFC curves of Brazilian and Malaysian cocoa butter. Brazilian cocoa butter does not have the necessary solid fat content at 25 and 30°C and thus will not lead to chocolate with the necessary snap and melting resistance.

Chaiseri & Dimick (1995a and 1995b) showed that under the same crystallization conditions (isothermal crystallization at 26.5°C under mild agitation), different cocoa butters nucleate at different rates. Cocoa butters from Malaysia and Ivory Coast show high nucleation rates, whereas cocoa butters from the Dominican Republic and Bahia (Brazil) have distinctively lower nucleation rates. Ghanaian and Ecuadorian samples have intermediate nucleation rates. Variation in the triacylglycerol composition was best correlated with the different crystallization induction times of cocoa butter. The same authors further showed that cocoa butters with high nucleation rates generally have high crystal growth rates and vice versa. Only the crystallization characteristics of the Ecuadorian sample deviate from this general rule in having a rather high nucleation rate but a low growth rate.

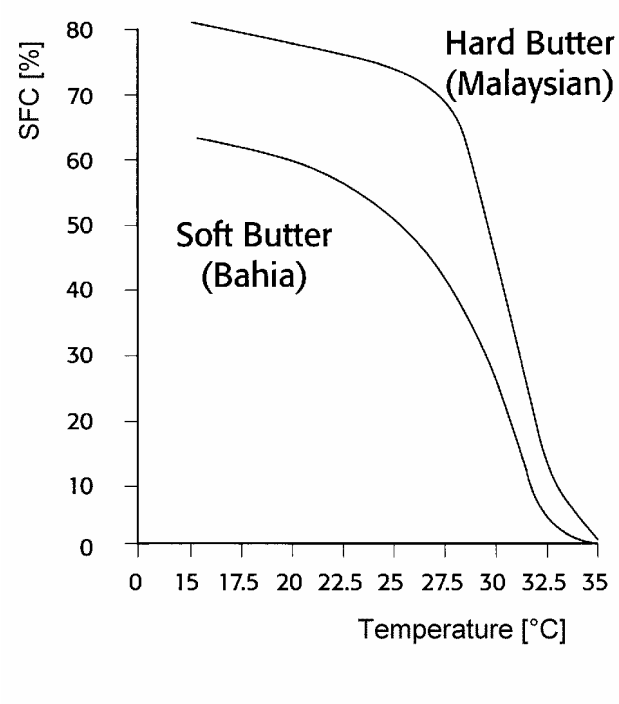

Figure 2.3 SFC curves of soft cocoa butter from Bahia (Brazil) and hard cocoa butter from Malaysia (Hanneman, 2000)

2.4.3 Polymorphism

The multiple melting points of cocoa butter coinciding with the different polymorphs have been recognized for several decades, but there is still controversy about the exact number of polymorphs and their nomenclature (Schlichter-Aronhime & Garti, 1988a). Table 2.3 gives a chronological overview and the following paragraphs give some more details on each of the classifications. Although the classification by Van Malssen et al. (1999) (see section 2.4.3.3) is the most recent and is obtained with the most sophisticated experimental techniques, the classifications with 6 (see section 2.4.3.1) and 4 (see section 2.4.3.2) polymorphs are still used by some research groups.

2.4.3.1 The existence of 6 polymorphs

In 1966 Wille & Lutton examined the polymorphism of a commercial cocoa butter with X-ray diffraction (XRD). They observed six polymorphs and denoted them with Roman numerals from I to VI in order of increasing melting point and stability. Chapman et al. (1971) used the same nomenclature and obtained comparable XRD data for West African cocoa butter. The melting points, however, differ significantly from those obtained by Wille & Lutton (1966). Huyghebaert & Hendrickx (1971) analyzed the polymorphism of twelve samples of cocoa butter of different origin by differential

scanning calorimetry (DSC) and also obtained six polymorphs. Their melting points coincide more or less with those of Chapman et al. (1971).

Table 2.3 Number of cocoa butter polymorphs and their nomenclature

6 polymorphs (Chapman et al., 1971, Huyghebaert & Hendrickx, 1971 and Wille & Lutton, 1966)	**4 polymorphs** (Merken & Vaeck, 1980 and Schlichter-Aronhime et al., 1988b)	**5 polymorphs** (Van Malssen et al., 1999)
I	γ	γ
II	α	α
III	β'	β' range
IV		
V	β	β(V)
VI		β(VI)

Table 2.4 gives an overview of the melting points and XRD data obtained by the different authors. From the long spacings reported in the table it can be deduced that only polymorphs V and VI are packed in pairs of three fatty acid chains (3L packing) (see also section 1.3.4).

The varying melting points in the different studies is probably explicable because in each study a different kind of cocoa butter was used, each butter having its specific chemical composition which influences the melting point.

Polymorph I is obtained when melted cocoa butter is crystallized at 0°C or lower (Wille & Lutton, 1966). Chapman et al. (1971) stated that it is difficult to determine whether such a rapid cooling of the melt produces a pure polymorph I or a mixture of polymorphs I and II. A DSC melting curve of the produced solid always shows a mixture, but it is possible that polymorph II is generated during heating. Moreover, Huyghebaert & Hendrickx (1971) always obtained a melting curve with two peaks.

Polymorph II is obtained when melted cocoa butter is quickly cooled to 0°C and stored for several minutes to an hour at this temperature. Attempts to crystallize polymorph II directly from the melt at temperatures ranging from 5 to 18°C invariably gave rise to higher melting polymorphs. Therefore, preparation of II appeared to require initial

Table 2.4 Overview of melting points and X-ray diffraction data (short spacings (SS) and long spacings (LS)) of the 6 polymorphs of cocoa butter as obtained by different authors

Polymorph	Wille & Lutton (1966)		Chapman et al. (1971)		Huyghebaert & Hendrickx (1971)
	Melting point [°C] [1]	SS and LS [Å]	Melting point [°C] [2]	SS and LS [Å]	Melting point [°C] [3]
I	17.3	3.70 and 4.19 (SS)		4.17 and 3.87 (SS) 54 (LS)	14.9
II	23.3	4.24 (SS) 49 (LS)		4.20 (SS) 51 (LS)	16.2-17.8
III	25.5	4.25 and 3.86 (SS) 49 (LS)		4.20 and 3.87 (SS) 51 (LS)	20.8-23.6
IV	27.5	4.15 and 4.35 (SS) 45 (LS)	25.6	4.32 and 4.13 (SS) 49 (LS)	23.7-25.8
V	33.8	4.58 and 3.98 (SS) 63.1 (LS)	30.8	4.58, 3.98 and 3.65 (SS) 66 (LS)	30.5-32
VI	36.3	4.59 and 3.70 (SS) 63.1 (LS)	32.3	4.53 and 3.67 (SS) 63 (LS)	32-35

[1] upper melting limit as determined by capillary method

[2] upper melting limit as determined from disappearance of diffraction lines

[3] peak maximum obtained by DSC at a heating rate of 4°C /min

formation of I and subsequent transition to II (Wille & Lutton, 1966). However, Chapman et al. (1971) obtained polymorph II directly from the melt by cooling at 2°C min^{-1}.

Polymorph III is obtained by crystallization of the melt at 5 to 10°C or by transition of polymorph II during storage at comparable temperatures (Wille & Lutton, 1966).

Polymorph IV is obtained by crystallization of the melt at 16 to 21°C or by transition of a lower melting polymorph during storage at the same temperatures (Wille & Lutton, 1966).

Polymorph V can be obtained directly from the melt after storage at room temperature for one week, by transition of lower melting polymorphs or by crystallization from solvents (Huyghebaert & Hendrickx, 1971 and Wille & Lutton, 1966).

Polymorph VI has never been obtained directly from the melt but only by transition of polymorph V. This transition occurs very slowly in comparison to other transitions; at room temperature it takes up to 4 months.

Figure 2.4 gives a schematic overview of the possible transitions (crystallization, melting and polymorphic transition) of cocoa butter according to Chapman et al. (1971).

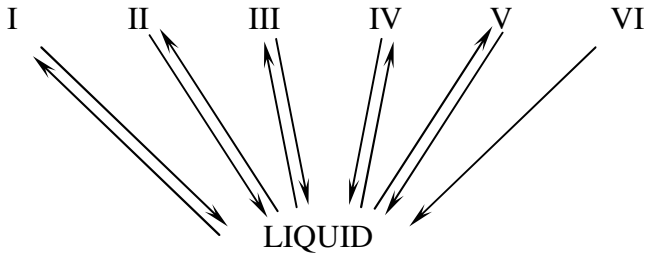

Figure 2.4 Possible transformations of cocoa butter according to Chapman et al. (1971)

2.4.3.2 The existence of 4 polymorphs

Merken & Vaeck (1980) re-investigated the polymorphism of cocoa butter with DSC. They rapidly (20°C min^{-1}) cooled a sample of commercial press cocoa butter to –30°C and heated it at rates varying between 0.31 and 40°C min^{-1}. At high heating rates they observed two peaks representing the γ and α polymorph. As the heating rate decreases the γ peak becomes smaller, the α peak becomes more pronounced and the peak temperatures decrease. The latter phenomenon can be explained by a decreasing effect of thermal lag. The peak temperatures do not decrease any longer from 10°C min^{-1} onwards showing that, from this heating rate, the thermal lag effect is negligible. From

2.5°C min^{-1} a third peak corresponding to the β' polymorph (peak maximum 23.2°C) is visible. At 0.62°C min^{-1} three peaks are visible which can be attributed to the polymorphs α (peak maximum 19.2°C), β' (peak maximum 24.5°C) and β (peak maximum at 30.9°C). At 0.31°C min^{-1} the β' peak splits into two peaks with maxima at 22°C and 25°C, which at first sight confirms the existence of two polymorphs, III and IV. This however is thermodynamically impossible since then a more stable polymorph with a higher melting point is formed from a less stable polymorph with a lower melting point. From this, the authors concluded that polymorph III of Wille & Lutton (1966) is not a separate polymorph but a mixture of polymorphs II and IV. They explained the separation of the β' peak by a strong development of the β polymorph from less stable polymorphs. This polymorphic transition is exothermic and interferes with the endothermic melting of the β' form giving the illusion that two peaks are formed.

Schlichter-Aronhime et al. (1988b) crystallized commercial cocoa butter at rates ranging from 0.02 to 0.3°C min^{-1} and heated the samples at a constant rate of 5°C min^{-1}. The peak maxima of the melting curves increase, as the crystallization rate is slower. They gradually change between those of polymorphs II and IV previously reported without corresponding to any of them. This supports the statement of Merken & Vaeck (1980) that polymorph III is a mixture of II and IV.

Merken & Vaeck (1980) and Schlichter-Aronhime et al. (1988b) also claimed that polymorph VI is not a distinct polymorph but is identical with form V but lacking the liquid triacylglycerols fraction. Their claim was based on the following observations. When keeping the cocoa butter melt at 32°C in the presence of solid germs for a long enough period, it is possible to obtain crystals with a melting point of 45°C and a composition different from that of the melt. This demonstrates that a fraction richer in high-melting triacylglycerols can crystallize under proper conditions. In another laboratory cocoa butter was crystallized at temperatures from 26 to 33°C and it was demonstrated that the proportion of SOS in the crystals and the melting point of the crystals formed at higher temperatures increase. Polymorph VI of cocoa butter is thus in reality a modification of polymorph V after the segregation of a liquid portion. Consequently the V to VI transition is not associated with polymorphism, since the latter is considered only when different crystalline forms exist, all belonging to the same chemical composition.

2.4.3.3 The existence of 5 polymorphs

Van Malssen et al. (1999) studied the polymorphism of cocoa butter from Cameroon by means of real-time XRD measurements. They crystallized cocoa butter isothermally at temperatures ranging from -20 to 40°C.

The γ polymorph is by far the least stable. It only stays unchanged for at least 10 days at temperatures lower than –10°C. It melts between –8 and 5°C. The α polymorph is formed easily either via a transition from the unstable γ polymorph or directly from the melt. The ease of this formation was emphasized by the observation that some α is formed before the start of γ formation even when the liquid cocoa butter is cooled at a rate of 360°C min^{-1}. The α phase melts between 17 and 22.5°C, is much more stable than γ but not stable enough to prevent its transition to β' within an hour or less at temperatures above 6°C.

There are various reasons to consider β' cocoa butter as a phase range rather than as separate (sub) phases: (i) seven different and apparently continuously varying β' XRD-patterns have been observed, (ii) melting ranges investigated at four points of the β' range show different melting characteristics (the melting starting point ranges from 19.6 to 24.2°C and the melting end point varies between 26.7 and 29°C), (iii) using DSC, Schlichter-Aronhime et al. (1988b) found more melting peaks for β' phases than the two corresponding with Wille & Lutton's polymorphs III and IV and (iv) there is a wide variety in β' melting points in literature. The physical basis of a β' phase range depends on cocoa butter being a mixture of triacylglycerols and solid cocoa butter existing as a conglomerate of crystallites with an individual triacylglycerol composition. Different cooling rates or crystallization temperatures will result in a different distribution of such crystallites and in a different distribution of individual melting and diffraction characteristics. This results in a different overall melting behaviour and diffraction pattern.

Two β polymorphs (melting ranges 28-32.5°C and 29-33.7°C) were observed with XRD patterns corresponding with polymorphs V and VI of Wille & Lutton (1966). Static crystallization of these two β phases, β(V) and β(VI) is only possible via a phase transition from the β' polymorph. Direct β crystallization only occurs when the liquid is not memory-free. It is, however, remarkable that not only β(V) but also β(VI) can be directly formed from β'.

All possible phase transitions (melting, crystallization and polymorphic transitions under isothermal and non-isothermal conditions) are summarized in the phase transition scheme in Figure 2.5. The phase transitions under non-isothermal conditions are known from literature and additional experiments.

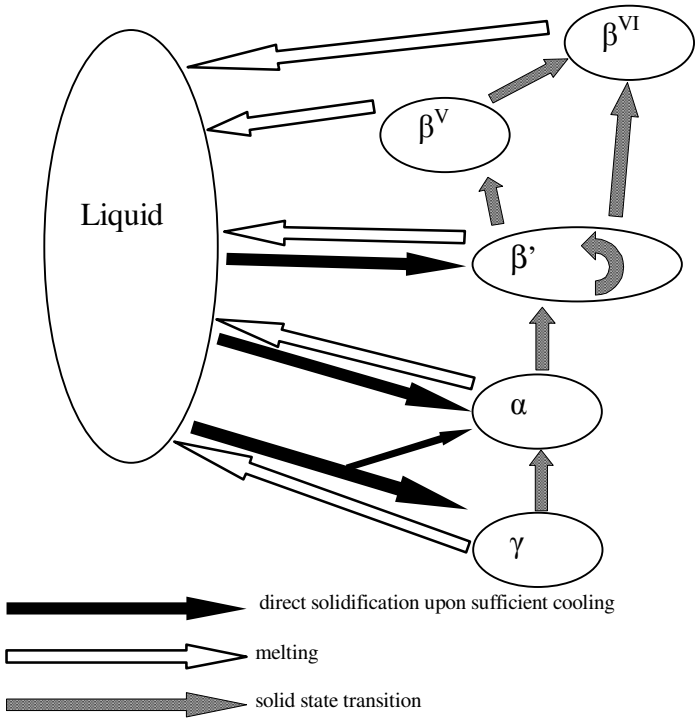

Figure 2.5 Cocoa butter phase transition scheme as proposed by Van Malssen et al. (1999)

2.5 Use of cocoa butter

Cocoa butter is used on a very small scale in the pharmaceutical industry for the preparation of suppositories and in the cosmetics industry for the preparation of lipstick and body lotions. Some decennia ago cocoa butter was used quite a lot for the production of cosmetics, but now it has mostly been replaced by synthetic products (Pontillon, 1998b).

The most important use of cocoa butter is, of course, the preparation of chocolate. The following sections describe the ingredients and the different steps in the manufacturing of chocolate.

2.5.1 Chocolate ingredients

Table 2.5 shows an example recipe for the preparation of milk and dark chocolate. It has to be stressed, however, that the ingredients and the proportions in which they are used can vary considerably.

Table 2.5 Typical recipe for milk and dark chocolate (Jackson, 1994)

	Milk chocolate	**Dark chocolate**
Cocoa mass [%]	10-14	35-43
Whole milk powder [%][1]	18-24	
Sugar [%]	46-55	48-50
Cocoa butter [%]	16-20	7-14
Lecithin [%]	0.35-0.4	0.3-0.35

[1] Whole milk powder is sometimes substituted with skimmed milk powder and butter oil

2.5.2 Mixing and grinding (Beckett, 1994)

The sugar, in a granulated or milled form, the cocoa butter and the milk powder (in the manufacturing of milk chocolate) are added to the cocoa mass. The ingredients are mixed and form a paste, which then can be passed through a five-roll refiner in order to make the particles small enough so that they are not detectable on the tongue. The actual size depends on the type of chocolate and the market where it is sold, but in general the vast majority of particles should be smaller than 40 μm.

2.5.3 Conching (De Ginestel, 1998a and Ley, 1994)

The grinded chocolate mass is then transferred to a conche. This is a robust mixing device with two or more axes and equipped with paddles or agitators. The design details depend on the constructor.

The main aims of the conching process are the development of the full desirable chocolate flavour and the conversion of the powdery, crumbly product into a flowable suspension of sugar, cocoa and milk powder particles in a liquid phase of cocoa butter.

To achieve these aims the conching process consists of two phases: the dry phase and the liquid phase (Figure 2.6). During dry conching the exerted shear forces lead to an increase of the temperature, controlled by a cooling circuit. The temperature at which the chocolate mass is conched will affect its rheology and organoleptic characteristics. In general, the temperature is kept under 80°C. During dry conching, the chocolate mass

loses part of its moisture and volatile components. As the conching progresses the viscosity is reduced and the flow properties improve. This is due to the reduced moisture content and the coating of cocoa butter across the surfaces of the particles.

During liquid conching, some cocoa butter is added first to facilitate the temperature decrease to approximately 60°C. At this temperature lecithin can be added. Considering the price difference between cocoa butter and lecithin, it is economically favourable to limit the amount of cocoa butter to the marginal amount necessary to obtain the desired rheological characteristics. European legislation allows chocolate to contain a maximum of 0.5 weight% of phosphatides. Bearing in mind that commercial lecithin contains approximately 60% of phosphatides, the allowed amount of lecithin is 0.8%. During further liquid conching, the ingredients are further homogenized by intense stirring and shearing.

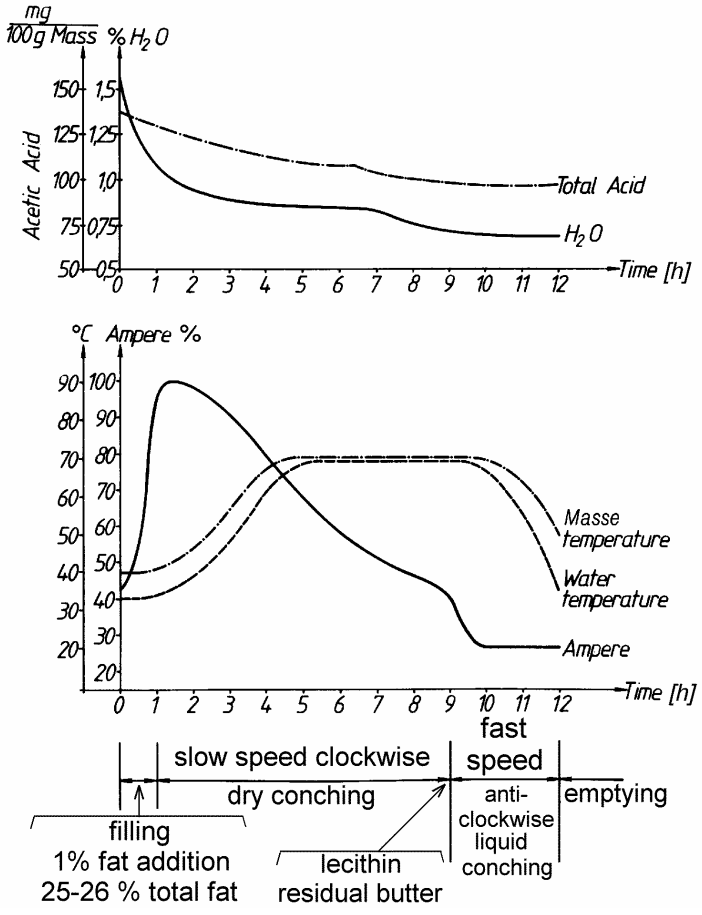

Figure 2.6 Machine operating conditions and changes in moisture and acidity during a conche cycle (Ley, 1994)

It is important to stress that conching should not be studied in isolation when investigating the development of chocolate flavour. Processes that have been initiated

during fermentation and roasting are being completed in the conche. As moisture is removed in the dry conching phase it takes with it many undesired flavour components (e.g. acetic acid and low-boiling aldehydes). The partial removal of these components is necessary to give the finished chocolate a full 'rounded' flavour. Furthermore a significant formation of free amino acids takes place during conching. Together with reducing sugars these free amino acids are the flavour precursors the variety of flavours develop from during heating by means of Maillard reactions. It has been proved that the shearing stress in the conche positively influences and accelerates the flavour development processes. This is probably due to the interactions occurring when the solid particles are forced against one another, in particular the sugar particles.

It cannot be overstressed however that the chemical and physical processes occur together during the traditional conching process and cannot be totally separated.

2.5.4 **Tempering** (Lopez et al., 1998 and Talbot, 1994b)

Before chocolate can be satisfactorily processed from liquid to solid, it must be tempered. This is a technique of controlled crystallization under shear necessary to induce a sufficient number of seed crystals in polymorph V (β polymorph). These are necessary to encourage the total fat phase to crystallize in this stable polymorph (see section 2.4.3 for details on the polymorphism of cocoa butter). Crystallization in the stable form V is needed because: (i) unstable polymorphs will undergo a polymorphic transition to more stable polymorphs during the shelf life of the chocolate leading to the development of chocolate fat bloom, (ii) the melting range of the unstable polymorphs is lower than the polymorph V melting range and that is why the chocolate will not have the desirable melting properties (see section 2.4) and (iii) unstable polymorphs will not shrink when cooling and thus will not easily demould.

The most commonly used tempering method consists of four steps. First, the chocolate is heated to approximately 50°C to ensure complete melting and then the melted chocolate is cooled. At first only sensible heat is removed but after some time the chocolate starts to crystallize in both stable and unstable polymorphs. At last the crystals in the unstable polymorph are melted off by raising the temperature. An example of a tempering sequence for milk chocolate is shown in Figure 2.7. Temperatures for dark chocolate are generally 2 to 3°C higher than those indicated for milk chocolate. However, precise temperatures vary depending on recipe, tempering equipment and even the purpose the chocolate will be used for.

In earlier times tempering was carried out by pouring the chocolate onto a marble slab and working it with a flexible spatula until it began to thicken. At this point both stable and unstable polymorphs were crystallized and the thick mush was mixed into a bowl of warm chocolate to melt off the unstable crystals. Although this method is still used by confectioners producing very small quantities of hand-made confections, many different tempering methods have been developed over the years and continuous automatic tempering units are now widely used. These are usually multi-stage heat exchangers.

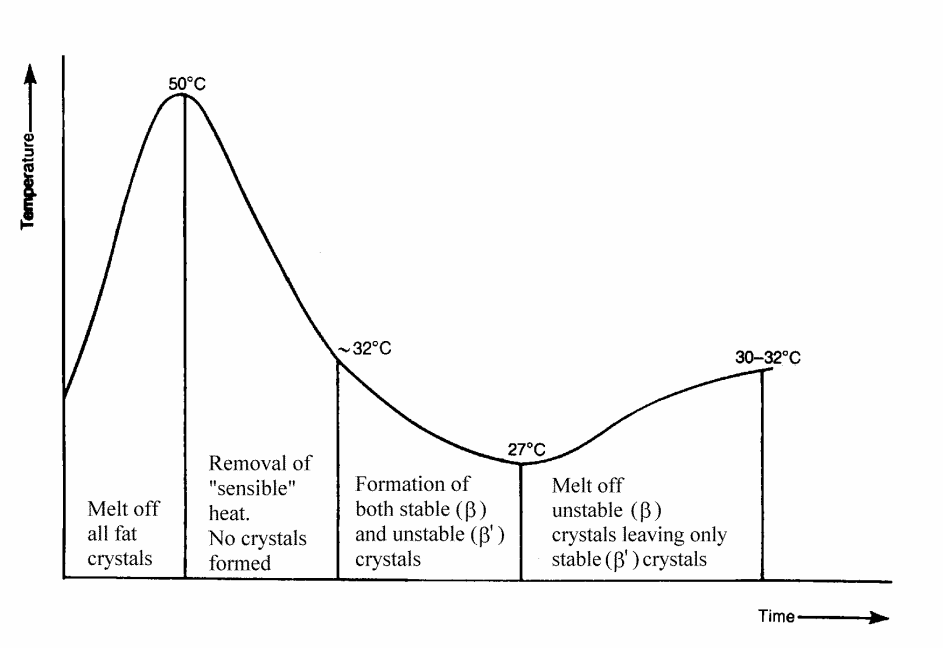

Figure 2.7 Milk chocolate tempering sequence (Talbot, 1994b)

2.5.5 **Enrobing or moulding and cooling** (Nelson, 1994)

When enrobing the chocolate is poured over some inner confection or other and before cooling any excess chocolate is removed by shaking or blowing. When moulding chocolate is poured into a mould where at least part of the chocolate is allowed to crystallize.

Although chocolate will crystallize at room temperature, it will not do so at the rate required by an industrial manufacturer. A series of cooling tunnels using a combination of conduction, convection and radiation are normally used. The cooling rate depends on tempering, chocolate type and thickness and largely determines the quality. To cool and crystallize chocolate properly it should first be allowed to cool gently.

2.6 Cocoa butter alternatives

In addition to cocoa butter, other vegetable fats, the so-called cocoa butter alternatives (CBAs), can also be used in chocolate and coatings. According to the nomenclature of Lipp & Anklam (1998), the CBAs can be subdivided into:

(i) cocoa butter equivalents (CBEs): non-lauric fats similar in their physical and chemical properties to cocoa butter and compatible with it in every amount without altering the properties of the cocoa butter;

(ii) cocoa butter substitutes (CBSs): lauric fats, chemically totally different from cocoa butter but with some physical similarities, almost not compatible with cocoa butter and consequently only suited to substitute cocoa butter for 100%;

(iii) cocoa butter replacers (CBRs): non-lauric fats with a fatty acid distribution similar to cocoa butter, but with a completely different triacylglycerol composition and therefore only compatible with cocoa butter in small ratios.

It has to be said that the nomenclature in this area is often confusing and that other authors may use another convention for subdividing the CBAs.

2.6.1 Cocoa butter equivalents

2.6.1.1 Legislation

The 2000 directive of the European Community concerning cocoa- and chocolate products (EG, 2000) allows the addition of 5% other vegetable fats than cocoa butter to chocolate if it is clearly indicated on the label. These vegetable fats, separate or in mixtures are cocoa butter equivalents and must meet the following criteria: (i) non-lauric vegetable fats, rich in symmetrical mono-unsaturated triacylglycerols of the type POP, POS and SOS, (ii) miscible with cocoa butter in every ratio and compatible with the physical properties of cocoa butter (melting point, crystallization temperature, melting rate, necessity of tempering) and (iii) obtained by refining and / or fractionation; enzymatic changes of the triacylglycerol composition are not allowed. According to these criteria the following vegetable fats are allowed: illipe, sal, shea, palm oil, kokum and mango kernel. More information about these fats is given hereafter.

2.6.1.2 Raw materials (Storgaard, 2000)

Illipe, also called Borneo tallow is obtained from the seed kernels of *Shorea stenoptera*, a wild crop in the jungle of South East Asia. The kernel contains between 40 and 70% fat. Illipe comes closest to matching cocoa butter in triacylglycerol composition, as it contains 86% of symmetrical mono-unsaturated triacylglycerols. Before it can be used as a CBE ingredient in chocolate, it generally undergoes only refining but no fractionation.

Sal fat is obtained from the kernels of the sal tree, *Shorea robusta*, a wild tree growing in India. The sal seed contains up to 18.5% of a greenish-brown hard fat with a characteristic odour and containing about 56% of symmetrical mono-unsaturated triacylglycerols. Before this fat can be used as a CBE ingredient in chocolate, it is generally refined and fractionated.

Shea butter (beurre de karité) is obtained from the seeds of a tree, *Butyrospermum parkii*, which grows in the wild in the African bush. As the trees grow in great numbers, there is a high potential of shea nuts but they are not frequently collected, because the trees are too far away from the villages. Because of its very slow growth and since it only provides a reasonable crop yield after many years, the tree is not commercially cultivated in plantations. The dry kernel contains between 40 and 60% fat on average. The fat contains approximately 39% of symmetrical mono-unsaturated triacylglycerols. Before it is used as a CBE ingredient, shea butter is usually refined and fractionated. Most often only the stearin fraction is used.

Palm oil is obtained from the reddish-yellow fruit flesh of the oil palm. It is the only raw material that is cultivated and produced industrially and commercially on a very large scale on plantations. Oil palms are mainly cultivated on big plantations in South East Asia, mainly in Malaysia and Indonesia. A fresh palm bunch contains about 20% palm oil, having about 38% of symmetrical mono-unsaturated triacylglycerols. Before palm oil is used as a CBE ingredient, it is refined and fractionated. The mid-fraction is mostly used for the preparation of a CBE.

Kokum butter is obtained from the fruit kernel of *Garcinia indica*, a tree in the savannah areas of the Indian subcontinent. The kokum kernel contains approximately 45% fat. This fat becomes appropriate for use in chocolate after refining (without fractionation). The obtainable yearly quantity of 300 to 800 tons is very low, so kokum fat is the least interesting raw material from a commercial point of view.

Mango butter is obtained from deshelled fruit kernels of the mango tree, *Magnifera indica*, native to sub-continental India and the tropics. The mango kernel contains 7 to 11% of a greyish-white fat. In order to become a CBE ingredient, this fat is refined and fractionated.

2.6.1.3 Commercial blends (Storgaard, 2000 and Talbot, 1994b)

None of the six raw materials discussed in section 2.6.1.2 alone can substitute cocoa butter. This is only possible by a combination of raw materials and their fractions. For example, by blending fractions of palm oil and shea butter with illipe butter, a typical West African cocoa butter can be matched closely. A blend of fractionated sal fat with the middle-melting fraction of palm oil is used to produce a CBE for tropical use.

2.6.1.4 Cocoa butter improvers (Lipp & Anklam, 1998)

It is also possible to produce a hard CBE that is able to improve the hardness of some of the softer qualities of cocoa butter. Such CBEs are known as cocoa butter improvers (CBIs). They have higher amounts of solid triacylglycerols than cocoa butter.

2.6.2 Cocoa butter substitutes (Talbot, 1994b)

Cocoa butter substitutes (CBSs) are fully refined fats produced from palm kernel and / or coconut oil by means of fractionation and hydrogenation. In this way fats can be produced with characteristics similar to those of cocoa butter in terms of hardness, mouth feel and flavour release. These fats, however, contain a high level of lauric fatty acids and have a completely different triacylglycerol composition compared to cocoa butter. The result is a considerable degree of incompatibility between CBSs and cocoa butter. About 5% cocoa butter is the safe maximum level of addition to CBSs. In practice this limits the added cocoa in recipes based on CBSs to low-fat cocoa powder or fat-free cocoa powder rather than cocoa mass. Usually no tempering is required in the production of CBS-based coatings.

2.6.3 Cocoa butter replacers (Talbot, 1994b)

Cocoa butter replacers (CBRs) are produced from non-lauric oils such as palm oil and soybean oil by hydrogenation and fractionation. Although these CBRs contain palmitic, stearic and oleic acid, their arrangement within the triacylglycerols is more random than in cocoa butter. In addition, a high content of trans fatty acids is present. Consequently, CBRs have a limited compatibility with cocoa butter. A maximum percentage of CBR may be added to cocoa butter (cocoa butter extender application) and a certain

maximum percentage of cocoa butter may be added to the fat phase of CBR-based coatings. CBRs have a greater tolerance to cocoa butter than the CBSs. In practical terms this means that cocoa mass can be used with CBRs resulting in a much more 'rounded' cocoa flavour than with CBSs where only low-fat cocoa powder is permissible. The production of these CBR-based coatings is similar to normal chocolate production but no tempering is required.

2.7 Conclusions

Due to its relatively simple chemical composition, cocoa butter is a strongly polymorphous fat. This polymorphism has a large impact on the product quality of chocolate and confectionaries. Knowledge of the polymorphs formed as a function of time and temperature is therefore of utmost importance not only to optimize production processes and to maintain product quality but also to explain some of the attributes of the crystallization kinetics. The chemical composition of cocoa butter can also vary slightly depending on the growing conditions and the age of the tree on the one hand, and on the production process of the cocoa butter from the cacao-beans and any refining of the cocoa butter on the other hand. These slight differences in chemical composition also lead to small differences in the physical properties, such as the crystallization kinetics.

3 DEVELOPMENT OF A DIFFERENTIAL SCANNING CALORIMETRY METHOD TO STUDY THE ISOTHERMAL CRYSTALLIZATION KINETICS OF COCOA BUTTER

3.1 Introduction

3.1.1 Principles of differential scanning calorimetry (DSC) and recent developments

Differential scanning calorimetry (DSC) is the most widely used of all thermal analysis techniques. It is a technique in which the difference in energy input into a sample and a reference material is measured as function of time or temperature while the sample and the reference material are subjected to a controlled time-temperature program. So it provides qualitative and quantitative information regarding transitions in materials that involve endothermic or exothermic processes or changes in heat capacity (Ladbrooke & Chapman, 1969).

Two types of DSC systems can be distinguished depending on the method of measurement used: power-compensation DSC and heat-flux DSC. In power-compensation DSC the sample and reference temperatures are controlled independently using separate (identical) ovens. The temperature difference between the sample and the reference is maintained to zero by varying the energy input into the two ovens. This type of DSC thus directly measures the energy flow to and from the sample and therefore the heat absorbed or released by the sample as it is subjected to a specific time-temperature program (Nicula, 2002).

In heat-flux DSC the sample and the reference material are enclosed in the same oven together with a metallic block (constantan disc) with high thermal conductivity that ensures a good heat flow between sample and reference. Figure 3.1 shows a cross-sectional diagram of a DSC-cell of the heat-flux type. The sample and the reference material are placed in pans sitting on raised platforms on the constantan disc. Heat is transferred through the disc and up into the sample and reference via the sample pans.

The differential heat flow to the sample and reference is monitored by chromel-constantan thermocouples, formed by the junction of the constantan and a chromel disc which covers the bottom of each platform. The ΔT output from these sample and reference thermocouples is fed to a variable high-gain amplifier where the signal is amplified, electronically scaled to read directly in heat flow units and finally displayed on one Y-axis (Ma & Harwalkar, 1991).

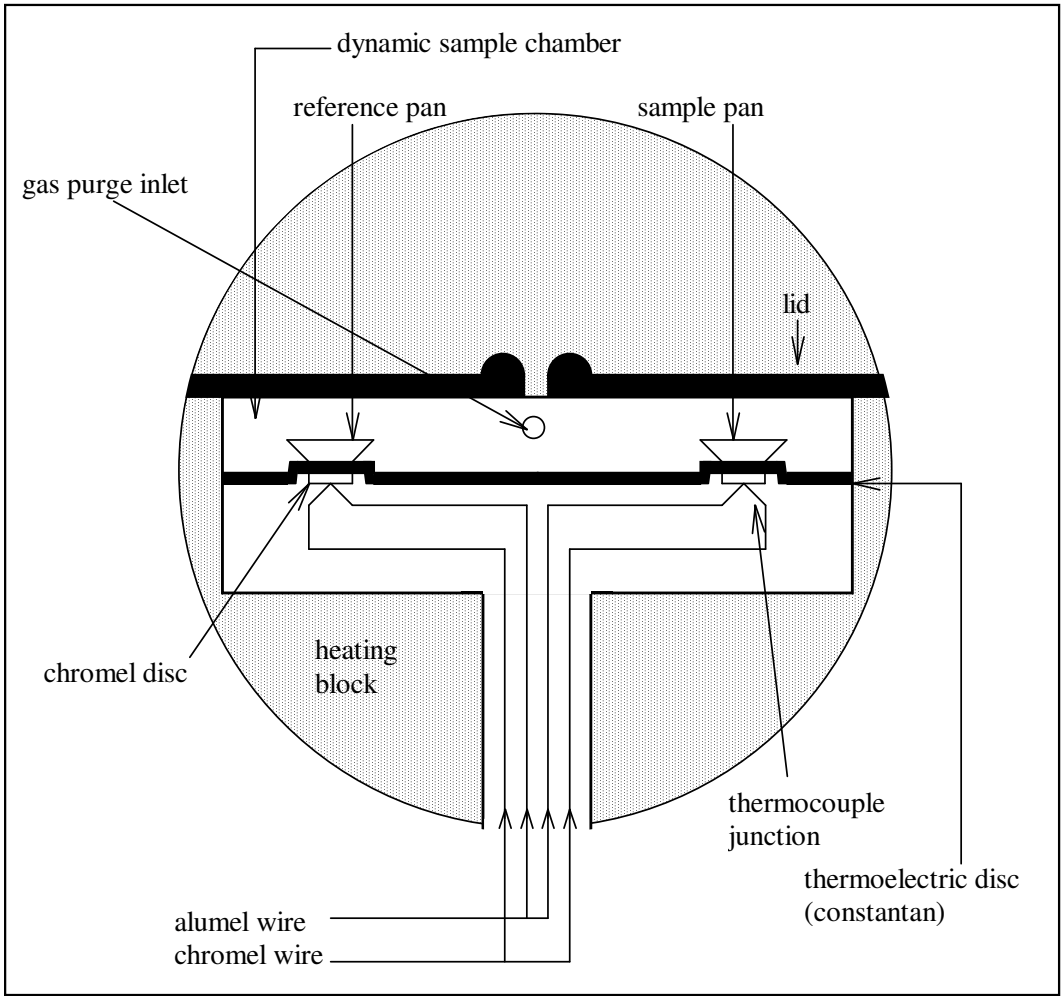

Figure 3.1 Cross sectional diagram of a DSC-cell of the heat-flux type (after Ma & Harwalkar, 1991)

The resultant heat flow between the sample and the reference in a DSC experiment is described by the general equation:

$$\frac{dQ}{dt} = C_p \times \frac{dT_K}{dt} + f(T,t) \qquad \textbf{[3.1]}$$

in which dQ/dt [W g^{-1}] is the heat flow, C_p [J g^{-1} K^{-1}] the heat capacity, dT_K/dt [K s^{-1}] the rate of change of the temperature and $f(T,t)$ [W g^{-1}] the heat flow from kinetic processes (Verdonck et al., 1999).

The main disadvantage of conventional DSC is that it is often difficult to interpret the heat flow from a DSC experiment, if multiple processes are involved. Modulated Temperature DSC (MTDSC) may help to overcome this limitation. In MTDSC a sinusoidal modulation is overlaid on the imposed time-temperature program. Consequently, the resultant heat flow, also termed the modulated heat flow, also varies periodically. In conventional DSC, only the sum of the two components in equation [3.1] is determined and is called the total heat flow. In MTDSC, the total heat flow and the two individual components can be distinguished as the heat capacity component or reversing heat flow and the kinetic component or non-reversing heat flow. The total heat flow is calculated from the average of the modulated heat flow. The heat capacity is calculated from the ratio of the modulated heat flow amplitude to the modulated heating rate amplitude by discrete Fourier transformation. Then the reversing heat flow is calculated by multiplication of C_p with the temperature change. The kinetic component or non-reversing heat flow is the arithmetic difference between the total heat flow and the reversing heat flow. In some cases overlapping processes can be distinguished with MTDSC since they are split in the reversing and the non-reversing heat flow. Additional advantages of MTDSC are its ability to detect subtle transitions more readily and without loss of resolution and its ability to measure the heat capacity in quasi-isothermal conditions (Verdonck et al., 1999).

Recently a new technology for measuring heat flow has been developed. This Tzero™ technology arises from a totally new DSC sensor design and heat flow measurement principal. The heat flow is now based on a four-term equation, including the conventional DSC signal and terms accounting for imbalances in thermal resistance, heat capacity and heating rate between the sample and the reference side of the sensor. This new technology allows a truer measurement of the sample heat flow than conventional DSC and results in a highly improved baseline and better resolution. The extra terms in the equation can be calculated by measuring the base temperature and the difference between the sample and the base temperature. The advanced Tzero™ heat flow model is yet another extension accounting for the effect of different heating rates between sample and reference pan (Tzero™ DSC Technology, 2001).

3.1.2 Use of DSC to study isothermal crystallization kinetics of fats

DSC has already been used in the past to study the isothermal crystallization kinetics of cocoa butter (Kerti, 1998, Metin & Hartel, 1998 and Ziegleder, 1990) and other natural fats (Dibildox-Alvarado & Toro-Vazquez, 1997, Kawamura, 1979 and Toro-Vazquez et al., 2000).

To transform the DSC crystallization peak into a crystallization curve representing the amount of heat released as function of time, the DSC peak area has to be integrated. The amount of heat released at a given time t [h], $\Delta H_{ts\text{-}t}$ [J g^{-1}], is calculated by taking the area enclosed by a baseline and the peak between t_s (the starting-point of crystallization) and t. The relative amount of heat released at time t is calculated by taking the ratio of $\Delta H_{ts\text{-}t}$ and the total heat of crystallization (ΔH [J g^{-1}]), the latter being the integration of the peak between t_s and t_e (the end point of crystallization). Figure 3.2 illustrates this procedure. Obviously, an important element is the determination of t_s and t_e. Toro-Vazquez et al. (2000) mentioned that t_s is calculated as the time from the start of the isothermal process to the beginning of crystallization (i.e. the time where the heat capacity of the sample has a significant departure from the baseline) using their DSC software library. However, the authors did not clarify the t_e determination. Kerti (2000) and Ziegleder (1990) showed a figure in which t_s and t_e are depicted. However, in these reports, as well as in other articles, the procedure for the actual calculation of t_s and t_e was not mentioned. It can be suspected this was done visually, a rather subjective method as is shown in section 3.4.1.1.

The aim of this part of the research was to reduce the variability on the data obtained from isothermal crystallization experiments with cocoa butter monitored by means of DSC. This chapter presents an objective calculation algorithm for the determination of t_s and t_e in the integration procedure eliminating the variability caused by the operator. Further, the time-temperature combination needed to eliminate all crystal nuclei prior to crystallization and the influence of the cooling rate to the isothermal crystallization temperature were investigated. Finally, the possible influence of the sample preparation procedure was studied.

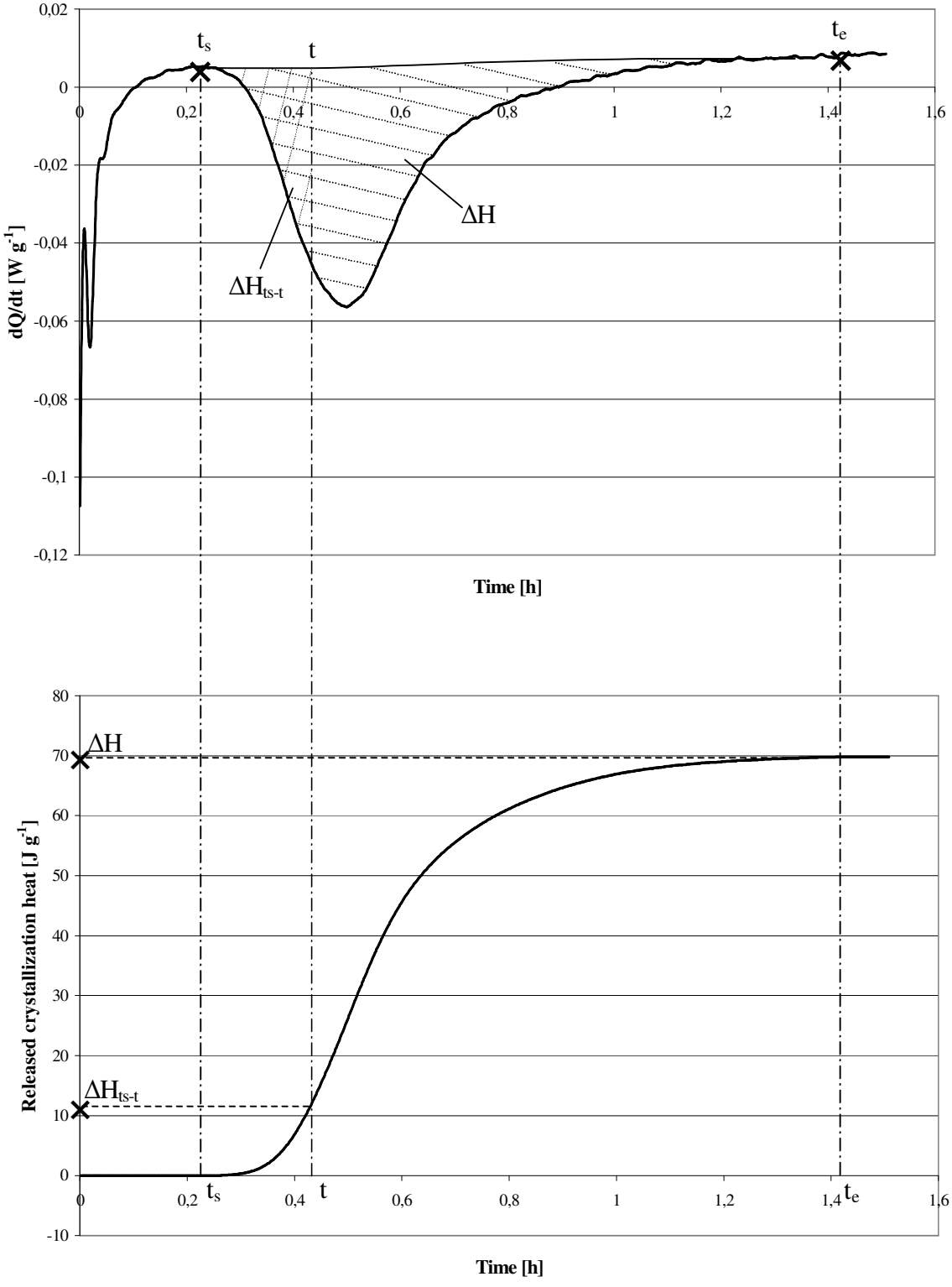

Figure 3.2 Integration of DSC crystallization peaks

3.2 Research strategy

First it was checked whether a visual determination of the integration limits (t_s and t_e) is indeed subjective, i.e. whether the limits are different when the same operator performs the integration several times and when different operators perform the integration. The variability introduced by a visual determination of the integration limits was compared with the sample variability. To be able to eliminate the former variability, a calculation algorithm allowing an objective determination of the integration limits was developed. The applicability of this algorithm was checked for crystallization data of different samples of cocoa butter at different crystallization temperatures (19-23°C). The integration limits obtained by a visual and an algorithmic determination were compared.

To investigate the influence of the cooling rate to the isothermal crystallization temperature the cocoa butter was cooled at 1, 5 and 8°C min^{-1}. To check the time-temperature combination needed to eliminate any memory effect due to remaining crystals (i.e. the necessary melting protocol), three different combinations were compared: 65°C for 15 min as proposed by Ziegleder (1990), 65°C for 30 min to check the influence of a longer holding time at the same temperature and 80°C for 15 min to check the effect of a higher temperature for the same holding time. Three repetitions were performed for each melting protocol. The potential influence on the following isothermal crystallization at 17.2°C was investigated by fitting the Avrami model to the data series and comparing the parameters obtained.

To check the influence of the sample preparation procedure, two different procedures (A and B) were used and it was checked whether the Avrami parameters of the following isothermal crystallization at 17.2°C differ significantly. Two repetitions of procedure A and three repetitions of procedure B were performed for each melting protocol.

3.3 Materials and methods

3.3.1 Cocoa butter

The cocoa butter used to study the influence of cooling rate, melting protocol and sample preparation procedure was a standard factory product (batch 1) supplied by Barry Callebaut (Wieze, Belgium). For testing the applicability of the calculation algorithm crystallization data of different samples of cocoa butter were used.

3.3.2 Sample preparation procedure

To study the influence of the sample preparation procedure on the isothermal crystallization kinetics of cocoa butter, two different preparation procedures (A and B) were used.

3.3.2.1 Sample preparation procedure A

(i) cocoa butter was taken from the cooling chamber (4°C), a sample (approximately 10-20 g) was taken with a knife and spoon cleaned with ethanol (Chem-Lab, Lichtervelde, Belgium) and transferred to a 50 ml beaker;

(ii) the beaker was covered with aluminum foil and placed in an oven at 60°C for 15 min to liquefy the cocoa butter;

(iii) a drop of liquefied cocoa butter was transferred to the DSC pan with a plastic micropipette.

3.3.2.2 Sample preparation procedure B

(i) cocoa butter was taken from the cooling chamber (4°C) and immediately placed in a desiccator;

(ii) a 50 ml beaker was cleaned with acetone (Roland, Brussels, Belgium), dried with hot air and put upside down in the desiccator;

(iii) when the cocoa butter was equilibrated to room temperature (which can take several hours depending on the sample size), a sample (approximately 10-20 g) was taken with a knife and spoon cleaned with acetone and transferred to the beaker;

(iv) the beaker was covered with aluminum foil and placed in an oven at 60°C for 15 min to liquefy the cocoa butter;

(v) a drop of liquefied cocoa butter was transferred to the DSC pan with a hot (110°C), glass Pasteur pipette cleaned with acetone.

3.3.3 DSC

The isothermal crystallization experiments were performed on a 2010 CE DSC (TA Instruments, New Castle, USA) with a Refrigerated Cooling System (TA Instruments, New Castle, USA). This is a regular heat-flux DSC (no modulated DSC). The DSC was calibrated with indium (TA Instruments, New Castle, USA), azobenzene (Sigma-Aldrich, Bornem, Belgium) and undecane (Acros Organics, Geel, Belgium) prior to

analyses. Nitrogen was used to purge the system. Hermetic aluminum pans were used and the reference was an empty pan. The sample size varied between 7.0 and 13.6 mg.

3.3.4 Time-temperature program

The first part of the time – temperature program was the melting part, which should eliminate all persisting crystals of cocoa butter. Three different melting protocols were compared: holding at 65°C for 15 min, holding at 65°C for 30 min and holding at 80°C for 15 min. After this melting period the sample was cooled at 8°C min^{-1} to the isothermal crystallization temperature of 17.2 ± 0.1°C and kept at that temperature until crystallization was completed (i.e. when the curve has returned to the baseline). The choice of 8°C min^{-1} as cooling rate was based on preliminary experiments discussed in section 3.4.2.

3.3.5 Integration of the crystallization curves

The amount of heat released up to time t [h] (ΔH_{ts-t} [J g^{-1}]) was determined by calculating the area between a horizontal sigmoid baseline and the DSC peak between t_s (the starting-point of crystallization) and t with t varying between t_s and t_e (the end point of crystallization). When t equals t_e the total heat of crystallization (ΔH [J g^{-1}]) was obtained. Thus:

$$\Delta H_{ts-t} = \int_{t_s}^{t} \frac{dQ}{dt} dt \quad \text{for all } t \text{ between } t_s \text{ and } t_e \qquad \textbf{[3.2]}$$

and

$$\Delta H = \int_{t_s}^{t_e} \frac{dQ}{dt} dt \qquad \textbf{[3.3]}$$

in which dQ/dt [W g^{-1}] is the heat flow as experimentally determined by DSC.

The determination of t_s and t_e was performed using an objective calculation algorithm as described in detail in section 3.4.1.2. The amount of heat released was calculated at 5-minute intervals. The integration was performed using the Universal Analysis software version 2.5 H (TA Instruments, New Castle, USA).

The start of the isothermal period (t = 0) was determined as follows: at the end of the cooling phase the temperature drops below the set point temperature (in this case

17.2°C) due to inertia effects. The controller causes the temperature to increase again and to oscillate to the set point temperature. The start of the isothermal period was determined as the time when the temperature increases for the first time after the cooling phase.

3.3.6 Parameter estimation

The Avrami model, a model frequently used in literature to describe the crystallization kinetics of fats (see section 1.4.4.1), was fitted to the data series. An extra parameter a_A [J g^{-1}], being the maximum amount of heat released, was added to the model to take into account that the phase transition in cocoa butter does not necessarily go to completion. The model can then be written as:

$$f(t) = a_A \times \left(1 - e^{-kt^m}\right) \quad \textbf{[3.4]}$$

where *f(t)* is the released crystallization heat ($\Delta H_{ts\text{-}t}$) [J g^{-1}] up to time *t* [h], a_A [J g^{-1}] the value for *f(t)* as *t* approaches infinity, *k* [h^{-m}] a crystallization rate constant which depends primarily on the crystallization temperature and *m* [-] the Avrami exponent, a combined function of the time dependence of nucleation and the number of dimensions in which crystal growth takes place.

Parameter estimations were performed by non-linear regression using the Sigmaplot 2000 software (SPSS Inc., Chicago, USA). This software uses the Levenberg-Marquardt algorithm to find the parameters giving the 'best fit' (expressed as the sum of squared residuals) between the model and the data.

3.3.7 Statistical analysis

To estimate whether the crystallization parameters differ significantly between groups of experiments and thus estimate whether there was a significant effect of the melting protocol and the sample preparation procedure, an adapted t-test was developed. This adapted t-test takes into account that the calculated parameters of the model are estimates themselves. In particular, it is assumed that each estimator $\hat{\omega}_{ji}$ has expectation ω_{ji} and variance $VAR(\omega_{ji})$ and that the parameter ω_{ji} is also a random variable with expectation ω_j and variance $VAR(\omega_j)$. This specifies a hierarchical model. The test statistic is calculated as:

$$t_w = \left| \frac{\overline{\omega_{(1)}} - \overline{\omega_{(2)}}}{\sqrt{s^2_{(1)} + s^2_{(2)}}} \right| \qquad \textbf{[3.5]}$$

with

$$\overline{\omega_{(j)}} = \frac{\hat{\omega}_{j1} + \hat{\omega}_{j2} + \ldots + \hat{\omega}_{jn}}{n_j} \qquad \text{j = 1,2} \qquad \textbf{[3.6]}$$

with $\hat{\omega}_{ji}$ the parameter value as estimated by Sigmaplot for repetition i (i = 1, …, n)

and

$$s^2_{(j)} = \frac{{s_j}^2}{n_j} + \frac{s^2_{j1} + s^2_{j2} + \ldots + s^2_{jn}}{{n_j}^2} \qquad \text{j = 1,2} \qquad \textbf{[3.7]}$$

Equation [3.7] calculates an estimator of the variance of $\overline{\omega}_{(j)}$, with s^2_{ji} being the estimator of the variance $VAR(\omega_{ji})$ of $\hat{\omega}_{ji}$ as calculated by Sigmaplot for repetition *i* and s^2_j the sample variance of the n_j parameter estimations $\hat{\omega}_{ji}$ for one specific condition, i.e. s^2_j is an estimator of $VAR(\omega_j)$. Note that $\overline{\omega}_{(j)}$ is an unbiased estimator for ω_j.

The standard deviations reported in the results and discussion section correspond to the variance as calculated in equation [3.7].

Since the parameter estimators $\hat{\omega}_{ji}$ are asymptotically normally distributed, the test statistic is asymptotically standard normal under the null hypothesis $\omega_1 = \omega_2$. For finite sample sizes, however, its null distribution is better approximated by a t-distribution. As the exact number of degrees of freedom is not straightforward to determine, the use of a lower bound, $n_1 + n_2 - 2$, was chosen. This choice results in a slightly conservative test. The test statistic has thus to be compared with the threshold value $t_{n1+n2-2,\ 0.05}$ under the student t-distribution where n_1 is the number of repetitions for group 1 and n_2 is the number of repetitions for group 2.

3.4 Results and discussion

3.4.1 Determination of the integration limits

The amount of crystallization heat released as function of time was calculated using equation [3.2]. To be able to use this equation t_s and t_e have to be determined. In most articles (Kerti, 1998 and Ziegleder, 1990) the procedure to determine t_s and t_e is not explicitly mentioned, but it can be suspected it is done visually, with t_s and t_e being the visually decided starting- and end point of crystallization or the moment where the crystallization curve deviates from and returns to the baseline respectively.

3.4.1.1 Subjectivity of a visual determination of the integration limits

To check the subjectivity of a visual determination of the integration limits, an experiment was organized. Eight DSC-experienced people were independently asked to visually determine the starting- and end point of a crystallization peak for three different samples of the same cocoa butter (different DSC pans) at three different moments in time. Using these visually determined integration limits the total area of the peak between starting- and end point (ΔH) was calculated with a horizontal sigmoid baseline. Table 3.1 reports the results of this experiment (only the values of ΔH are given). It occurred that the coefficient of variation of t_s between the different determinations by the same operator (the mean value of the coefficients of variation for the three samples is reported) varies between 1 and 2.7%, while the difference between the lowest and the highest value obtained by one operator for one sample ranges between 0.04 and 2.37 min (detailed results not shown). For t_e the differences are even larger: the coefficient of variation ranges from 4.9 to 17.2% and the difference between the lowest and the highest value obtained by one operator for one sample varies between 1.61 and 46.09 min (detailed results not shown). Evidently, this spreading on the values of t_s and t_e influences the area of the crystallization peak: for ΔH the coefficient of variation ranges between 2.8 and 16.8% while the lowest and highest value obtained by one operator for one sample differ by 0.9 to 21.12 J g^{-1} (Table 3.1). Taking into account the different operators the overall coefficient of variation (one sample integrated by eight operators at three different moments in time) of t_s varies around 3%, while the difference between the lowest and the highest value obtained for one sample varies around 4 min (detailed results not shown). For t_e the coefficient of variation varies around 17% and the difference between the lowest and the highest value obtained for

one sample varies between 58 and 96 min (detailed results not shown). Most importantly, the coefficient of variation for ΔH varies between 7 and 12.5%, while the difference between the lowest and the highest value for one sample ranges between 10 and 28 J g^{-1} (Table 3.1). Since the values of ΔH vary dramatically, also the values of $\Delta H_{ts\text{-}t}$ and consequently also the crystallization model parameter values will differ, depending on the integration when a visual determination of the integration limits is performed.

The variability introduced by a visual determination of t_s and t_e was compared with the sample variability, i.e. the variability originating from using different samples of the same cocoa butter. To do so, the total variability on the ΔH values obtained in this experiment was split up into the sample, the inter-operator and the intra-operator variability. The inter-operator variability is the variability originating from different operators performing the integration of the same crystallization peak, while the intra-operator variability is the variability obtained when the same operator performs the integration of the same crystallization peak several times. The different variabilities were determined using an ANOVA analysis with sample and operator as random factors.

The effect of the factor sample allows to calculate the sample variability, the effect of the factor operator allows to calculate the inter-operator variability and the residual error allows to calculate the intra-operator variability. The standard deviations corresponding to these variabilities are quoted in Table 3.2. From this table it can be concluded that the variability introduced by a visual determination of the integration limits (inter and intra-operator variability) is considerably larger than the sample variability, proving that it is worth to develop and use an objective, mathematical calculation algorithm to determine t_s and t_e of the crystallization peaks.

Table 3.1 Visual determination of integration limits as performed by eight persons on three different samples of the same cocoa butter at three different moments in time. The calculated values of ΔH [J g^{-1}] are reported.

Sample (time of integration) / operator	**1**	**2**	**3**	**4**	**5**	**6**	**7**	**8**	**mean value using visual determination**	**value using calculation algorithm[2]**
1(1)	47.73	46.58	44.14	39.44	44.35	44.95	42.75	47.61		
1(2)	46.90	47.70	47.53	46.76	46.63	47.55	21.63	44.57	44.61	46.47
1(3)	46.64	46.00	**49.38**	41.50	46.95	46.79	39.11	47.49		
2(1)	44.70	45.22	44.19	38.23	43.53	39.57	40.83	44.00		
2(2)	45.88	42.12	44.95	44.27	43.63	46.98	31.90	44.55	43.33	48.60
2(3)	48.36	47.68	**49.38**	43.86	42.73	47.95	30.44	45.13		
3(1)	44.74	50.45	46.35	41.08	44.94	42.50	40.74	43.65		
3(2)	48.23	47.30	47.53	42.12	41.47	45.98	41.72	47.65	45.22	49.84
3(3)	50.39	45.46	**51.22**	42.08	42.29	47.78	41.57	47.92		
mean coefficient of variation (%)[1]	3.74	4.44	5.66	6.10	2.82	6.34	16.79	3.37		

The underlined and bold values are the minimum and maximum values obtained for one sample by the different operators at different moments in time

[1] The mean coefficient of variation is the mean value of the coefficients of variation calculated for each of the three samples

[2] The calculation algorithm used to determine these values is discussed in section 0

Table 3.2 Split-up of the total variability into sample, inter-operator and intra-operator variability. The standard deviations corresponding to the variabilities are quoted.

Type of variability	Standard deviation [J g^{-1}]
sample	0.77
inter-operator	3.32
intra-operator	3.24

3.4.1.2 Objective calculation algorithm for the determination of the integration limits

To eliminate the variability introduced by a visual determination of the integration limits (section 3.4.1.1), an objective calculation algorithm for determining these limits was developed.

Figure 3.3 displays an example of a DSC curve (dQ/dt [W g^{-1}] as function of time) and its slope. Exothermal events, such as crystallization, are plotted downwards, a convention that will be used throughout this whole work. The first part of the DSC curve is the period when the temperature decreases and equilibrates to the isothermal crystallization temperature (= equilibration). The main part of the DSC curve is the exothermal crystallization peak. After the crystallization the heat flow returns to the baseline (= end phase).

Taking into account the DSC heat flow equation [3.1] it can be assumed that under isothermal conditions ($dT_K/dt = 0$) the slope of the heat flow curve will be zero when no crystallization ($f(T,t) = 0$) is occurring. For non-isothermal measurements, however, this reference slope will not be zero, so the reference slope will have to be estimated first.

During the equilibration period a decreasing negative heat flow and the resulting positive slope can be seen (Figure 3.3). This is caused by the change in dT_K/dt in this period. Once the temperature is stabilized and the crystallization has not started yet, the slope is zero, in theory. However, in practice, this is, due to noise, never exactly the case. Once crystallization starts, the heat flow will start to increase to negative values and the heat flow curve will show a certain negative slope. After the crystallization peak maximum the slope becomes positive. At the end of crystallization the heat flow curve returns to the baseline and consequently the slope changes from positive to zero in

theory. However, due to noise the heat flow curve will vary around the final value with alternating positive and negative slopes (Figure 3.3).

Therefore, it was decided to determine t_s as the point where the slope changes from a positive (equilibration period) to a negative (crystallization) value, and t_e as the point where the slope changes sign for the y^{th} time after the peak maximum.

Figure 3.4 to Figure 3.6 give an overview of this algorithm that can easily be programmed in a spreadsheet.

Part 1 of the algorithm (Figure 3.4) consists of some preparation steps to determine the sign changes in the corrected slope and to number them. The corrected slope has been calculated in periods of x minutes.

Part 2 of the algorithm (Figure 3.5) determines t_s. In the most straightforward situation t_s is determined as the time where the slope changes sign from positive to negative before the peak maximum. However, it is possible that several sign changes exist before the peak maximum (in that case the peak maximum does not correspond to the second sign change). This can be caused by a bump (i.e. a deviation from the normal course of the heat flow curve) in the equilibration phase or in the first part of the crystallization curve. In this case the time corresponding to the sign change with the highest heat flow value is taken as t_s. However, only the sign changes from positive to negative are taken into account. In the example in Figure 3.3, the peak maximum corresponds to the fourth sign change. Sign changes j_1 and j_3 qualify for t_s as sign changes from positive to negative but j_1 is selected because it corresponds to a higher heat flow value.

Part 3 of the algorithm (Figure 3.6) determines t_e. However, only the sign changes at the real end of crystallization (i.e. in the end phase) should be taken into account and not the sign changes caused by a bump in the second part of the crystallization peak. Therefore, the heat flow value (dQ/dt) at each sign change after the peak maximum is compared to the last available heat flow value (dQ/dt_f). To eliminate the influence of an outlier, the median of the last five data points (i.e. the last five minutes) is taken as dQ/dt_f. If the difference between dQ/dt and dQ/dt_f is higher than three times the noise on the baseline (σ_n [W g^{-1}]), the sign change still belongs to the crystallization peak and is thus not counted to determine t_e.

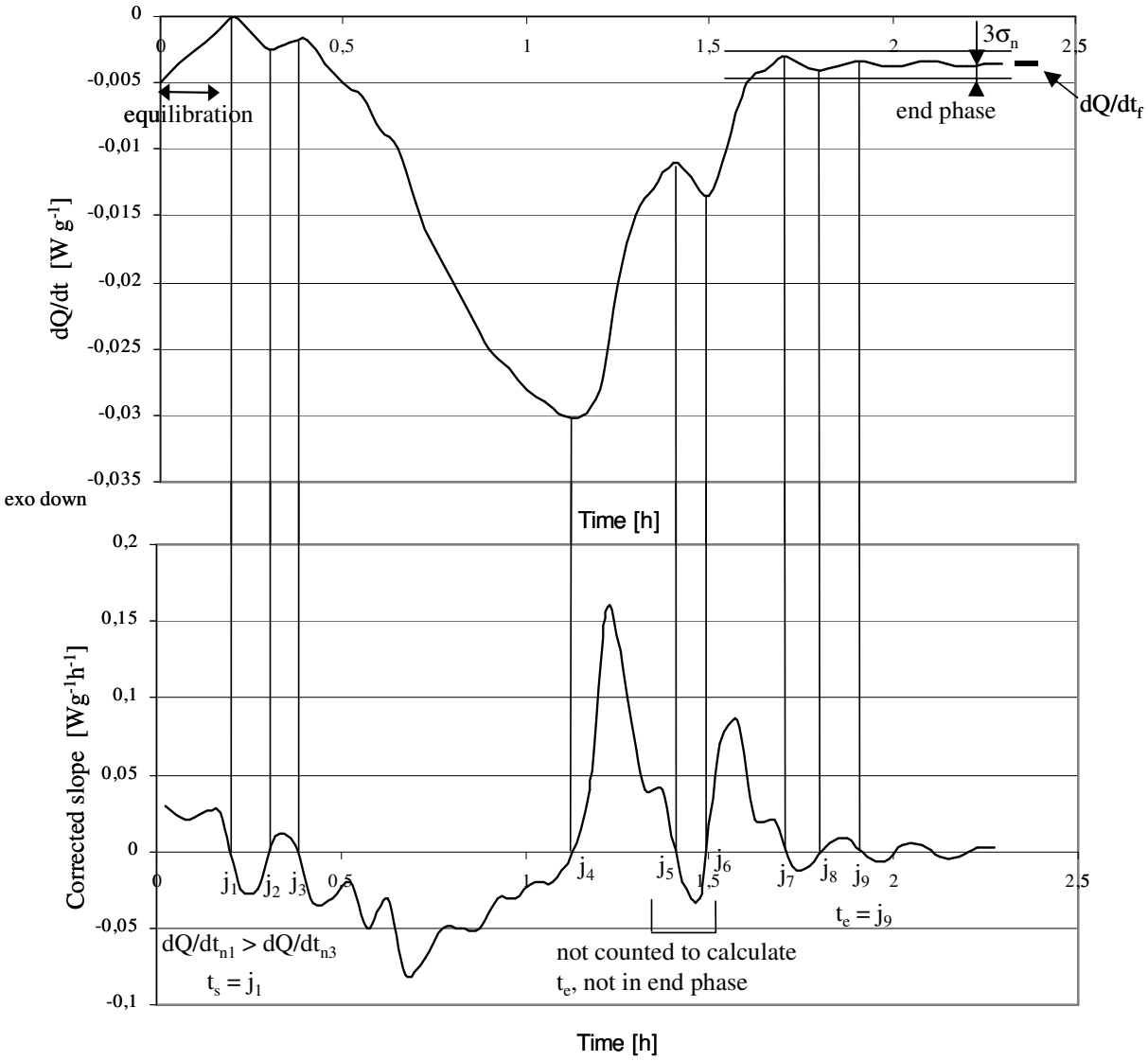

Figure 3.3 Calculation algorithm for the determination of the integration limits

In the example in Figure 3.3 j_5 and j_6 are not counted because the difference between their corresponding heat flow values and dQ/dt_f is larger than $3\sigma_n$. These sign changes are caused by the bump in the heat flow curve. Sign change 7 is the first for which the difference between dQ/dt and dQ/dt_f is smaller than $3\sigma_n$ and is thus the first sign change in the end phase. Consequently t_e corresponds to j_9. The value of σ_n is determined by considering a run or part of a run where no kinetic processes are happening (i.e. a straight baseline) and performing a linear regression on these data.

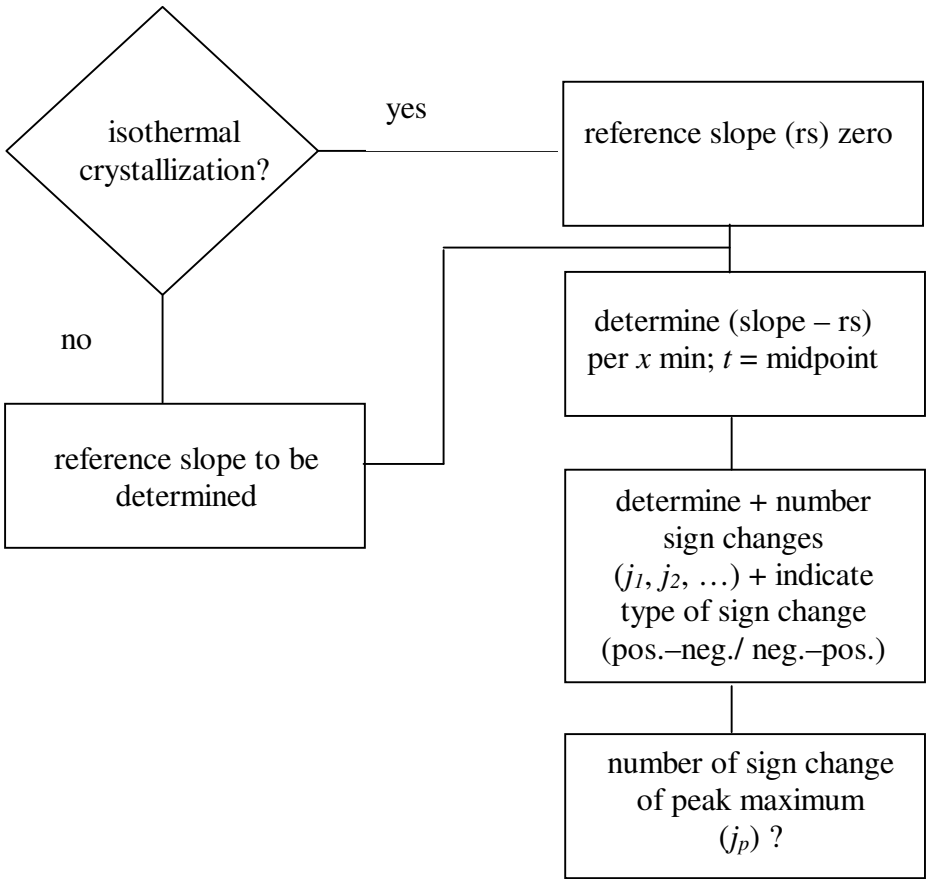

Figure 3.4 Calculation algorithm for determination of t_s and t_e: preparation step

The regression provides the sum of squared residuals (SSR [$W^2\ g^{-2}$]). The value of σ_n is then expressed by equation [3.8]:

$$\sigma_n = \sqrt{\frac{SSR}{z-2}} \qquad \textbf{[3.8]}$$

where z [-] is the number of data points used to calculate the regression.

The value of σ_n may be different for various instruments. For the instrument used in this research a value of 0.000154 W g^{-1} was obtained. This value will be used throughout this whole work. The optimum values for x (the length of the period for which the slope is determined) and y (the number of the sign change after the peak maximum taken as t_e) may also change from instrument to instrument. For the instrument used in this research optimum values for x and y were 7 min and 3 respectively.

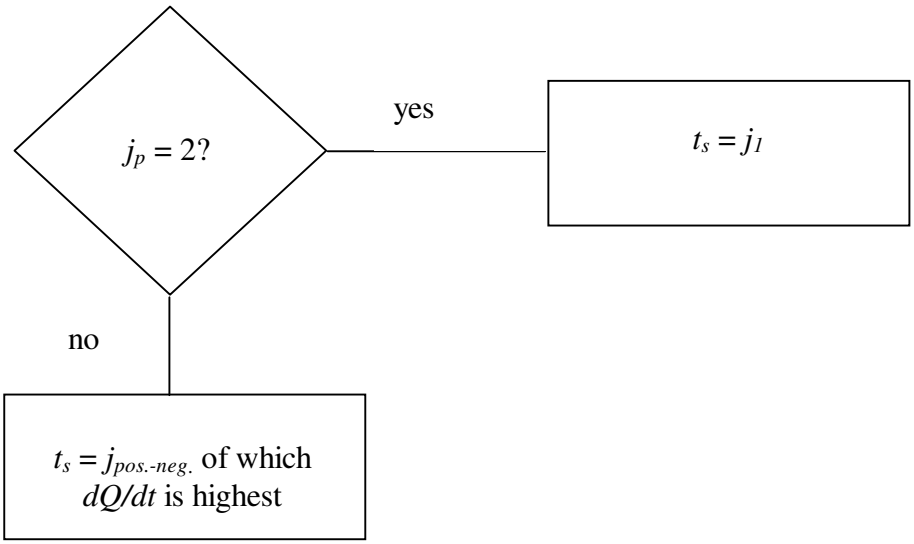

Figure 3.5 Calculation algorithm for determination of t_s and t_e: determination of t_s

3.4.1.3 Comparison of visual and algorithmic determination of integration limits

The values of the algorithmic determination using the calculation algorithm were compared with those of the visual determination. Conclusions are that for two of the three samples the algorithmic value for t_s is situated between the minimum and maximum value obtained by visual determination (by different operators at different moments in time), for the other sample it is slightly lower than the lowest visual value. For two samples, the algorithmic value for t_e is higher than the highest visual value, for the other sample some visual values are higher than the algorithmic value. An explanation for the fact that in most cases the algorithmic value of t_e is larger than the visual value is that when the crystallization peak is not enlarged enough for visual determination of t_e, it can appear the curve has already returned to the baseline at a specific point, which is in reality not the case. The consequence for the integration is that the value of ΔH determined by using the algorithmic integration limits is on average about 9% higher than the mean of the values determined by using the visual integration limits (Table 3.1). However, for two of the three samples some values obtained by using visual limits are higher than the value using algorithmic limits.

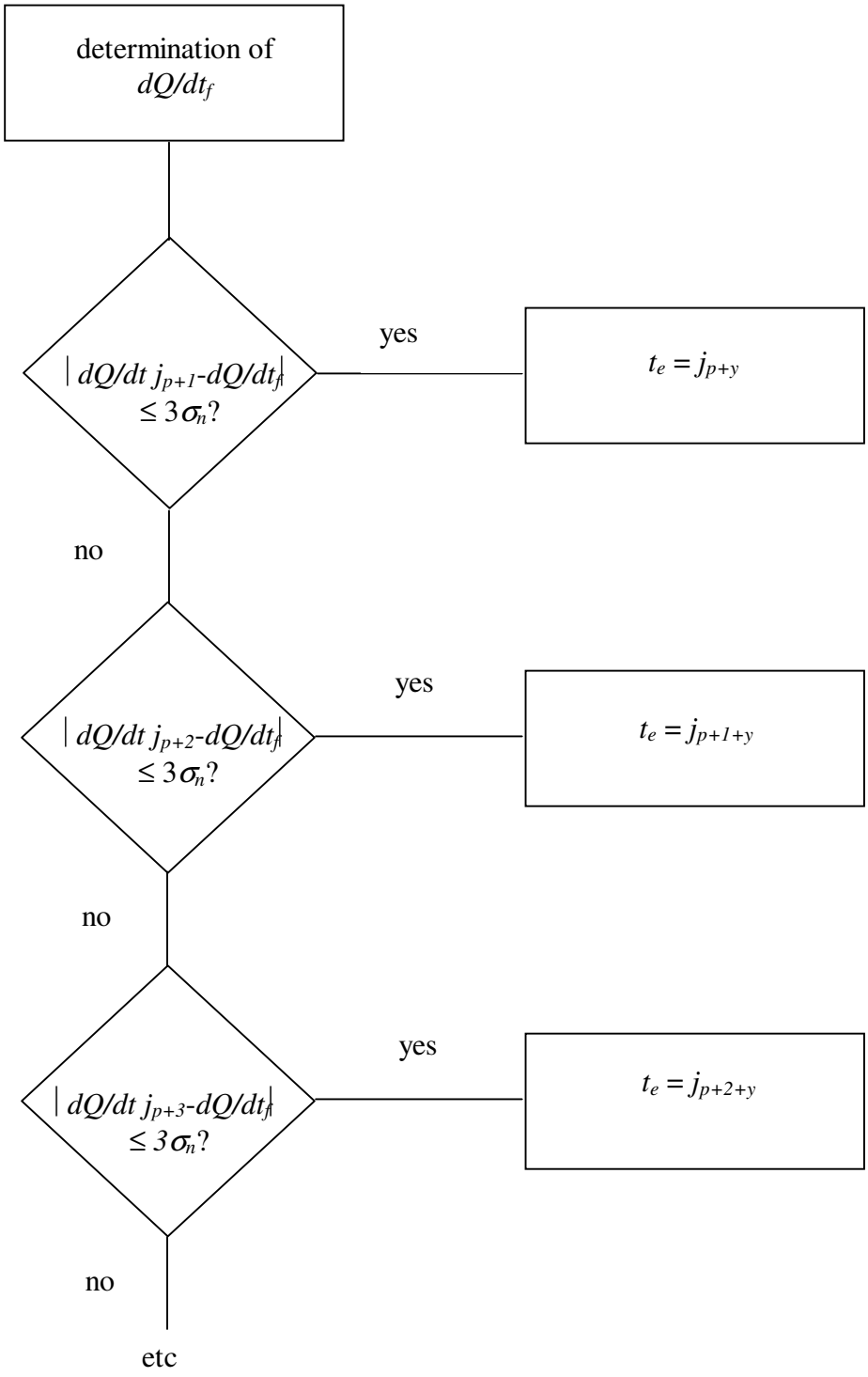

Figure 3.6 Calculation algorithm for determination of t_s and t_e: determination of t_e

3.4.2 Choice of cooling rate

A cooling rate of 8°C min^{-1} was chosen considering, on the one hand, that the cooling rate should be high enough to prevent the melt from forming a lamellar structure in the liquid state, which would influence the subsequent crystallization process. Toro-Vazquez et al. (2001) showed that this effect takes place when using a cooling rate of 1°C min^{-1} when compared to 10°C min^{-1}. On the other hand the apparatus should be able to keep up with the cooling rate under all conditions, since otherwise the reproducibility will be lowered. The possibility to maintain a specified cooling rate was checked by evaluating the plot of the actual temperature versus time (which should be a straight line) and by looking for a warning signal of the apparatus when the specified cooling rate could not be kept. The highest possible cooling rate was determined to be 8°C min^{-1}.

To get more insight in the effect of cooling rate, an experiment was designed in which three different cooling rates (1, 5 and 8°C min^{-1}) were compared. For each cooling rate three repetitions (three different pans of the same cocoa butter) were performed. The DSC curves showed that when cooling at 1°C min^{-1} some crystallization already occurs during the cooling phase, an undesired phenomenon since it was the aim to study isothermal crystallization. The Avrami model was fitted to the isothermal crystallization data after cooling at 5 and 8°C min^{-1}. No significant differences ($\alpha = 0.05$) between its parameters were found (detailed results not shown) despite the fact that in literature (Martini et al., 2001 and Toro-Vazquez et al., 2001) an effect of cooling rate has been found. The cooling rates used in this experiment, however, were much closer to each other than these in literature.

As in theory the sample should be quench cooled to the isothermal temperature, it was decided to use the highest cooling rate attainable by the apparatus, thus 8°C min^{-1}.

3.4.3 Influence of melting protocol

The aim of the melting part of the time-temperature program is to eliminate all homogeneous crystal nuclei so they cannot have any effect on the subsequent crystallization. As a reference, holding at 65°C for 15 min (as used by Ziegleder (1990)) was chosen. To check whether this time-temperature combination is adequate to melt all homogeneous nuclei, it was compared with holding at 65°C for 30 min and holding at

80°C for 15 min. To compare the different crystallization processes, the Avrami model was fitted to the data series and its parameters were compared.

To study the effect of the melting protocol, only the experiments performed with sample preparation procedure B were taken into account. Figure 3.7 shows the crystallization curves for the different melting protocols and proves no obvious difference between the three protocols can be detected.

Table 3.3 gives an overview of the mean values and the standard deviations calculated for the three Avrami parameters for each of the melting protocols. Significance of differences was checked with the adapted t-test. The three melting protocols were compared two by two and for none of the parameters any significant difference (α = 0.05) was detected. This means that holding at 65°C for 15 min is enough to melt all homogeneous nuclei and eliminate any memory effect on the crystallization process. This confirms the results of Hachiya et al. (1989) and Van Malssen et al. (1996) who reported that to eliminate memory effects in cocoa butter, the temperature has to be

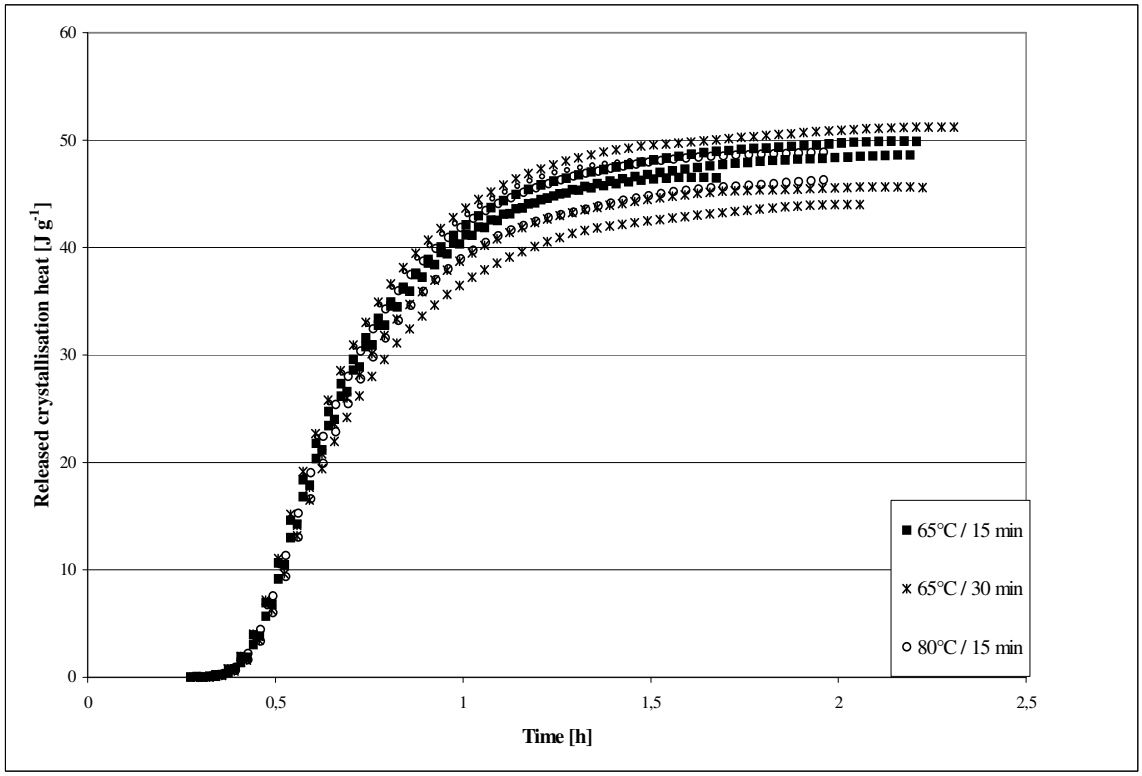

raised only slightly above the melting point.

Figure 3.7 Influence of melting protocol on the isothermal crystallization of cocoa butter (sample preparation method B)

Table 3.3 Influence of melting protocol on the isothermal crystallization of cocoa butter (mean ± standard deviation (corresponding to $s^2(j)$ as calculated in [3.7]) for three repetitions)

Crystallization parameter / melting protocol	Avrami a_A [J g^{-1}]	Avrami k [h^{-m}]	Avrami m [-]
65°C / 15 min	46.85±1.02[a]	2.66±0.37[a]	3.38±0.18[a]
65°C / 30 min	45.66±2.25[a]	2.50±0.16[a]	3.30±0.15[a]
80°C / 15 min	46.78±1.01[a]	2.71±0.21[a]	3.47±0.15[a]

[a, b] indicate whether the sample preparation method has a significant effect; means with the same superscript are not significantly different at $\alpha = 0.05$

Whether a specific time-temperature combination is sufficient to melt all nuclei, is independent of the temperature at which the following isothermal crystallization is performed. Therefore the result obtained for an isothermal crystallization at 17.2°C can be generalized to other isothermal crystallization temperatures.

3.4.4 Influence of sample preparation procedure

The potential influence of the sample preparation procedure was investigated by comparing the isothermal crystallization of samples prepared in two different manners (sample preparation procedure A and B as described in section 3.3.2). For each melting protocol two repetitions using procedure A and three repetitions using procedure B were performed. Figure 3.8 shows the influence of the sample preparation procedure on the crystallization curves. For clarity reasons, only the crystallization curves recorded with a melting protocol of 65°C for 15 min are shown. It can clearly be noticed that the sample preparation procedure has an influence on the crystallization curve: when using sample preparation procedure A the induction time is longer and the final value is higher.

Table 3.4 gives an overview of the mean values and the standard deviations calculated for the three Avrami parameters for each sample preparation procedure and this for the three melting protocols separately and irrespective of the melting protocol. Using the

adapted t-test it was investigated whether the parameters are significantly influenced by the sample preparation procedure.

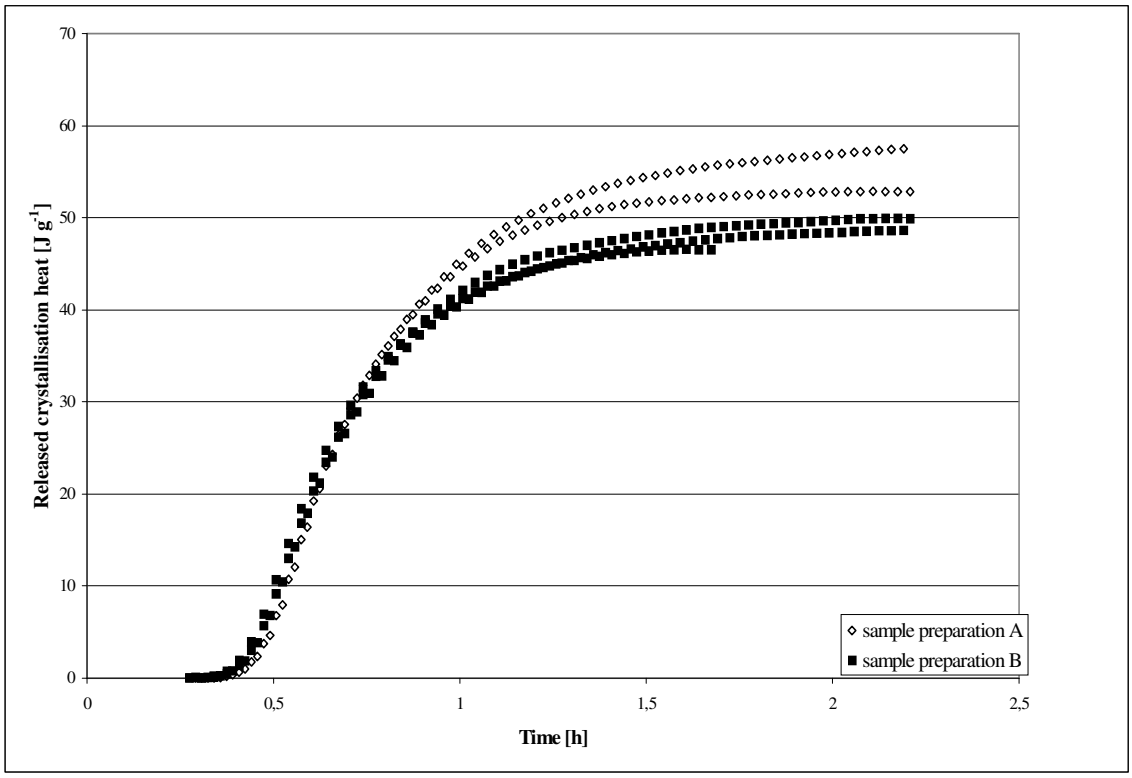

Figure 3.8 Influence of sample preparation procedure on the isothermal crystallization of cocoa butter (melting protocol 65°C / 15 min)

First, the influence of the sample preparation procedure was studied regardless of the melting protocol used. Significant differences were found for both the a_A and k parameters ($\alpha = 0.05$). The higher values for a_A when using sample preparation procedure A are also illustrated clearly in Figure 3.8. The adapted t-test was also performed on the data for each melting protocol separately. No significant differences were found. However, when studying the data in Table 3.4, the same trends (higher a_A values and lower k values) are noticed for each melting protocol separately. The lack of significance when the melting protocols were considered separately is probably related to the smaller number of repetitions, which reduces the power of the statistical methods.

Although the experiments were only performed at one crystallization temperature, it can be expected that also at other temperatures the sample preparation procedure may have a significant influence on the crystallization process. Consequently, it is very important to keep the sample preparation procedure constant at all times when preparing DSC samples. Otherwise a difference between two groups could be wrongfully attributed to a

difference between the groups, the real reason being a difference in the sample preparation procedure. By eliminating the variability caused by a difference in sample preparation procedure, the variability on the data can be lowered and so the quality of the data will increase.

Table 3.4 Influence of sample preparation procedure on the isothermal crystallization of cocoa butter (mean ± standard deviation (corresponding to $s^2(j)$ as calculated in [3.7]) for two repetitions of method A and three repetitions of method B)

Crystallization parameter / melting protocol / sample preparation procedure		**Avrami a_A [J g^{-1}]**	**Avrami k [h^{-m}]**	**Avrami m [-]**
65°C / 15 min	A	53.72±2.21[a]	2.08±0.33[a]	3.35±0.26[a]
	B	46.85±1.02[a]	2.66±0.37[a]	3.38±0.18[a]
65°C / 30 min	A	50.58±1.17[a]	2.20±0.15[a]	3.46±0.18[a]
	B	45.66±2.25[a]	2.50±0.16[a]	3.30±0.15[a]
80°C / 15 min	A	49.82±0.52[a]	2.35±0.17[a]	3.54±0.19[a]
	B	46.78±1.01[a]	2.71±0.21[a]	3.47±0.15[a]
all heating protocols	A	51.37±1.02[a]	2.21±0.13[a]	3.45±0.12[a]
	B	46.43±0.81[b]	2.62±0.14[b]	3.38±0.09[a]

[a, b] indicate whether the sample preparation method has a significant effect; means with the same superscript are not significantly different at $\alpha = 0.05$

3.5 Conclusions

To transform a DSC crystallization peak into a crystallization curve representing the amount of heat released as function of time, the DSC peak area has to be integrated. When the integration limits of such a crystallization peak are determined visually, the result (ΔH and thus $\Delta H_{ts\text{-}t}$ and thus the parameters of the crystallization model) will strongly depend on the operator and will also differ when the same operator performs the integration several times. To eliminate the high variability introduced by this visual determination of the integration limits, an objective calculation algorithm was developed to determine these limits.

It was also shown that there is no significant difference between a melting protocol of 65°C for 15 min, 65°C for 30 min and 80°C for 15 min. This means 65°C for 15 min is

sufficient to melt all homogeneous nuclei of cocoa butter. For that reason, this time-temperature combination was used further in this work.

Finally, it could be concluded that it is important to keep the sample preparation procedure constant since a change in this procedure can influence the subsequent crystallization process and therefore increase the variability on the data. It was chosen to use sample preparation method B during this whole work.

4 A NEW MODEL TO DESCRIBE THE CRYSTALLIZATION KINETICS OF FATS

4.1 Introduction

Understanding when and to what extent different fat components crystallize under specific conditions is important for controlling operations in the food industry to produce the desired product characteristics (Metin & Hartel, 1998). Probably because of that importance, quite some articles were published in the last decennia in which the isothermal crystallization kinetics of fats is mathematically modelled to enable quantification of differences in crystallization behaviour between different products and process conditions. Section 1.4.4 gives an overview of the models used to describe the crystallization kinetics of fats. The following paragraph gives a brief summary of these models.

The Avrami model (Avrami, 1939 and Avrami, 1940) is the most frequently used model. It was initially developed for metals, later it was also used a lot for polymers and fats. Some authors applied a modified Avrami model, a reparameterization of the original model possibly leading to better parameter estimations. However, it does not differ from the original model from a curve-fitting point of view. The Avrami model can be adapted to account for the fact that not necessarily all fat is crystallized at equilibrium. An extra parameter a_A [J g^{-1} or % solid fat depending on the measuring technique], representing the maximum amount of crystallization, is therefore added to the model, which is consequently written as:

$$f(t) = a_A \times \left(1 - e^{-kt^m}\right) \qquad \textbf{[4.1]}$$

It is also possible to add a fourth parameter to the Avrami model to account for an induction time t_ind_A [h] (Lambrigger, 1996). The model in [4.1] then changes to:

$$f(t) = a_A \times \left(1 - e^{-k(t - t\_ind_A)^m}\right) \qquad \textbf{[4.2]}$$

A few authors have used a reparameterized Gompertz model (Zwietering, 1990):

$$f(t) = a_G \times \exp\left\{-\exp\left[\frac{\mu_G \times e}{a_G} \times (\lambda_G - t) + 1\right]\right\} \quad \textbf{[4.3]}$$

This model originates from demography but was mainly used to describe bacterial growth.

The Avrami and Gompertz models have some advantages and disadvantages. Advantages of the Avrami model are the firm theoretical basis and the frequent use. Disadvantages are the assumptions the theory is based on and which may not always be valid in the case of fat crystallization, and the rather bad fit as shown in Figure 1.7. Advantages of the Gompertz model are the straightforward physical interpretation of the parameters and the better fit when compared to the Avrami model. Still the fit is not yet perfect (Figure 1.7). The weak theoretical basis is the main disadvantage of the Gompertz model.

The aim of this chapter is to present a new model able to better describe the isothermal crystallization kinetics of fats. It was chosen to derive a model in the form of a differential equation, which has some advantages as will be discussed in section 4.4.1. To show its universality, the model was fitted to isothermal crystallization data of some completely different fats, measured at different isothermal crystallization temperatures and using different measuring techniques. The qualities of the proposed model were compared to those of the Avrami (with and without induction time) and Gompertz models.

4.2 Research strategy

A new model to describe the crystallization kinetics of fats was developed. The original differential equation was simplified, mainly based on parameter estimation studies. This simplified version could also be solved for isothermal conditions leading to an algebraic equation allowing easier parameter estimation. The influence of the model parameters on the course of a crystallization curve was investigated.

The quality of the proposed model was compared to that of the Avrami (with and without induction time) and Gompertz models using different mathematical criteria. To do this, fourteen different samples of cocoa butter were isothermally crystallized at 20±0.05°C using DSC. Each sample was analyzed three times. To check the influence of crystallization temperature on the quality of the models, one type of cocoa butter was isothermally crystallized at 19, 21, 22 and 23°C (±0.05°C), also using DSC. To check

the influence of the type of fat on the quality of the models, milk fat was isothermally crystallized in the DSC at 20.7±0.05°C and 23.7±0.05°C. Two samples of milk fat containing extra minor components were also crystallized in the DSC at 23.7±0.05°C. To check the influence of the measuring technique on the quality of the models, pNMR was used to record the isothermal crystallization kinetics of three milk fat fraction samples at 17.5, 21.5 and 26°C (±0.2°C) respectively. The models were also compared on the basis of their visual quality of fit, the errors on their parameter estimates and their ability to fit asymmetric curves.

4.3 Materials and methods

4.3.1 Materials

Fourteen different samples of cocoa butter (CB A-N) originating from Africa, South America as well as Asia were analyzed. They were obtained from ADM Cocoa (Koog aan de Zaan, the Netherlands), Barry Callebaut (Wieze, Belgium) and Barry Callebaut (Bussum, the Netherlands). Milk fat (MF A) was obtained from Aveve Dairy Products (Klerken, Belgium). Extra minor components were added to purified milk fat samples: 0.5% water in a first sample (MF B) and 0.75% water and 0.075% phospholipids in a second sample (MF C). Aveve Dairy Products (Klerken, Belgium) also supplied the three milk fat fraction samples (MF D-F).

4.3.2 Isothermal crystallization experiments using DSC

The DSC experiments were performed with a 2010 CE DSC (TA Instruments, New Castle, USA) with a Refrigerated Cooling System (TA Instruments, New Castle, USA). The DSC was calibrated with indium (TA Instruments, New Castle, USA), azobenzene (Sigma-Aldrich, Bornem, Belgium) and undecane (Acros Organics, Geel, Belgium) prior to analyses. Nitrogen was used to purge the system.

Cocoa butter (7.3-15.6 mg) was sealed in hermetic aluminum pans (using sample preparation procedure B as described in section 3.3.2.2) and an empty pan was used as a reference. The time-temperature program used in the experiments was (see chapter 3): holding at 65°C for 15 minutes to ensure a completely liquid state, cooling at 8°C min^{-1} to the isothermal crystallization temperature and keeping at that temperature until crystallization had finished.

Milk fat samples (2-5 mg) were transferred into an aluminum DSC pan using a micropipette. The melting part of the time-temperature program was 70°C for

10 minutes instead of 65°C for 15 minutes. The rest of the time-temperature program was the same as for cocoa butter.

The changes in the heat flow during isothermal DSC operation at the crystallization temperature were recorded.

The amount of heat released as function of time was calculated by integration of the crystallization peaks using a horizontal sigmoid baseline. The starting- and end points of the peak were determined using the objective calculation algorithm as described in section 3.4.1.2. In between starting- and end points the area (and thus the amount of heat released up to that moment) was calculated at 5-minute intervals. More frequent data sampling led to auto-correlated residuals with underestimated errors on the parameter estimates as a consequence (see Annex III.2 for more details). The integration was performed using the Universal Analysis software version 2.5 H (TA Instruments, New Castle, USA). The start of the isothermal period was determined as described in section 3.3.5.

4.3.3 Isothermal crystallization experiments using pNMR

The pNMR experiments were performed with a Minispec pc 20 (Bruker, Karlsruhe, Germany). Liquefied milk fat was transferred to pNMR tubes. To eliminate any thermal history these tubes were kept at 60°C for 30 minutes and then placed in a thermostatic water bath at crystallization temperature. Readings of the amount of solid fat were taken at appropriate time intervals. The start of the isothermal period was taken one minute after transfer to the water bath.

4.3.4 Parameter estimation

The different algebraic models (Avrami model with and without induction time, Gompertz model and algebraic version of proposed model) were fitted to the data series by non-linear regression using the Sigmaplot 2000 software (SPSS Inc., Chicago, USA). This software uses the Levenberg-Marquardt algorithm to find the parameters offering the best fit between the model and the data. This algorithm seeks the values of the parameters minimizing the sum of squared differences between the observed and predicted values of the dependent variable. This process is iterative: the curve fitter begins with a guess at the parameters, checks to see how well the model fits and then continues to make better guesses until the sum of squared residuals no longer decreases

significantly. This condition is known as convergence. Varying the initial values, step size and tolerance, avoid the iterative process to stop in a local minimum.

The parameter estimations of the proposed model in its differential equation form were performed in WEST (Hemmis NV, Kortrijk, Belgium) using the Simplex algorithm (Nelder & Mead, 1964).

More information on parameter estimation is found in Annex III.3 and III.4.

4.3.5 Mathematical model selection

Several methods exist to evaluate the quality of different models after fitting each model to the data. These methods can be subdivided into information criteria, methods that go back to statistics and techniques in which an analysis is made of the residuals between model predictions and measured data. Vanrolleghem and Dochain (1998) give an overview of the model selection methods. The methods used in this study are summarized in the following sections.

4.3.5.1 Information criteria

The two best-known information criteria are the Final Prediction Error (*FPE*) and Akaike's Information Criterion (*AIC*):

$$FPE = \frac{SSR}{N_d} \times \left(1 + \frac{2 \times n_p}{N_d - n_p}\right) \quad \textbf{[4.4]}$$

$$AIC = N_d \times \log\left(\frac{SSR}{N_d}\right) + 2 \times n_p \quad \textbf{[4.5]}$$

where *SSR* is the sum of squared residuals, n_p is the number of parameters in the model and N_d is the number of data points. The model with the smallest criterion value was selected for each data series. These criteria have the disadvantage that they are not consistent (i.e. they do not guarantee that the probability of selecting the wrong model tends to zero as the number of data points tends to infinity).

Examples of consistent criteria are the Bayesian Information Criterion (*BIC*) and *LILC*:

$$BIC = N_d \times \log\left(\frac{SSR}{N_d}\right) + n_p \times \log\left(N_d\right) \quad \textbf{[4.6]}$$

$$LILC = N_d \times \log\left(\frac{SSR}{N_d}\right) + n_p \times \log(\log(N_d)) \quad \textbf{[4.7]}$$

The model with the lowest criterion value was selected.

All these information criteria are based on *SSR* and thus give an indication of how much the predicted curve differs from the actually measured curve, compensating in different ways for model complexity.

4.3.5.2 Methods that go back to statistics

The statistical F-test is probably the most frequently applied method to decide whether the more complex model j is significantly (with a significance level α) better than model i. The test statistic is calculated as:

$$F_w = \frac{(SSR_i - SSR_j)/(n_{p_j} - n_{p_i})}{SSR_j/(N_d - n_{p_j})} \quad \textbf{[4.8]}$$

The obtained value of the test statistic has to be compared with tabulated values for $F_\alpha(n_{pj} - n_{pi}, N_d\text{-}n_{pj})$.

4.3.5.3 Analysis of residuals

The quality of a model can also be assessed by analysis of the properties of the calculated residuals ε (measured value minus predicted value). Two approaches can be used to check whether the residuals are independent of each other.

The so-called run test evaluates the number of sign changes in the residual sequence and compares it to the expected number $N_d/2$.

The auto-correlation test consists of comparing the value of the auto-correlation *AC* for each time lag φ with the limit value $N(0,1)/\sqrt{N_d}$ with *N(0,1)* the standard normal distribution. For a significance level α = 0.05 this means that only 5% of the auto-correlations may be larger than $1.96/\sqrt{N_d}$. The auto-correlation with time lag φ quantifies the dependency of a variable at any time t_k and the variable at time t_k-φ:

$$AC(\varphi) = \frac{1}{\sum_{k=1}^{N_d} \varepsilon(t_k)\varepsilon(t_k)} \times \sum_{k=1}^{N_d-\varphi} \varepsilon(t_k - \varphi) \times \varepsilon(t_k) \quad \textbf{[4.9]}$$

The value for the auto-correlation test is the amount of auto-correlations higher than the threshold $1.96/\sqrt{N}_d$.

4.3.5.4 PRESS

The Sigmaplot software provided an additional criterion: the predicted residual error sum of squares (PRESS) which gauges how well a model predicts new data. The smaller the PRESS statistic is, the better the predictive ability of the model will be. The PRESS statistic is computed by summing the squares of the prediction errors (differences between predicted and observed values) for each observation, with that point deleted from the computation of the regression equation.

4.4 Results and discussion

4.4.1 The proposed model

A new model to describe the crystallization kinetics of fats was developed. In contrast to the Avrami and Gompertz models, it was developed in the form of a differential equation. This has the advantage that (i) it is often easier to interpret the model mechanistically, (ii) it is easier to make minor changes to the model on the basis of acquired knowledge and (iii) by incorporation of secondary models describing the temperature dependency of the parameters, the model can be used to describe non-isothermal crystallization kinetics.

In contrast, an algebraic solution is obtained assuming isothermal conditions, making its use for non-isothermal ones impossible. On the other hand, an algebraic solution offers the advantage that parameter estimation is easier because of more readily available software packages capable of non-linear regression of algebraic equations. Therefore the simplified version of the differential equation was solved for isothermal conditions.

4.4.1.1 Remaining crystallizable fat

The Avrami and Gompertz models express the absolute amount of crystallization f as function of time. The proposed model is, however, written in terms of a related variable h [-], the relative amount of remaining crystallizable fat:

$$h = \frac{a_P - f}{a_P} \qquad \textbf{[4.10]}$$

where a_P [J g^{-1} or % solid fat depending on measuring technique] is the value of the variable f [J g^{-1} or % solid fat depending on measuring technique] for t [h] approaching

infinity. In contrast to *f*, which increases in time in a sigmoid way, this new variable *h* is related to the remaining supersaturation (i.e. the driving force for crystallization) and thus decreases in time in a sigmoid way.

4.4.1.2 Building of the model

To build the model, the approach of Wünderlich (1990) was followed. He stated that phase transitions (such as crystallization) can be written in the form of a chemical reaction

A (in this case melt) $\rightleftharpoons$ B (in this case crystals)

and that for the thermodynamic and kinetic description of phase transitions the same equations as for chemical reactions can be used. Furthermore, he stated that all transitions between the melted and the crystalline phase are usually assumed to be first-order transitions. Common causes, however, for a deviation of a first order transition are impurities and a distribution of phases with different perfections.

The proposed model represents the crystallization process as if it was a combination of a first-order forward reaction and a reverse reaction of order *n* [-] with rate constants K_i for each of the reactions. In this way the dynamics of *h* can mathematically be written as:

$$\frac{dh}{dt} = K_n \times h^n - K_1 \times h \qquad \textbf{[4.11]}$$

K_1 [h^{-1}] and K_n [h^{-1}] are the rate constants of the first order forward reaction and the n^{th} order reverse reaction respectively.

To calculate the values of *h* as function of time according to equation [4.11], the initial value for *h*, *h(0)*, needs to be specified:

$$h(0) = \frac{a_P - f(0)}{a_P} \qquad \textbf{[4.12]}$$

with *f(0)* the initially present amount of crystals (nuclei?).

4.4.1.3 Simplification of the proposed model

Parameter estimation studies (for details on parameter estimation in WEST, see Annex III.3) revealed a difference between K_1 and K_n of only between 1.10^{-4} and 1.10^{-7} h^{-1}. Furthermore, the quality of the 5-parameter model was not significantly better than that of a 4-parameter model for which $K_1 = K_n$. For some data series a higher *SSR* value was

obtained for the 5-parameter than for the 4-parameter model. Taking into account that the more complex model should always have a better quality of fit than the simpler one, this meant that the real optimum for the 5-parameter model was not reached. Varying the settings for accuracy, changing the initial values and changing to another optimization algorithm (Praxis) did not lead to lower values for *SSR*. The most probable explanation for this contradiction is that the data series do not contain enough information to estimate five parameters.

Taking the above-mentioned into account, it was decided to put K_n equal to K_1 and simplify the model to:

$$\frac{dh}{dt} = K \times (h^n - h)$$
$$h(0) = \frac{a_P - f(0)}{a_P} \qquad \textbf{[4.13]}$$

where a_P [J g^{-1} if measuring by DSC or % solid fat if measuring by pNMR] is the value of f as t approaches infinity, K the rate constant [h^{-1}], n the order of the reverse reaction [-] and $f(0)$ the initially present amount of crystals [J g^{-1} if measuring by DSC or % solid fat if measuring by pNMR]. This simplified model thus has a total of four parameters.

An additional advantage of simplifying the model is the possibility of solving equation [4.13] for isothermal conditions (see section 4.4.1.7). The obtained algebraic equation allows easier parameter estimation in a multitude of software packages capable of non-linear regression.

4.4.1.4 Model with variable order of the forward reaction

The behaviour of the generalized form of equation [4.13], with n_2 as the order of the forward reaction instead of a fixed value of one, was also explored. The result was differential equation [4.14]:

$$\frac{dh}{dt} = K \times (h^n - h^{n_2})$$
$$h(0) = \frac{a_P - f(0)}{a_P} \qquad \textbf{[4.14]}$$

Parameter estimation studies revealed that the fit of this generalized equation was not significantly better than that of equation [4.13]. As for the original 5-parameter model, for some data series the obtained fit was even worse than that of the 4-parameter model

with the order of the forward reaction fixed on one. The reason is probably the same as for the original 5-parameter model: not enough information in the data series to estimate five parameters. Typical values obtained for n_2 are 0.88, 0.89 and 0.92, which is close to the original fixed value of one. It was thus decided to keep the order of the forward reaction fixed on one.

4.4.1.5 Influence of model parameters on crystallization curve

Figure 4.1 to Figure 4.4 show the influence of the four parameters of the simplified model (equation [4.13]) on the crystallization curve. Figure 4.1 shows the influence of varying a_P between 40 and 70 J g^{-1} or % solid fat.

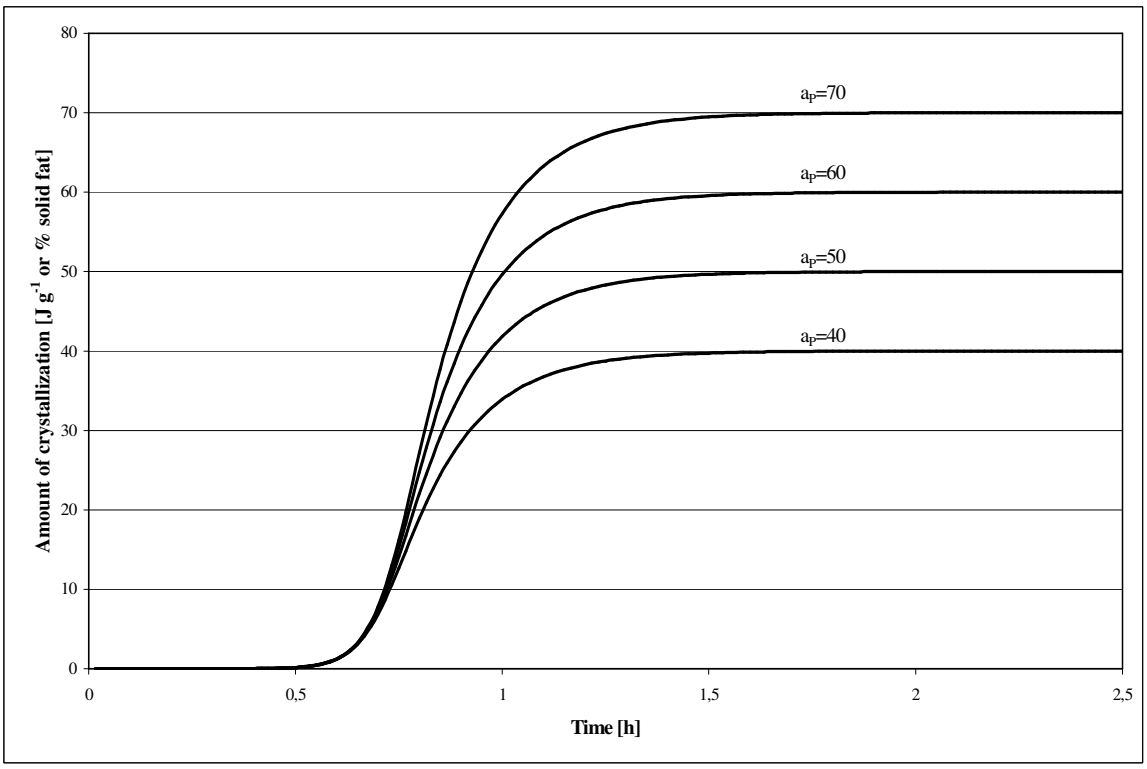

Figure 4.1 Influence of varying a_P [J g^{-1} or % solid fat] on the crystallization curve ($f(0)$=1.10^{-5} J g^{-1} or % solid fat, K=6 h^{-1}, n=5)

The parameter a_P is indeed the height of the plateau of the curve and thus directly related to the a_A and a_G values of the Avrami and Gompertz models respectively.

Figure 4.2 shows the influence of varying $f(0)$ between 1.10^{-7} and 1.10^{-4} J g^{-1} or % solid fat. The parameter $f(0)$ is clearly related to the induction time of the crystallization process. Section 4.4.1.8 will make this relationship clearer mathematically.

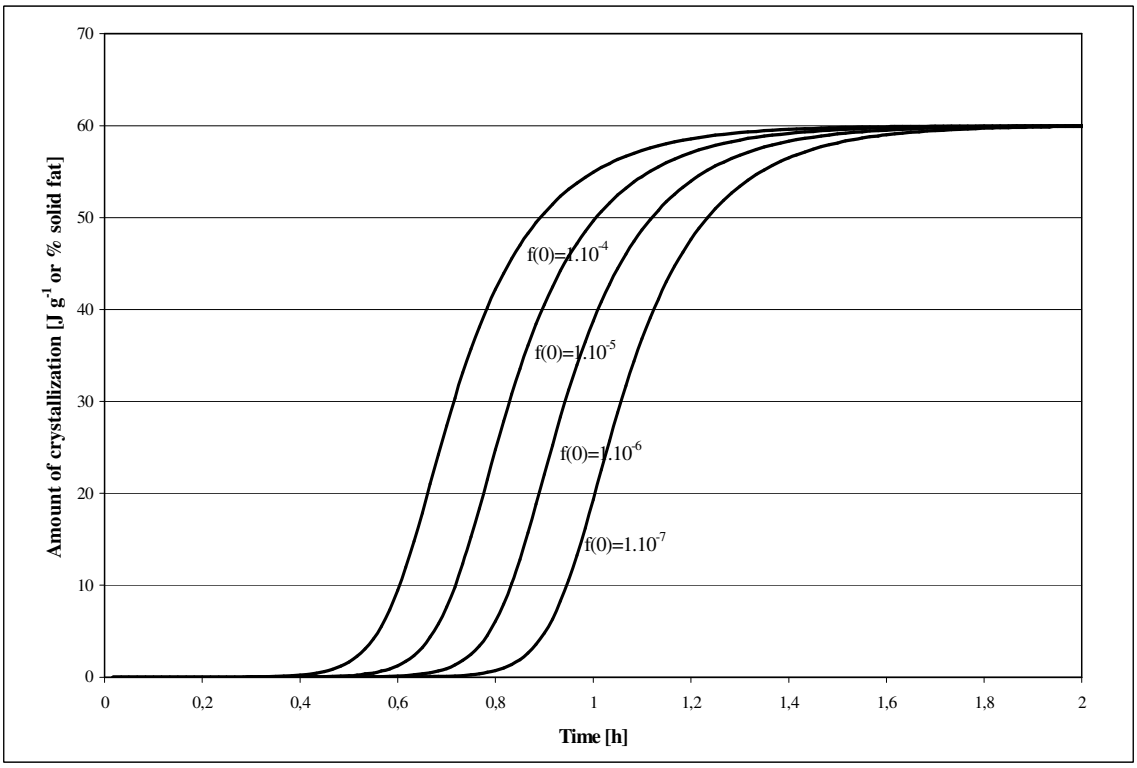

Figure 4.2 Influence of varying *f(0)* [J g^{-1} or % solid fat] on the crystallization curve (a_P=60 J g^{-1} or % solid fat, *K*=6 h^{-1}, *n*=5)

Figure 4.3 shows the influence of varying *K* between 3 and 12 h^{-1}.

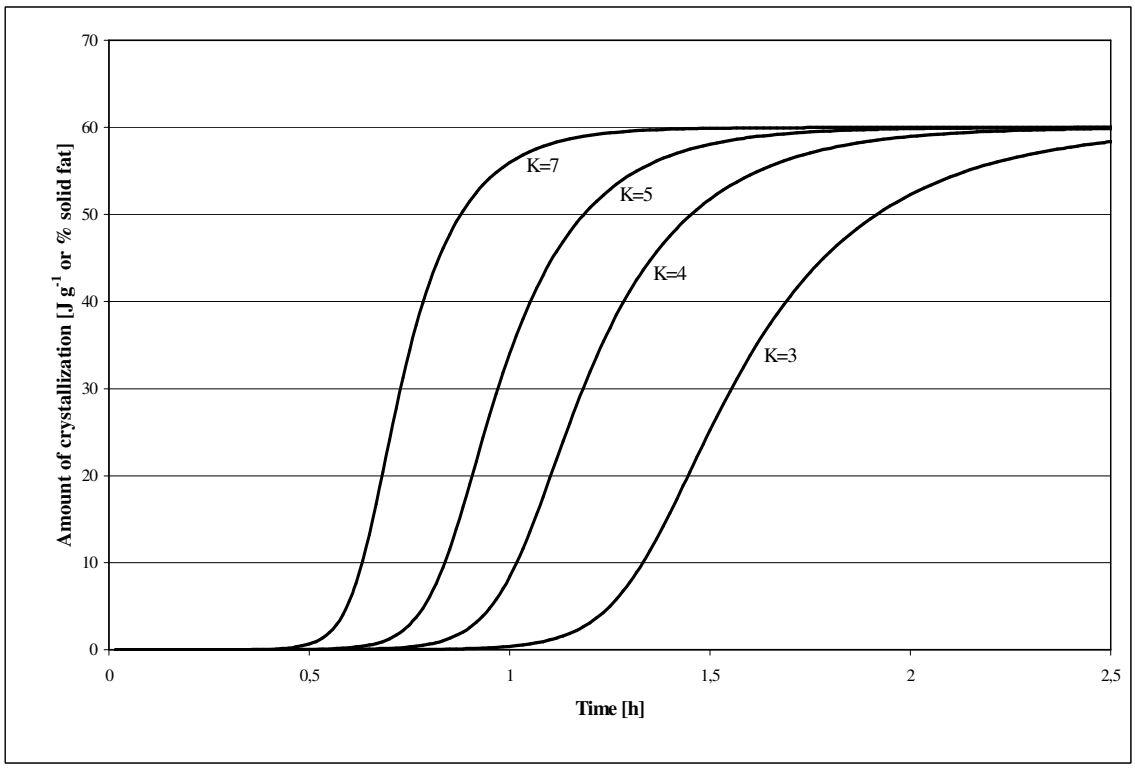

Figure 4.3 Influence of varying *K* [h^{-1}] on the crystallization curve (a_P=60 J g^{-1} or % solid fat, *f(0)*=1.10^{-5} J g^{-1}or % solid fat, *n*=5)

The rate of crystallization obviously increases when the K parameter increases with the result that the higher the value of K is, the shorter the time needed to reach a measurable amount of crystallization and the faster the rest of the crystallization process takes place. In the case of K=3 h^{-1} the crystallization rate is so slow that the plateau has not been reached yet after 2.5 h.

Figure 4.4 shows the influence of varying n between 1.5 and 7.

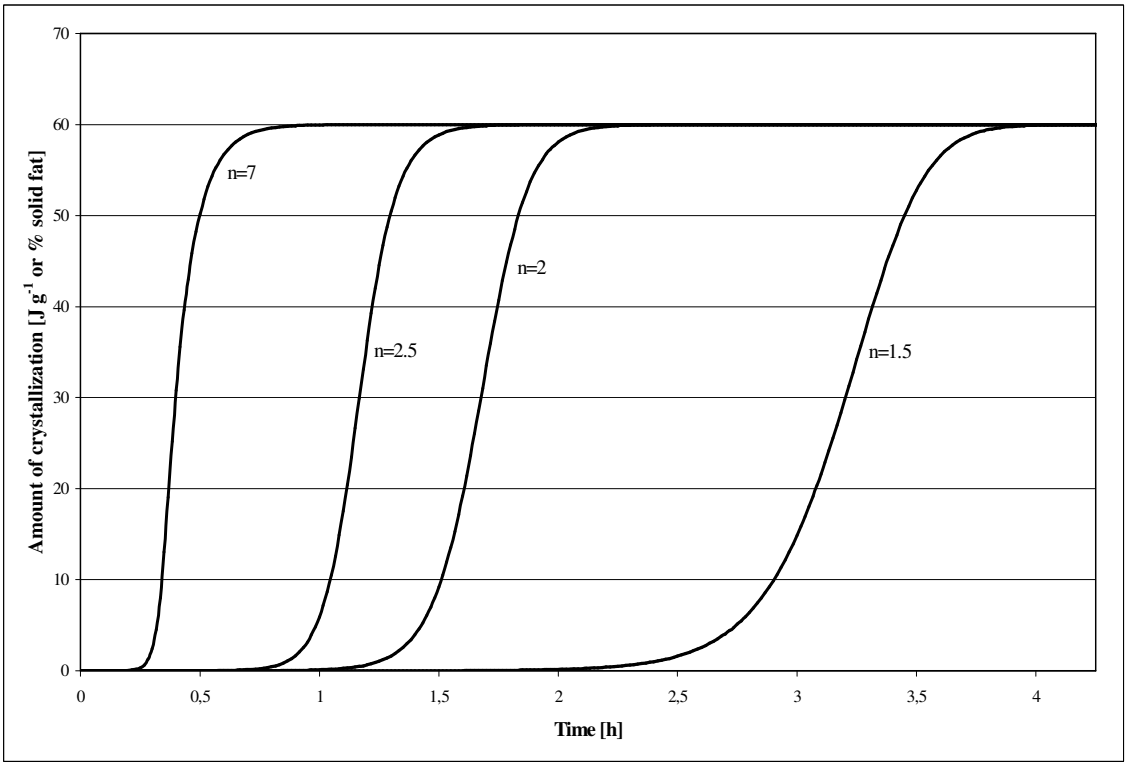

Figure 4.4 Influence of varying n [-] on the crystallization curve (a_P=60 J g^{-1}, K=10 h^{-1}, $f(0)$=1.10^{-5} J g^{-1} or % solid fat)

The parameter n also has an influence on the time needed to reach a measurable amount of crystallization. This can be explained as follows: the higher the n value (the order of the reverse reaction), the faster the term $K\ h^n$ will become negligible and the faster a measurable amount of crystallization will be formed. However, the value of n is also linked with the degree of curve asymmetry. When the value of n is 2, the sigmoid curve is perfectly symmetric. When the value is larger than 2, the beginning of the crystallization process is faster than the end. The more n exceeds 2, the larger the difference between the rates of the beginning and end stages becomes. When the value is smaller than 2, the beginning of the process is slower than the end. This influence of n on the curve asymmetry will be mathematically shown in section 4.4.2.4.3. Figure 4.5 more clearly illustrates the influence of n on the degree of curve asymmetry. In this

figure the time-axis is normalized by rescaling time so that all curves intersect at 50% of their ultimate value.

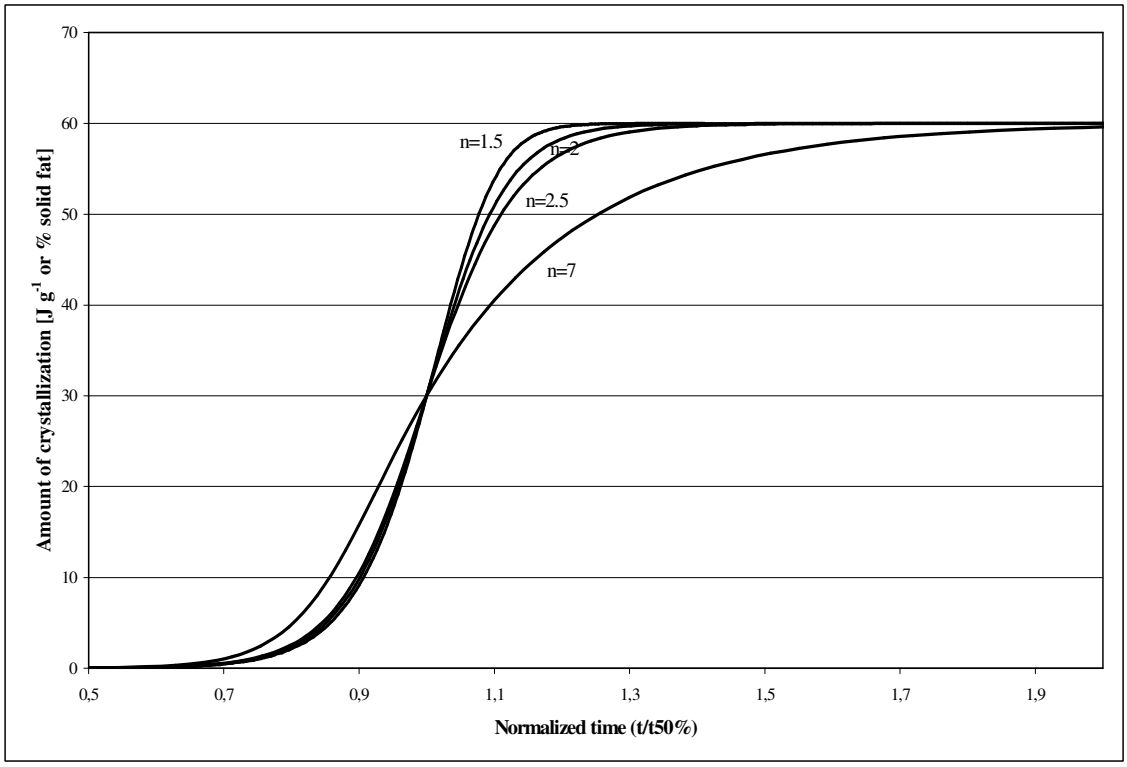

Figure 4.5 Influence of *n* [-] on curve asymmetry (a_P=60 J g^{-1}, K=10 h^{-1}, $f(0)$=1.10^{-5} J g^{-1} or % solid fat)

4.4.1.6 Typical parameter ranges

Table 4.1 shows some typical parameter ranges obtained for the analyzed data series. The parameters obviously show a temperature and sample dependency. The influence of temperature and sample on the model parameters will be discussed further in chapters 6 and 7.

4.4.1.7 *Algebraic solution*

To simplify parameter estimation the simplified model was converted to its algebraic solution, assuming isothermal conditions. To solve the differential equation [4.13] it was rewritten as:

$$h^{-n}\frac{dh}{dt} + K \times h^{1-n} - K = 0 \qquad \textbf{[4.15]}$$

When h^{1-n} was substituted by w, this led to the first order differential equation:

$$\frac{1}{1-n}\frac{dw}{dt} + K \times w = K \qquad \textbf{[4.16]}$$

with as a solution:

$$w = 1 + \left(w(0) - 1\right) \times e^{-(1-n) \times K \times t} \quad \textbf{[4.17]}$$

Re-substitution into the original variable *h* led to:

$$h = \left[1 + \left(h(0)^{1-n} - 1\right) \times e^{-(1-n) \times K \times t} \right]^{\frac{1}{1-n}} \quad \textbf{[4.18]}$$

Taking into account equations [4.10] and [4.12], equation [4.18] was rewritten to obtain an expression of the absolute amount of crystallization *f* as function of time.

$$f(t) = a_P \times \left[1 - \left[1 + \left((1 - \frac{f(0)}{a_P})^{1-n} - 1 \right) \times e^{-(1-n) \times K \times t} \right]^{\frac{1}{1-n}} \right] \quad \textbf{[4.19]}$$

Equation [4.19] can be used in many software packages capable of parameter estimation of non-linear algebraic equations. More details on parameter estimation of the algebraic equation are found in Annex III.4.

Table 4.1 Typical parameter ranges of the proposed model

Data series	a_P **[J g^{-1}]**	K **[h^{-1}]**	n **[-]**	$f(0)$ **[J g^{-1}]**
Cocoa butter isothermally crystallized at 20°C by means of DSC	60 - 70	4 - 7	3 - 6	1.10^{-5} - 1.10^{-3}
Cocoa butter isothermally crystallized at 22°C by means of DSC	55 - 65	2.5 - 3.5	3.5 - 4	1.10^{-3} - 2.10^{-2}
Milk fat samples measured by means of DSC	10 - 20	3 - 12	3 - 6	1.10^{-6} - 1.10^{-3}

4.4.1.8 *Use of induction time as model parameter*

As stated in section 4.4.1.5 the model parameter *f(0)* is related to the induction time of the crystallization process. To make this relationship clearer, *f(0)* was mathematically related to the induction time t_ind_F [h], defined in this study as the time needed to reach *F%* of crystallization, where *F* for example could be 0.01. To obtain a mathematical expression for t_ind_F, *f(t)* (as defined in equation [4.19]) was divided by a_P and put equal to *F*. The following expression for t_ind_F was thus obtained:

$$t\_ind_F = \frac{-\ln\left(\frac{(1-F)^{1-n}-1}{(1-\frac{f(0)}{a_P})^{1-n}-1}\right)}{(1-n)\times K} \qquad \textbf{[4.20]}$$

From equation [4.20] it was concluded that the induction time depends on a_P, *f(0)*, *K* and *n*.

Since the physical interpretation of the parameter induction time is more straightforward than that of the parameter *f(0)*, since the induction time can be more easily found back on a crystallization curve and since the induction time is an important industrial parameter (Ziegleder, 1990), it was decided to represent the model as function of t_ind_F instead of *f(0)*. To realize this, *f(0)* was written as function of t_ind_F and this expression was inserted in equation [4.19]. The algebraic version of the proposed model thus became:

$$f(t) = a_P \times \left[1 - \left[1 + ((1-F)^{1-n} - 1) \times e^{-(1-n)\times K\times(t-t\_ind_F)}\right]^{\frac{1}{1-n}}\right] \qquad \textbf{[4.21]}$$

Another advantage of equation [4.21] is that the error on the parameter estimate of t_ind_F is smaller than the one on *f(0)*. Parameter estimation of the differential equation with t_ind_F as one of the parameters, was also worked out in WEST (see Annex III.3.4).

Equation [4.21] was preferred for parameter estimation in this study.

4.4.1.9 *Nature of reverse reaction*

The proposed model comprises a first order forward reaction and a reverse reaction of order *n* (equation [4.13]). To gain more insight into the nature of this reverse reaction and its effect on the crystallization process, Figure 4.6 shows a graph in which the two reactions of the proposed model are separately plotted. The rate of the first order

forward reaction is represented by dh/dt_1, the rate of the reverse reaction by dh/dt_2. It has to be stressed that the values of dh/dt_1 and dh/dt_2 are calculated on the basis of the h value of the complete model. That is why dh/dt_1 and dh/dt_2 do not represent the situation when only that part of the reaction takes place.

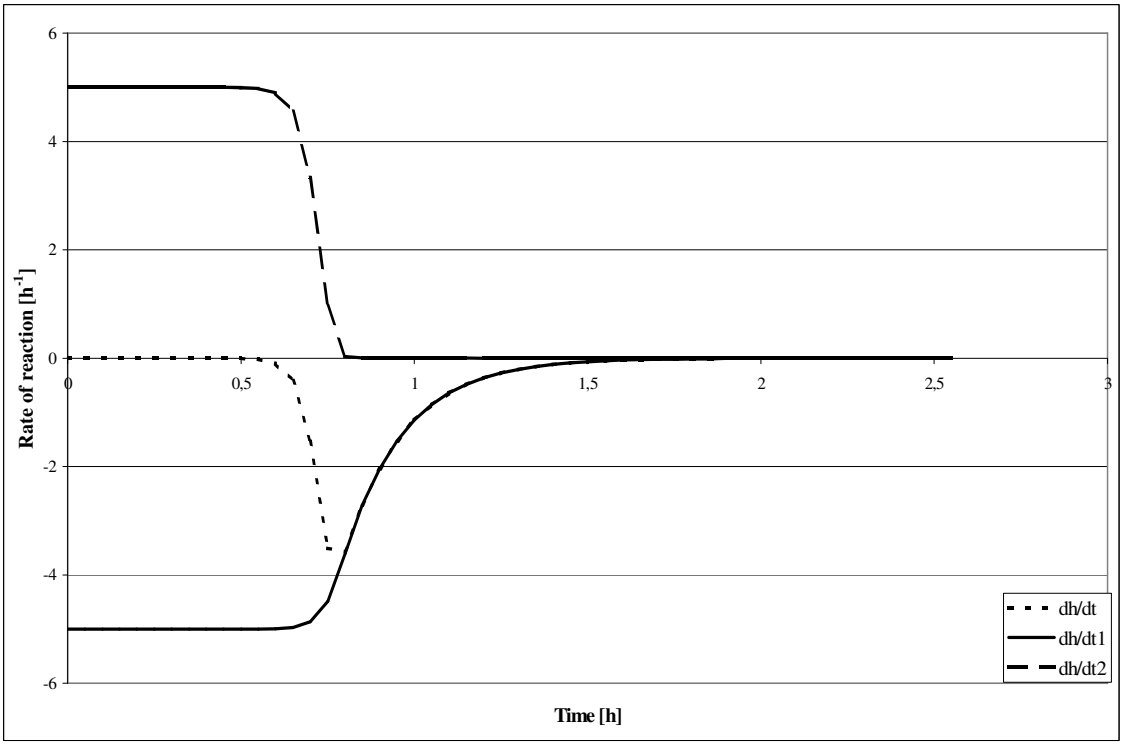

Figure 4.6 Split-up of the proposed model in its two components: forward and reverse reaction

From Figure 4.6 it can be deduced that initially the two reactions nearly have the same rate and thus the overall rate dh/dt is nearly zero and the amount of crystallization remains at a very low level. At a certain moment dh/dt_2 starts to decrease quicker than dh/dt_1 which makes that dh/dt increases (to negative values) and thus the amount of crystallization also increases. At a certain moment dh/dt_2 becomes zero and thus dh/dt is only influenced by the forward reaction. The higher the value of n, the faster the rate of the reverse reaction decreases and the faster it ultimately loses its effect.

Several hypotheses were formulated concerning the detailed nature of the reverse reaction:

(i) As the forward reaction takes place, latent heat of crystallization is released. Locally, this causes the temperature to rise, which may lead to a local melting of crystals if the local temperature rises above the melting point of these crystals. As the rate of the forward reaction decreases, the amount of

local latent heat released will decrease and consequently the rate of the reverse reaction will also decrease.

(ii) Formed crystals may redissolve. This possibility was proposed by Smith et al. (2001) who showed that, at thermal equilibrium, an exchange of molecules between pools in solid and dissolved form takes place. Their experiments were performed on a model system of β crystals of tripalmitin as the solid phase, and tripalmitin dissolved in a medium chain triacylglycerol oil as the liquid phase. A surface specific exchange rate of 11 mg h^{-1} m^{-2} was obtained. It could be argued that a similar phenomenon takes place during crystallization. As the crystallization goes on, the surface to volume ratio decreases due to crystal growth and thus the rate of the reverse reaction decreases.

(iii) A combination of several processes takes place: e.g. a combination of remelting, redissolving and diffusion of the molecules away from the crystals. It is possible that the importance of each process depends on the crystallization temperature. The values of *n* well above one are an argument in favour of this hypothesis. For a simple remelting or redissolving reaction, a reaction order around one would be expected.

Counterdiffusion of non-crystallizing species away from the crystal surface as suggested by Hartel (1992) was another possibility. But then an increase of the rate of the reverse reaction would be expected since the concentration of non-crystallizing species will probably increase as function of time. Since the rate of the reverse reaction decreases with time (Figure 4.6) this hypothesis seems less plausible.

It may be possible to get a clearer view on the detailed nature of the reverse reaction when the influence of temperature and chemical composition on the value of *n* is studied (chapter 6 and 7).

4.4.2 Model comparison

The four models - Avrami with and without induction time, Gompertz and proposed model - were compared with the mathematical model selection criteria as described in section 4.3.5 (section 4.4.2.1) and by visual comparison of their quality of fit (section 4.4.2.2). The errors on the parameter estimates were compared too (section 4.4.2.3). To gain a clear insight into the differences between the models their ability to fit

asymmetric curves was investigated (section 0). Section 0 summarizes the differences between the models.

4.4.2.1 Mathematical model selection based on quality of fit

For each data series, Table 4.2 shows the results of the model selection using the different mathematical model selection criteria (see section 4.3.5).

The four information criteria (FPE, AIC, BIC and LILC) and the PRESS criterion give the same result for most of the data series: the proposed model performs the best for most of the data series (between 41 and 44 out of 53). For some data series the quality of fit of both the Gompertz and the proposed model is so similar that, depending on the criterium either the Gompertz model or the proposed model is selected.

The statistical F-test showed that for all data series the proposed model with four parameters performs significantly ($\alpha = 0.01$ except for one data series, $\alpha = 0.05$) better than the Avrami model without induction time having only three parameters, and for most of the data series (41 out of 53) also significantly better than the Gompertz model also only having three parameters.

To gain a better insight in the magnitude of the difference between the Gompertz and the proposed model the values for the mean sum of squared residuals (MSR) (= $SSR/(N_d-n_p)$) for both models are presented in Table 4.3 for each data series. The MSR value consists of the measurement error and the model error. Since the measurement error can be assumed as constant, the model is better when the value of MSR is lower, and the larger the difference is between the values for MSR, the larger the difference is between the quality of the models. From Table 4.3 it can be deduced that the MSR value is much more constant for the proposed model than for the Gompertz model. For some data series the values for the Gompertz model are only slightly higher, and for some data series even slightly lower than for the proposed model, while for other data series the MSR value for the Gompertz model is much higher than the one for the proposed model. For the data series where the proposed model performs worse, the difference between the two values is small. These results indicate that the proposed model is more flexible in describing the crystallization kinetics of fats. It gives a good fit for all the data series used in this study, while the Gompertz model gives some very good fits as well as some significantly poorer fits.

Table 4.2 Model selected on the basis of different model selection criteria. A = Avrami, Ai = Avrami with induction time, G = Gompertz, P = proposed

Data series[1]	FPE	AIC	BIC	LILC	PRESS	F-test (α=0.01) [1]α=0.05	Run test	Auto-correlation test
CB A/20 (1) DSC	P	P	P	P	P	P	P	A/Ai/P/G
CB A/20 (2) DSC	P	P	P	P	P	P	P	A/Ai/P/G
CB A/20 (3) DSC	P	P	P	P	P	P	P	P
CB B/20 (1) DSC	P	P	P	P	P	P	G	A/Ai/P/G
CB B/20 (2) DSC	P	P	P	P	P	P	P	A/Ai/P/G
CB B/20 (3) DSC	P	P	P	P	P	P	P	A/Ai/P
CB C/20 (1) DSC	P	P	P	P	P	P	P	P
CB C/20 (2) DSC	P	P	P	P	P	P	P	Ai/P/G
CB C/20 (3) DSC	P	P	P	P	P	P	P	P/G
CB D/20 (1) DSC	P	P	P	P	P	P	P	A/Ai/P
CB D/20 (2) DSC	P	P	P	P	P	P	P	A/Ai/P/G
CB D/20 (3) DSC	G	G	G	G	G	G	G	P/G
CB E/20 (1) DSC	G	G	G	G	G	G[1]	P/G	A/Ai/P/G
CB E/20 (2) DSC	P	P	P	P	G	P	P	A/Ai/P/G
CB E/20 (3) DSC	G	G	G	G	G	G	P	P
CB F/20 (1) DSC	P	P	P	P	P	P	P	A/Ai/P/G
CB F/20 (2) DSC	G	G	G	P	P	G	P	P/G
CB F/20 (3) DSC	P	P	P	P	P	P	P	A/Ai/P/G
CB G/20 (1) DSC	G	G	G	G	G	P/G	P	A/Ai/P/G
CB G/20 (2) DSC	P	P	P	P	P	P	Ai/P	A/Ai/P/G
CB G/20 (3) DSC	P	P	P	P	P	P	P	A/Ai/P/G
CB H/20 (1) DSC	P	G	G	P	G	P/G	P	P/G
CB H/20 (2) DSC	G	G	G	G	G	G	G	A/Ai/P/G
CB H/20 (3) DSC	G	G	G	G	G	G[1]	Ai/P	A/Ai/P/G
CB I/20 (1) DSC	P	P	P	P	P	P	P	A/Ai/P/G
CB I/20 (2) DSC	P	P	P	P	P	P	P	A/Ai/P/G
CB I/20 (3) DSC	P	P	P	P	P	P	P	P/G
CB J/20 (1) DSC	G	G	G	G	G	P/G	P	A/Ai/P/G
CB J/20 (2) DSC	P	P	P	P	P	P	P	A/Ai/P/G
CB J/20 (3) DSC	P	P	P	P	P	P[1]	G	A/Ai/P/G
CB K/20 (1) DSC	P	P	P	P	P	P	P	P
CB K/20 (2) DSC	P	P	P	P	P	P	P	P
CB K/20 (3) DSC	P	P	P	P	P	P	P	P
CB L/20 (1) DSC	G	G	G	G	G	P/G	P	P
CB L/20 (2) DSC	G	G	G	G	G	G	P	P
CB L/20 (3) DSC	P	P	P	P	P	P	Ai/P	A/Ai/P/G
CB M/20 (1) DSC	P	P	P	P	P	P	Ai/P	Ai/P/G
CB M/20 (2) DSC	P	P	P	P	P	P	Ai/P/G	A/Ai/P/G
CB M/20 (3) DSC	P	P	P	P	P	P	P	P
CB N/20 (1) DSC	P	P	P	P	P	P	P	A/Ai/P/G
CB N/20 (2) DSC	P	P	P	P	P	P	P	G
CB N/20 (3) DSC	P	P	P	P	P	P	P	P/G
CB N/19 DSC	P	P	P	P	P	P	Ai/P	Ai/P/G
CB N/21 DSC	P	P	P	P	P	P	P	A/Ai/P/G
CB N/22 DSC	P	P	P	P	P	P	P	P/G
CB N/23 DSC	P	P	P	P	P	P	P	P
MF A/20.7 DSC	P	P	P	P	P	P	Ai/P	Ai/P
MF A/23.7 DSC	P	P	P	P	P	P	P	P/G
MF B/23.7 DSC	P	P	P	P	P	P	P	A/Ai/P/G
MF C/23.7 DSC	P	P	P	P	P	P	P	A/Ai/P/G
MF D / 17.5 pNMR	G	G	P	P	P	P/G	P	A/Ai/P/G
MF E / 21.5 pNMR	P	P	P	P	P	P[1]	Ai/P/G	A/Ai/P/G
MF F / 26 pNMR	P	P	P	P	P	P	Ai/P	A/Ai/G/P
Model A selected	0/53	0/53	0/53	0/53	0/53	0/53	0/53	0/53
Model Ai selected	0/53	0/53	0/53	0/53	0/53	0/53	0/53	0/53
Model P selected	42/53	41/53	42/53	44/53	42/53	41/53	39/53	10/53
Model G selected	11/53	12/53	11/53	9/53	11/53	7/53	4/53	1/53
Models P/G selected	0/53	0/53	0/53	0/53	0/53	5/53	1/53	8/53
Model Ai/P selected	0/53	0/53	0/53	0/53	0/53	0/53	7/53	1/53
Models Ai/P/G selected	0/53	0/53	0/53	0/53	0/53	0/53	2/53	3/53
Models A/Ai/P selected	0/53	0/53	0/53	0/53	0/53	0/53	0/53	2/53
All models equal	0/53	0/53	0/53	0/53	0/53	0/53	0/53	28/53

[1] Sample (CB = cocoa butter, MF = milk fat) / crystallization temperature (number of repetition) measuring technique

When modelling, the residuals are assumed to be random and independent. As explained in section 4.3.5, the run and auto-correlation tests give an idea of how good this assumption is satisfied. For the DSC as well as the pNMR measurements the value for the run test should be around 10 (knowing that the number of data points fluctuates around 20). The values obtained for each of the four models are between 3 and 6 for most data series. The model with the highest number of sign changes can be regarded as the best. Table 4.2 shows that for nearly all data series the proposed model was selected as (one of) the best.

The auto-correlation may only be larger than 0.44 (approximate value for $1.96/\sqrt{N}$) for 1 time lag (i.e. 5% of the 18 calculated lags). For the proposed model a maximum of one auto-correlation above the threshold was found for all data series. For the other models a limited number of data series showed more than one auto-correlation above the threshold. In Table 4.2 the model with the lowest amount of auto-correlations above the threshold was indicated as the best.

4.4.2.2 Visual model selection

Besides mathematical tools, the quality of a model can also be assessed visually. Figure 4.7 to Figure 4.10 show the measured data points and the predicted curves calculated with the Avrami (with and without induction time), the Gompertz and the proposed model and the residuals for each of the models. Figure 4.7 and Figure 4.8 represent data series CB N/19, for which the difference between the Gompertz and the proposed model is the largest in favour of the proposed model, while Figure 4.9 and Figure 4.10 represent data series CB D/20(3), for which the difference between the two models is the largest in favour of the Gompertz model. For both data series it is obvious that the Gompertz and the proposed models are much closer to the data than the Avrami model. For data series CB N/19 (Figure 4.7 and Figure 4.8) the Avrami model with induction time seems to have a comparable quality of fit with the Gompertz model, a fit which is however considerably worse than that of the proposed model. For data series CB D/20(3) the fit of the Avrami model with induction time is worse than those of the Gompertz and the proposed models. When comparing the Gompertz and proposed models it can be seen that for data series CB N/19 (Figure 4.7 and Figure 4.8) the Gompertz model still deviates quite a lot from the measured data points, while the proposed model hardly shows any deviation from the data points. For data series CB D/20(3) (Figure 4.9 and Figure 4.10) both models fit the data points very well, the

Table 4.3 Values for the mean sum of squared residuals (MSR) for the Gompertz and proposed model

Data series[1]	MSR Gompertz	MSR proposed
CB A/20 (1) DSC	0.345	0.117
CB A/20 (2) DSC	0.250	0.115
CB A/20 (3) DSC	0.244	0.076
CB B/20 (1) DSC	0.092	0.038
CB B/20 (2) DSC	0.073	0.035
CB B/20 (3) DSC	0.213	0.003
CB C/20 (1) DSC	1.630	0.003
CB C/20 (2) DSC	0.895	0.085
CB C/20 (3) DSC	0.621	0.041
CB D/20 (1) DSC	0.345	0.097
CB D/20 (2) DSC	0.138	0.021
CB D/20 (3) DSC	0.046	0.318
CB E/20 (1) DSC	0.044	0.079
CB E/20 (2) DSC	0.063	0.037
CB E/20 (3) DSC	0.017	0.093
CB F/20 (1) DSC	0.562	0.055
CB F/20 (2) DSC	0.010	0.057
CB F/20 (3) DSC	0.478	0.059
CB G/20 (1) DSC	0.128	0.180
CB G/20 (2) DSC	0.328	0.116
CB G/20 (3) DSC	0.431	0.215
CB H/20 (1) DSC	0.138	0.127
CB H/20 (2) DSC	0.017	0.120
CB H/20 (3) DSC	0.045	0.095
CB I/20 (1) DSC	0.409	0.061
CB I/20 (2) DSC	0.638	0.012
CB I/20 (3) DSC	0.282	0.039
CB J/20 (1) DSC	0.107	0.127
CB J/20 (2) DSC	0.213	0.096
CB J/20 (3) DSC	0.087	0.072
CB K/20 (1) DSC	0.228	0.075
CB K/20 (2) DSC	0.109	0.032
CB K/20 (3) DSC	0.117	0.031
CB L/20 (1) DSC	0.075	0.084
CB L/20 (2) DSC	0.034	0.100
CBL/20 (3) DSC	0.085	0.040
CB M/20 (1) DSC	0.193	0.070
CB M/20 (2) DSC	0.605	0.098
CB M/20 (3) DSC	0.194	0.014
CB N/20 (1) DSC	0.637	0.085
CB N/20 (2) DSC	0.576	0.142
CB N/20 (3) DSC	0.286	0.007
CB N/19 DSC	1.831	0.010
CB N/21 DSC	0.092	0.025
CB N/22 DSC	0.095	0.007
CB N/23 DSC	0.280	0.053
MF A/20.7 DSC	0.084	0.029
MF A/23.7 DSC	0.010	0.001
MF B/23.7 DSC	0.150	0.073
MF C/23.7 DSC	0.036	0.012
MF D /17.5 pNMR	0.047	0.042
MF E /21.5 pNMR	0.036	0.018
MF F /26 pNMR	0.464	0.065
Mean	0.286	0.071
Minimum	0.010	0.001
Maximum	1.831	0.318

[1] Sample (CB = cocoa butter, MF = milk fat) / crystallization temperature (number of repetition) measuring technique

Gompertz model performing a little better in the beginning of the crystallization process.

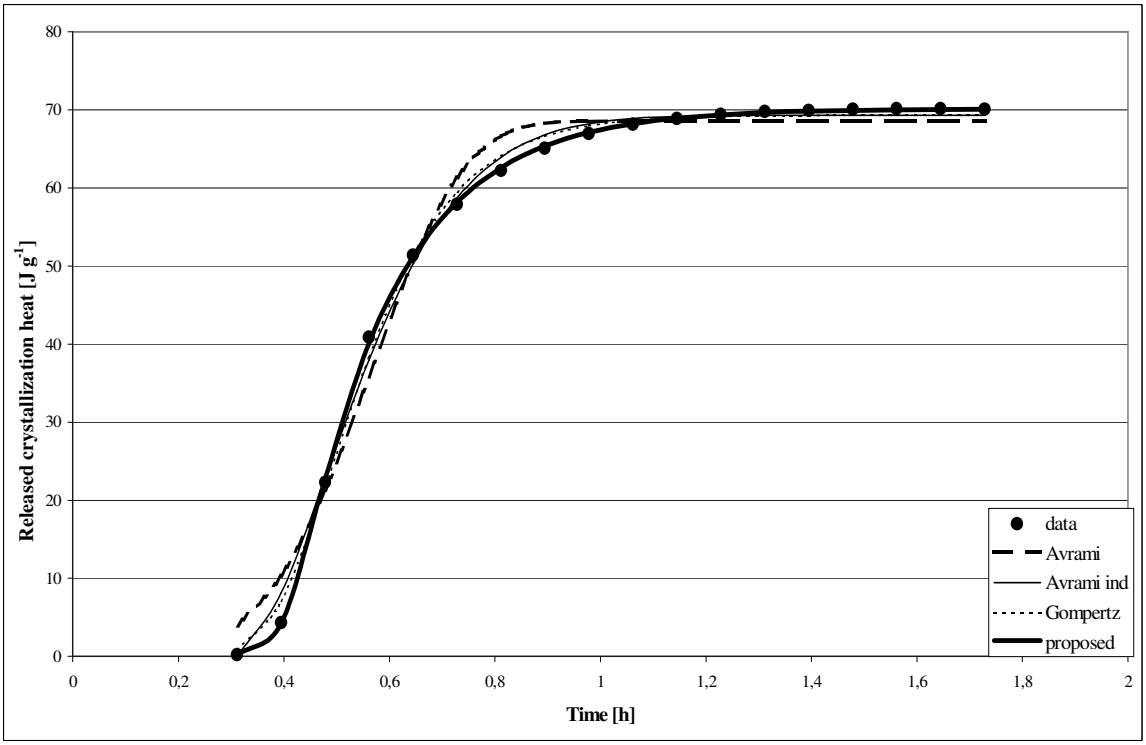

Figure 4.7 Visual representation of the quality of fit of the different models: measured data points and predicted curves for the four models for data series CB N/19 as measured by DSC

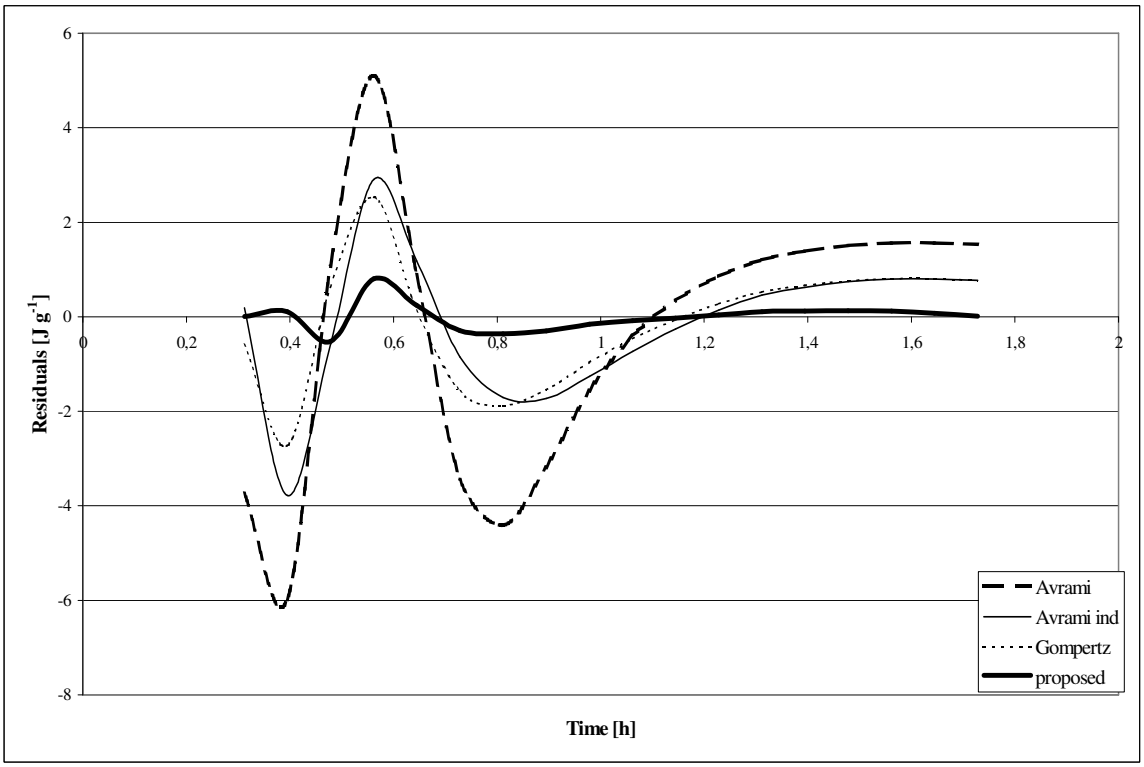

Figure 4.8 Visual representation of the quality of fit of the different models: residuals as function of time for the four models for data series CB N/19 as measured by DSC

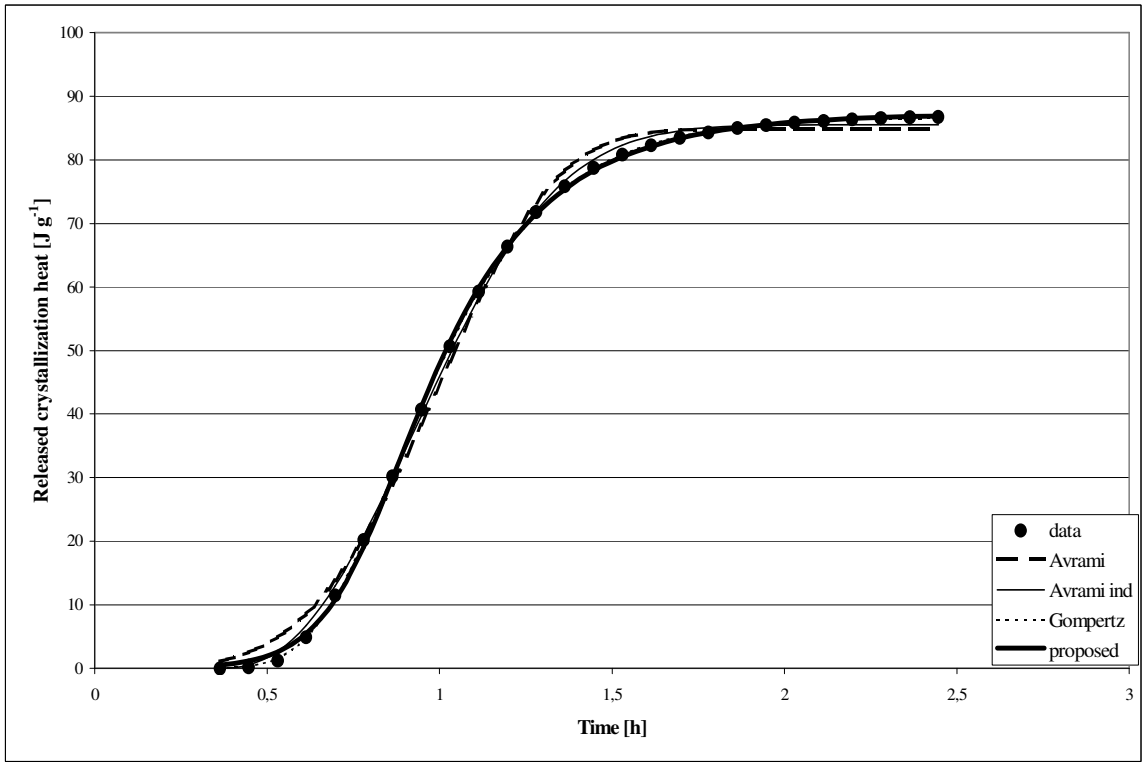

Figure 4.9 Visual representation of the quality of fit of the different models: measured data points and predicted curves for the four models for data series CB D/20(3) as measured by DSC

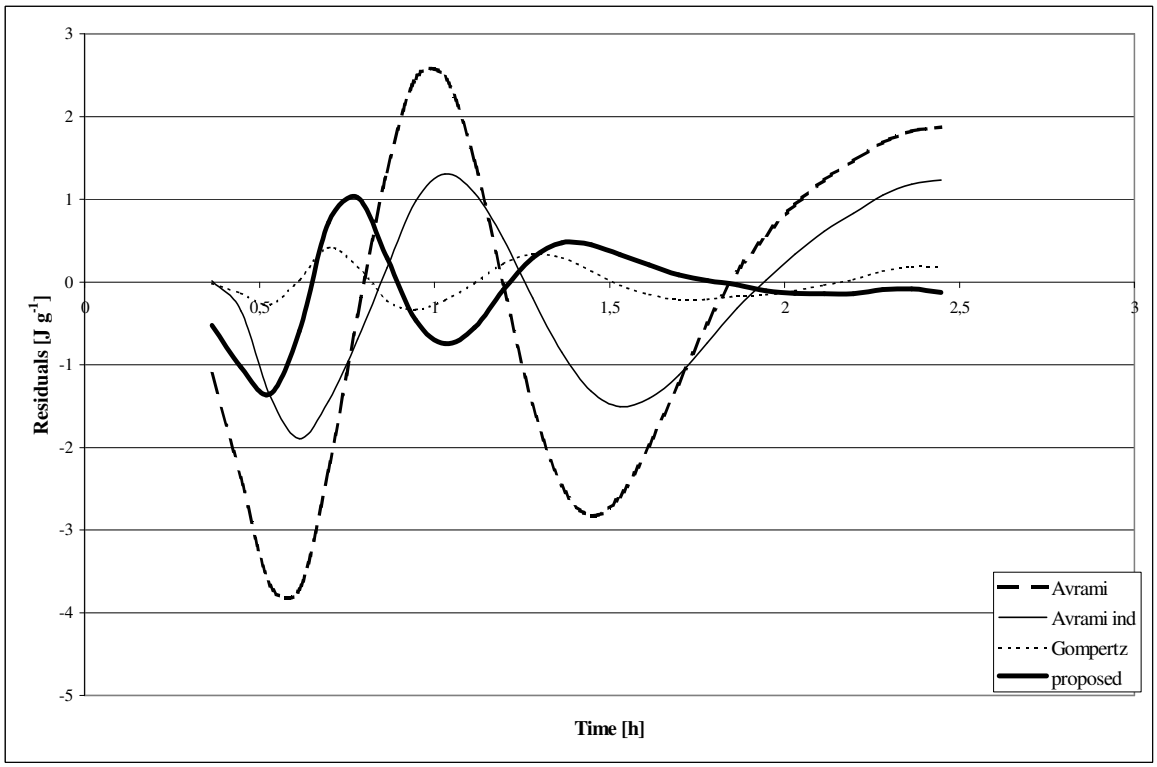

Figure 4.10 Visual representation of the quality of fit of the different models: residuals as function of time for the four models for data series CB D/20(3) as measured by DSC

4.4.2.3 Errors on parameter estimates

Table 4.4 compares the errors on the parameter estimates as calculated by Sigmaplot (and confirmed by WEST for the proposed model) for each model.

The table shows that the errors are largest for the Avrami model (with and without induction time). The errors on the parameter estimates of the Gompertz and proposed models are of similar magnitude, except for the error on the *n* parameter of the proposed model, which is higher. However, this was to be expected since more parameters have to be estimated from the same data series.

Table 4.4 Comparison of the errors on the parameter estimates (mean values are reported and parameters with a comparable meaning are reported on the same line)

Avrami		**Avrami induction**		**Gompertz**		**Proposed**	
Parameter	**Error [%]**	**Parameter**	**Error [%]**	**Parameter**	**Error [%]**	**Parameter**	**Error [%]**
k	10	k	7.5	μ_G	1.5	K	1.5
m	5	m	7.5				
		t_ind_A	7.5	λ_G	0.75	t_ind_F	1.5
a_A	1	a_A	0.5	a_G	0.25	a_P	0.2
						n	4

4.4.2.4 Ability to fit asymmetric curves

To gain a clear insight into the differences between the models, their ability to fit an asymmetric curve was tested. The asymmetry of a curve was defined as:

$$asym = \frac{t_{90\%} - t_{50\%}}{t_{50\%} - t_{10\%}} \quad \textbf{[4.22]}$$

where $t_{F\%}$ [h] is the time needed to reach $F\%$ crystallization. A symmetric curve has a value of 1 for *asym*. Of course, alternatives with other percentages of crystallization are also possible to define the asymmetry of the crystallization curves.

The *asym* value was calculated for the four models. First, the time needed to reach $F\%$ of crystallization was calculated as function of the model parameters. The thus obtained formula with different values for F was used to calculate the *asym* value according to equation [4.22].

4.4.2.4.1 Avrami model (with and without induction time)

For the original Avrami model $t_{F\%}$ was calculated from equation [4.1] as:

$$t_{F\%} = \sqrt[m]{\frac{-\ln(1-F)}{k}} \quad \textbf{[4.23]}$$

After some simplifications, the *asym* value could be written as:

$$asym = \frac{\sqrt[m]{-\ln 0.1} - \sqrt[m]{-\ln 0.5}}{\sqrt[m]{-\ln 0.5} - \sqrt[m]{-\ln 0.9}} \quad \textbf{[4.24]}$$

For the Avrami model with induction time the same expression for *asym* was obtained.

From equation [4.24] it was deduced that the asymmetry of the Avrami model (with and without induction time) is only dependent on the value of the Avrami exponent *m*. Also was calculated that the Avrami model is symmetric for *m* equal to 3.26. For *m* values higher than 3.26, the *asym* value is lower than 1, meaning that the start of the crystallization process is slower than the end. The inverse is valid for *m* values lower than 3.26. The value of 3.26 is independent of the values for *F%* chosen in the definition of the *asym* value.

The values of *m* of the original Avrami model obtained for the crystallization experiments described in this chapter ($3 < m < 6$) coincide with *asym* values around 1 or smaller, meaning that the start of the crystallization is slower than the end. This is, however, not concordant with the experimental data (see e.g. Figure 4.7 and Figure 4.8), which may explain why the Avrami model does not provide good fits.

The Avrami model with induction time takes account of the induction time before the start of crystallization. Obtained *m* values for the Avrami model with induction time coincide with *asym* values larger than 1, which is concordant with the experimental data. This probably explains why the Avrami model with induction time fits the data significantly better than the original Avrami model.

4.4.2.4.2 Gompertz model

From equation [4.3] $t_{F\%}$ was calculated as:

$$t_{F\%} = \lambda - \frac{a_G}{\mu_G \times e} \times (\ln(-\ln(F)) - 1) \quad \textbf{[4.25]}$$

After simplification this led to:

$$asym = \frac{-\ln(-\ln(0.9)) + \ln(-\ln(0.5))}{-\ln(-\ln(0.5)) + \ln(-\ln(0.1))} = 1.57 \quad \textbf{[4.26]}$$

This proved that the *asym* value is fixed at 1.57 for the Gompertz model, an important feature of this model since it means that it does not offer any flexibility concerning the asymmetry of the curve. This probably explains why the Gompertz model fits certain datasets very well (those showing an *asym* value around 1.57) and others considerably worse. The calculation of the *asym* value can therefore be used as a method of a priori model selection, since the evaluation of the *asym* value of a data series would allow to decide beforehand whether the Gompertz model will fit well or not.

4.4.2.4.3 Proposed model

The same calculations were performed on the algebraic solution of the proposed model (equation [4.19]). For $t_{F\%}$ this resulted in:

$$t_{F\%} = \frac{-\ln\left(\frac{(1-F)^{1-n}-1}{\left(1-\frac{f(0)}{a_P}\right)^{1-n}-1}\right)}{(1-n)\times K} \quad \textbf{[4.27]}$$

After some simplifications equation [4.27] led to:

$$asym = \frac{\ln(0.5^{1-n}-1) - \ln(0.1^{1-n}-1)}{\ln(0.9^{1-n}-1) - \ln(0.5^{1-n}-1)} \quad \textbf{[4.28]}$$

From equation [4.28] it was deduced that the asymmetry of the proposed model is only dependent on *n*. For *n* equal to 2, a symmetric curve is obtained. Table 4.5 gives the *asym* values for some selected values of the model parameter *n*.

4.4.2.4.4 Alternative definition for model (a)symmetry

An alternative method to define the symmetry of a curve was also explored. A symmetric model was defined as a model for which the *f* value at the inflection point equals 0.5 *a*, meaning that exactly half of the attainable crystallization is already reached at the inflection point. This way of defining the symmetry led to precisely the same results: the Avrami model is symmetric for an *m* value of 3.26, the Gompertz model is never symmetric and the proposed model is symmetric for an *n* value of 2.

Table 4.5 Relationship between the model parameter *n* of the proposed model and the asymmetry of the curve

n	***asym***
1.5	0.81
2	1
3	1.37
4	1.69
5	1.94
6	2.12
7	2.27
8	2.37

4.4.2.5 Summary of model comparison

The newly developed model is capable of describing the isothermal crystallization kinetics of fats much better than the generally used Avrami model. Several authors (Metin & Hartel, 1998, Toro-Vazquez et al., 2000, Wright et al., 2000 and Ziegleder, 1990) using the Avrami model have described the fit as very good, stating a correlation coefficient always larger than 0.96 (Wright et al., 2000), an R-value between 0.993 and 0.998 (Metin & Hartel, 1998) and a regression coefficient larger than 0.998 (Toro-Vazquez et al., 2000). In this study, a mean value for R^2 of 0.9998 (R = 0.9999) was obtained for the proposed model. Moreover, Figure 4.7 to Figure 4.10 show that the fit for the Avrami model is far from being perfect when compared to the one of the proposed model. It has to be remarked that Metin & Hartel (1998) and Toro-Vazquez et al. (2000) linearized the Avrami model to estimate its parameters (which is statistically questionable, see Annex III.1) while in this study non-linear regression was used to fit the data.

The Avrami model with induction time fits the data significantly better than the original Avrami model and this for most of the data series (detailed results not presented). However, the fit of the proposed model is still much better.

The Gompertz model introduced by Kloek et al. (2000) already offers a large improvement compared to the Avrami model. This can be seen in Figure 4.7 to Figure 4.10 and as well when comparing the values for the information and PRESS criteria (detailed data not presented). When the Gompertz model is compared with the Avrami

model with induction time, the Gompertz model nearly always performs better even though it uses one parameter less.

The proposed model, however, performs even better than the Gompertz model and this for the majority of the data series. Also, it offers the advantage that it fits all data series used (different fats, different crystallization temperatures, different measuring methods) nearly as good, while the Gompertz model performs excellent on certain data series but significantly poorer on others. This is most probably related to the fact that the Gompertz model does not offer any flexibility regarding the model asymmetry whereas for the proposed model the asymmetry can take any value by changing the value of the parameter n.

The errors on the parameter estimates are of the same order of magnitude for the proposed model as for the Gompertz model, except for one parameter of the proposed model, that has a higher error because an extra parameter has to be estimated. The errors on the Avrami parameter estimates (with and without induction time) are higher.

An additional advantage of the proposed model is that it has been built in the form of a differential equation, making it easier to give a mechanistic interpretation (compare equation [4.13] to equations [4.1], [4.2], [4.3] and [4.21]) and to apply the model in non-isothermal conditions for example. Moreover, an analytical solution is available for the isothermal situation, facilitating non-linear parameter estimation in a multitude of software packages.

4.5 Conclusions

A new model able to describe the isothermal crystallization kinetics of fats was developed. The model was built in the form of a differential equation, but the analytical solution under isothermal conditions was also calculated. It was proved that the proposed model always performs better than the often-used Avrami model (with and without induction time) and performs better than the Gompertz model for the majority of the data series. The main difference between the Gompertz and the proposed model is the flexibility of the latter to fit crystallization curves with different degrees of asymmetry. The universality of the proposed model was shown by fitting the model to data series obtained by crystallizing two completely different fats (cocoa butter and milk fat) at different temperatures and using different measuring techniques.

5 MULTI-METHODOLOGICAL INVESTIGATION OF THE ISOTHERMAL COCOA BUTTER CRYSTALLIZATION

5.1 Introduction

5.1.1 X-ray diffraction and recent developments

X-rays are electromagnetic radiation with typical photon energies in the range of 100 eV - 100 keV. For diffraction applications, only short wavelength X-rays (hard X-rays) are used. Because the wavelength of X-rays is comparable to the size of atoms, they are ideally suited for probing the structural arrangement of atoms and molecules in a wide range of materials (Materials Research Laboratory, 2003). If suitable single crystals are available, X-ray diffraction analysis permits determination of the atomic positions in the unit cell with high precision, from which in turn the molecular conformation can be derived. Most of the information obtained by X-ray diffraction on crystals of triacylglycerols is, however, based on the study of polycrystalline materials using X-ray powder diffraction methods (Kellens, 1992).

Depending on the detection angle relative to the incoming ray, small angle X-ray diffraction (SAXS) and wide angle X-ray diffraction (WAXD) can be differentiated. Bragg's law (equation [5.1]), describing the relationship between the scattering angle θ [°] and the distance between the reflecting entities d [Å], shows that large distances scatter at small angles and that this angle also depends on the wavelength used (λ [Å]).

$$s = \frac{1}{d} = \frac{2\sin\theta}{\lambda} \qquad \textbf{[5.1]}$$

Historically, WAXD intensities are presented as function of 2θ, while SAXS curves are drawn as function of s [$Å^{-1}$], the reciprocal distance (Goderis & Reynaers, 2002).

X-rays are produced generally by either X-ray tubes or synchrotron radiation. In an X-ray tube, which is the primary X-ray source used in laboratory X-ray instruments, X-rays are generated when a focused electron beam accelerated across a high voltage field bombards a stationary or rotating solid target. A typical experiment using such laboratory X-ray instruments easily takes more than an hour and these instruments are thus not suited to perform measurements under DSC conditions. Therefore, in recent

years, synchrotron facilities have become widely used as preferred sources for X-ray diffraction measurements. These powerful sources are thousands to millions of times more intense than laboratory X-ray tubes allowing the exposure time to be reduced to a few seconds or even less. Synchrotron radiation is emitted when electrons are travelling at near light speed and are obliged to change direction under the influence of a magnetic field (Goderis & Reynaers, 2002 and Materials Research Laboratory, 2003).

5.1.2 Isothermal phase behaviour of cocoa butter

Cocoa butter polymorphism as described in section 2.4.3 has a large impact on the product quality of chocolate and confectioneries. Knowledge of the (isothermal) phase behaviour of cocoa butter is therefore of utmost importance to optimize production processes and to maintain product quality (Van Malssen et al., 1999).

Based on the melting range, Ziegleder (1990) concluded that under conditions of isothermal crystallization at temperatures between 19°C and 23°C cocoa butter crystallizes in the β' polymorph. With XRD, Metin & Hartel (1998) showed that after three hours of isothermal crystallization at 17°C also the β' polymorph was formed.

Van Malssen et al. (1999) developed a cocoa butter phase scheme covering all isothermal phase transitions in the temperature range from –20°C to 40°C and a time span of ten days based on wide-angle X-ray diffraction (WAXD) measurements. Using WAXD, the short spacings that are characteristic of each polymorph (see section 1.3.1) can be determined. The phase scheme shows that the initial cocoa butter polymorph depends heavily on the crystallization temperature. At temperatures lower than 21°C α crystals are formed within a time span of seconds to minutes. Below 4°C γ crystals are formed. Between 22 and 27°C β' crystals develop within a time span of hours to days. Above 28°C no sign of crystallization is observed. The initially formed polymorphs can transform into more stable polymorphs: below 4°C γ crystals rather quickly transform into α, above 4°C α crystals transform into the β' phase and above 14°C β' crystals transform into the most stable β phase.

Van Langevelde et al. (2001) used small angle X-ray scattering (SAXS) to study the isothermal crystallization of cocoa butter. Using SAXS, the long spacings, i.e. the thickness of the layers formed by the side-by-side arrangement (see also section 1.3.4), can be determined. Apart from the packing mode (2L or 3L) and the length of the molecules the long spacings also depend on the angle of tilt between the chain axis and

the methyl end group plane. So the long spacings can also provide valuable information on the different polymorphs of cocoa butter. The authors discovered that the γ polymorph develops at temperatures below 5°C. Between 5°C and 15°C cocoa butter crystallizes in the α polymorph, which disappears at longer crystallization times in favour of the β' polymorph.

Mainly based on DSC results, Marangoni & McGauley (2003) constructed their own phase scheme for statically, isothermally crystallized cocoa butter. At some time-temperature combinations the present polymorphs were confirmed by WAXD. The scheme shows that both γ and α polymorphs are present at low temperatures (between –20°C and –15°C). A pure α polymorph is initially observed at temperatures ranging from –10°C to 20°C. At temperatures above 0°C the α polymorph later transforms into β', a transition which is completed faster at higher temperatures. At temperatures from 21 to 26°C formation of the β' polymorph takes place directly.

Hindle et al. (2002) used WAXD to characterize the crystal polymorphs formed in cocoa butter oil in water emulsions during isothermal crystallization at 15°C. They found out that cocoa butter initially crystallizes in the α polymorph. After longer crystallization times, diffraction lines of both the α and β' polymorph are present. During overnight crystallization further polymorphic transition takes place as the α diffraction lines disappear.

None of the above-mentioned articles provided information about the relative amounts of the different polymorphs as function of time. It was thus the aim of the research described in this chapter to not only investigate which polymorphs are formed during the isothermal cocoa butter crystallization but also to have an idea of the amount of each polymorph. From this information more insight into the details of formation of the different polymorphs can be gained. For example, an answer to the question whether the β' crystals are formed by polymorphic transition of α crystals or by direct crystallization from the melt or by a combination of both is aimed at. Different experimental techniques (DSC, pNMR, real-time XRD (WAXD and SAXS) and polarized light microscopy (PLM)) were used to attain this goal. Each of these techniques measures another property related to phase transitions. DSC measures the released crystallization heat while pNMR measures the difference in relaxation behaviour of triacylglycerols in the solid and liquid like state. By real-time XRD, the

short and long spacings as function of time are determined, thus providing unambiguous phase information at each moment in time. By PLM the morphology of the crystals can be studied.

5.2 Research strategy

Cocoa butter was isothermally crystallized using DSC at temperatures between 17°C and 23°C (± 0.05°C). To gain more insight into the type of polymorphs formed during isothermal crystallization, the crystallization process was stopped at different moments in time and the sample was heated again (stop and return technique). The thus obtained melting profile provides an idea of the polymorph(s) present and the amount of cocoa butter already crystallized. Experiments using pNMR were performed at temperatures between 17°C and 23°C (± 0.2°C). Real-time XRD experiments using synchrotron radiation were performed at 17, 20 and 23°C (± 0.1°C). PLM was used to visualize the morphology of the crystals as function of time when isothermally crystallizing at 20°C (±0.2°C). Combining the information obtained from the different experimental techniques, a mechanism for the formation of the different polymorphs during isothermal crystallization of cocoa butter at 20°C, was proposed.

5.3 Materials and methods

5.3.1 Cocoa butter

The cocoa butter used in the experiments was a standard factory product (batch 2) supplied by Barry Callebaut (Wieze, Belgium).

5.3.2 DSC

The DSC experiments were performed with a 2010 CE DSC (TA Instruments, New Castle, USA) with a Refrigerated Cooling System (TA Instruments, New Castle, USA). The DSC was calibrated with indium (TA Instruments, New Castle, USA), azobenzene (Sigma-Aldrich, Bornem, Belgium) and undecane (Acros Organics, Geel, Belgium) prior to analyses. Nitrogen was used to purge the system.

Cocoa butter (2.3-8.4 mg) was sealed in hermetic aluminum pans (using sample preparation procedure B as described in section 3.3.2.2) and an empty pan was used as a reference.

5.3.2.1 Isothermal crystallization experiments

The following time-temperature program was applied (see chapter 3): holding at 65°C for 15 minutes to ensure a completely liquid state, cooling at 8°C min^{-1} to the isothermal crystallization temperature and keeping at that temperature until crystallization had finished.

The crystallization peaks were integrated using a horizontal sigmoid baseline and the starting- and end points were determined using the calculation algorithm as described in section 3.4.1.2. The integration was performed with the Universal Analysis software version 2.5 H (TA Instruments, New Castle, USA). The start of the isothermal period was determined as described in section 3.3.5.

5.3.2.2 Stop and return experiments

The same pan as for the isothermal crystallization experiment at that crystallization temperature was used. The sample was melted (65°C for 15 minutes), cooled (8°C min^{-1}) to the crystallization temperature, kept at that temperature for the desired time and heated up to 65°C at a rate of 5°C min^{-1}. This heating rate was chosen because it is fast enough to prevent polymorphic transitions from taking place during heating and slow enough to eliminate the effects of thermal lag.

When integrating the melting peaks a problem occurred since no stable baseline was available at the low temperature side. It was decided to integrate the peaks using a linear baseline with the end point at the visual end of the melting peak and the starting-point at the same y-value as the end point as shown in Figure 5.1. It has to be stressed that this method only gives an approximation of the area of the melting peak. The peak maximum, however, is independent of the integration procedure. The integration was performed with the Universal Analysis software version 2.5 H (TA Instruments, New Castle, USA).

5.3.3 pNMR

The pNMR experiments were performed with a Minispec pc 20 (Bruker, Karlsruhe, Germany). Liquefied cocoa butter was transferred to pNMR tubes and these were put at 65°C for 1 hour to eliminate any thermal history. Then they were placed in a thermostatic water bath at crystallization temperature. The sample temperature then decreased exponentially with an initial rate of 25°C min^{-1}. Readings of the amount of solid fat were taken at appropriate time intervals and a separate tube was used for every

measurement. The start of the isothermal period was taken 3.1 minutes after transfer to the water bath.

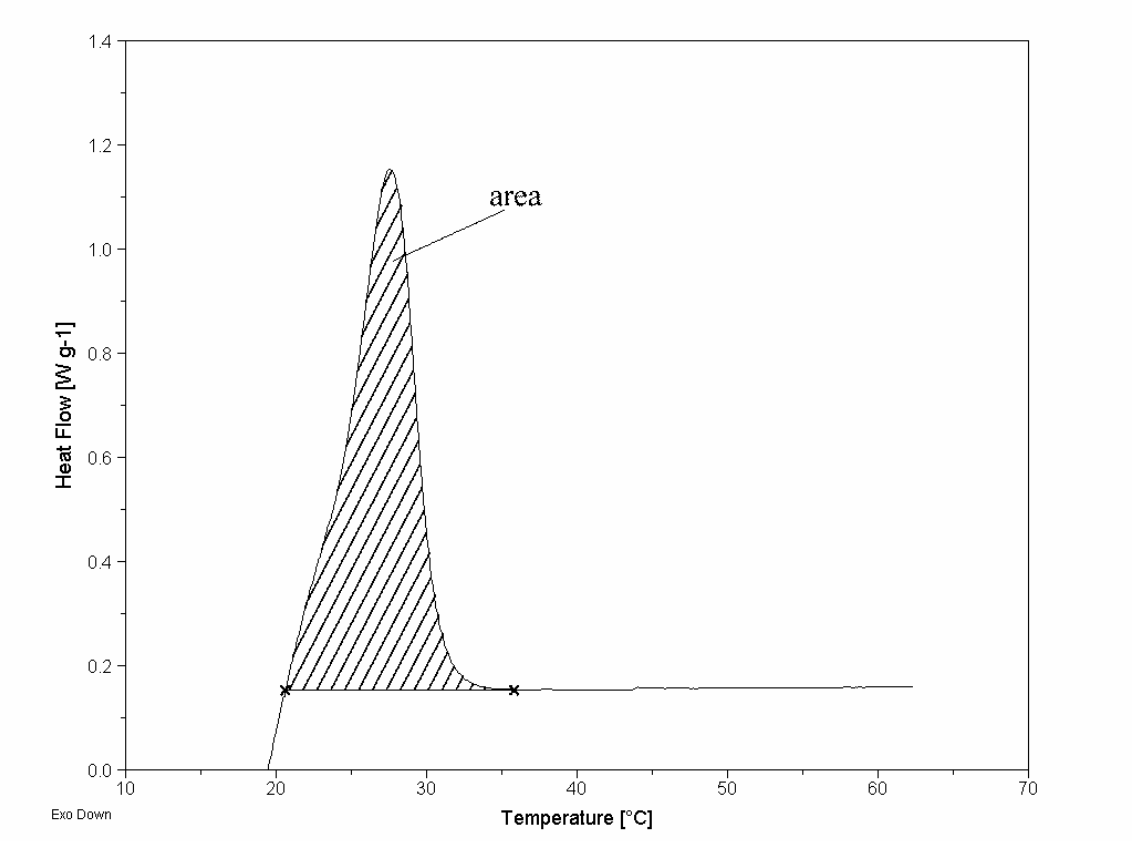

Figure 5.1 Integration of melting peaks obtained by stop and return experiments

5.3.4 Real-time XRD

Real-time XRD measurements were performed on the DUBBLE beamline BM26a of the synchrotron facility ESRF in Grenoble (France). The experiments were done at a fixed wavelength of 1.24Å. Two detectors were used: a curved 1D WAXD detector to determine the short spacings, characteristic of the different crystal lattice types and a 2D SAXS detector to determine the long spacings related to the longitudinal stacking of the molecules in lamellae.

A small amount of cocoa butter was placed into copper rings (7 mm) and covered with mica. These rings were placed into a Linkam cooling stage allowing to perform temperature-controlled experiments. The following time-temperature program was applied: heating to 65°C, holding at that temperature for 15 minutes, cooling at 8°C min^{-1} to the crystallization temperature and keeping at that temperature until crystallization was completed. Images were taken each 40 seconds from the start of cooling.

The known reflections of silverbehenate and silicium powder were used to calibrate the SAXS and WAXD angles respectively. Data processing for WAXD was performed using a method developed by colleagues of the Laboratory of Macromolecular Structural Chemistry, Catholic University Leuven (Belgium). This method is explained in more detail in Annex IV.

5.3.5 Polarized light microscopy

One drop of liquefied cocoa butter was put on a carrier glass and a covering slide was used to cover the sample. Then the sample was placed on a temperature-controlled stage Linkam PE94 (Linkam Scientific Instruments, Surrey, UK). The following time-temperature combination was applied: heating to 65°C and holding for 15 minutes to eliminate all crystal nuclei, followed by cooling at 8°C min^{-1} to the crystallization temperature of 20°C. The sample was kept at that temperature until crystallization had finished. The formed crystals were visualized with a polarized light microscope Leitz Diaplan (Leitz, Wetzlar, Germany). The start of the isothermal period was taken as the moment when the temperature reached the crystallization temperature ± 0.2°C.

5.4 Results and discussion

5.4.1 Isothermal crystallization behaviour as measured by DSC

Figure 5.2 shows a crystallization curve obtained by DSC at a temperature of 19°C. The first part of the curve coincides with melting and cooling (see section 5.3.2.1). After cooling the temperature equilibrates to the crystallization temperature causing some sinusoidal variation in the crystallization curve. On top of that variation a more or less pronounced small peak is visible. Because of its overlap with the temperature equilibration it is, however, impossible to integrate this peak. After this the crystallization curve returns to the baseline for a very short period of time. This means that no phase transition occurs in this period. After this period a clear crystallization peak is visible.

Ziegleder (1990) also detected a small peak immediately after cooling. He attributed this to undefined components present in cocoa butter causing a spontaneous turbidity of the melt. But as he could not detect an influence on the main crystallization peak, he decided not to take it into account in the rest of his research.

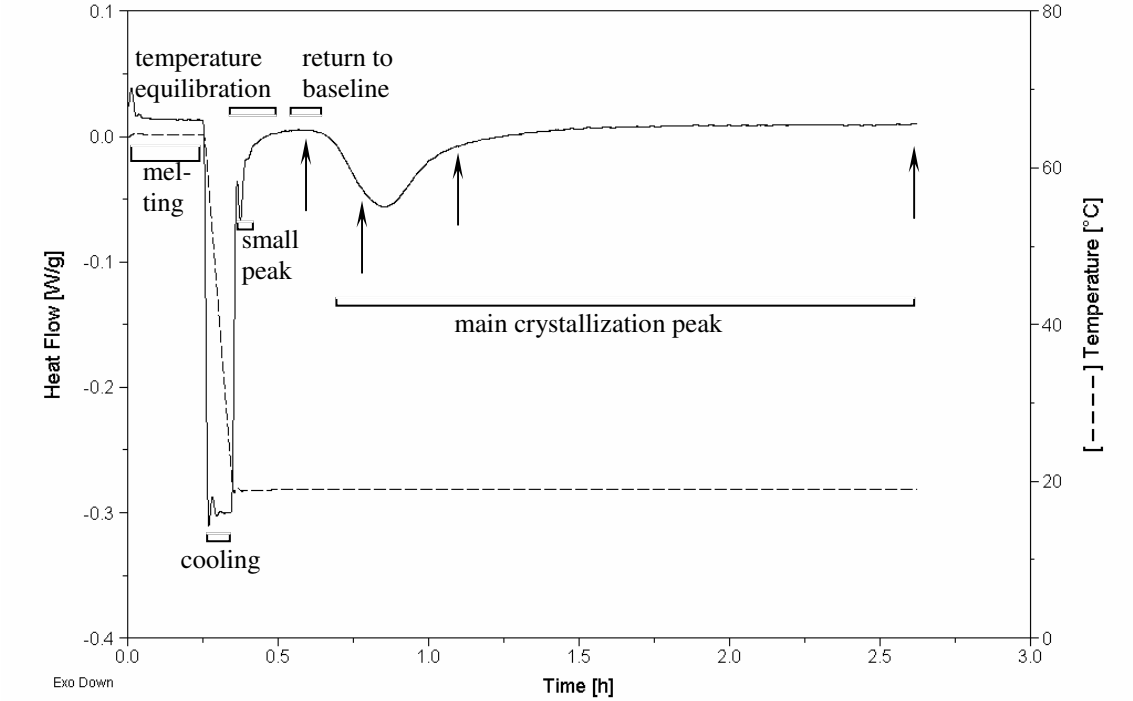

Figure 5.2 Isothermal crystallization of cocoa butter at 19°C as measured by DSC

Comparable crystallization curves were obtained for temperatures from 19.5°C up to 23°C. However, as the crystallization temperature increases, the period without phase transition increases, the main crystallization peak shifts to longer crystallization times and is broader. These temperature effects are discussed in more detail in chapter 6.

At temperatures below 19°C the crystallization curve does not return to the baseline before the start of the main crystallization peak (Figure 5.3). In some cases some crystallization already occurs during cooling, leading to a peak that is superimposed on the normal curve at the end of the cooling phase. Such a superimposed peak is visible in Figure 5.3 for example.

5.4.2 Stop and return experiments by DSC

To gain more insight into the polymorphs formed during the isothermal crystallization, stop and return experiments using DSC were performed.

The principle of the stop and return technique is to interrupt the isothermal crystallization at different moments in time and subsequently heat up the sample in order to obtain a melting profile of the crystallized cocoa butter. Such a melting profile gives an idea of the amount of crystallized cocoa butter (peak area) and the polymorph

in which the cocoa butter has crystallized (peak maximum). To attribute the different melting peaks to the different polymorphs, the melting points as described in section 2.4.3 were used.

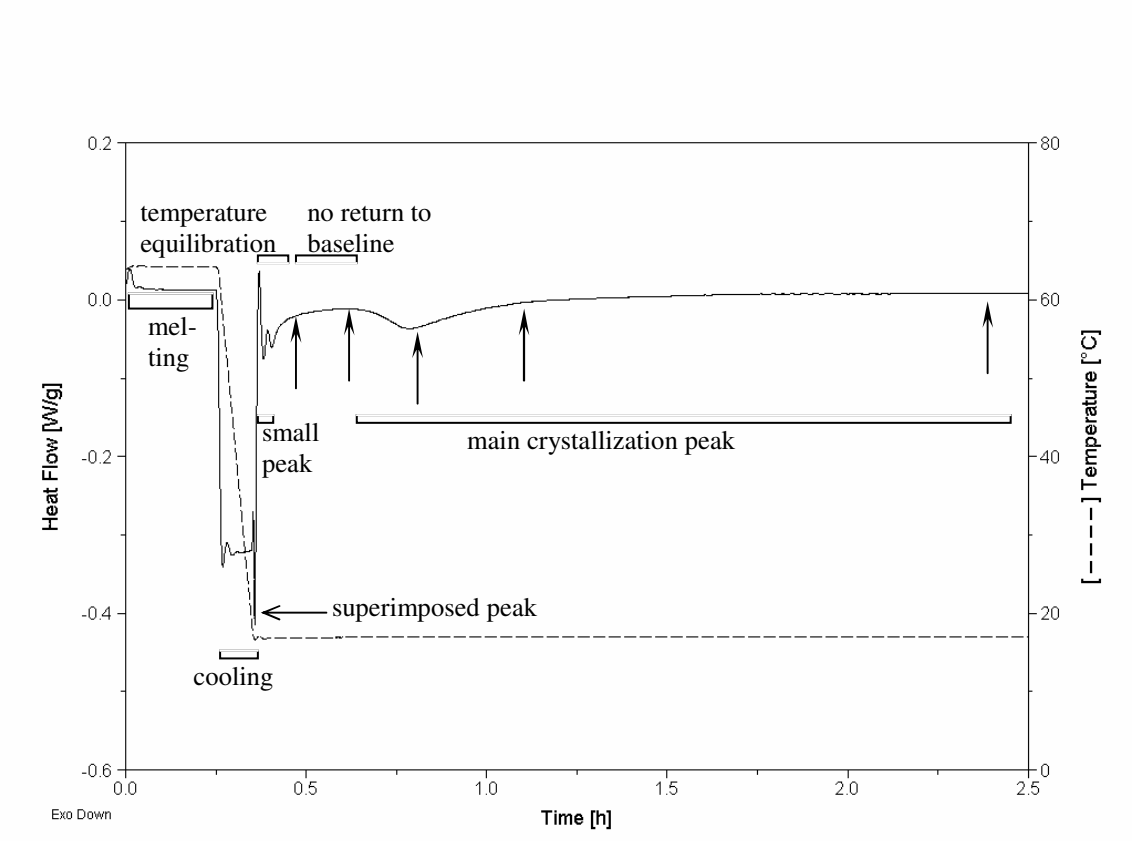

Figure 5.3 Isothermal crystallization of cocoa butter at 17°C as measured by DSC

The result for isothermal crystallization at 19°C is depicted in Figure 5.4. The isothermal times at which the crystallization is stopped, are indicated with arrows in Figure 5.2. When the crystallization is stopped before the main peak a melting profile with one peak with a maximum at 22.96°C and an area of 17 J g^{-1} is obtained. This means mainly α crystals are formed at this moment. When the crystallization is stopped in the first part of the main peak two melting peaks are obtained: the first one with a maximum of 23.47°C and an area of 10 J g^{-1}, the second one with a maximum at 26.90°C and an area of 13 J g^{-1}. These two melting peaks correspond to the α and β' polymorph respectively. When the crystallization is stopped in the final part of the main peak one melting peak with a maximum at 27.61°C and an area of 63 J g^{-1} is obtained. A small shoulder on the low temperature side, indicative of some remaining α crystals, seems to be present. At the end of the crystallization a single melting peak with peak maximum at 27.22°C and an area of 86 J g^{-1} is obtained. It is difficult to judge whether the shoulder at the low temperature side is still present.

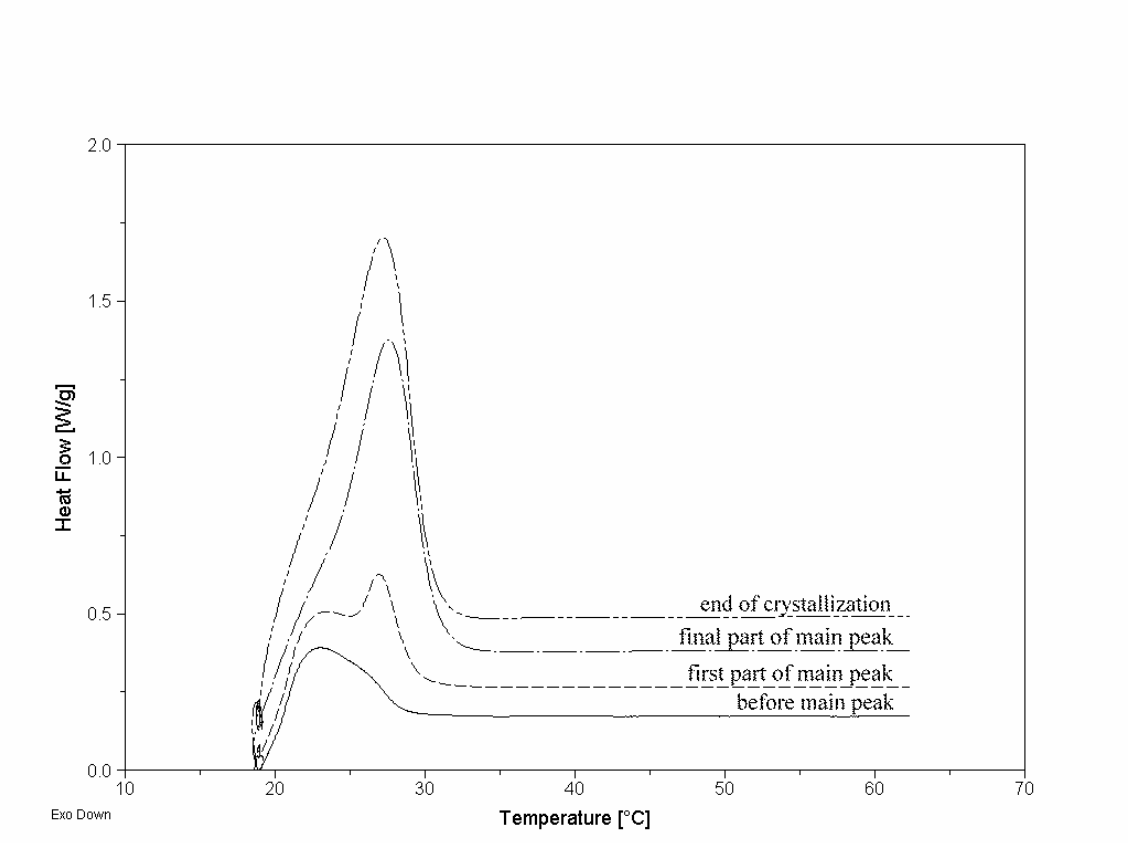

Figure 5.4 Melting profiles after isothermal crystallization at 19°C for different periods of time

The conclusion is that some crystallization already takes place before the main crystallization peak, giving rise to the small exothermic peak observed during or immediately after the equilibration phase. The formed crystals are mainly in the α polymorph. During the main crystallization peak β' crystals are formed and α crystals disappear, most probably due to a polymorphic transition from α to β'. The increase of the area of the β' peak is, however, much higher than the decrease of the area of the α peak even when taking account of the difference in melting enthalpy between both polymorphs (around 80 J g^{-1} for the α polymorph and around 100 J g^{-1} for the β' polymorph (Chapman et al., 1971 and Riiner, 1970)). Additional formation of β' crystals is thus expected to take place.

The same conclusions as for 19°C could be drawn from the stop and return experiments at 20°C, 21°C, 22°C and 23°C.

The result of the stop and return experiments at a crystallization temperature of 17°C are depicted in Figure 5.5. The moments at which the crystallization is stopped are indicated with arrows in Figure 5.3.

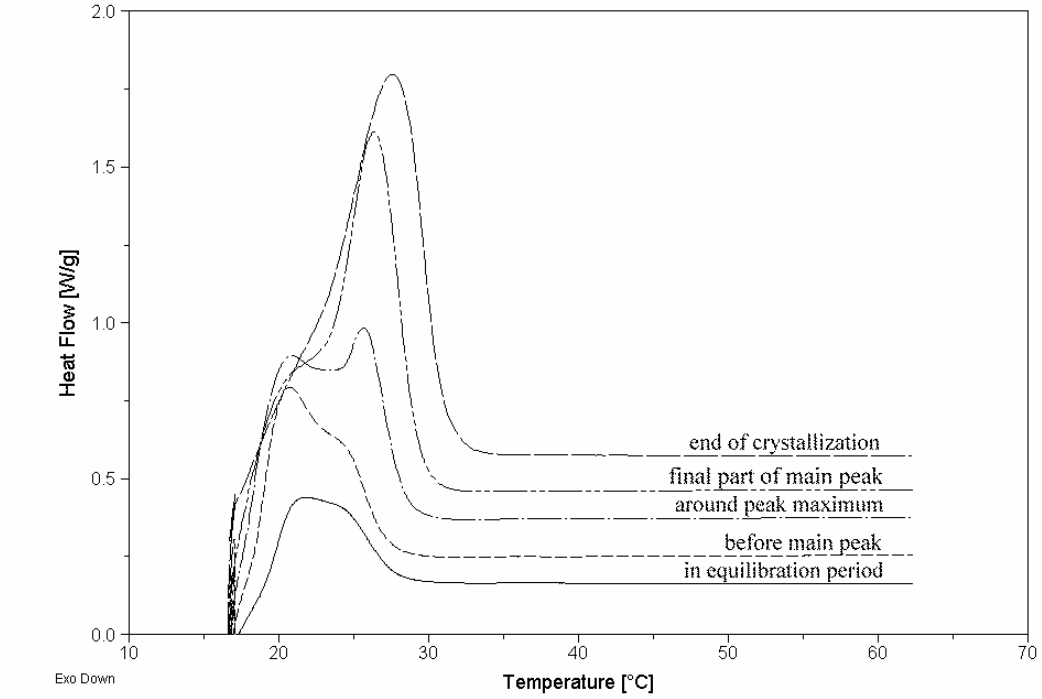

Figure 5.5 Melting profiles after isothermal crystallization at 17°C for different periods of time

When the crystallization is stopped in the equilibration period, one melting peak with a maximum at 21.81°C and an area of 21 J g^{-1}, indicative of mainly α crystals, is obtained. When the crystallization is stopped before the main peak, a melting peak with maximum at 20.69°C and an area of 36 J g^{-1} but with a clear shoulder on the high temperature side, is obtained. This means that β' crystals are already formed before the start of the main crystallization peak. When the crystallization is stopped around the maximum of the main crystallization peak, two melting peaks are detected: one with a maximum at 20.99°C and an area of 24 J g^{-1} corresponding to α crystals, and one with a maximum at 25.65°C and an area of 27 J g^{-1} corresponding to β' crystals. When the crystallization is stopped in the final part of the main crystallization peak, one melting peak with a maximum at 26.33°C and an area of 75 J g^{-1}, is obtained. A clear shoulder on the low temperature side, indicative of some remaining α crystals, is also present. At the end of the crystallization the melting profile shows a single peak with a maximum at 27.59°C and an area of 93 J g^{-1}. It is difficult to judge whether a shoulder at the low temperature side is still present.

This means that also at 17°C, the formation of α crystals is followed by the formation of β' crystals by polymorphic transition from α (decrease of the α peak area) and a supplementary process (increase in β' peak area higher than decrease in α peak area).

5.4.3 Isothermal crystallization behaviour as measured by pNMR

Figure 5.6 shows isothermal crystallization curves at 17°C, 19°C and 20°C as measured by pNMR.

The crystallization curve obtained at 20°C indicates that at this temperature crystallization is clearly a two-step process. First the amount of solid fat increases without an appreciable induction time, then the value remains more or less constant for a while but after that it increases drastically. Finally, the amount of solid fat levels off to a second plateau.

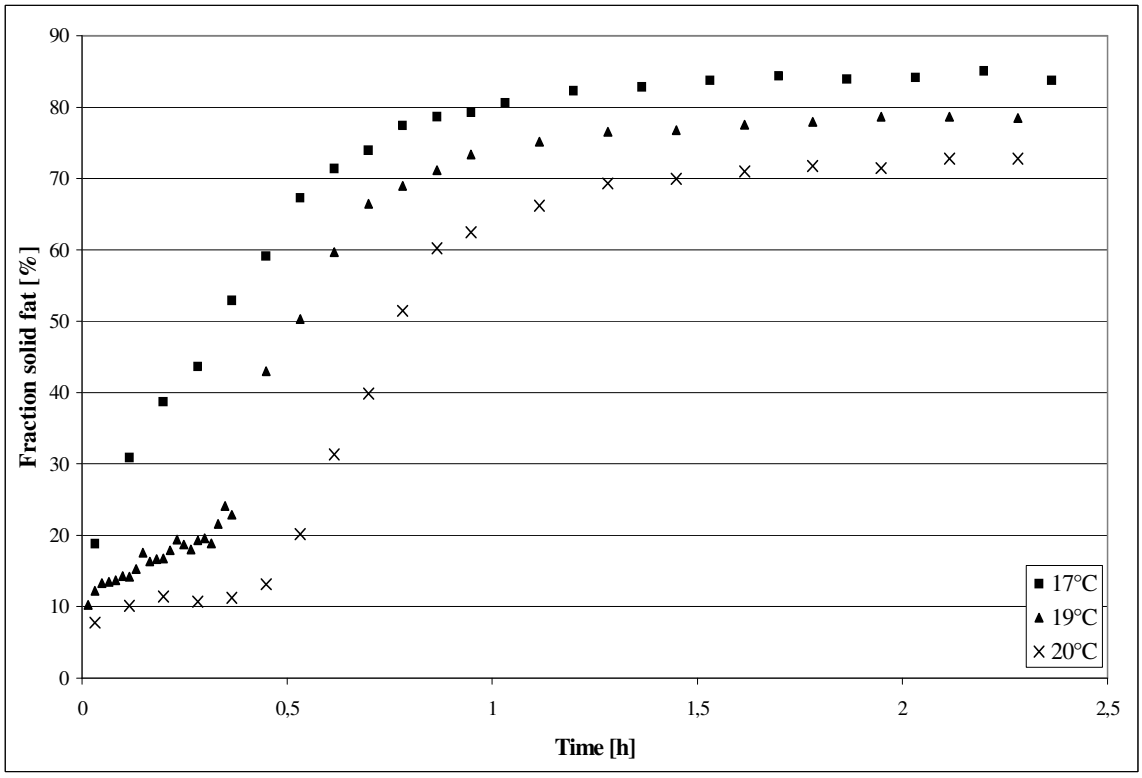

Figure 5.6 Isothermal crystallization of cocoa butter at 17°C, 19°C and 20°C as measured by pNMR

Crystallization curves comparable to the one obtained at 20°C, were observed for temperatures between 21°C and 23°C. As the temperature increases, the length of the first plateau increases but its height decreases as well as the rate of crystallization in the second step and the final plateau. These temperature effects are discussed in more detail in chapter 6.

When crystallizing at temperatures lower than 20°C, no intermediate period with a constant amount of solid fat can be detected making it more complicated to distinguish the two steps of the crystallization process. But a period when the crystallization starts to slow down, is followed by an increase in the rate of crystallization. This indicates that, also at these lower temperatures, crystallization takes place in two steps.

5.4.4 Isothermal crystallization behaviour as measured by real-time XRD

5.4.4.1 Isothermal crystallization behaviour as measured by WAXD

Figure 5.7 shows the mass fractions of the α and β' polymorph and the non-crystalline fraction as function of the isothermal time at a crystallization temperature of 20°C. These mass fractions were calculated from the diffraction patterns as described in Annex IV.

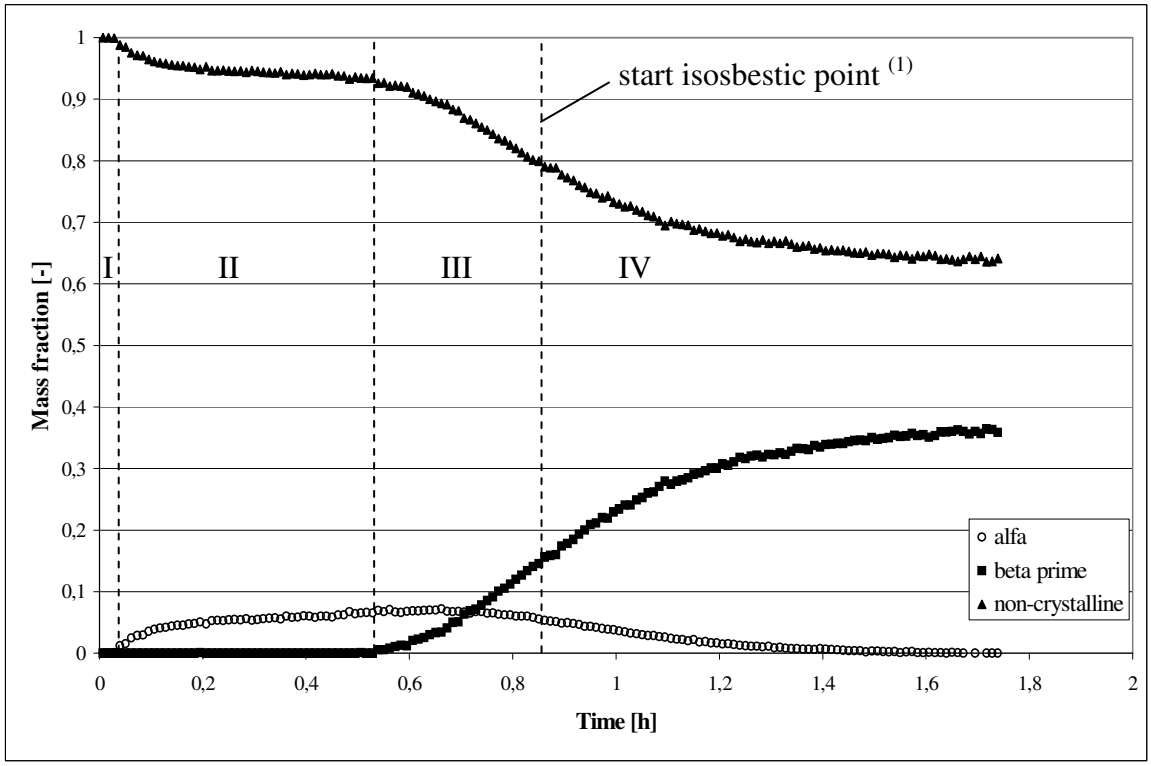

Figure 5.7 Mass fraction of α and β' polymorphs and non-crystalline fraction during isothermal crystallization of cocoa butter at 20°C as measured by WAXD

(1) see section 5.4.4.2

The figure shows a first step of the crystallization process where α crystals are formed. The α crystallization starts almost immediately after reaching the isothermal temperature, but its rate slows down rather quickly (period II in Figure 5.7, period I is the time span where no crystallization takes place). After some time the increase in the

mass fraction of α crystals is very slow though it seems like no real plateau is reached at the moment the β' crystals start to form after approximately 0.55 h. Also at later times no real plateau is reached. The mass fraction of β' crystals increases in a sigmoid way (period III in Figure 5.7). About 0.15 h after the start of the β' formation the mass fraction of α crystals starts to decrease. The disappearance of the last α crystals seems to coincide with the moment the mass fraction of β' no longer increases.

5.4.4.2 Isothermal crystallization behaviour as measured by SAXS

Figure 5.8 show the SAXS diffraction patterns for the isothermal crystallization at 20°C at different moments in time. To keep the figure clearly structured, only one frame out of ten is presented. Literature data (Loisel et al., 1998a and Van Langevelde et al., 2001) were used to allocate the different peaks to the different polymorphs. Both the α and β' polymorph show a 2L packing mode.

The results about the appearance and disappearance of the different polymorphs obtained by WAXD were confirmed by SAXS. Figure 5.8 however also shows that from 0.85 h onwards and until the end of crystallization the diffraction patterns of all frames pass through one point. Such an isosbestic point indicates that the total volume remains constant or increases stoechiometrically during a chemical reaction or a physical change of the sample. This means that the α phase is transferred into the β' phase without a change of the total volume occupied by α + β'.

When isothermally crystallizing at 17°C no isosbestic point was observed (detailed results not shown). However, it has to remarked that this experiment was stopped before the end of crystallization.

Vanhoutte (2002) also demonstrated the existence of an isosbestic point during isothermal crystallization of milk fat (fractions) at a supercooling of 15°C and higher. In contrast with the crystallization of cocoa butter the isosbestic point for milk fat (fractions) is already visible from the moment of appearance of the β' diffraction lines.

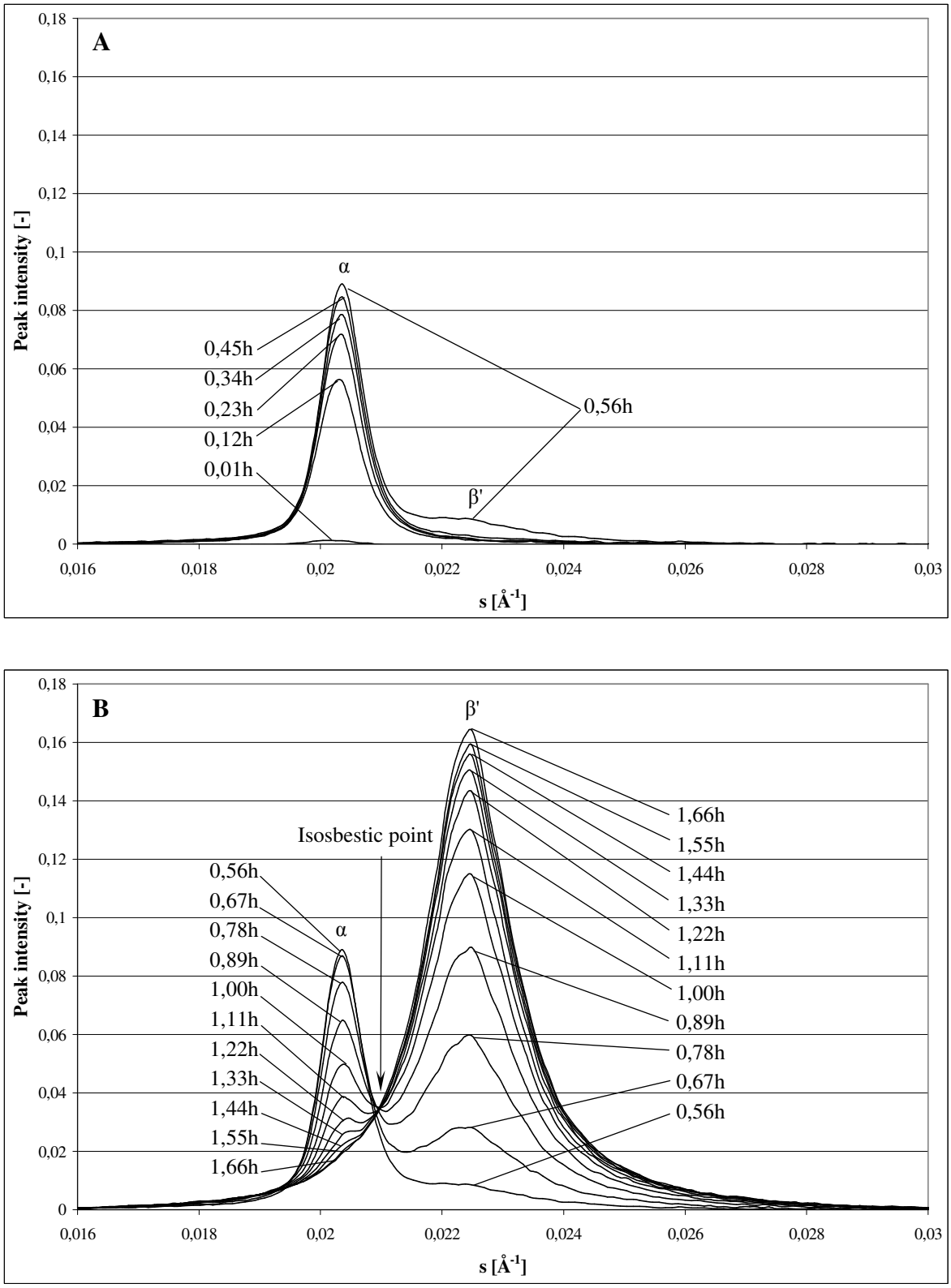

Figure 5.8 Isothermal crystallization of cocoa butter at 20°C: SAXS diffraction patterns as function of time. A : Time span 1, up to 0.56 h, B : Time span 2, from 0.56 h onwards

5.4.5 Isothermal crystallization as visualized by PLM

Microscopic examination of the isothermal crystallization at 20°C showed that crystals are formed from the start of the isothermal period. The amount of crystals quickly increases in the first minutes of the isothermal crystallization to already reach a saturation level after 0.04 h. The same image persists until about 0.5 h. In the next 0.25 h a dramatic change in the image is observed: it seems like the remaining liquid regions (black spots) fill up with small crystals (white spots) resulting in a less apparent form of the initial crystals. From 0.75 h onwards, no more change in the image is observed. This moment more or less coincides with the start of the appearance of an isosbestic point in SAXS. Figure 5.9 shows three pictures in the transition phase between 0.5 and 0.75 h.

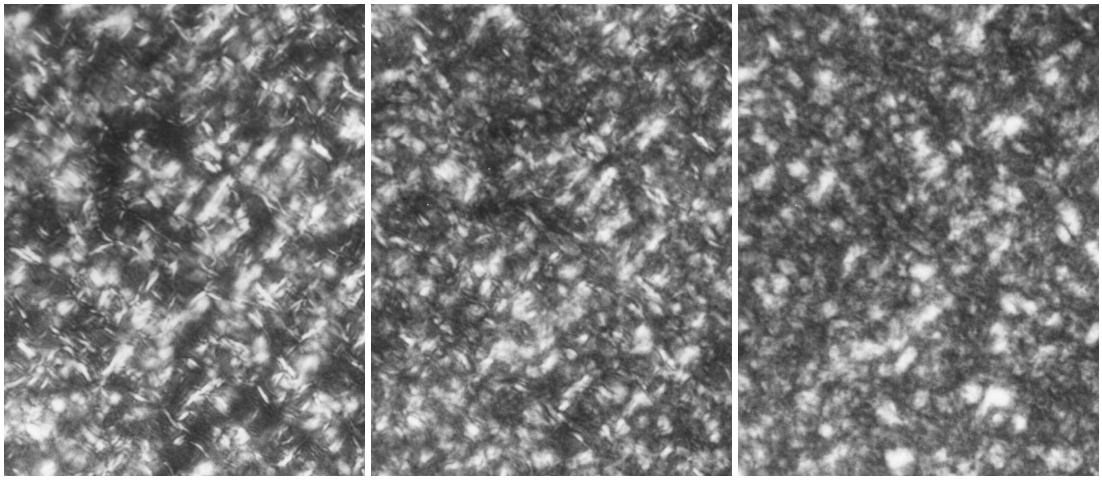

A B C

Figure 5.9 Isothermal crystallization of cocoa butter at 20°C: PLM images at different moments in time (A = 0.45 h, B = 0.58 h, C = 0.68 h)

5.4.6 Discussion

5.4.6.1 Introduction

When the results obtained with the different measuring techniques are compared it has to be taken into account that, apart from measuring different properties, some other differences can exist that affect crystallization. Differences in weight or volume of the samples and in equipment design may have an effect on the heat and mass transfer conditions existing in each measurement device (Toro-Vazquez et al., 2002). Although a sample from the same batch was used for each experiment, still some inhomogeneity can be present within one batch. The crystallization temperature can differ a little

despite the fact that the temperature was kept to the preset temperature as good as possible and this for each technique. A small difference in time zero of the isothermal period can exist despite the fact that this time was determined as accurately as possible for each technique.

5.4.6.2 Isothermal crystallization as a two-step process

The results obtained with the different techniques showed that the isothermal crystallization of cocoa butter at temperatures between 17°C and 23°C is a two-step process. From DSC experiments it can be concluded that the two steps (small peak and main crystallization peak) are separated from 19°C onwards, as reflected by a return to the baseline before the main crystallization peak. However, at the lowest temperatures it is difficult to judge if indeed the crystallization curve returns to the baseline for some time. In the pNMR experiments a plateau with a constant amount of solid fat is only observed from 20°C onwards. In the WAXD experiments it seems like, even at 20°C, the mass fraction of α crystals is still slightly increasing at the moment the β' crystals start to form. This means that no period without a phase transition exists. This difference may be explained by the higher sensitivity of WAXD compared to DSC and pNMR. When following the crystallization with PLM a period without remarkable changes was also detected.

Taking into account the remarks in section 5.4.6.1, it can be concluded that the isothermal times at which the two steps of the crystallization process start and end, more or less coincide.

The stop and return experiments by DSC and the real-time XRD experiments suggested that the first and second step involve formation of α and β' crystals respectively.

From the cocoa butter phase diagrams obtained by Van Malssen et al. (1999) and Marangoni & McGauley (2003) and the results of Hindle et al. (2002) a kind of two-step process with the presence of the α polymorph followed by the presence of the β' polymorph can also be deduced. At lower degrees of supercooling, thus higher crystallization temperatures, the crystallization behaviour changes to a one-step process, more specifically a direct crystallization into β'. This was observed for temperatures from 22°C (Van Malssen et al., 1999) and 21°C onwards (Marangoni & McGauley, 2003). In this research a two-step process is still observed at 23°C (results not shown). Investigating the isothermal crystallization behaviour at even higher temperatures was

practically impossible due to the very slow crystallization rates. The difference in highest possible temperature for a two-step process between the studies may be explained by the use of a different cocoa butter: Van Malssen et al. (1999) used cocoa butter from Cameroon, a standard factory product from mainly Ivory Coast beans was used in the present study and Marangoni & McGauley (2003) did not report the kind of cocoa butter they used.

Herrera et al. (1999a) and Vanhoutte (2002) for milk fat (fractions) and Chen et al. (2002) for refined palm oil also described the isothermal crystallization at high degrees of supercooling as a two-step process.

An explanation for this two-step process with first crystallization in the less stable α polymorph was given by Rousset (1997) (see also section 1.3.1): the α polymorph has a lower critical activation free energy for nucleation and thus a higher nucleation rate despite the larger difference in chemical potential and thus the larger driving force for crystallization for the more stable polymorphs.

5.4.6.3 Mechanistic interpretation

Based on the results obtained with the different techniques a mechanism for the formation of both polymorphs can be proposed for isothermal crystallization of cocoa butter at 20°C. The crystallization is divided in different periods, which are also indicated in Figure 5.7.

Period I: no diffraction patterns (XRD);

Period II: increase in α mass fraction (WAXD);

increase in amount of solid fat (pNMR);

some heat release but no clear interpretation possible due to overlap (DSC).

Period III: slight increase in mass fraction α crystals followed by a decrease (WAXD);

increase in mass fraction β' crystals (WAXD);

no isosbestic point (SAXS);

increase in amount of solid fat (pNMR);

release of heat (DSC).

Period IV: decrease in mass fraction α crystals (WAXD);

continued increase in mass fraction β' crystals (WAXD);

isosbestic point meaning that only a polymorphic transition takes place (SAXS);

continued increase in amount of solid fat (pNMR);

continued heat release (DSC).

These observations were combined in the following mechanism. No crystallization takes place in period I. In period II part of the melt crystallizes in the α polymorph. After some time the rate of α crystallization decreases drastically owing to the lowering of the supersaturation. At a certain moment (start of period III) α crystals start transforming into β' crystals. Because of this polymorphic transition the supersaturation for the α polymorph increases again, allowing extra melt to crystallize in the α polymorph. The so formed α crystals also transform into β'. Both processes, i.e. the polymorphic transition from α to β' and the crystallization from the melt in the α polymorph, occur simultaneously. The mass fraction of α crystals remains constant at first and decreases afterwards. Consequently the rates of both reactions (polymorphic transition and melt crystallization) are equal first, later on the rate of the polymorphic transition is faster than the α crystallization, probably because the α crystallization slows down because of less supersaturation. At a certain moment (start of period IV) the α crystallization stops and only a transition from α to β' takes place thus leading to the existence of an isosbestic point. In this proposed mechanism the β' crystallization would thus be α mediated.

When the start of the isosbestic behaviour is extrapolated to the curves representing the amount of solid fat (Figure 5.6) it may seem remarkable that during period IV, when only a polymorphic transition takes place, the amount of solid fat still increases by more than 10%. This may be explained by the presence of liquid-like end group regions with disordered chains in the α polymorph, as suggested by Hernqvist & Larsson (1982) (Figure 5.10). They deduced this structure model from a plot of the long spacings as function of chain length for the different polymorphs and from Raman spectroscopy. The former shows that the intercept obtained by extrapolating to chain length zero

(corresponding to the space occupied by the glycerol groups and the gap between the methyl end groups in adjacent layers) is much larger in the α polymorph compared to the β' polymorph. The latter shows a significant 'liquid' contribution in the spectra of the α polymorph compared to the β' and β polymorphs. When a polymorphic transition from α to β' takes place the chains in the liquid-like end group regions of the α polymorph order themselves leading to a higher crystallinity of the β' polymorph.

The increase in amount of solid fat during the polymorphic transition from α to β' is even clearer for the isothermal crystallization of milk fat where the complete second step of crystallization coincides with only a polymorphic transition from α to β' but is still accompanied by an increase in the amount of solid fat (Vanhoutte, 2002).

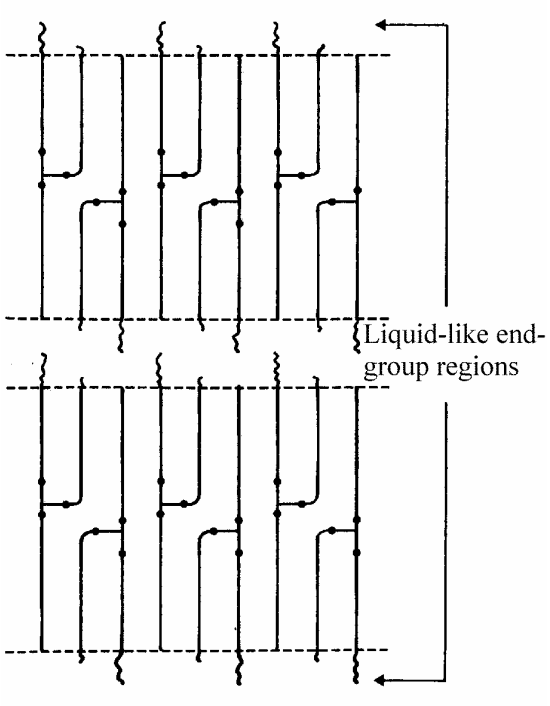

Figure 5.10 Proposed structure of the α polymorph of triacylglycerols. The main part of the hydrocarbon chains are oscillating and hexagonally close-packed; the methyl end group regions are somewhat more disordered, as in liquid crystals (Hernqvist & Larsson, 1982)

5.4.6.4 Equilibrium crystallinity as measured by different techniques

It is remarkable that the final crystallinity as measured by WAXD is much smaller than the final amount of solid fat as measured by pNMR: 36% in WAXD compared to 72.5% in pNMR at 20°C. The mass fraction α crystals formed in the first step also shows this difference: about 7% in WAXD compared to 11% in pNMR (20°C).

From the released crystallization heat as measured by DSC, the amount of crystallized fat can be calculated when the latent heat is known. For the α polymorph the latent heat is about 80 J g^{-1}, for the β' polymorph it is about 100 J g^{-1} (Chapman et al., 1971 and Riiner, 1970). The area of the small peak corresponding to α crystallization could not be determined, but the area of the melting peak after isothermal crystallization up to the start of the main peak was determined in stop and return experiments. This area could be used to calculate the mass fraction of α crystals. For isothermal crystallization at 20°C a value of around 8% was obtained. For the second step of crystallization the peak area was around 77 J g^{-1} corresponding to 77% β' crystals. The polymorphic transition of the α crystals formed in the first step also releases some heat but this is negligible (0.08 X 20 J g^{-1} = 1.6 J g^{-1}). The total amount of solid fat is thus around 85%.

These differences in crystallinity obtained by different measuring techniques can be attributed to the fact that the different techniques measure different physical features of the material. According to Le Botlan et al. (1999), the determination of the absolute crystallinity should be performed by XRD because the presence of an amorphous phase is, due to its melting enthalpy, seen as solid by DSC. This amorphous phase is also partly seen as solid by pNMR. This would explain the highest values obtained for the DSC total crystallinity, the intermediate values for the pNMR total crystallinity and the lowest ones for the WAXD total crystallinity.

5.5 Conclusion

Using DSC, pNMR and real-time XRD it was shown that at temperatures between 17°C and 23°C isothermal crystallization of cocoa butter is a two-step process with formation of α crystals in the first step and formation of β' crystals in the second step. From WAXD experiments the mass fractions of both polymorphs were calculated as function of time. A mechanism for the formation of both polymorphs was proposed for isothermal crystallization at 20°C. In the first step part of the melt crystallizes in the α polymorph, while the second step consists of α mediated β' crystallization. The latter means that the already formed α crystals transform into β' leading to the formation of extra α crystals, which in turn transform into β'. No β' crystals are formed directly from the melt. In the last part of the second step only a polymorphic transition from α to β' takes place which is reflected by the presence of an isosbestic point in SAXS.

6 INFLUENCE OF TEMPERATURE ON THE ISOTHERMAL COCOA BUTTER CRYSTALLIZATION

6.1 Introduction

Ziegleder (1990) studied the isothermal cocoa butter crystallization by DSC and established a strong temperature dependence in the range 19°C - 23°C. The main crystallization peak starts later and is broader as the temperature is higher. The author integrated the peak and fitted the Avrami model to the data. A plot of the logarithm of the Avrami rate constant *k* versus temperature shows a decreasing straight line at temperatures from 20°C onwards. This was attributed to the strong temperature dependence of the nucleation rate since the crystal growth rate is only very slightly dependent on temperature in the studied range. At temperatures below 20°C, *k* increases less than expected from the linear relationship. According to Ziegleder (1990) this is caused by an increase in the melt viscosity at these lower temperatures. The logarithm of the onset time (i.e. the intersection of the baseline with the line tangent to the curve at the inflection point), giving an indication of the start of the process, is also linearly correlated with temperature. This was again explained by the exponentially increasing nucleation rate at decreasing temperatures. It has to be remarked, however, that Ziegleder (1990) attributes the main crystallization peak to β' crystallization from the melt and does not recognize the small peak appearing before the main crystallization peak as a first step of the crystallization. In chapter 5 it was proved that this interpretation is not correct. Before the main DSC crystallization peak part of the melt has already crystallized in the α polymorph and all β' crystals are formed by a polymorphic transition from the α polymorph.

From the isothermal phase transition scheme developed by Van Malssen et al. (1999) for statically crystallized cocoa butter, it was concluded that both the start of the α crystallization and the occurrence of the first β' crystals take place later when the temperature is higher.

Marangoni & McGauley (2003) used pNMR to study the effect of temperature on the isothermal crystallization kinetics of cocoa butter. Both the induction time and the level

at which the curves level off, are function of temperature: the former increases while the latter decreases with increasing temperature. The authors fitted the Avrami model to their data. They observed two different regions in a plot of the Avrami exponent *m* versus temperature coinciding with crystallization in metastable and stable polymorphs. The induction time is also very sensitive to the formed polymorph: discontinuities in a plot of the induction time versus temperature are indicative of a change in nucleation rate due to crystallization of different polymorphs or different fractions.

The aim of this chapter is to describe the influence of temperature on the isothermal cocoa butter crystallization. The temperature dependence of the four parameters of the model developed in chapter 4 was studied based on isothermal DSC measurements between 19°C and 23°C. Supplementary information was obtained by scanning diffusive light scattering (SDLS) and pNMR experiments.

6.2 Research strategy

The isothermal crystallization of two different cocoa butters was monitored by pNMR at temperatures between 19°C and 22°C or 23°C (±0.2°C) (depending on the cocoa butter used). Experiments were performed at 1°C intervals. At each temperature one crystallization curve was obtained using a different tube for every measurement (i.e. every isothermal time). The pNMR crystallization curves show the two steps of the process (see Figure 5.6).

To gain a clear insight in the initial phase of crystallization (i.e. crystallization of part of the melt in the α polymorph, see chapter 5) SDLS experiments were performed on one kind of cocoa butter at temperatures between 19°C and 23°C (±0.1°C) with an interval of 0.5°C. Two repetitions were done at each temperature. SDLS is a very sensitive technique and is therefore well suited to determine the induction time of α crystallization. Since the crystal signal saturates very quickly, no information about the later stages of crystallization could be obtained.

The influence of temperature on the second step of crystallization was studied by DSC. Two different cocoa butters were isothermally crystallized at temperatures between 19°C and 22.5°C or 23°C (±0.05°C) (depending on the kind of cocoa butter used) with an interval of 0.5°C. At each temperature five independent repetitions were performed. The main crystallization peak was integrated and the model developed in chapter 4 was

fitted to the data series. The model parameters were plotted as function of temperature. The amount of cocoa butter crystallizing in the α polymorph before the main peak was estimated by stop and return experiments.

The lowest crystallization temperature was limited to 19°C, because at lower temperatures, crystallization already took place during cooling, which is undesirable in a study of isothermal crystallization. With DSC and pNMR it was impossible to perform measurements at temperatures above 23°C because the crystallization rate was too slow to yield high quality data.

6.3 Materials and methods

6.3.1 Cocoa butters

A standard factory product (batch 2) and a Nigerian cocoa butter were used. Both cocoa butters were supplied by Barry Callebaut (Wieze, Belgium).

6.3.2 pNMR

The pNMR experiments were performed with a Minispec pc 20 (Bruker, Karlsruhe, Germany). Liquefied cocoa butter was transferred to pNMR tubes and these were warmed up to 65°C for 1 hour to eliminate any thermal history. Then they were placed in a thermostatic water bath at crystallization temperature. The sample temperature decreased exponentially with an initial rate of 25°C min^{-1}. Readings of the amount of solid fat were taken at appropriate time intervals and a separate tube was used for each measurement. The start of the isothermal period was taken 3.1 minutes after transfer to the water bath.

6.3.3 SDLS

An NK60-CPA (Phase Technology, Richmond, Canada) light-scattering analyzer was used to follow the initial phases of the isothermal cocoa butter crystallization. The principle of operation is as follows (Figure 6.1): multiple optical detectors are positioned above the sample, the temperature of which is monitored by a platinum resistance thermometer controlled by a thermoelectric module. In the absence of an organized solid phase, the sample is optically transparent and an incident light beam is reflected away from the detectors. But when crystals are formed, the light beam is diffusively scattered into the detector cone. The matrix of sensors designed to cover the

entire sample area eliminates blind spots during the measurement (Toro-Vazquez et al., 2002).

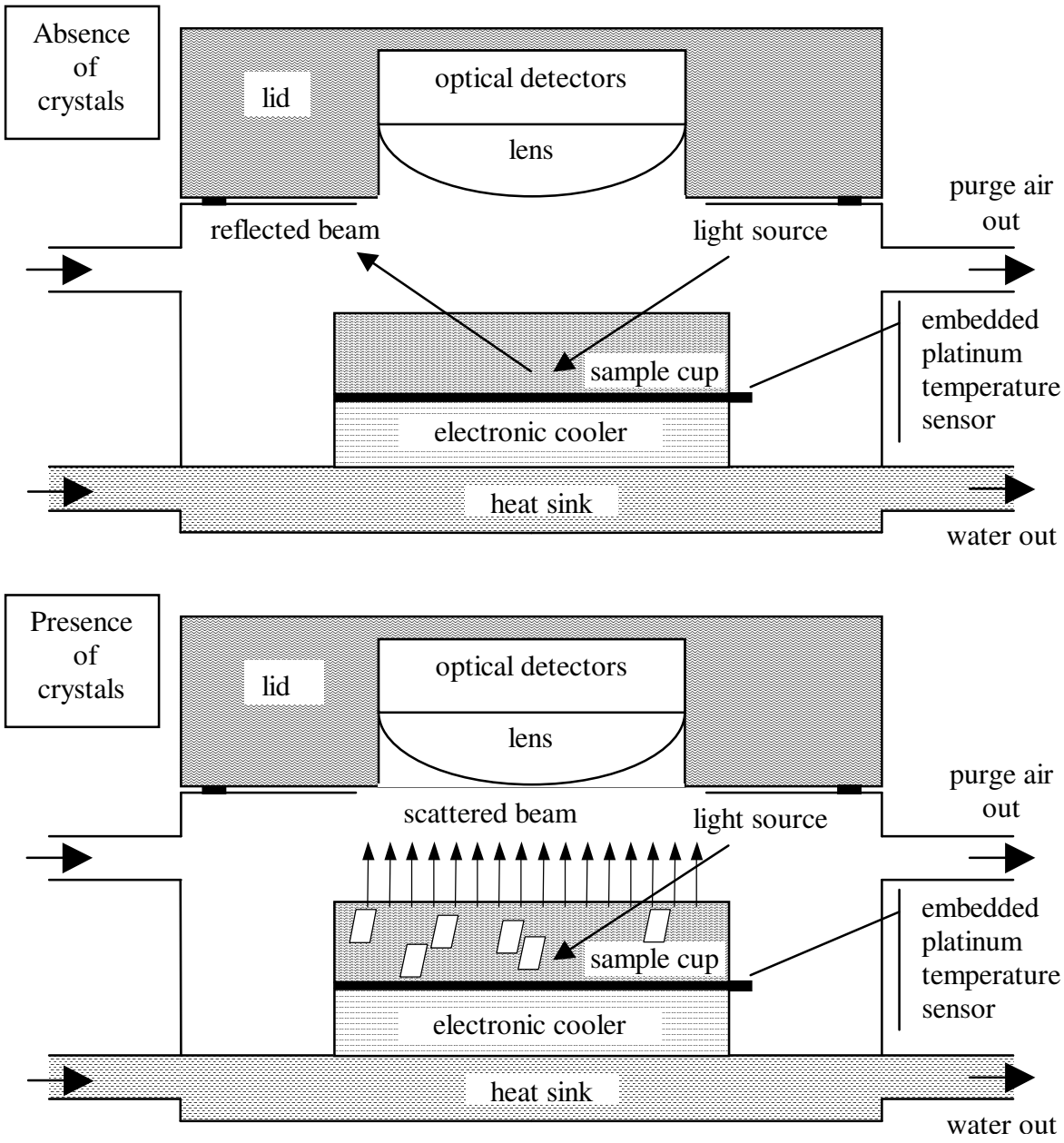

Figure 6.1 Principle of scanning diffusive light scattering

Liquefied cocoa butter (150 µl) was placed in the sample compartment, heated up to 65°C at 25°C min^{-1} and held at that temperature for 15 minutes. Next, the sample was cooled at 8°C min^{-1} to the crystallization temperature where it was kept until saturation of the signal (i.e. a value of 250).

The start of the isothermal period was taken at the moment when the crystallization temperature ± 0.1°C was reached.

The induction time for α crystallization (t_ind_α) was determined as the time when the crystal signal had increased 5 units above the minimum value.

6.3.4 DSC

The DSC experiments were performed with a 2010 CE DSC (TA Instruments, New Castle, USA) with a Refrigerated Cooling System (TA Instruments, New Castle, USA). The DSC was calibrated with indium (TA Instruments, New Castle, USA), azobenzene (Sigma-Aldrich, Bornem, Belgium) and undecane (Acros Organics, Geel, Belgium) prior to analyses. Nitrogen was used to purge the system.

Cocoa butter (2.7-15.3 mg) was sealed in hermetic aluminum pans (using sample preparation procedure B as described in section 3.3.2.2) and an empty pan was used as a reference.

6.3.4.1 Isothermal crystallization experiments

The following time-temperature program was used (see chapter 3): holding at 65°C for 15 minutes to ensure a completely liquid state, cooling at 8°C min^{-1} to the isothermal crystallization temperature and keeping at that temperature until crystallization had finished.

The crystallization peaks were integrated using a horizontal sigmoid baseline and the starting- and end points were determined with the calculation algorithm as described in section 3.4.1.2. In between starting- and end points the area (and thus the amount of heat released up to that moment) was calculated at 5-minute intervals. The integration was performed with the Universal Analysis software version 2.5 H (TA Instruments, New Castle, USA). The start of the isothermal period was determined as described in section 3.3.5.

The algebraic solution of the model developed in chapter 4, written as function of the induction time (equation [4.21]), was fitted to the data series by non-linear regression using the Sigmaplot 2000 software (see also section 4.3.4).

6.3.4.2 Stop and return experiments

The same pan as for the isothermal crystallization experiment at that crystallization temperature was used. The starting-point of the integration in the isothermal crystallization experiment was chosen as the end of the isothermal crystallization in the stop and return experiment. The used time – temperature program was: heating to 65°C

and holding for 15 minutes, cooling at 8°C min^{-1} to the crystallization temperature, holding at that temperature for the desired time and heating up to 65°C at a rate of 5°C min^{-1} (see section 5.3.2.2 for more information on why this heating rate was chosen). As a result an indication of the amount of heat released before the start of the main crystallization peak was obtained. The melting peak was integrated as described in section 5.3.2.2. The integration was performed using the Universal Analysis software version 2.5 H (TA Instruments, New Castle, USA).

6.3.5 Detection of statistically significant differences

To check the general influence of the independent variable temperature on the different crystallization parameters ANOVA was performed (SPSS for Windows 10.0.5, SPSS Inc., Chicago, USA). A significance level of 0.05 was used at all times. To check what temperatures differed significantly (post-hoc tests) the adapted t-test as described in section 3.3.7, was used. This test takes into account that the calculated model parameters themselves are estimates. A significance level of 0.05 was also used here.

6.4 Results and discussion

6.4.1 Influence of temperature as measured by pNMR

Figure 6.2 and Figure 6.3 show the amount of solid fat as function of time for the standard factory product at temperatures between 19°C and 23°C and for the Nigerian cocoa butter at temperatures between 19°C and 22°C.

The same trends as function of temperature are observed for both cocoa butters. Both the rate of the first step and the height of the plateau after the first step decrease as the temperature increases. The second step starts later and the crystallization occurs slower as the temperature is higher. The equilibrium amount of solid fat decreases as the temperature increases.

Comparable results for the equilibrium amount of solid fat and the mass fraction of solid fat after the first step were obtained by Herrera et al. (1999a) and Vanhoutte (2002) for milk fat (fractions) and by Ng & Oh (1994) for palm oil. As already mentioned in section 6.1 Marangoni & McGauley (2003) found lower values for the equilibrium amount of solid fat for cocoa butter at higher temperatures.

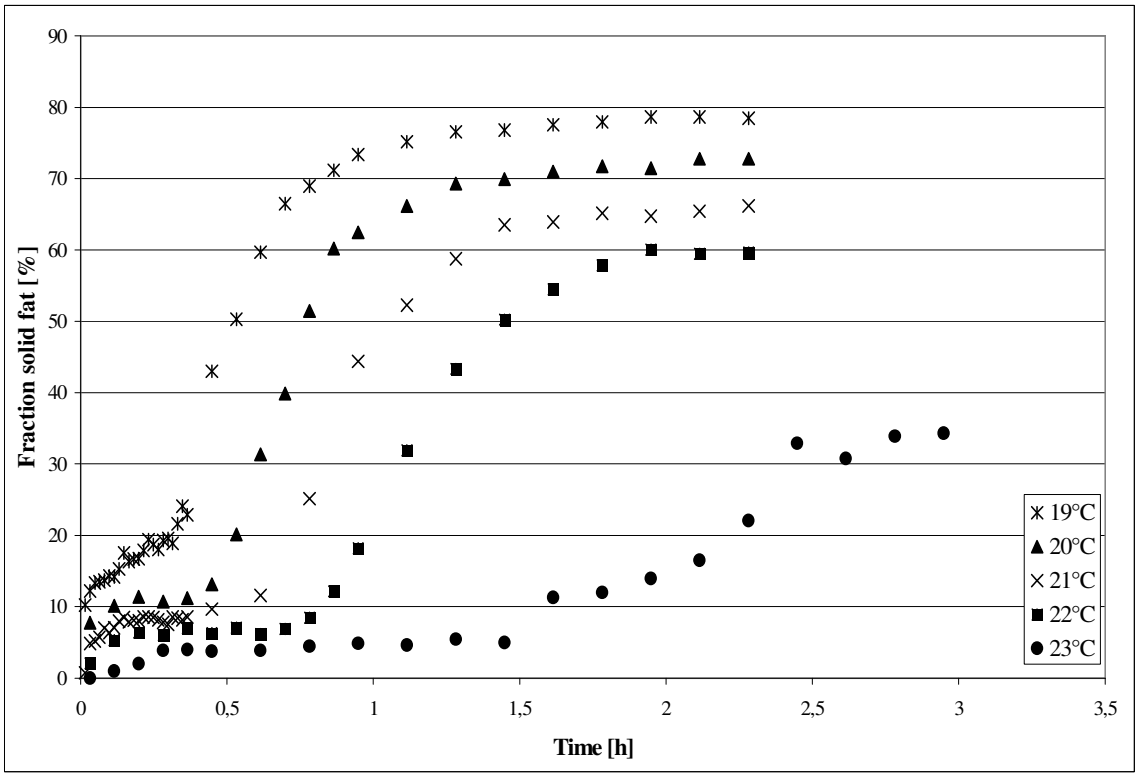

Figure 6.2 Influence of isothermal crystallization temperature on amount of solid fat versus time curves (standard factory product cocoa butter)

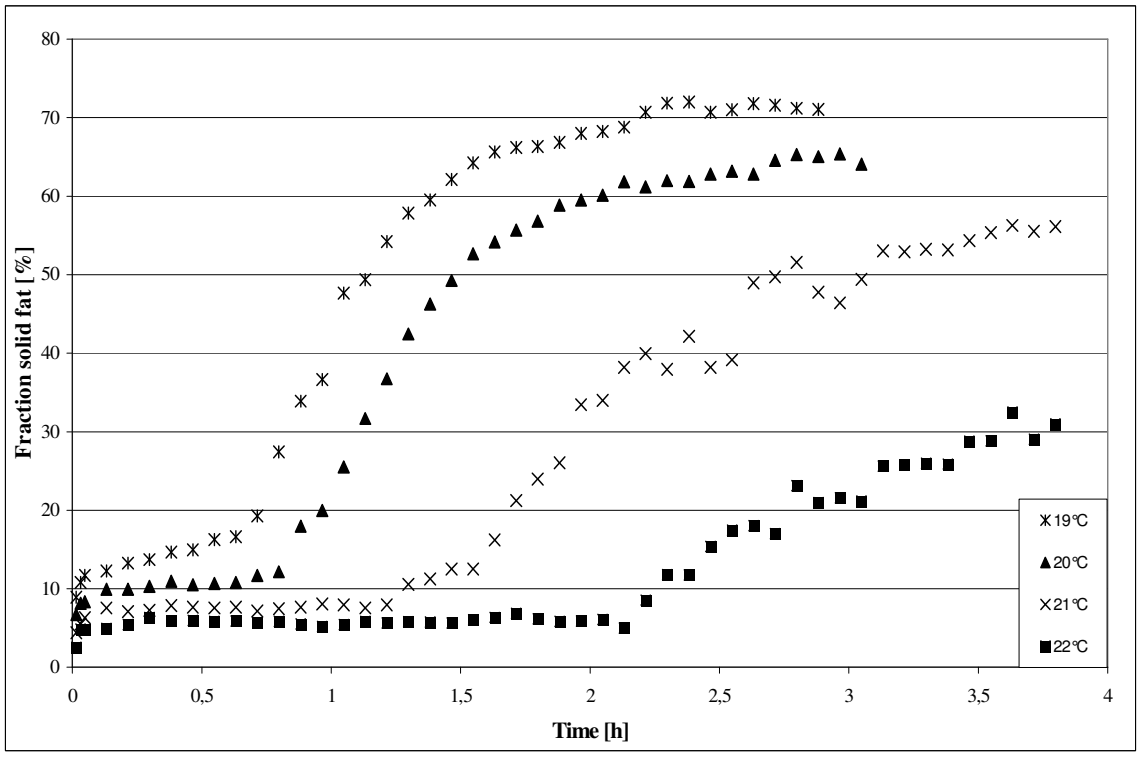

Figure 6.3 Influence of isothermal crystallization temperature on amount of solid fat versus time curves (Nigerian cocoa butter)

These results can be explained by the higher solubility at higher temperatures as described by the Hildebrand equation (see also section 1.2.1.2):

$$\ln C_s = \frac{\Delta H_m}{R_g}\left(\frac{1}{T_{Km}} - \frac{1}{T_K}\right) \quad \textbf{[6.1]}$$

where C_s is the concentration at saturation and T_{Km} and ΔH_m are respectively the absolute melting temperature [K] and the molar enthalpy variation in the system during the transition [J mole^{-1}] of the specific polymorph.

6.4.2 Influence of temperature on the α induction time as determined by SDLS

SDLS was used to study the initial phase of the first crystallization step, i.e. the crystallization of part of the melt in the α polymorph. Figure 6.4 shows the effect of temperature on the α induction time which was determined as the time when the crystal signal had increased 5 units above the minimum value.

The figure shows that the α induction time increases in a more or less exponential way with temperature. No jump in the curve can be observed, meaning that the same polymorph was formed (Ng, 1990) in the whole temperature range. This phenomenon was expected as it was already proved in chapter 5 that some α crystals are initially formed at all temperatures.

Taking account of the rather low supercooling at which crystallization occurs, heterogeneous nucleation can be suspected to take place. The temperature dependence of heterogeneous nucleation is however the same as for homogeneous nucleation (Rousset, 1997). The latter is described in section 1.2.1.2.

Using equations [1.4], [1.8], [1.10] and [1.11] (the Turnbull-Fisher equation) and considering that the induction time is inversely proportional to the nucleation rate, the induction time can be written as function of temperature as:

$$t\_ind_\alpha = \frac{cst1}{T_K} e^{\left(\frac{cst2 \times T_{Km}^2}{\Delta T^2 \times T_K}\right)} \quad \textbf{[6.2]}$$

with *cst1* and *cst2* combinations of variables independent of temperature. The critical activation free energy ΔG^* can be calculated from *cst2* as indicated in equation [6.3]:

$$\Delta G^* = \frac{cst2 \times k_B \times T_{Km}^2}{\Delta T^2} \qquad \textbf{[6.3]}$$

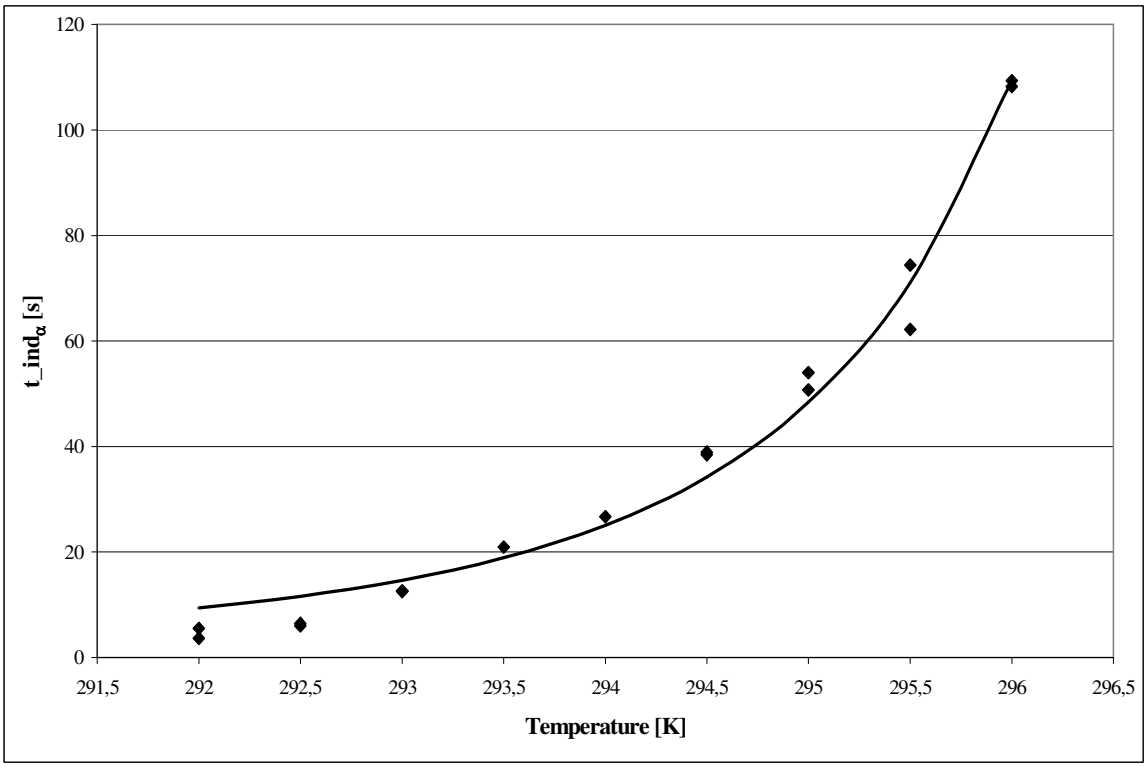

Figure 6.4 Influence of temperature on the α induction time as measured by SDLS (standard factory product cocoa butter) and Turnbull-Fisher equation fitted to these data (T_{Km} = 309 K)

To obtain equation [6.2] the volume diffusion term of equation [1.11] was neglected. Except for glass transitions, the value of this term is indeed small and can be considered constant as long as the temperature does not vary too much (Rousset, 1997). Figure 6.4 also indicates that the induction times do not increase again at lower temperatures, as would be expected if the volume diffusion term becomes rate limiting.

Equation [6.2] has been successfully applied to natural fats and oils (Herrera et al., 1999a, Litwinenko et al., 2002, Toro-Vazquez et al., 2002 and Wright & Marangoni, 2002), despite its original development for single-component systems. Using the curve fitting option of the Sigmaplot 2000 software (SPSS Science, Chicago, USA) (see also section 4.3.4) it was investigated whether equation [6.2] could be fitted to the data points in Figure 6.4. It was established that the quality of the obtained fit depends rather strongly on the chosen value of T_{Km} with the best fit at a value of 310.45 K or 37.45°C.

Then there is the question of what value has to be used for the melting point. In other words, how is the melting point defined for a product with a melting range and the melting point of which polymorph has to be used. Herrera et al. (1999a) used the Mettler dropping point whereas Litwinenko et al. (2002) used the peak maximum of a DSC melting profile (heating at 5°C min^{-1}) of the stable sample. With the latter definition, the melting point of the standard factory product cocoa butter was established at 36°C or 309K. Using this value for T_{Km} a good fit (R^2 = 0.984) was obtained as the curve in Figure 6.4 shows. The obtained parameter values are: 75 K s for *cst1* and 3.2 K for *cst2*. Using the value of *cst2* and equation [6.3] a value of $1.46.10^{-20}$ J $molecule^{-1}$ was obtained for ΔG^* for a crystallization temperature of 19°C. This value is equivalent to 8.8 kJ $mole^{-1}$, a value of the same order of magnitude as reported in literature by Toro-Vazquez et al. (2002) for tripalmitin in sesame oil, by Herrera et al. (1999a) and Wright & Marangoni (2002) for milk fat (fractions) and by Litwinenko et al. (2002) for palm based shortening.

6.4.3 Influence of temperature on DSC main crystallization peak

The main DSC crystallization peak was integrated and the model developed in chapter 4 (equation [4.21]) was fitted to the data series. This main peak most probably represents α mediated β' crystallization of part of the melt and transformation of the α crystals that are formed before the start of the main peak into the β' form (see chapter 5). The contribution of the latter is negligible compared to the one of the former (see also section 6.4.4).

6.4.3.1 Influence of temperature on parameter a_P

Figure 6.5 shows the influence of temperature on the a_P parameter for both cocoa butters. Taking into account that the latent heat of the β' polymorph is 100 J g^{-1} (Chapman et al., 1971 and Riiner, 1970), the a_P value equals the mass fraction β' crystals formed in the second step of crystallization neglecting the heat released by the polymorphic transition of the already formed α crystals. This mass fraction β' crystals is related to the difference in solubility of the α and β' polymorph since it is the lower solubility of the β' polymorph which makes that the crystallization can continue from the moment β' crystals are formed (see chapter 5).

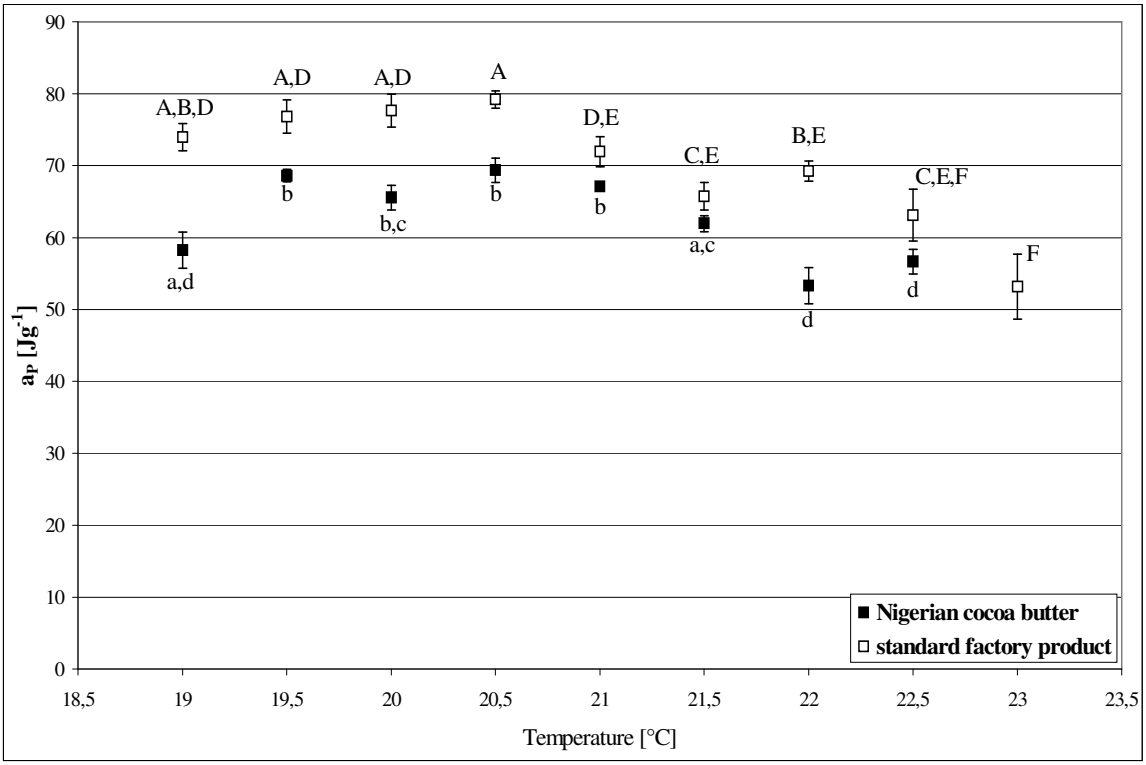

Figure 6.5 Influence of temperature on a_P for a standard factory product and a Nigerian cocoa butter. Error bars represent the standard deviation as calculated from equation [3.7]. The letters indicate the significant differences as calculated by adapted t-tests, values with the same letter are not significantly different.

It is clear that the a_P value remains more or less constant or slightly increases up to a temperature of 20.5°C and then decreases as the temperature further rises. The initial increase is more pronounced in the Nigerian cocoa butter.

ANOVA detected a significant effect of temperature on a_P for both cocoa butters. Adapted t-tests were used to obtain more details on what temperatures differ significantly and the results are indicated in Figure 6.5 with letters. Values with the same letter are not significantly different at the 5% level.

6.4.3.2 Influence of temperature on t_ind$_F$

Figure 6.6 shows the influence of temperature on the t_ind_F parameter for both cocoa butters. This parameter represents the induction time of the second step of crystallization, i.e. the α mediated β' crystallization.

It is obvious that t_ind_F increases as function of temperature in a more or less exponential way. No jump is observed in Figure 6.6 indicating that always the same polymorph is formed in the studied temperature range (Ng, 1990). The formation of the

β' crystals by a polymorphic transition of already formed α crystals was demonstrated in chapter 5.

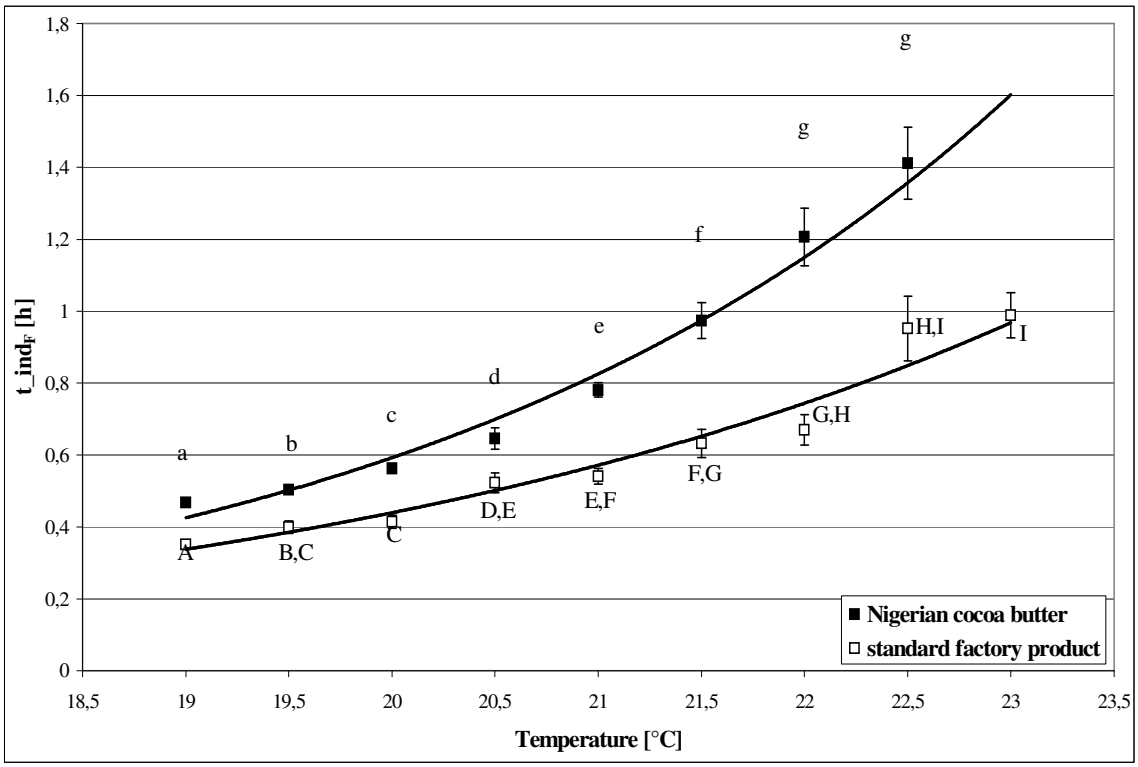

Figure 6.6 Influence of temperature on *t_ind*$_F$ for a standard factory product and a Nigerian cocoa butter and exponential curve fitted to the data. Error bars represent the standard deviation as calculated from equation [3.7]. The letters indicate the significant differences as calculated by adapted t-tests, values with the same letter are not significantly different.

ANOVA showed that temperature has a significant influence on *t_ind*$_F$ for both cocoa butters. Adapted t-tests showed that most of the differences between the values at different temperatures are significant. Details of the significant differences are indicated in Figure 6.6.

As already stated in section 6.1, Ziegleder (1990) also crystallized cocoa butter isothermally at different temperatures. He obtained a linear relation between the logarithm of the onset time (the intersection of the baseline with the line tangent to the curve at the inflection point) and the crystallization temperature. The onset time gives an indication of the start of a process and is in such a way related to the induction time *t_ind*$_F$. The linear correlation between the logarithm of the onset time and the crystallization temperature obtained by Ziegleder (1990) would correspond with an exponential relationship between *t_ind*$_F$ and temperature. For the standard factory product a rather good exponential relationship was obtained (R^2 = 0.87). In contrast to

the results of Ziegleder no deviation from the exponential relationship was observed at temperatures between 19°C and 20°C. For the Nigerian cocoa butter an R^2 of 0.93 was obtained also without a deviation at the lower temperatures.

Since the second step of the crystallization process probably starts by the polymorphic transition from α to β' (see chapter 5), this would mean that t_ind_F reflects the time needed to initiate this polymorphic transition. The DSC results indicate that this time is longer as the crystallization temperature is higher. The same result was obtained by real-time XRD (see chapter 5): the higher the temperature, the later the β' diffraction lines appear. McGauley & Marangoni (2003) and Van Malssen et al. (1999) obtained similar results. However, ten Grotenhuis et al. (1999) stated that the stability of the α polymorph of milk fat is higher at lower temperatures, leading to a diminished driving force for polymorphic transition and thus a later start of the transition at lower temperatures. Sato & Kuroda (1987) showed that the rate of the isothermal polymorphic transition from α (formed by rapid cooling of the melt to 0°C) to β in tripalmitin increases with a rising temperature.

A possible explanation for this contradiction is that the induction time as measured by DSC is primarily associated with crystal growth (Toro-Vazquez et al., 2002) because a considerable heat flow is only measured when the β' crystals are growing. Due to the very low supercooling for the β' polymorph (only about 5°C at the highest isothermal crystallization temperature) the crystal growth may be retarded, especially at the highest temperatures. This would mean that it takes a longer time before a considerable amount of heat is released. Still it is possible that β' nuclei already exist quite some time before the moment when the β' crystals have grown enough to release enough heat to be detected by DSC. It is thus also possible that the first β' nuclei appear earlier at higher temperatures. In milk fat and tripalmitin the difference between the melting points of both polymorphs is higher causing the smallest possible supercooling for β' formation by polymorphic transition to be higher (α polymorphs can only be formed up to the melting point of α). This may mean that crystal growth is not that much retarded and that is why the faster nucleation in the more stable polymorph at higher temperatures may predominate. This may explain why Vanhoutte (2002) did not find a clear relationship between temperature and the induction time for isothermal polymorphic transition from α to β'.

A crystal of some dimension is also needed for XRD to detect diffraction lines of a specific polymorph. This possibly explains why also in the XRD measurements a longer induction time was found at higher temperatures.

6.4.3.3 Influence of temperature on K

Figure 6.7 shows the influence of temperature on the *K* parameter for both cocoa butters. This parameter represents the rate constant of the crystallization process.

It is obvious that for the standard factory product the *K* value remains more or less constant up to 20°C but decreases strongly at higher temperatures. For the Nigerian cocoa butter the *K* value at the lowest temperatures is much lower than the values of the standard factory product. However, at higher temperatures the difference is less pronounced. As a consequence the decrease at higher temperatures is less clear for the Nigerian cocoa butter.

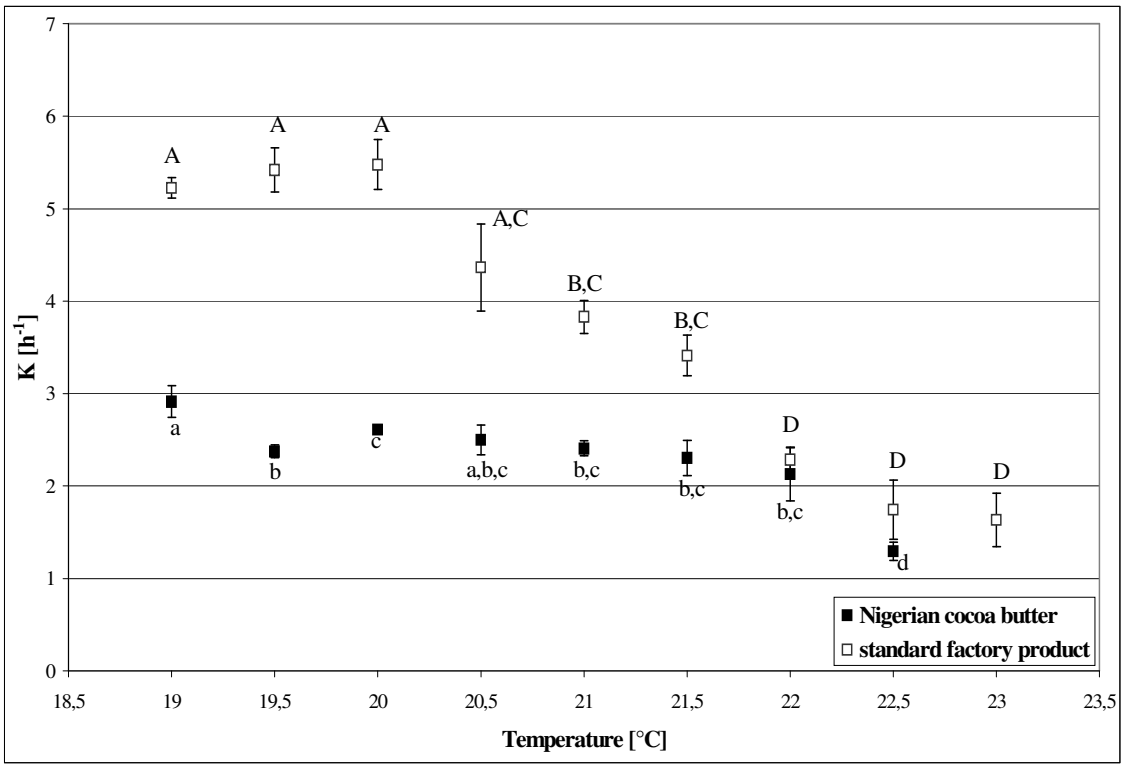

Figure 6.7 Influence of temperature on *K* for a standard factory product and a Nigerian cocoa butter. Error bars represent the standard deviation as calculated from equation [3.7]. The letters indicate the significant differences as calculated by adapted t-tests, values with the same letter are not significantly different.

ANOVA showed a significant influence of temperature on *K* for both cocoa butters. The results of the adapted t-tests also reflect the difference between both cocoa butters in the influence of temperature as indicated in Figure 6.7.

As already mentioned in section 6.1, Ziegleder (1990) observed a linear dependence of the logarithm of the Avrami rate constant *k* on temperature from 20°C onwards. This corresponds with an exponential relationship between *k* and temperature from 20°C onwards. He attributed the lower than expected values for temperatures lower than 20°C, to the increase of the melt viscosity. A similar result was obtained by Supaphol and Spruiell (2001) for melt crystallization of polymers. They described the temperature dependency of the crystallization rate constant with a bell-shaped curve and ascribed this type of curve to the nucleation control effect at low supercooling and the diffusion control effect at high supercooling.

The data for the standard factory product can be described rather well by the right side of such a bell-shaped curve, which shows that, as expected, the viscosity influence is not that pronounced in the temperature interval studied. The data of the Nigerian cocoa butter can hardly be described by a bell-shaped curve. Possibly the rate constant *K* only starts to decrease strongly at higher temperatures.

It should be noted that the DSC main crystallization peak relates to crystallization from the melt in the α polymorph and polymorphic transition from α into β'. That is why the crystallization rate constant *K* may depend on both rates. Sato & Kuroda (1987) observed increasing rates of polymorphic transition at higher temperatures. However, as already stated in section 6.4.3.2, the growth of β' crystals is retarded in cocoa butter compared to tripalmitin due to the lower supercooling. This may lead to a decreasing rate of the polymorphic transition at higher temperatures and explain why the temperature dependence of *K* agrees (at least for the standard factory product) with the temperature dependence that is expected for the rate constant of a simple crystallization from the melt.

6.4.3.4 Influence of temperature on n

Figure 6.8 shows the influence of temperature on the *n* parameter for both cocoa butters. This parameter represents the order of the reverse reaction of the crystallization process, which reflects how long this reverse reaction affects the crystallization process. The higher *n*, the shorter its influence.

It is clear that the *n* value initially decreases but remains more or less constant from 20.5°C (standard factory product) or 21.5°C (Nigerian cocoa butter) onwards.

ANOVA showed a significant influence of temperature on *n*. The results of the adapted t-tests are indicated in Figure 6.8.

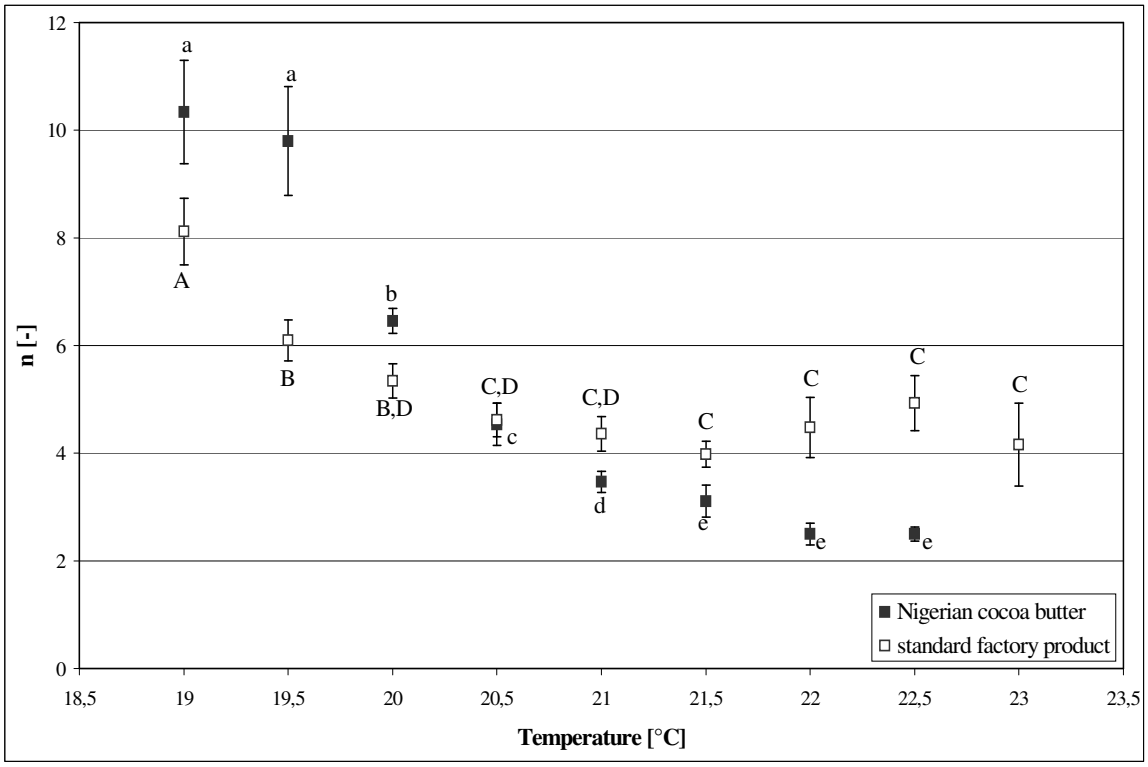

Figure 6.8 Influence of temperature on *n* for a standard factory product. Error bars represent the error (1 standard deviation) on the parameter estimation. The letters indicate the significant differences as calculated by adapted t-tests, values with the same letter are not significantly different.

In section 4.4.1.9 three hypotheses were already formulated concerning the detailed nature of the reverse reaction. The first hypothesis attributes the reverse reaction to a local remelting of crystals due to a local temperature increase caused by the release of latent heat. Remelting may be suspected to be less plausible at lower temperatures, as the temperature has to increase more before the melting point is reached. This would cause the reverse reaction to lose its effect faster and thus lead to higher *n* values at lower temperatures. This agrees with the observed results. However, it should also be taken into account that the crystals are smaller at lower temperatures and thus melt more easily due to a higher surface energy.

A second hypothesis explains the reverse reaction by redissolving of molecules from the crystals. As the crystals grow the surface-to-volume ratio decreases and the reverse reaction slows down. The expectation is then that, at lower temperatures, when more nuclei are formed and the crystals remain smaller, the rate of the reverse reaction

decreases less and thus lower *n* values are obtained. This is in contrast to the observations. However, it is also of importance that the solubility is higher at higher temperatures (see the Hildebrand equation [6.1]) and for that reason redissolving may be more favoured at these higher temperatures leading to a lower value of *n*.

A combination of several processes was a third hypothesis. The temperature influence may then be explained by a different dominating process leading to another order of the reaction. Remelting may dominate at higher temperatures due to the smaller temperature difference between crystallization and melting temperature, whereas at lower temperatures redissolving may be favoured because of the smaller crystal size. Redissolving may be considered then as a more complex reaction, depending directly on *h* but also on several variables (e.g. the size of the crystals), which are in turn affected by *h.* This may explain the higher order of the overall reaction.

The temperature dependence consequently does not really rule out any of the three hypotheses.

6.4.4 Influence of temperature on α crystallization as determined by DSC stop and return experiments

The amount of α crystallization was estimated by DSC by holding the sample at the crystallization temperature up to the starting-point of the integration of the main peak and then heating up the sample. The area of the obtained peak is plotted as function of temperature in Figure 6.9. It has to be taken into account that due to baseline problems the area could only be approximated (see section 5.3.2.2).

Despite this approximation a rather good repeatability (an average coefficient of variation of 10%) is obtained for the standard factory product. The results for the Nigerian cocoa butter show a worse repeatability (average coefficient of variation of nearly 30%). The area of the melting profile decreases as function of temperature for both cocoa butters.

Considering that the latent heat of the α polymorph is around 80 J g^{-1} (Chapman et al., 1971 and Riiner, 1970), the mass fraction α crystals can be calculated from the area of the melting peak. For the standard factory product this mass fraction decreases from 14.7% at 19°C to 2.4% at 22°C while for the Nigerian cocoa butter a decrease from 16.4% at 19°C to 2.8% at 22.5°C was observed. The same decrease of the mass fraction

α crystals as function of temperature was observed using pNMR (height of the first plateau in Figure 6.2).

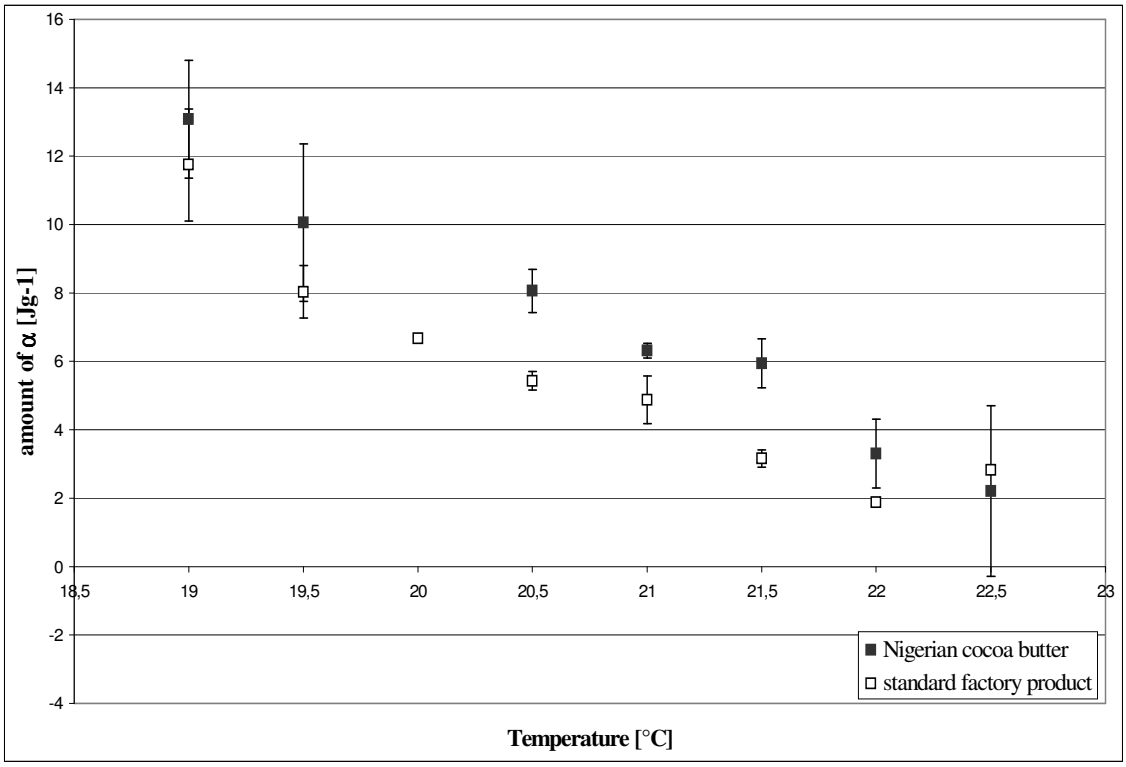

Figure 6.9 Area of DSC melting profile after isothermal crystallization up to starting-point of main crystallization peak for standard factory product and Nigerian cocoa butter. The error bars represent 1 standard deviation; when no error bars are depicted, only 1 repetition was performed.

Using these mass fractions of α crystals formed in the first crystallization step, the contribution to the main DSC crystallization peak of their transformation to β' can be calculated taking account of the heat of polymorphic transition of approximately 20 J g^{-1}. The contribution appears to be 3.3 J g^{-1} at the most and is thus negligible compared to the total area of the main peak, which is between 50 and 80 J g^{-1}.

By adding the mass fraction α formed in the first step to a_P (i.e. the mass fraction β' formed in the second step) the equilibrium amount of solid fat could be calculated from the DSC experiments (Table 6.1). These values were then compared with the equilibrium amount of solid fat measured by pNMR (Figure 6.2). The pNMR values turned out to be lower for both cocoa butters and this holds for all crystallization temperatures. A possible explanation for this difference was already given in section 5.4.6.4. Another reason may be that the pNMR experiments were terminated too early and so the equilibrium amount of solid fat was not reached yet.

Table 6.1 Total amount of solid fat as calculated from isothermal DSC experiments and DSC stop and return experiments (calculations based on mean values of the available results) and comparison with pNMR results (estimated values from curves).

Temperature [°C]	Total amount of solid fat [%]			
	Standard factory product		Nigerian cocoa butter	
	DSC	PNMR	DSC	pNMR
19	89	79	75	71
19.5	87		81	
20	86	74	[1]	65
20.5	86		80	
21	78	66	75	57
21.5	70		69	
22	72	60	57	30
22.5	67		59	
23	[1]	35		

[1] Value that could not be calculated due to missing stop and return experiments

The lower mass fraction α crystals as well as the lower equilibrium amount of solid fat at higher temperatures can be explained by the higher solubility at higher temperatures. This was already discussed in section 6.4.1.

6.5 Conclusion

The influence of temperature on the isothermal crystallization of cocoa butter at temperatures between 19°C and 23°C was studied by pNMR, SDLS and DSC for two different cocoa butters. The influence of temperature is more or less comparable for both cocoa butters. Furthermore, it was determined that the nucleation in the α polymorph agrees the Turnbull-Fisher equation describing a higher induction time at higher temperatures. Also, the induction time of the second part of the crystallization process (t_ind_F), i.e. the induction time for the polymorphic transition from α to β', increases with temperature. Likely, the value of t_ind_F is more related to the growth of the β' crystals, thus explaining its temperature dependence. The rate constant K decreases as the temperature increases, especially at higher temperatures. The order of the reverse reaction n decreases up to a certain temperature and then remains equal.

Both the mass fraction α crystals and the equilibrium amount of solid fat decrease as function of temperature, in accordance with the solubility principle.

7 INFLUENCE OF CHEMICAL COMPOSITION ON THE ISOTHERMAL COCOA BUTTER CRYSTALLIZATION

7.1 Introduction

The chemical composition of cocoa butter varies depending on the growing conditions and the age of the plant (see also section 2.3). The production process of the cocoa butter from the cacao-beans and any refining of the butter may also influence the composition (see also section 2.2). In section 2.4.2 the effect of these differences in chemical composition on the physical properties was already discussed briefly. The introduction of this chapter gives a more detailed overview of the literature dealing with the effect of chemical composition (triacylglycerol profile and minor components) on the cocoa butter crystallization properties. Where no or very little information on cocoa butter is available, the effect of chemical composition on the crystallization of other fats is also discussed.

7.1.1 Triacylglycerol profile

The induction time of crystallization as well as the solid fat content mainly depend on the triacylglycerol composition (Chaiseri & Dimick, 1989 and Shukla, 1995).

Pontillon (1998a) observed a moderate correlation between the solid fat content on the one hand and the amount of tri-saturated and tri-unsaturated triacylglycerols on the other hand. However, the amount of di-unsaturated triacylglycerols correlates the best with the solid fat content. Chaiseri & Dimick (1989) also found that cocoa butter containing a high concentration of di-unsaturated triacylglycerols is softer and thus has a lower SFC. They explained this phenomenon by the double bond in the fatty acid in the sn-3 position of the di-unsaturated triacylglycerols, which causes extra kinking in the structure and so interrupts the molecular packing of the major components, the mono-unsaturated triacylglycerols. In a later study the same authors (Chaiseri & Dimick, 1995a) discovered that samples containing a higher concentration of POO and SOO and concomitantly a lower POS and SOS concentration, have longer induction times when they are isothermally crystallized at 26.5°C under mild agitation.

Davis & Dimick (1989) also crystallized cocoa butter isothermally at 26.5°C. After three hours they observed seed crystals with a melting point of 72.4°C and a high concentration of tri-saturated triacylglycerols. Loisel et al. (1998a) found that during cooling of cocoa butter, SSS crystallizes first as a separate fraction due to its limited solubility in mono- and di-unsaturated triacylglycerols. Adding extra SSS consequently shortens the induction time of the first crystallization step but does not affect the crystallization of the remaining triacylglycerols. Hachiya et al. (1989) studied the effect of seeding on the crystallization kinetics of cocoa butter and dark chocolate. They concluded that SSS in the β form does not remarkably accelerate the crystallization despite its high melting point, whereas SOS in the β form remarkably enhances the crystallization rate.

7.1.2 Minor components

Gutshall-Zakis & Dimick (1993) showed that the refining of cocoa butter has a significant impact on its crystallization kinetics (crystallization at 26.5°C under agitation). They attributed this phenomenon to the removal of the majority of phospholipids, free fatty acids and other minor components. They also observed that refined cocoa butter contains a higher percentage of solid fat compared to unrefined samples.

Wright et al. (2000) discovered that nucleation occurs later when the minor components are removed from milk fat or when their concentration is doubled. At lower levels these minor components thus serve as nucleating sites and aid in crystallization but at higher concentrations they begin to interfere with crystallization. These authors did not find an influence of the amount of minor components on the equilibrium amount of solid fat.

7.1.2.1 Free fatty acids

Pontillon (1998a) observed that free fatty acids increase the crystallization time of cocoa butter but only at concentrations above 2%. Loisel et al. (1998b) showed that increased levels of free stearic acid slow down the crystallization of the mono-unsaturated triacylglycerols in chocolate.

From their study Smith et al. (1994) concluded that free lauric acid increases the growth rate of trilaurin under non-isothermal conditions. Free fatty acids dissimilar in chain length, either have little influence on or only slightly increase the growth rate of trilaurin (Smith & Povey, 1997).

Gordon & Rahman (1991) studied the addition of free fatty acids to coconut oil. The addition of free lauric and oleic acid dramatically increases the induction time whereas free palmitic acid has a smaller effect. It is likely that palmitic acid precipitates out of coconut oil on cooling and initiates nucleation. Lauric acid, however, is likely to be incorporated into the growing embryo prior to nucleation and thereby retards formation of a nucleus.

Jacobsberg & Oh Chuan (1976) found that an increase in the free fatty acid content of palm oil decreases the SFC and shifts the melting point to lower temperatures. They attributed this to the formation of a eutectic mixture.

7.1.2.2 Monoacylglycerols

Chaiseri & Dimick (1995a) stated that monoacylglycerols will not affect the cocoa butter crystallization much because of their low concentrations.

In general however, micelles of monoacylglycerols are suspected to act as templates for crystallization and may induce heterogeneous nucleation (Walstra, 1987). Indeed, Sambuc et al. (1980) showed that the addition of 4% of a mixture of monopalmitin and monostearin decreases the induction time of vegetable fats. Smith et al. (1994) found that monolaurin increases the growth rate of trilaurin under non-isothermal conditions while monoacylglycerols dissimilar in chain length, either have little influence on or only slightly increase the growth rate of trilaurin (Smith & Povey, 1997). Addition of 0.05% to 0.25% milk fat monoacylglycerols does not affect the crystallization behaviour of milk fat much (Vanhoutte, 2002).

7.1.2.3 Diacylglycerols

Shukla (1995) and Ziegleder (1988) noticed that cocoa butters with a higher diacylglycerol level exhibit a slower crystallization. Chaiseri & Dimick (1995a) showed that rapid-nucleating cocoa butters (isothermal crystallization at 26.5°C under mild agitation) contain significantly higher concentrations of stearic acid in the diacylglycerol fraction. Wähnelt et al. (1991) added 10% extra diacylglycerols to cocoa butter and observed a retarded crystallization with 1,2-diacylglycerols having more effect than 1,3-diacylglycerols.

Cebula & Smith (1992) observed that diacylglycerols promote nucleation in cocoa butter equivalents but retard crystal growth and polymorphic transitions.

Vanhoutte (2002) found that milk fat diacylglycerols in concentrations between 0.5% and 2% retard the start of crystallization and decrease the growth rate. Gordon & Rahman (1991) concluded that dilaurin retards the nucleation of coconut oil whereas diolein does not have a significant effect. Smith et al. (1994) showed that dilaurin retards the growth rate of trilaurin and acts as a stabilizer for metastable polymorphs while diacylglycerols dissimilar from the host, have less pronounced effects (Smith & Povey, 1997). Siew & Ng (1996) and Wright & Marangoni (2002) also remarked that the effect of diacylglycerols depends on their compatibility with the surrounding triacylglycerols.

Siew & Ng (1996) observed a decreased SFC of palm olein in the presence of diacylglycerols. Jacobsberg & Oh Chuan (1976) also found that an increase in the diacylglycerol content of palm oil decreases the SFC and shifts the melting point to lower temperatures. They attributed this to the formation of a eutectic mixture.

7.1.2.4 Phospholipids

Davis & Dimick (1989) isothermally crystallized cocoa butter at 26.5°C and observed seed crystals with a melting point of 72.4°C after three hours of crystallization. These seed crystals contain a higher proportion of phospholipids, in particular phosphatidylethanolamine and phosphatidylcholine, compared to the original cocoa butter. Gutshall-Zakis & Dimick (1993) showed that slow nucleating cocoa butters contain higher amounts of phospholipids. However, neither Savage & Dimick (1995) nor Chaiseri & Dimick (1995a) found any correlation between the nucleation times and the total phospholipid concentration. They did find a significant correlation between the concentration of phosphatidylinositol and phosphatidylcholine and the nucleation time.

Smith (2000) showed that also in palm oil the interaction between phospholipids and triacylglycerols depends on the phospholipid nature and the similarity in chain length between the phospholipid and the triacylglycerol. This causes some types of phospholipids to delay nucleation while others have a more pronounced effect on the growth rate. Vanhoutte (2002) showed that phospholipids delay the onset of crystallization at intermediate levels (0.0175%), whereas at higher levels (0.03 – 0.07%) they retard the growth rate.

7.1.3 Aim of the chapter

It is the aim of this chapter to chemically characterize (fatty acid profile, triacylglycerol profile and minor components) a series of cocoa butters and to investigate whether these chemical composition variables influence the isothermal cocoa butter crystallization. This crystallization was followed by DSC and described by the four parameters of the model developed in chapter 4. Supplementary information on the effect of chemical composition on nucleation was obtained by SDLS (scanning diffusive light scattering).

7.2 Research strategy

Twenty different cocoa butters were isothermally crystallized at 20°C (± 0.05°C) in the DSC. Each cocoa butter was analyzed five times. The main crystallization peak was integrated and the model developed in chapter 4 was fitted to the data series. To gain more insight in the initial crystallization phase, SDLS experiments were performed on some cocoa butters.

For each cocoa butter the following chemical composition variables were determined: fatty acid profile (in double), triacylglycerol profile, diacylglycerol content, free fatty acid content (in double), phosphorus content related to the phospholipid content (in triple), iron content (in triple), soap content (in double), amount of unsaponifiable matter (in double), peroxide value (in double), p-anisidine value. HPLC and thin layer chromatography experiments showed that the amount of monoacylglycerols in cocoa butter was negligible and so these were not quantified.

With principal component analysis and forward linear regression the influence of the different chemical composition variables on the crystallization parameters was investigated.

7.3 Materials and methods

7.3.1 Cocoa butters

Twenty different cocoa butters were used. Table 7.1 gives a short description of each cocoa butter and the supplier.

Table 7.1 Overview of used cocoa butters

Sample name	Sample description and supplier
CB A	Cocoa butter from West-Africa (ADM Cocoa, Koog aan de Zaan, the Netherlands)
CB B	Cocoa butter from Ivory Coast (1st sample) (Barry Callebaut, Wieze, Belgium)
CB C	Cocoa butter from Nigeria (Barry Callebaut, Wieze, Belgium)
CB D	Cocoa butter from Ivory Coast (2nd sample) (Barry Callebaut, Wieze, Belgium)
CB E	Cocoa butter from Indonesia (Barry Callebaut, Wieze, Belgium)
CB F	Cocoa butter from Malaysia (ADM Cocoa, Koog aan de Zaan, the Netherlands)
CB G	Cocoa butter from San Domingo (Barry Callebaut, Wieze, Belgium)
CB H	Cocoa butter from Ecuador (Barry Callebaut, Wieze, Belgium)
CB I	Cocoa butter from Brazil (1st sample) (Barry Callebaut, Wieze, Belgium)
CB J	Unsteamed cocoa butter of unknown origin (Barry Callebaut, Bussum, the Netherlands)
CB K	Steamed cocoa butter of unknown origin (Barry Callebaut, Bussum, the Netherlands)
CB L	Standard factory product (batch 1) (Barry Callebaut, Wieze, Belgium)
CB M	Hard cocoa butter (unknown origin) (Barry Callebaut, Wieze, Belgium)
CB N	Standard factory product (batch 2) (Barry Callebaut, Wieze, Belgium)
CB O	Cocoa butter from a mixture of beans from Ivory Coast, Brazil and Indonesia (ADM Cocoa, Koog aan de Zaan, the Netherlands)
CB P	Cocoa butter from Brazil (2nd sample) (Barry Callebaut, Wieze, Belgium)
CB Q	Cocoa butter causing crystallization problems in production (1st sample) (Barry Callebaut, Wieze, Belgium)
CB R	Cocoa butter causing crystallization problems in production (2nd sample) (Barry Callebaut, Wieze, Belgium)
CB S	Cocoa butter causing crystallization problems in production (3rd sample) (Barry Callebaut, Wieze, Belgium)
CB T	Cocoa butter causing crystallization problems in production (4th sample) (Barry Callebaut, Wieze, Belgium)

7.3.2 Isothermal crystallization experiments by DSC

The DSC experiments were performed with a 2010 CE DSC (TA Instruments, New Castle, USA) with a Refrigerated Cooling System (TA Instruments, New Castle, USA). The DSC was calibrated with indium (TA Instruments, New Castle, USA), azobenzene (Sigma-Aldrich, Bornem, Belgium) and undecane (Acros Organics, Geel, Belgium) prior to analyses. Nitrogen was used to purge the system.

Cocoa butter (2.5-15.0 mg) was sealed in hermetic aluminum pans (using sample preparation procedure B as described in section 3.3.2.2) and an empty pan was used as a reference.

The applied time-temperature program was (see chapter 3): holding at 65°C for 15 minutes to ensure a completely liquid state, cooling at 8°C min^{-1} to 20°C and keeping at that temperature until crystallization had finished.

The crystallization peaks were integrated using a horizontal sigmoid baseline and the starting- and end points were determined using the calculation algorithm as described in section 3.4.1.2. In between the starting- and end points, the area (and thus the amount of heat released up to that moment) was calculated at 5-minute intervals. The integration was performed with the Universal Analysis software version 2.5 H (TA Instruments, New Castle, USA). The start of the isothermal period was determined as described in section 3.3.5.

The algebraic solution of the model developed in chapter 4 written as function of the induction time (equation [4.21]) was fitted to the data series by non-linear regression using the Sigmaplot 2000 software (see also section 4.3.4).

7.3.3 Determination of α induction time by SDLS

An NK60-CPA (Phase Technology, Richmond, Canada) light-scattering analyzer was used. The principle of operation is described in section 6.3.3. Liquefied cocoa butter (150 µl) was placed in the sample compartment, heated to 65°C at 25°C min^{-1} and kept at that temperature for 15 minutes. Then the sample was cooled at 8°C min^{-1} to 20°C where it was kept until saturation of the signal (i.e. a value of 250). The start of the isothermal period was taken at the moment the crystallization temperature ± 0.1°C was reached.

The induction time for α crystallization (t_ind_α) was determined as the time when the crystal signal has increased 5 units above the minimum value.

7.3.4 Determination of chemical composition

7.3.4.1 *Fatty acid profile* (De Meulenaer & Huyghebaert, 2002)

7.3.4.1.1 Principle

The fatty acids were esterified with methanol in the presence of the catalyst potassium hydroxide. Then the methylesters were separated by gas liquid chromatography. The fatty acids were identified by comparing their retention times with those of familiar fatty acids. The peak areas were correlated with the quantities of the respective fatty acids.

7.3.4.1.2 Materials

- 20 ml test tubes with screw cap;
- 1 ml and 10 ml pipettes;
- gaschromatography tubes;
- gaschromatographic equipment: GC 3380 (Varian, Sint-Katelijne Waver, Belgium) with WCOT CP-sil 88 column, split injector and flame ionization detector;
- hexane (Chem-Lab, Zedelgem, Belgium);
- esterifying solution: 2N potassium hydroxide (Merck, Darmstadt, Germany) in methanol (Chem-Lab, Zedelgem, Belgium).

7.3.4.1.3 Method

- put 4 droplets of melted cocoa butter in a test tube, add 9 ml hexane and 1 ml esterifying solution and shake for 30 s;
- fill the tubes of the gaschromatographic equipment;
- conditions of gaschromatographic analysis: temperature of injector: 250°C, temperature of detector: 250°C, flow rate of mobile phase (helium): 1 ml min^{-1}, flow rate of hydrogen: 40 ml min^{-1}, flow rate of air: 120 ml min^{-1}, injection volume: 1 µl, column oven temperature: 120°C for 2 minutes followed by heating at 5°C min^{-1} to 200°C and holding at that temperature for 20 minutes.

7.3.4.2 Triacylglycerol profile

7.3.4.2.1 Principle

Cocoa butter was separated by high resolution capillary gas chromatography into triacylglycerol fractions according to their molecular weight and degree of unsaturation using a thermostable polarizable capillary column. The triacylglycerols appear in order of increasing number of carbon atoms and of increasing degree of unsaturation for the same number of carbon atoms. The peaks were identified by comparison of the retention times of the sample with those of standards. The peak areas were correlated with the quantities of the respective triacylglycerols.

7.3.4.2.2 Materials

- analytical balance (Sartorius MC210P, Göttingen, Germany);
- volumetric flasks;
- 1 ml and 10 ml pipettes;
- gas chromatograph: cold on-column injection system, flame ionization detector, carrier gas: hydrogen, column: CP-TAP (0.25 mm X 25 m, 0.1 µm);
- isooctane (Merck, Darmstadt, Germany).

7.3.4.2.3 Method

- weigh 0.50 g of liquefied cocoa butter in a volumetric flask and add 9.5 ml isooctane;
- pipette 0.5 ml of the solution into another volumetric flask and add 9.5 ml of isooctane;
- inject 0.5 µl of the solution into the gas chromatographic system;
- operating conditions: initial temperature: 100°C, heat at 95°C min^{-1} to 115°C, heat at 65°C min^{-1} to 175°C, heat at 45°C min^{-1} to 300°C and heat at 35°C min^{-1} to the final temperature of 365°C, flow rate 1 ml min^{-1}.

7.3.4.3 Diacylglycerols

7.3.4.3.1 Principle

The amount of diacylglycerols present in cocoa butter was determined by HPLC with an evaporative light scattering detector (ELSD). The diacylglycerol peaks were identified

by comparison of the retention times of the sample with those of dipalmitin and distearin standards. The peak areas were correlated with the quantities of diacylglycerols.

7.3.4.3.2 Materials

- dipalmitin and distearin standards (Nu-check Prep, Elysian, United States);
- acetonitrile (Chem-Lab, Zedelgem, Belgium);
- dichloromethane (Merck, Darmstadt, Germany);
- HPLC system: Gilson (Den Haag, the Netherlands) 811C chromatograph with two pumps and a manometric module, 20 µl injection valve, Spherisorb ODS-2 column (150 X 4.6 mm, 3 µm particles) (Varian, Sint-Katelijne Waver, Belgium), reversed phase 3 µm pre-column (Varian, Sint-Katelijne Waver, Belgium), column oven (Model 7990, Jones Chromatography, Hengoed, United Kingdom), ELSD detector (Model 2000, Alltech, Lokeren, Belgium) at 1.7 bar and 64°C, carrier gas: nitrogen.

7.3.4.3.3 Method

- dissolve a liquefied cocoa butter sample in dichloromethane in a concentration of 1 mg ml^{-1};
- inject into the HPLC system using a mobile phase consisting of 67:33 acetonitrile: dichloromethane, a flow rate of 0.6 ml min^{-1} and a column temperature of 30°C.

7.3.4.3.4 Calculation

The percentage of diacylglycerols in cocoa butter, expressed on triacylglycerol basis, was calculated according to equation [7.1]:

$$\%\ diacylglycerols = \frac{area\ diacylglycerol\ peaks \times \%_{GLC}}{area\ triacylglycerol\ peaks} \quad \textbf{[7.1]}$$

The area of the triacylglycerol peaks is the sum of the areas of the five main triacylglycerol peaks detectable via HPLC (POP, POS, SOS, SOO and POO). With gas chromatography (see section 7.3.4.2) the percentagewise contribution of these five triacylglycerols to the total amount of triacylglycerols was calculated (= $\%_{GLC}$). Then this value was used to correct the percentage of diacylglycerols.

7.3.4.4 Free fatty acids (AOCS Official Method Ca 5a-40, 1996)

7.3.4.4.1 Principle

The amount of free fatty acids was determined by dissolving a known quantity of fat in ethanol and by titration with aqueous sodium hydroxide.

7.3.4.4.2 Materials

- 25 ml burette;
- analytical balance (Sartorius A02119, Göttingen, Germany);
- 250 ml conical flask;
- 10 ml plastic pipettes;
- sodium hydroxide (0.01 N);
- 1% phenolphtalein (Merck, Darmstadt, Germany) solution in ethanol;
- mixture of diethylether (Chem-Lab, Zedelgem, Belgium) and 95% ethanol (Chem-Lab, Zedelgem, Belgium) (1:1 v/v) with 3 ml phenolphtalein solution per litre.

7.3.4.4.3 Method

- weigh approximately 2.00 g of liquefied cocoa butter in the conical flask;
- add 50 ml of the diethylether / ethanol / phenolphthalein solution and shake;
- titrate with sodium hydroxide shaking vigorously until the appearance of the first permanent pink colour.

7.3.4.4.4 Calculation

The amount of free fatty acids expressed as % oleic acid (molecular weight 282 g mole^{-1}) was calculated with equation [7.2]:

$$\%\, free\, fatty\ acids = \frac{V_{NaOH}\,[ml] \times 0.01 \times 282}{sample\ mass\,[g] \times 10} \qquad \textbf{[7.2]}$$

7.3.4.5 Phosphorus (AOCS recommended practice Ca 20-99, 1999)

7.3.4.5.1 Principle

The amount of phosphorus in cocoa butter was determined by inductively coupled plasma-atomic emission spectroscopy. With this technique liquid samples are nebulized and carried into the excitation source by a flowing gas. Atoms are quantified by

measuring the specific emission lines produced by atoms decaying from high energy levels.

7.3.4.5.2 Materials

- inductively coupled plasma-atomic emission spectrometer (Atomscan, Thermo Jarrel Ash, Franklin, USA);
- analytical balance (Sartorius, Göttingen, Germany);
- glass test tubes with screw cap;
- disposable plastic pipettes;
- beaker;
- hot water bath (Rikakikai, Tokio, Japan);
- kerosene (Sigma-Aldrich, Steinheim, Germany);
- peanut oil (commercial sample from supermarket);
- high standard solution containing 80 ppm phosphorus, 2 ppm iron, 2 ppm calcium and 2 ppm magnesium, prepared from commercially available single element organic based standards (Merck, Darmstadt, Germany).

7.3.4.5.3 Method

- put 2.00 g of liquefied cocoa butter in a test tube and add kerosene to 10.00 g;
- shake the test tube and put it in a hot water bath to ensure that the sample remains in solution with the solvent and also to avoid solidification of the sample;
- perform a wavelength calibration to identify and determine the entire wavelength region;
- perform a peak search with the high standard solution to fine-tune the selected wavelength for phosphorus (214.9 nm);
- standardize at the phosphorus wavelength, first with the solvent (kerosene) and then with the high standard solution, repeat this standardization every ten or less samples;
- measure the cocoa butter samples (measurement is performed in triplicate in the apparatus).

7.3.4.5.4 Calculation

The concentration of phosphorus [ppm] was calculated from the peak area with the linear regression formula calculated from the area and concentration of the blank and the standard taking the correct dilution factor into account.

7.3.4.6 Iron

The amount of iron was determined by inductively coupled plasma-atomic emission spectroscopy. The iron determination was executed in the same run as the phosphorus determination. A wavelength of 259.94 nm was used for the iron determination.

7.3.4.7 *Traces of soap* (AOCS Recommended practice Cc 17-79, 1990 and Pontillon & Cros, 1998)

7.3.4.7.1 Principle

When cocoa butter is mixed with hydrated acetone two layers are formed. The soap, being the more polar constituent, goes to the upper layer. The amount is determined by titration.

7.3.4.7.2 Materials

- 250 ml conical flask;
- 25 ml burette;
- 25 ml pipette;
- analytical balance (Sartorius model A02119, Göttingen, Germany);
- 100 ml and 1 l volumetric flask;
- bromophenol blue indicator solution: put 0.2 g of bromophenol blue (Janssen Chimica, Geel, Belgium) in a 100 ml volumetric flask and fill with acetone (Vel, Leuven, Belgium);
- hydrochloric acid (Merck, Darmstadt, Germany) solution: 0.01 N in acetone (Vel, Leuven, Belgium)
- neutralized acetone: put 30 ml demineralized water, 1 ml bromophenol blue indicator solution and 800 ml acetone (Vel, Leuven, Belgium) in a 1 l volumetric flask and add some drops of the hydrochloric acid solution until the mixture turns yellow to light green and fill to 1 l with acetone.

7.3.4.7.3 Method

- clean all glassware and spoons with neutralized acetone before usage to eliminate possible sites of alkalinities;
- weigh approximately 20.00 g of melted cocoa butter in the conical flask;
- add 25 ml of the neutralized acetone and mix vigorously with a spoon (top layer turns blue to green in the presence of soap);
- titrate with the hydrochloric acid solution until the top layer turns light green.

7.3.4.7.4 Calculation

The amount of soap expressed in ppm sodium stearate (molecular weight 306 g mole^{-1}) was calculated with equation [7.3]:

$$amount\ of\ soap = \frac{3.06 \times V_{HCl}\,[ml] \times 1000}{sample\ mass\,[g]} \qquad \textbf{[7.3]}$$

7.3.4.8 *Amount of unsaponifiable matter* (AOCS Official Method Ca 6a-40, 1989)

7.3.4.8.1 Principle

Unsaponifiable matter includes those substances frequently dissolved in fats and oils, which cannot be saponified by the usual caustic treatment, but are soluble in ordinary fat and oil solvents. This group of compounds includes higher aliphatic alcohols, sterols, pigments and hydrocarbons. To determine the amount of unsaponifiable matter the sample is saponified with ethanolic potassium hydroxide. Then the unsaponifiable matter is separated from the matrix by an extraction with petroleum ether and dried until constant mass. Finally a correction for the free fatty acids is taken into account.

7.3.4.8.2 Materials

- analytical balance (Sartorius model A02119, Göttingen, Germany);
- oven;
- 250 ml flask;
- 500 ml separatory funnels;
- 500 ml conical flask;
- pipettes;
- ethanol (95%) (Chem-Lab, Zedelgem, Belgium);

- 50 % (w/w) potassium hydroxide: dissolve 30 g potassium hydroxide (Chem-Lab, Zedelgem, Belgium) in 20 ml distilled water;
- petroleum ether (Lamers & Pleuger, ‘s Hertogenbosch, the Netherlands);
- 0.004 N sodium hydroxide;
- 1% phenolphthalein (Merck, Darmstadt, Germany) indicator solution in 95% ethanol;
- sodium sulfate (Chem-Lab, Zedelgem, Belgium);

7.3.4.8.3 Methods

- weigh approximately 5.00 g of melted cocoa butter in the flask and add 30 ml of ethanol and 5 ml of the potassium hydroxide solution;
- boil gently but steadily under reflux for 1 h;
- transfer to the separatory funnel and wash with 5 ml ethanol, complete the transfer with twice 20 ml hot distilled water, wash the flask with 5 ml petroleum ether and add to the separatory funnel;
- cool the contents to room temperature and add 50 ml petroleum ether;
- insert the stopper and shake vigorously for at least 1 minute and let settle until both layers are clear;
- draw off the lower aqueous layer into another separatory funnel, collect the petroleum ether extract (containing the unsaponifiable matter) in the conical flask;
- repeat the extraction of the aqueous phase six times, each time using 50 ml petroleum ether; collect all petroleum ether extracts in the conical flask;
- transfer the extracts to a separatory funnel and wash the conical flask with petroleum ether;
- wash the extracts three times with 25 ml 10% ethanol in distilled water, shaking vigorously and drawing off the aqueous alcohol layer after each extraction;
- filtrate the petroleum ether extract over sodium sulfate, transfer to a tared beaker and evaporate to dryness;
- after evaporating all the solvent, complete the drying to constant weight in an oven at 105°C;

- cool in a desiccator and weigh (= O in calculation);
- after weighing, take up the residue in 50 ml warm (50°C) 95% ethanol, containing phenolphthalein indicator and previously neutralized to the phenolphthalein endpoint;
- titrate with 0.004 N sodium hydroxide to the same final colour, a reagent blank correction should be determined;
- correct the mass of the residue for free fatty acid content, using the relationship that 1 ml of 0.004N sodium hydroxide is equivalent to 1.13 mg oleic acid, the grams of fatty acid determined by this titration becomes P in the calculation;
- correct for any reagent blank by conducting the unsaponifiable matter procedure without any cocoa butter present, the blank determined by this procedure becomes M in the calculations.

7.3.4.8.4 Calculation

The percentage of unsaponifiable matter in cocoa butter was calculated with equation [7.4]:

$$unsaponifiable\,matter = \frac{O-(P+M)}{sample\,mass}\times 100 \qquad \textbf{[7.4]}$$

All masses should be expressed in g.

7.3.4.9 Peroxide value (AOCS Official Method Cd 8b-90, 1996)

7.3.4.9.1 Principle

The acetic acid – isooctane method was used to determine the peroxide value.

This method determines all substances, in terms of milliequivalents of peroxide per 1000 grams of sample, that oxidize potassium iodide under the conditions of the test. These substances are generally assumed to be peroxides or other similar products of fat oxidation.

7.3.4.9.2 Material

- 1 ml glass pipette;
- 25 ml burette;
- 250 ml conical flask;
- volumetric flasks;

- analytical balance (Sartorius model A02119, Göttingen, Germany);
- acetic acid (Chem-Lab, Zedelgem, Belgium) – isooctane (Chem-Lab, Zedelgem, Belgium) solution (3:2, v/v);
- potassium iodide solution: dissolve 20 g potassium iodide (Chem-Lab, Zedelgem, Belgium) in 25 ml water;
- sodium thiosulfate (Merck, Darmstadt, Germany) solution 0.01 N;
- starch indicator solution: take 1 g of starch (Chem-Lab, Zedelgem, Belgium), fill to 200 ml with water, boil until clear, take 50 ml of this solution and fill to 1 l with water, add 0.5 ml of 0.1 N jodium.

7.3.4.9.3 Method

- weigh approximately 5.00 g of melted cocoa butter in the 250 ml conical flask;
- add 50 ml of the acetic acid – isooctane solution and swirl to dissolve the sample;
- add 0.5 ml of the potassium iodide solution and shake vigorously for one minute;
- add 50 ml of the starch indicator solution and titrate with the sodium thiosulfate solution until the blue-purple colour has disappeared;
- conduct a blank determination of the reagents daily.

7.3.4.9.4 Calculation

The peroxide value (milliequivalents peroxide per 1000 g sample) was calculated according to equation [7.5]:

$$Peroxide\ value = \frac{1000 \times \left(V_{Na_2S_2O_3\,sample}\,[ml] - V_{Na_2S_2O_3\,blank}\,[ml] \right) \times 0.01}{sample\,mass\,[g]} \quad \textbf{[7.5]}$$

7.3.4.10 P-anisidine value (AOCS Official Method Cd 18-90, 1996)

7.3.4.10.1 Principle

The p-anisidine value defines the amount of aldehydes in the cocoa butter sample by reaction in an acetic solution of the aldehydic compounds in the cocoa butter and the p-anisidine. The absorbance is determined at 350 nm.

7.3.4.10.2 Materials

- 50 ml conical flask;
- 5 ml pipette;
- 50 ml volumetric flask;
- 10 ml test tube;
- 1000 µl automatic pipette;
- spectrofotometer (Ultrospec 1000, Biochrom, Cambridge, United Kingdom);
- analytical balance (Sartorius model A02119, Göttingen, Germany);
- 1 cm glass cells;
- isooctane (Chem-Lab, Zedelgem, Belgium);
- glacial acetic acid (Chem-Lab, Zedelgem, Belgium);
- 0.25 g p-anisidine (Merck, Darmstadt, Germany) per 100 ml glacial acetic acid solution.

7.3.4.10.3 Method

- weigh 0.50 g of melted cocoa butter in the volumetric flask and fill it with isooctane;
- measure the absorbance of this solution (= Ab) at 350 nm with isooctane as the blank;
- pipette 5 ml of the cocoa butter in isooctane solution in a test tube, add exactly 1 ml of the p-anisidine solution and shake;
- measure the absorbance after exactly 10 minutes (= As) using isooctane mixed with the p-anisidine solution as a blank.

7.3.4.10.4 Calculation

The p-anisidine value is defined by convention as 100 times the optical density measured at 350 nm in a 1 cm cell of a solution containing 1.00 g of the cocoa butter in 100 ml of a mixture of solvent and reagent.

$$p-anisidine\,value = \frac{25\times(1.2\times As - Ab)}{sample\,mass\left[g\right]} \qquad \textbf{[7.6]}$$

7.3.5 Principal component analysis

Principal component analysis (PCA) is a mathematical procedure that transforms a number of (possibly) correlated variables into a number of uncorrelated variables called principal components. These principal components are linear combinations of the original variables. The coefficients of the original variables in these linear combinations are chosen so that the first principal component accounts for as much of the variability in the data as possible and each succeeding component accounts for as much of the remaining variability as possible. Instead of working with all original variables, PCA can be performed and only the first two or three principal components can be used in subsequent analyses. The objective of PCA is thus to reduce the dimensionality (number of variables) of the data set while retaining most of the original variability in the data.

PCA was used in this research to reduce the dimensionality of the data set obtained from the determination of the fatty acid and triacylglycerol profile. Then the principal components explaining most of the variability, were used in the multiple linear regression.

SPSS for Windows 10.0.5 (SPSS Inc., Chicago, USA) was used to perform the PCA. Since the variables (the percentages of the different fatty acids and triacylglycerols) differed in magnitude, PCA was performed on the standardized variables. A Varimax rotation was applied to the principal components with an eigenvalue above 1.

7.3.6 Forward multiple linear regression

To investigate which chemical composition variables influence the crystallization parameters, forward multiple linear regression was used. Multiple regression calculates a linear model between a dependent variable (the different crystallization parameters) and different independent variables (chemical composition variables). Each independent variable has a partial regression coefficient indicating its influence on the dependent variable. A multiple regression model can be built in two ways. With standard methods all independent variables are entered into the model at the same time, whereas with stepwise methods the independent variables are entered step by step, based on an F-test. Such an F-test allows to decide whether a more complex model is significantly better than the simpler model (see also 4.5.5.2). In this research a stepwise method, more specifically forward regression was used. This means that the independent variable with the highest F-value (lowest significance) and thus the highest correlation with the dependent variable is added to the model first. In a second step the variable, which then

has the highest F-value is added. The model is complete when all variables with an F-value above a minimum value (F-to-enter (FIN)) or a significance value below a maximum value (PIN), are added. A PIN value of 0.05 was used in this research.

The different independent variables may not be correlated too much among each other because they then measure more or less the same and it is no longer possible to determine the influence of every separate variable. Consequently, the validity of the model can be jeopardized. This problem is circumvented by the tolerance principle. For every independent variable a multiple correlation coefficient is calculated explaining that independent variable based on all other independent variables. The tolerance or the unexplained variance is calculated then as one minus the square of the correlation coefficient. If the unexplained variance is too low, the variable is a combination of the others and should not be entered into the model. A tolerance value of 0.0001 was used in this research.

The regression analysis was performed with SPSS for Windows 10.0.5 (SPSS Inc., Chicago, USA). The means of the chemical composition variables were used because the number of repetitions was not always the same. For the crystallization kinetics parameters the individual values of the five repetitions were used.

7.4 Results and discussion

7.4.1 Isothermal crystallization measured by DSC

The isothermal crystallization at 20°C of the different cocoa butters was measured by DSC. The main crystallization peak was integrated and the model developed in chapter 4 was fitted to the data series. Taking into account the proposed mechanism of the crystallization process as formulated in chapter 5, this main peak represents the α mediated β' crystallization and the polymorphic transition of already formed α crystals into β'. The contribution of the latter is however negligible as was shown in section 6.4.4. Parameter a_P represents the total amount of heat released in the second step of crystallization, equaling the mass fraction β' crystals formed in this second step (taking account of the latent heat of the β' polymorph of 100 J g^{-1}). Parameter t_ind_F represents the induction time of the second step of crystallization, thus the induction time of the polymorphic transition from α to β'. This parameter may, however, also be related to the growth rate of the β' crystals as was discussed in section 6.4.3.2. K is the rate

constant and *n* the order of the reverse reaction. The latter reflects how long this reverse reaction affects the crystallization process: the higher *n*, the shorter its influence.

ANOVA (SPSS for Windows 10.0.5 (SPSS Inc., Chicago, USA) demonstrated that the type of cocoa butter has a significant ($\alpha = 0.05$) influence on each of the crystallization model parameters.

Table 7.2 shows the mean values and standard deviations of the four crystallization parameters for each of the cocoa butters. The a_P parameter varies from 49.1 J g^{-1} for one of the Brazilian cocoa butters (CB P) to 78.9 J g^{-1} for the hard cocoa butter of unknown origin (CB M). The other Brazilian cocoa butter (CB I) and the cocoa butter partly from Brazilian beans (CB O) also have low a_P values. The Asian cocoa butters (CB E and F from Indonesia and Malaysia respectively) have high a_P values. Shukla (1995) observed low SFC values for Brazilian cocoa butters and high SFC values for Malaysian cocoa butter. This coincides with the results obtained in this study although it has to be remarked that a_P only reflects the amount of crystallization in the second step of the process. The t_ind_F parameter varies from 0.412 h for the hard cocoa butter of unknown origin (CB M) to 1.45 h for one of the Brazilian cocoa butters (CB P). The other Brazilian cocoa butter (CB I) and the cocoa butter partly from Brazilian beans (CB O) also have high t_ind_F values. The *K* parameter varies from 2.61 h^{-1} for the Nigerian cocoa butter (CB C) to 6.64 h^{-1} for the West African cocoa butter (CB A). The *n* parameter varies from 2.11 for one of the Brazilian cocoa butters (CB P) to 6.46 for the Nigerian cocoa butter (CB C). The other Brazilian cocoa butter (CB I) and the cocoa butter partly from Brazilian cacao-beans (CB O) also have low *n* values.

Clearly the Brazilian cocoa butters (and the cocoa butter partly from Brazilian beans) have comparable crystallization characteristics. The crystallization of the other South American cocoa butters (CB G and H) is, however, quite different. No similarity between the crystallization parameters of the African cocoa butters (CB A to D) could be detected. The crystallization of both Asian cocoa butters (CB E and F) is more similar. It is also remarkable that the crystallization parameters of both standard factory products (CB L and N) are quite different. The same applies for the cocoa butters with crystallization problems in production (CB Q to T).

Table 7.2 Parameters of the model developed in chapter 4 for twenty different cocoa butters. Mean and standard deviations from 5 repetitions are reported. The standard deviation for each cocoa butter is calculated according to equation [3.7].

Sample	a_P [J g^{-1}]	t_ind_F [h]	K [h^{-1}]	n [-]
A	71.9 ± 2.0	0.445 ± 0.004	6.64 ± 0.15	4.02 ± 0.15
B	70.8 ± 0.9	0.520 ± 0.011	4.45 ± 0.10	4.22 ± 0.17
C	65.6 ± 1.7	0.563 ± 0.011	2.61 ± 0.03	6.46 ± 0.23
D	75.1 ± 3.3	0.500 ± 0.021	4.41 ± 0.30	4.34 ± 0.20
E	76.0 ± 1.9	0.506 ± 0.017	4.39 ± 0.11	4.58 ± 0.27
F	75.7 ± 2.1	0.421 ± 0.013	4.59 ± 0.23	5.34 ± 0.24
G	71.2 ± 1.5	0.547 ± 0.012	6.44 ± 0.37	3.86 ± 0.26
H	69.0 ± 3.2	0.498 ± 0.006	4.12 ± 0.22	4.00 ± 0.13
I	58.6 ± 0.5	1.16 ± 0.05	4.55 ± 0.40	3.00 ± 0.17
J	76.2 ± 2.2	0.532 ± 0.012	4.17 ± 0.19	3.82 ± 0.10
K	74.6 ± 1.0	0.578 ± 0.020	4.61 ± 0.31	4.14 ± 0.27
L	65.5 ± 2.1	0.523 ± 0.021	5.01 ± 0.47	3.92 ± 0.33
M	78.9 ± 2.3	0.412 ± 0.005	5.67 ± 0.34	4.90 ± 0.42
N	77.7 ± 2.3	0.414 ± 0.018	5.48 ± 0.27	5.35 ± 0.32
O	60.5 ± 1.3	0.707 ± 0.044	2.87 ± 0.26	3.39 ± 0.27
P	49.1 ± 2.6	1.45 ± 0.17	3.86 ± 0.91	2.11 ± 0.43
Q	75.6 ± 1.9	0.478 ± 0.028	3.80 ± 0.51	3.93 ± 0.23
R	76.3 ± 2.2	0.655 ± 0.012	3.15 ± 0.37	4.71 ± 0.31
S	65.3 ± 2.1	0.758 ± 0.031	2.72 ± 0.37	3.85 ± 0.36
T	72.4 ± 0.2	0.513 ± 0.018	5.06 ± 0.25	3.69 ± 0.10
Mean	70.3	0.61	4.4	4.2
Standard deviation.[a]	7.6	0.26	1.1	0.9

[a] Standard deviation only taking into account the mean values for the different cocoa butters

7.4.2 Chemical composition of different cocoa butters

7.4.2.1 Fatty acid and triacylglycerol profile

7.4.2.1.1 General remarks

The fatty acid profile of the different cocoa butters was determined with gas chromatography. The five main fatty acids detected are palmitic, stearic, oleic, linoleic and arachidic acid. This matches the results of Talbot (1994b). Apart from these five main fatty acids, traces of myristic and palmitoleic acid are present. However, there is no pronounced difference in amount between the various cocoa butters. The relative amounts of each fatty acid are presented in Annex V.1.

ANOVA (SPSS for Windows 10.0.5 (SPSS Inc., Chicago, USA)) showed a significant ($\alpha = 0.05$) effect of the type of cocoa butter on the percentage of all fatty acids except for arachidic acid. The value of the latter is rather constant at about 1%.

The triacylglycerol profile was determined by gas chromatography and the relative amounts of each triacylglycerol are presented in Annex V.2.

As reported by Schlichter-Aronhime & Garti (1988a), the three main triacylglycerols are POP, POS and SOS. Together they account for about 85% of the triacylglycerols.

7.4.2.1.2 Principal component analysis on fatty acid and triacylglycerol profile

To reduce the dimensionality of the data from the fatty acid and triacylglycerol profile and thus facilitate the interpretation of the data, PCA was applied. The theory of PCA is explained in section 7.3.5.

The first and second principal component, respectively explain 36.5% and 19.2% of the total variance of the data set. Figure 7.1 shows the values of these first two principal components for each of the cocoa butters. The main group of cocoa butters has a value between 0 and 1 for the first principal component and a value between -1 and 1 for the second principal component. Cocoa butters P and I (both from Brazil) form a group that is characterized by very low values of the first principal component but intermediate values of the second principal component. Cocoa butters G (cocoa butter from San Domingo), J (unsteamed cocoa butter of unknown origin) and O (cocoa butter partly from Brazilian beans) form a group that is characterized by slightly negative values of the first principal component and intermediate values of the second principal component. A fourth group consists of cocoa butters N (standard factory product) and K

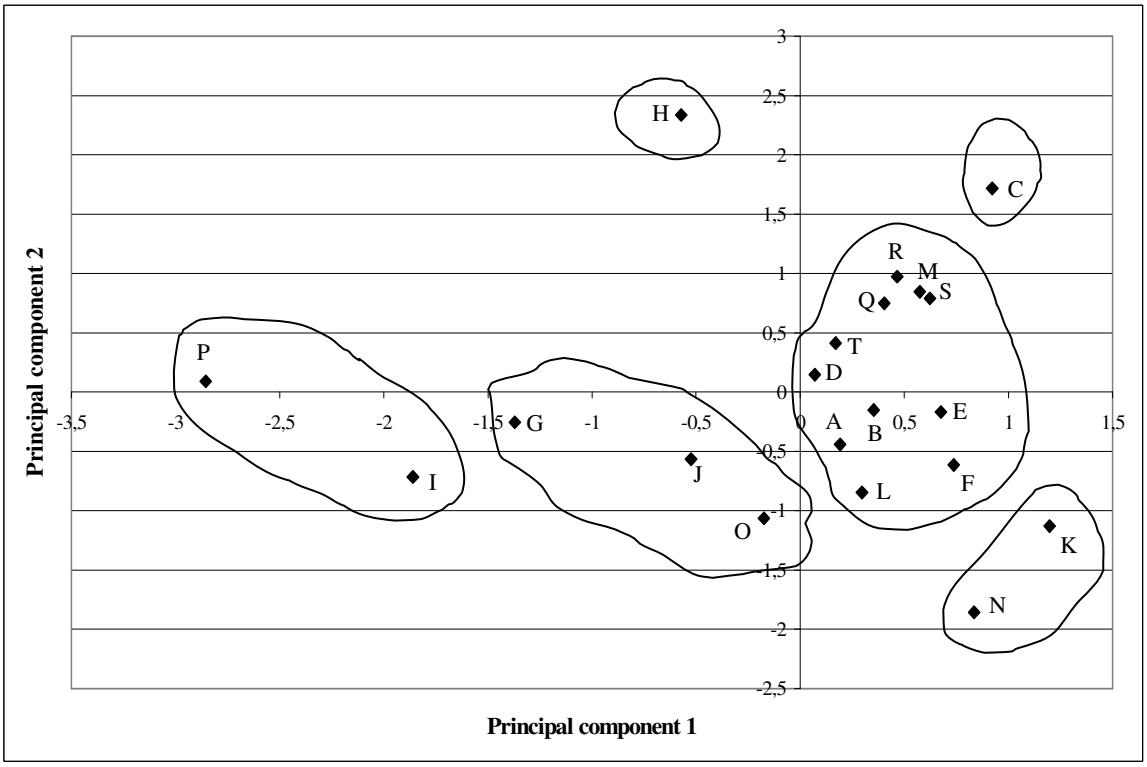

Figure 7.1 Separation of cocoa butters based on the first two principal components

(steamed cocoa butter of unknown origin). They both have rather high values for the first principal component but they are mainly characterized by a higher than average negative value for the second principal component. Cocoa butters H (cocoa butter from Ecuador) and C (Nigerian cocoa butter) also deviate from the main group of cocoa butters. The former has a very high positive value for the second principal component together with a slightly negative value of the first principal component, whereas the latter has a high positive value for the second principal component combined with a rather high value of the first principal component.

The third principal component explains another 15.2% so that the first three principal components together explain 70.9% of the total variance in the data set. Based on the third principal component (not shown in Figure 7.1) it is mainly CB J (unsteamed cocoa butter of unknown origin), which differentiates itself based on a high positive value.

Figure 7.2 shows the loading plot of the first two principal components. The loadings are the coefficients that are used to compute the principal components from the original variables. A loading plot shows which of the original variables determine the values of the principal components the most. The loadings of the first three principal components are also indicated in Table 7.3.

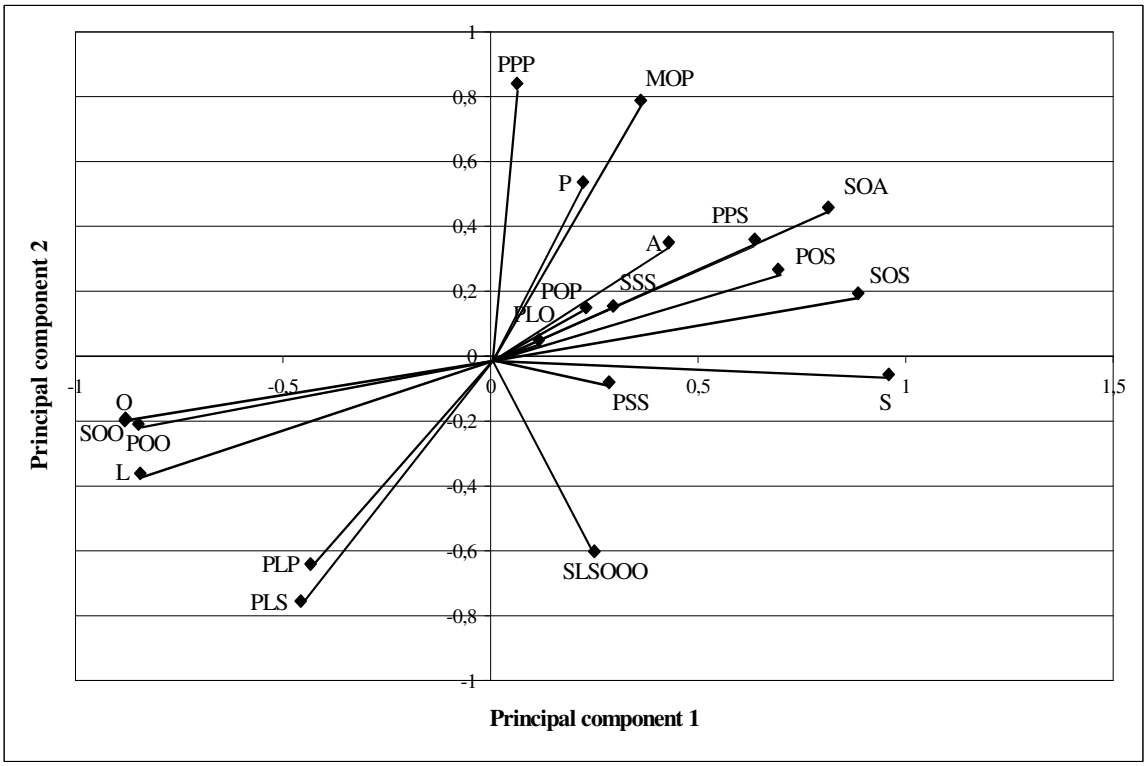

Figure 7.2 Loading plot of the first two principal components

The first principal component is mainly determined by the ratios of saturated to unsaturated fatty acids and mono-unsaturated to di-unsaturated triacylglycerols. Cocoa butters containing a high percentage of unsaturated fatty acids and di-unsaturated triacylglycerols have a high negative value for the first principal component and vice versa. This means that the Brazilian cocoa butters (CB P and I), the cocoa butter partly from Brazilian beans (CB O) and the other South American cocoa butters (CB G and H) contain relatively more unsaturated fatty acids and di-unsaturated triacylglycerols. This agrees with the results of Chaiseri & Dimick (1989), Klagge & Sen Gupta (1990), Schlichter-Aronhime & Garti (1988a) and Shukla (1995).

The second principal component is mainly influenced by the percentage of PPP, MOP and palmitic acid (positive influence) and the percentage of PLP, PLS and SLS + OOO (negative influence). As shown in Figure 7.1 the second principal component does not lead to a strong grouping of the cocoa butters. The high values for cocoa butters H (Ecuadorian cocoa butter) and C (Nigerian cocoa butter) reflect their higher PPP, MOP and palmitic acid contents. The high negative values for cocoa butters N (standard factory product) and K (steamed cocoa butter of unknown origin) reflect their higher PLS and SLS + OOO contents.

Table 7.3 Loadings of the first three principal components

	Principal component 1	**Principal component 2**	**Principal component 3**
Palmitic acid	0.223	0.537	0.475
Stearic acid	0.959	-0.056	0.101
Oleic acid	-0.879	-0.192	-0.318
Linoleic acid	-0.844	-0.361	-0.206
Arachidic acid	0.429	0.351	-0.469
PPP	0.064	0.840	-0.307
MOP	0.362	0.789	-0.009
PPS	0.636	0.360	0.566
POP	0.230	0.150	-0.055
PLP	-0.434	-0.641	-0.118
PSS	0.285	-0.084	0.841
POS	0.693	0.268	-0.152
POO	-0.881	-0.198	-0.215
PLS	-0.457	-0.754	-0.276
PLO	0.116	0.054	0.575
SOO	-0.848	-0.209	-0.214
SLS+OOO	0.250	-0.601	-0.355
SOA	0.814	0.458	0.012
SSS	0.295	0.155	0.763
SOS	0.885	0.194	0.274

The third principal component is mainly influenced by the percentage of the tri-saturated triacylglycerols PSS, SSS and PPS and by the percentage of PLO. All four triacylglycerols have a positive influence on the third principal component. Cocoa butter J (unsteamed cocoa butter of unknown origin) has a high value for the third principal component because of its high percentage of the tri-saturated triacylglycerols PPS, PSS and SSS.

7.4.2.2 Diacylglycerols

The percentage of diacylglycerols (expressed on triacylglycerol basis) in the different cocoa butters is presented in Table 7.4. The amount varies from 0.59% for the West African cocoa butter (CB A) to 2.22% for the cocoa butter from a mixture of beans from Ivory Coast, Brazil and Indonesia (CB O). The range of the values corresponds to the results of Shukla (1995) and Pontillon (1998a).

Both Brazilian cocoa butters (CB I and P) contain rather low amounts of diacylglycerols although the cocoa butter partly from Brazilian cacao-beans (CB O) shows the highest diacylglycerol content. All cocoa butters causing crystallization problems in production contain rather low amounts of diacylglycerols, which may be surprising taking their rather high free fatty acid levels into account (see section 7.4.2.3). It is, however, possible that the diacylglycerols hydrolyse further. This would not be surprising, bearing in mind that the kinetics of attack of a diacylglycerol is faster than that of a triacylglycerol due to the lower amounts present (Pontillon, 1998a).

7.4.2.3 Free fatty acids

ANOVA (SPSS for Windows 10.0.5 (SPSS Inc., Chicago, USA)) showed a significant ($\alpha = 0.05$) effect of the kind of cocoa butter on the amount of free fatty acids.

Table 7.4 gives an overview of the free fatty acid content, expressed as percentage oleic acid, in the different cocoa butters. It shows that the content of free fatty acids varies from 1.16% for the hard cocoa butter of unknown origin (CB M) to 2.77% for the Nigerian cocoa butter (CB C). This range of values matches the results found in literature (Chaiseri & Dimick, 1989 and Shukla, 1995).

According to European legislation, the different types of cocoa butter must meet some quality criteria: pure press cocoa butter as well as expeller and refined cocoa butter must not contain more than 1.75% free fatty acids (EG, 2000). Six out of the twenty cocoa butter samples contain an amount of free fatty acids significantly ($\alpha = 0.05$) higher than this limit: CB B (cocoa butter from Ivory Coast), CB C (Nigerian cocoa butter), CB L (standard factory product) and CB R to T (problem causing cocoa butters). Also the fourth problem causing cocoa butter (CB Q) has a rather high free fatty acid content. In literature some authors try to link the amount of free fatty acids to the country of origin: Jinap et al. (1994) discovered that cocoa-bean samples from Brazil and countries from the Far East are highly acidic, while samples from West African countries have medium

acidity and samples from Central and South American (outside Brazil) beans are the least acidic. Chaiseri & Dimick (1989) and Shukla (1995) observed that cocoa butters with a high free fatty acid content above the legal limit, originate from Nigeria, Ivory Coast, Ecuador, Malaysia and Peru.

Table 7.4 Diacylglycerol and free fatty acid content of twenty different cocoa butters.

Sample	Diacylglycerol content expressed on triacylglycerol basis [%]	Free fatty acid content [% oleic acid][a]
A	0.59	1.62 ± 0.02
B	0.70	2.18 ± 0.02
C	1.1	2.77 ± 0.02
D	1.1	1.91 ± 0.06
E	0.81	1.58 ± 0.02
F	1.2	1.20 ± 0.04
G	0.69	1.32 ± 0.04
H	1.1	1.18 ± 0.02
I	0.72	1.66 ± 0.02
J	0.62	1.52 ± 0.01
K	1.3	1.37 ± 0.04
L	0.72	2.25 ± 0.07
M	0.81	1.16 ± 0.01
N	0.72	1.38 ± 0.01
O	2.2	1.79 ± 0.02
P	0.86	1.60 ± 0.02
Q	0.88	1.72 ± 0.01
R	0.81	1.93 ± 0.04
S	0.78	1.91 ± 0.02
T	0.64	2.08 ± 0.02
Mean	0.92	1.7
Standard deviation	0.36	0.4

[a] Mean values and standard deviation of two repetitions are reported.

These links between the country of origin and the amount of free fatty acids neither match each other nor the results of this research. This is probably because not so much the country of origin but the production process and possible refining determines the amount of free fatty acids. High free fatty acid values can be due to the use of beans from diseased pods, hydrolysis by lipase from mould contamination caused by insufficient drying, extended fermentation or too quick drying of the beans, which does not allow for an adequate loss of the volatile acids (Chaiseri & Dimick, 1989, Hancock & Fowler, 1994 and Pontillon, 1998a).

7.4.2.4 Phosphorus

The phosphorus content was determined by inductively coupled plasma-atomic emission spectroscopy. The results are presented in Table 6.5.

To recalculate the amount of phosphorus to the amount of phospholipids 1 ppm phosphorus was equated to 25 ppm phospholipids, leading to 1 ppm phosphorus equalling 0.0025% phospholipids (Christie, 1982). Since the phosphorus content varies from 2.30 ppm for the cocoa butter from San Domingo (CB G) to 63 ppm for the Malaysian cocoa butter (CB F), the phospholipids content varies from 0.006 to 0.16 %. This range of values is lower than what is generally reported in literature (see section 2.3.3). Only Chaiseri & Dimick (1995a) also report rather low values from 0.1 to 0.2%.

The South American - but not Brazilian cocoa butters - (CB G and H) contain very low amounts of phosphorus, while the Brazilian cocoa butters (CB I and P) contain intermediate to high amounts. All African cocoa butters (CB A to D) contain rather low levels. These results do not coincide with the tendency, as found by Parsons et al. (1969), that African cocoa butters contain lower amounts of phospholipids than American cocoa butters. This may mean that the phospholipid content does not primarily depend on the country of origin but on the production process of the cocoa butter from the beans and any refining of the butter (Pontillon, 1998a). It can be remarked that all problem causing cocoa butters (CB Q to T) contain above average amounts of phosphorus and thus phospholipids.

7.4.2.5 Iron

The iron content was also determined by inductively coupled plasma-atomic emission spectroscopy. The results are presented in Table 7.5.

Table 7.5 Phosphorus and iron content of twenty different cocoa butters

Sample	Phosphorus content [ppm][a]	Iron content [ppm][a]
A	22.6 ± 0.1	0.836 ± 0.074
B	16.9 ± 0.4	0.565 ± 0.099
C	11.5 ± 0.2	1.00 ± 0.03
D	15.9 ± 0.7	1.66 ± 0.61
E	18.7 ± 0.1	0.938 ± 0.174
F	63.0 ± 1.0	1.17 ± 0.04
G	2.30 ± 0.20	0.140 ± 0.037
H	2.71 ± 0.05	1.17 ± 0.23
I	41.6 ± 0.3	1.77 ± 0.04
J	39.8 ± 0.5	2.55 ± 0.08
K	35.3 ± 0.6	2.86 ± 0.04
L	35.6 ± 0.4	1.66 ± 0.08
M	49.8 ± 0.2	1.75 ± 0.07
N	41.6 ± 0.2	2.71 ± 0.04
O	7.70 ± 0.20	0.573 ± 0.150
P	26.5 ± 0.3	0.302 ± 0.047
Q	37.1 ± 0.4	5.71 ± 0.09
R	39.4 ± 0.4	5.56 ± 0.08
S	48.4 ± 0.5	5.18 ± 0.07
T	38.9 ± 0.4	4.27 ± 0.06
Mean	29.8	2.12
Standard Deviation	16.8	1.76

[a] Mean and standard deviation of three repetitions are reported

The cocoa butter from San Domingo (CB G) contains the lowest amount of iron (0.140 ppm) whereas one of the problem causing cocoa butters (CB Q) contains the highest amount (5.71 ppm). All problem causing cocoa butters contain very high amounts of iron compared to the average. Furthermore, it may be surprising that the standard factory products (CB L and N) also contain rather high amounts of iron. These high iron contents may be due to old machines or press devices used in the production

and refining of cocoa butter. No real trend as function of country of origin could be detected. In literature no information about the concentration of iron in cocoa butter could be found.

7.4.2.6 Traces of soap

ANOVA (SPSS for Windows 10.0.5 (SPSS Inc., Chicago, USA)) showed a significant influence of the kind of cocoa butter on the soap content.

Table 7.6 reports the soap content, expressed as ppm sodium stearate, for the twenty cocoa butters. The values range from 0 ppm for one of the cocoa butters from Ivory Coast (CB D) and the cocoa butter from a mixture of beans of different origin (CB O) to 329 ppm for the Malaysian cocoa butter (CB F). Also the other Asian cocoa butter from Indonesia (CB E) contains a high amount of soap. The problem causing cocoa butters (CB Q to T) as well as the standard factory products (CB L and N) contain high levels of soap.

Pontillon (1998a) states that cocoa butter of good quality should contain less than 200 ppm soap and that cocoa butter is of inferior quality when the value is higher than 4000 ppm. Only two cocoa butters (CB F, the Malaysian cocoa butter and CB R, one of the problem causing cocoa butters) have values significantly ($\alpha = 0.05$) higher than 200 ppm. None of the cocoa butters comes close to the 4000 ppm limit.

High soap contents in cocoa butter may be due to alkalizing of the cocoa nib or mass prior to pressing. If this alkalizing is not carefully performed, saponification can take place (Cros & Bianchi, 1998 and Meursing, 1994).

7.4.2.7 Unsaponifiable matter

ANOVA (SPSS for Windows 10.0.5 (SPSS Inc., Chicago, USA)) showed a significant ($\alpha = 0.05$) effect of the kind of cocoa butter on the amount of unsaponifiable matter.

The amounts of unsaponifiable matter in the different cocoa butters are presented in Table 7.6. The amount of unsaponifiable matter varies from 0.31% for one of the cocoa butters from Ivory Coast (CB B) to 0.53 % for the Nigerian cocoa butter (CB C). Included in the unsaponifiable matter are compounds such as higher aliphatic alcohols, sterols, pigments and hydrocarbons.

Table 7.6 Soap content and amount of unsaponifiable matter for twenty different cocoa butters

Sample	Soap content [ppm sodium stearate]	Amount of unsaponifiable matter [%] [b]
A	69.4 ± 29.0[a]	0.34 ± 0.04
B	124 ± 7[b]	0.31 ± 0.02
C	3.05 ± 0.01[b]	0.53 ± 0.00
D	0 ± 0[b]	0.40 ± 0.05
E	172 ± 19[c]	0.38 ± 0.01
F	329 ± 0[b]	0.35 ± 0.05
G	27.4 ± 4.2[b]	0.42 ± 0.01
H	7.62 ± 2.16[b]	0.43 ± 0.01
I	157 ± 2[b]	0.43 ± 0.00
J	220 ± 5[b]	0.37 ± 0.05
K	165 ± 4[b]	0.37 ± 0.01
L	149 ± 0[b]	0.35 ± 0.04
M	82.4 ± 4.2[b]	0.33 ± 0.00
N	195 ± 53[d]	0.39 ± 0.05
O	0 ± 0[b]	0.36 ± 0.04
P	51.9 ± 4.4[b]	0.44 ± 0.03
Q	188 ± 26[b]	0.45 ± 0.07
R	248 ± 4[b]	0.34 ± 0.01
S	207 ± 16[b]	0.41 ± 0.00
T	165 ± 5[b]	0.38 ± 0.02
Mean	128	0.39
Standard deviation	94	0.05

[a] Mean and standard deviation of four repetitions
[b] Mean and standard deviation of two repetitions
[c] Mean and standard deviation of three repetitions
[d] Mean and standard deviation of six repetitions

European legislation (EG, 2000) limits the amount of unsaponifiable matter to a maximum of 0.35% for pure press cocoa butter and 0.50% for expeller and refined cocoa butter. Although the mean of quite a lot of samples is higher than the threshold of

0.35%, t-tests (SPSS for Windows 10.0.5 (SPSS Inc., Chicago, USA)) showed that only six cocoa butters out of the twenty contain an amount of unsaponifiable matter significantly ($\alpha = 0.05$) higher than the 0.35% threshold. These six cocoa butters include all South American cocoa butters (CB G, H, I and P), the Nigerian cocoa butter (CB C) and the Indonesian cocoa butter (CB E). Only the Nigerian cocoa butter (CB C) has a significantly ($\alpha = 0.05$) higher value than the 0.50% threshold.

Literature does not report information about the amount of unsaponifiable matter in cocoa butter.

7.4.2.8 Peroxide value

The peroxide values, expressed as milliequivalents peroxide per 1000 g of sample, of the different cocoa butters are reported in Table 7.7. ANOVA (SPSS for Windows 10.0.5 (SPSS Inc., Chicago, USA)) showed that the kind of cocoa butter has a significant influence on the peroxide value. These values range from 0 for the cocoa butter from a mixture of beans from different origins (CB O) to 7.9 for one of the cocoa butters causing problems in production (CB R). It is obvious, that all problem causing cocoa butters have a high peroxide value. Other cocoa butters with a high value are one of the standard factory products (CB L) and the Nigerian cocoa butter (CB C). No real trend as function of the country of origin could be detected. In literature no peroxide values for cocoa butter are reported. A general guideline for fats and oils is that freshly produced fat should have a peroxide value below 1 meq peroxide kg^{-1} and that fat starts to have undesirable properties from 10 meq peroxide kg^{-1} onwards (De Meulenaer & Huyghebaert, 2002). None of the cocoa butters exceeds the latter limit.

7.4.2.9 P-anisidine value

For all cocoa butters negative or extremely low p-anisidine values were obtained. This means that hardly any secondary oxidation products are present. As a result, the low peroxide values are due to the fact that hardly any oxidation has taken place and not to the fact that the primary oxidation products (peroxide) have been decomposed into secondary oxidation products. This chemical characteristic was not further taken into account.

Table 7.7 Peroxide value of twenty different cocoa butters

Sample	Peroxide value [milliequivalents peroxide per 1000 g sample] [a]
A	0.05 ± 0.07
B	0.20 ± 0.14
C	1.8 ± 0.1
D	0.35 ± 0.07
E	0.54 ± 0.06
F	0.64 ± 0.07
G	0.44 ± 0.07
H	0.83 ± 0.19
I	0.20 ± 0.14
J	0.55 ± 0.07
K	0.64 ± 0.08
L	3.1 ± 0.4
M	0.30 ± 0.01
N	1.1 ± 0.1
O	0 ± 0
P	0.15 ± 0.07
Q	4.4 ± 0.2
R	7.9 ± 0.8
S	4.7 ± 0.9
T	2.8 ± 0.5
Mean	1.5
Standard Deviation	2.1

[a] Mean and standard deviation of two repetitions are presented.

7.4.2.10 Correlation between different chemical composition variables

Pearson correlation coefficients were calculated by SPSS for Windows 10.0.5 (SPSS Inc., Chicago, USA). Two rather high correlations were discovered: the phosphorus content is positively correlated with the soap content (Pearson correlation coefficient +0.822) and the iron content is positively correlated with the peroxide value (Pearson

correlation coefficient +0.832). A possible explanation for the first observation is that some refining treatments remove phospholipids as well as traces of soap (Gutshall-Zakis & Dimick, 1993). The second observation can most probably be explained by the pro-oxidant activity of iron. Hashim et al. (1997) showed that the presence of a pro-oxidant such as iron, accelerates the oxidation of refined cocoa butter.

7.4.3 Influence of chemical composition on isothermal crystallization kinetics

Forward multiple linear regression was used to investigate which chemical composition variables have the most important influence on the different crystallization kinetics parameters. The theory of forward multiple linear regression is explained in section 7.3.6.

To reduce the dimensionality of the data from the fatty acid and triacylglycerol profile, the three principal components obtained in section 7.4.2.1.2 were used as independent variables in the regression instead of the percentages of all fatty acids and triacylglycerols separately.

7.4.3.1 Influence of chemical composition on a_P

The value of the crystallization parameter a_P corresponds to the amount of crystallization in the second step of the crystallization process and is thus related to the equilibrium amount of solid fat. The amount of α crystallization (not determined in this research) should, however, be added to a_P to obtain the total equilibrium amount of solid fat.

The results of the forward multiple linear regression with a_P as the dependent variable are presented in Table 7.8 and Table 7.9. Table 7.8 gives the order in which the different independent variables are added to the regression model and the corresponding R^2 values. This R^2 value corresponds to the amount of variance of the dependent variable that is explained by the regression model, thus by the independent variables entered in the regression model.

Table 7.8 Variables entered in forward multiple linear regression with a_P as dependent variable

Variables entered	**R^2**
principal component 1	0.382
principal component 1 + free fatty acids	0.503
principal component 1 + free fatty acids + diacylglycerols	0.596

It can be deduced that the first principal component explains most of the variance (38.2%) of a_P. Other chemical composition variables having a significant (α = 0.05) influence on a_P, include the amount of free fatty acids and diacylglycerols. These three independent variables together explain nearly 60 % of the variance of a_P.

Table 7.9 reports the regression equation for the model with the three independent variables entered. The regression coefficients indicate the change in the dependent variable when the value of that independent variable increases with one unit, while the influence of the other independent variables is kept constant. The standardized regression coefficients are also reported in Table 7.9. These are dimensionless and give an indication of the relative importance of each independent variable: the variable with the highest absolute value has the most important influence on the dependent variable. The sign of the standardized regression coefficient indicates whether an increase in the value of the independent variable leads to an increase or a decrease in the value of the dependent variable.

Table 7.9 Resulting regression model of forward multiple linear regression with a_P as dependent variable

Independent variable	Regression coefficient	Standardized regression coefficient
principal component 1	6.2	0.72
free fatty acids	-8.2	-0.39
diacylglycerols	-6.8	-0.29
intercept	91	

It can be deduced that the value of the first principal component has the most important influence on a_P: when the percentage of saturated fatty acids and mono-unsaturated triacylglycerols increases (see section 7.4.2.1.2), a_P increases. This result matches the findings of Chaiseri & Dimick (1989), Pontillon (1998a) and Shukla (1995). The first authors explained the lower equilibrium amount of solid fat for cocoa butters with a high concentration of di-unsaturated triacylglycerols by the double bond in the sn-3 position. This causes extra kinking in the structure and so interrupts the molecular packing of the mono-unsaturated triacylglycerols. Another possible explanation for the lower equilibrium amount of solid fat is that the di-unsaturated triacylglycerols do not crystallize at 20°C, due to their β' melting point below the crystallization temperature

(2.5°C for POO and 8.6°C for SOO (Hagemann, 1988)). Consequently, a lower percentage of triacylglycerols is able to crystallize under the given conditions.

Table 7.9 also shows that higher amounts of free fatty acids and diacylglycerols have a negative influence on a_P. Jacobsberg & Oh Chuan (1976) obtained similar results for palm oil and attributed the effect to the formation of a eutectic mixture. For cocoa butter Gutshall-Zakis & Dimick (1993) observed that refining, which involves elimination of minor components like free fatty acids and diacylglycerols, increases the amount of solid fat.

7.4.3.2 Influence of chemical composition on t_ind$_F$

Table 7.10 and Table 7.11 represent the results of the forward linear regression with t_ind_F as the dependent variable. This parameter represents the induction time of the second step of crystallization, i.e. the α mediated β' crystallization.

Table 7.10 Variables entered in forward multiple linear regression with t_ind_F as dependent variable

Variables entered	**R^2**
principal component 1	0.549
principal component 1 + principal component 3	0.605
principal component 1 + principal component 3 + phosphorus	0.671
principal component 1 + principal component 3 + phosphorus + free fatty acids	0.709
principal component 1 + principal component 3 + phosphorus + free fatty acids + diacylglycerols	0.752

It is obvious that the value of the first principal component has by far the most important influence on t_ind_F. This variable alone already explains 55% of the variance of t_ind_F. The higher the percentage of the saturated fatty acids and the mono-unsaturated triacylglycerols is (see section 7.4.2.1.2), the lower the value of t_ind_F is. Four other independent variables have a significant ($\alpha = 0.05$) influence on t_ind_F: the amount of diacylglycerols, phosphorus and free fatty acids have a positive influence while the value of the third principal component has a negative influence on t_ind_F. The latter means that a high percentage of tri-saturated triacylglycerols leads to a shorter induction time for the second step of crystallization (see section 7.4.2.1.2).

Table 7.11 Resulting regression model of forward multiple linear regression with t_ind_F as dependent variable

Independent variable	Regression coefficient	Standardized regression coefficient
principal component 1	-0.25	-0.91
principal component 3	-0.06	-0.24
phosphorus	0.006	0.39
free fatty acids	0.17	0.25
diacylglycerols	0.17	0.22
intercept	-0.02	

The parameter t_ind_F represents the induction time of the second step of crystallization and thus depends on the induction time for the polymorphic transition from α to β' (see chapter 5 for more details). It was, however, explained in section 6.4.3.2 that the β' crystals have to grow before sufficient heat is released so the DSC can detect it. That is why t_ind_F may not only depend on the induction time for the polymorphic transition from α to β' but also on the growth rate of the β' crystals. It may be expected then that the chemical composition variables influencing the rate constant K, also influence t_ind_F but in the opposite way, since a higher rate constant leads to a shorter induction time. Three of the five chemical composition variables influencing the rate constant K (see section 7.4.3.3), have an opposite influence on t_ind_F.

To have an idea of the induction time of the first step of crystallization, i.e. the crystallization of part of the melt in the α polymorph, SDLS experiments were performed on some cocoa butters. The results for cocoa butters D (cocoa butter from Ivory Coast), H (Ecuadorian cocoa butter) and T (problem causing cocoa butter) are similar with values between 15 and 30 s. The induction time of one of the Brazilian cocoa butters (CB P) is however much longer (339 s). Based on these results some relation between the influence of chemical composition on both induction times (first and second step of crystallization) may be suspected as Brazilian cocoa butters have a long induction time for both crystallization steps.

7.4.3.3 Influence of chemical composition on K

Table 7.12 and Table 7.13 present the results of the forward linear regression with the rate constant K of the crystallization process as the dependent variable.

It can be deduced that it is only possible to explain 53.7% of the variance of *K* with the chemical composition variables determined in this research.

K is the only crystallization parameter on which the ratios of saturated to unsaturated fatty acids and mono-unsaturated to di-unsaturated triacylglycerols (reflected by the value of the first principal component) do not have the most important influence. The first and second principal component have an impact on the rate constant but this influence is less important than that of the amount of free fatty acids, diacylglycerols and soap. The first principal component has a positive influence, while the second one has a negative influence. This means that the higher the percentage of unsaturated fatty acids and di-unsaturated triacylglycerols is, the lower the rate constant is.

Table 7.12 Variables entered in forward multiple linear regression with *K* as dependent variable

Variables entered	**R^2**
free fatty acids	0.145
free fatty acids + diacylglycerols	0.302
free fatty acids + diacylglycerols + peroxide value	0.388
free fatty acids + diacylglycerols + peroxide value + unsaponifiable matter	0.433
free fatty acids + diacylglycerols + peroxide value + unsaponifiable matter + soap	0.460
free fatty acids + diacylglycerols + peroxide value + unsaponifiable matter + soap + principal component 2	0.508
free fatty acids + diacylglycerols + peroxide value + unsaponifiable matter + soap + principal component 2 + principal component 1	0.537

Furthermore, an increase in the percentage of PPP and MOP or a decrease in the percentage of PLP, PLS and SLS + OOO leads to a lower rate constant. Chaiseri & Dimick (1995a) also observed that higher percentages of di-unsaturated triacylglycerols retard the crystallization of cocoa butter. They attributed this phenomenon to the interference of their extra oleate chain with the molecular packing of the mono-unsaturated triacylglycerols. The influence of the triacylglycerols with the most importance in the second principal component has never been studied before. It may, however, be expected that triacylglycerols containing a fatty acid with two double

bonds (such as PLP, PLS and SLS), have an effect comparable to that of triacylglycerols with two fatty acids with one double bond each (di-unsaturated triacylglycerols). However, from this research it was concluded that triacylglycerols with one di-unsaturated fatty acid have an opposite effect.

Table 7.13 Resulting regression model of forward multiple linear regression with *K* as dependent variable

Independent variable	Regression coefficient	Standardized regression coefficient
free fatty acids	-1.3	-0.41
diacylglycerols	-2.2	-0.61
peroxide value	-0.02	-0.04
unsaponifiable matter	-3.8	-0.15
soap	-0.007	-0.49
principal component 2	-0.47	-0.36
principal component 1	0.28	0.21
intercept	11	

The variables with the most important influence on the rate constant are the amount of diacylglycerols and the amount of free fatty acids. Both have a negative influence. Pontillon (1998a) also observed that free fatty acids decrease the crystallization rate of cocoa butter. Shukla (1995) and Ziegleder (1988) also noticed that cocoa butters with a higher diacylglycerol level display a slower crystallization. The negative effect of diacylglycerols on the crystallization rate of milk fat was explained by Wright et al. (2000): as the diacylglycerols become incorporated in the solids, they create irregularities in the growing crystal because of the hydroxyl group they contain instead of a fatty acid chain. This polar region, or the structural vacancy created in the lattice, may hinder the incorporation of triacylglycerol molecules into the crystal and thus the subsequent crystallization.

Another chemical composition variable with a significant ($\alpha = 0.05$) influence on the rate constant is the amount of soap. The higher the amount of soap is, the lower the rate constant is. The influence of soap on the crystallization kinetics of fats has never been studied in detail but it is known by chocolate manufacturers that cocoa butters containing high soap contents, show crystallization problems.

7.4.3.4 Influence of chemical composition on n

Table 7.14 and Table 7.15 present the results of the forward linear regression with *n* as the dependent variable. This crystallization parameter represents the order of the reverse reaction of the crystallization process. In section 4.4.1.9 some hypotheses about the detailed nature of the reverse reaction were given: local remelting, redissolving or a combination of both could be the reason for the existence of a reverse reaction. The order of the reaction reflects how long this reaction affects the crystallization process: the higher *n* is, the shorter its influence.

Table 7.14 Variables entered in forward multiple linear regression with *n* as dependent variable

Variables entered	**R^2**
principal component 1	0.442
principal component 1 + unsaponifiable matter	0.506
principal component 1 + unsaponifiable matter + iron	0.558
principal component 1 + unsaponifiable matter + iron + diacylglycerols	0.586
principal component 1 + unsaponifiable matter + iron + diacylglycerols + peroxide value	0.605
principal component 1 + unsaponifiable matter + iron + diacylglycerols + peroxide value + phosphorus	0.627

Table 7.15 Resulting regression model of forward multiple linear regression with *n* as dependent variable

Independent variable	**Regression coefficient**	**Standardized regression coefficient**
principal component 1	0.90	0.87
unsaponifiable matter	7.3	0.36
iron	-0.40	-0.65
diacylglycerols	-0.39	-0.14
peroxide value	0.17	0.32
phosphorus	0.02	0.20
intercept	1.9	

It can be deduced that the six chemical composition variables having a significant ($\alpha = 0.05$) influence on *n*, together explain 62.7% of the variance of *n*. The value of the first principal component has the most important (positive) influence, meaning that higher percentages of saturated fatty acids and mono-unsaturated triacylglycerols (see section 7.4.2.1.2) increase the value of *n*. A higher percentage of saturated fatty acids and mono-unsaturated triacylglycerols may increase the melting point of the cocoa butter. As the crystallization temperature remains equal, the necessary temperature increase for local remelting increases and so the reverse reaction may lose its influence faster, leading to an increase in the value of *n*.

Other chemical composition variables with a positive influence include the amount of unsaponifiable matter, the peroxide value and the amount of phosphorus. The amount of iron and the diacylglycerol content have a negative influence on *n*. The influence of the diacylglycerols may be explained as follows: partial glycerides such as diacylglycerols may act as a template and thus induce a larger number of nuclei and crystals (Vanhoutte, 2002) which, consequently, remain smaller. Smaller crystals have a higher surface to volume ratio and thus promote redissolving of molecules. Then the importance of the reverse reaction decreases slower reflecting in a lower value for *n*. It is possible that iron molecules act as heterogeneous nuclei and also lead to a higher amount of smaller crystals and a lower value of *n*. No reasonable explanation could be found for the positive influence of the amount of unsaponifiable matter and phosphorus and the peroxide value.

7.5 Conclusions

The type of cocoa butter has a significant effect on the fatty acid and triacylglycerol profile. The cocoa butters from South America and especially the cocoa butters from Brazil contain higher percentages of unsaturated fatty acids and di-unsaturated triacylglycerols. Consequently they could be separated rather well from the main group of cocoa butters using principal component analysis. Also the contents of minor components (diacylglycerols, free fatty acids, phospholipids, iron, soap, unsaponifiable matter and oxidation products) of the different cocoa butters differ significantly. However, the contents of the different minor components do not show a clear relationship with the country of origin, probably because they are more influenced by the production and refining processes of the cocoa butter than by the country of origin. The differences in chemical composition cause differences in the crystallization

kinetics. A significant influence of the type of cocoa butter on each crystallization parameter was observed. The ratios of saturated to unsaturated fatty acids and mono-unsaturated to di-unsaturated triacylglycerols have the most important influence on all crystallization parameters except on the rate constant K. The diacylglycerols and free fatty acids have a similar influence on crystallization: they have a negative influence on a_P and K but a positive influence on t_ind_F. Other minor components with an important influence on the crystallization kinetics are the phospholipids and traces of soap. The former prolong the induction time of the second step of crystallization, whereas the latter have a negative influence on the rate constant.

GENERAL CONCLUSIONS

A lot of food products contain an important amount of fat, of which a substantial amount is present in the crystallized form. Insight in the crystallization kinetics of fats, i.e. when and to what extent fat components crystallize under certain conditions, is important for controlling the operations in the manufacturing process which are based on fat crystallization. Quite some studies have therefore been published in which the differences in the crystallization behaviour between different products and crystallization conditions are quantified using a mathematical model to describe the isothermal crystallization kinetics of fats. The Avrami model and its modified version are the most often used models in these studies. Recently, some authors also used the Gompertz model. It was shown that the Gompertz model provides a better quality of fit than the Avrami model but that neither of them fits the data satisfactorily. Models to describe the non-isothermal crystallization kinetics of fats were not found in literature despite the fact that quite some industrial processes are based on non-isothermal crystallization (chapter 1). The main aim of this research was therefore to develop a model which is able to describe the isothermal crystallization kinetics of fats better and which can be adapted for use under non-isothermal conditions. To satisfy the latter, a model written in the form of a differential equation was chosen. This kind of model has indeed the advantage that by incorporation of secondary models it can also be used under time-varying conditions, as e.g. non-isothermal crystallization where the temperature varies as function of time. Additional advantages of a differential equation are that it is often easier to interpret such a model mechanistically and that it is easier to make minor changes to the model on the basis of acquired knowledge. This model was then used to quantify the influence of temperature and chemical composition on the cocoa butter crystallization. After all, the chemical composition of cocoa butter varies slightly depending on the growth conditions and age of the tree on the one hand and on the production process including any refining on the other hand. This variation in chemical composition also leads to small differences in the crystallization properties.

To develop a new model high quality experimental data are necessary. A literature review (chapter 1) revealed that differential scanning calorimetry (DSC) and pulsed nuclear magnetic resonance (pNMR) are the preferred experimental techniques, each having advantages and disadvantages. As DSC was used for the majority of the

experiments, the method to study the isothermal cocoa butter crystallization by means of DSC was first optimized and standardized (chapter 3). Emphasis was put on the numerical integration of the obtained crystallization peaks. This integration is necessary to obtain a (mostly sigmoid) crystallization curve representing the amount of heat released as function of time. It was shown that when the starting- and end point of such an integration are determined visually, the result strongly depends on the operator and also differs when the same operator performs the integration several times. To eliminate the high variability introduced by a visual determination of the integration limits, an objective calculation algorithm to determine these limits was developed. Furthermore, it was shown that 65°C for 15 minutes is sufficient to melt all homogeneous nuclei of cocoa butter prior to the crystallization process. Finally, it could be concluded that a change in the sample preparation procedure can influence the subsequent crystallization process and should therefore be avoided.

To develop the new model able to better describe the crystallization kinetics of fats (chapter 4), the crystallization process was described as a first order forward reaction and a reverse reaction of order *n*. This reverse reaction may be related to local remelting of crystals and / or redissolving of crystals. Furthermore, the model was written in terms of the variable 'relative amount of remaining crystallizable fat', a variable which is related to the remaining supersaturation, i.e. the driving force for crystallization. The proposed model has a total of four crystallization parameters: a_P is the amount of crystallization as time approaches infinity, t_ind_F the induction time defined as the time needed to reach *F%* (e.g. 1%) of crystallization, *K* the rate constant and *n* the order of the reverse reaction. The proposed model was compared to the Avrami and Gompertz models using a large number of data series from cocoa butter and milk fat, isothermally crystallized at different temperatures and using different analytical techniques (DSC and pNMR). Objective model selection criteria showed that the proposed model always has a better quality of fit than the Avrami model. For the majority of the data series its quality of fit is also better than that of the Gompertz model, whereas for the other data series it performs only slightly worse. In comparison with the Gompertz model, the proposed model has an important feature: its ability to fit crystallization curves with different asymmetries. To simplify parameter estimation the differential equation was converted to its algebraic solution, assuming isothermal conditions. It was also shown that the amount of data points had to be reduced to eliminate autocorrelation problems.

Since cocoa butter is a strongly polymorphous fat, knowledge of the polymorphs formed as function of time and temperature is important to optimize production processes and to maintain product quality but also to explain some of the attributes of the crystallization kinetics. To gain a better insight into the polymorphs formed, their relative amounts and their formation mechanism (crystallization from the melt, polymorphic transition?) the isothermal cocoa butter crystallization was studied using different analytical techniques: DSC, pNMR, polarized light microscopy and real-time wide and short angle X-ray diffraction (chapter 5). It was shown that in the studied temperature range (17 - 23°C) crystallization is a two-step process. A mechanism for these two steps was proposed. In the first step part of the melt crystallizes in the α polymorph while the second step is initiated by the polymorphic transition of existing α crystals to the β' polymorph. The latter allows more fat to crystallize in the α polymorph and subsequently transform into the β' polymorph. This proposed mechanism implies that no β' crystals are formed directly from the melt. In the later stages of the second step only a polymorphic transition from α to β' takes place, leading to the existence of an isosbestic point.

Next, the influence of temperature on the isothermal cocoa butter crystallization was investigated (chapter 6). Scanning diffusive light scattering was used to determine the induction time of α crystallization. In the studied temperature range, the Turnbull-Fisher equation was successfully fitted to these data showing that the classical nucleation theory from which this equation is derived, is valid for isothermal cocoa butter crystallization. DSC and pNMR were used to study the latter stages of the crystallization process. It was shown that the percentage of fat that crystallizes in the α polymorph in the first crystallization step, decreases with temperature. The amount of heat released during the second crystallization step, however, only decreases from around 20.5°C onwards. The induction time of the second step of crystallization, i.e. the induction time for the polymorphic transition from α to β', increases with increasing temperature. Likely, the value of this induction time is more related to the growth rate of the β' crystals, which is expected to decrease at higher temperatures thus leading to a higher induction time. The rate constant decreases with increasing temperature, as expected. The order of the reverse reaction decreases up to a certain temperature and then remains constant.

The study of the influence of chemical composition on the isothermal cocoa butter crystallization comprised the last part of this research (chapter 7). It was revealed that there is a significant difference in the chemical composition variables (fatty acid and triacylglycerol profile as well the amounts of several minor components) as well as in the crystallization parameters between the different investigated cocoa butters. The dimensionality of the data from the fatty acid and triacylglycerol profiles was reduced using principal component analysis and the influence of the chemical composition variables on the four model parameters was investigated by means of forward linear regression. It was shown that the ratios of saturated to unsaturated fatty acids and mono-unsaturated to di-unsaturated triacylglycerols have the most important effect on all crystallization parameters except on the rate constant K. The latter is mainly influenced by the diacylglycerol content. Other minor components with a rather important influence on different crystallization parameters are the free fatty acids, the phospholipids and traces of soap.

Summarized, this PhD thesis proposed an alternative model for the description of the crystallization kinetics of fats, with important advantages over the existing Avrami and Gompertz models. Its possibilities were shown by applying it to quantify the influence of temperature and chemical composition on the isothermal, static cocoa butter crystallization. The necessary data series were mostly obtained by DSC using an improved method, mainly for the integration of the crystallization peaks. More insight into the details of the crystallization process was obtained by a combination of analytical techniques, among which real-time X-ray diffraction using synchrotron radiation.

In the future, knowledge about the details of the crystallization (relative amounts of the different polymorphs and their formation mechanism) under different processing conditions, as obtained by combining different analytical techniques including real-time X-ray diffraction, can be used to extend the proposed model. The model can also be applied to the data obtained by these X-ray diffraction experiments which represent the amount of each polymorph as function of time instead of the total amount of solid fat as function of time.

After enlarging the range of isothermal crystallization temperatures studied, secondary models describing the temperature dependency of the model parameters can be developed. The results discussed in chapter 6 are already a first step in this

development. These models will allow the extension of the proposed model for application under non-isothermal conditions as often used in industry and for which up to now no model is available in the fats and oils literature. Since industrial crystallization processes also often take place under shear (i.e. crystallization takes place in an agitated system), a similar extension to describe crystallization under varying shear is also important. To be able to build these models, new and improved experimental techniques are necessary since DSC can only be applied under isothermal conditions, linear cooling rates and combinations thereof and without shear. The possibilities of other experimental techniques will have to be verified and the methods optimized.

The proposed model can also be used to quantify the influence of processing conditions and chemical composition on the crystallization of other substrates than cocoa butter. Secondary models describing the influence of chemical composition can also be developed.

Finally, all developed models can be combined to one overall model describing the crystallization of a fat with a specific chemical composition under a specific combination of time, temperature and shear. This model should allow to simulate industrial processes and to predict the influence of changes in processing conditions or to find out what changes are necessary to compensate for a specific change in chemical composition. This will ultimately lead to a better product quality.

REFERENCES

AOCS OFFICIAL METHOD Ca 5a-40 (1996). Free fatty acids. Champaign, AOCS Press, 1p.

AOCS OFFICIAL METHOD Ca 6a-40 (1989). Unsaponifiable matter. Champaign, AOCS Press, 2p.

AOCS OFFICIAL METHOD Cd 8b-90 (1996). Peroxide value. Acetic Acid – Isooctane Method. Champaign, AOCS Press, 2p.

AOCS OFFICIAL METHOD Cd 18-90 (1996). p-Anisidine Value. Champaign, AOCS Press, 2p.

AOCS RECOMMENDED PRACTICE Cc 17-79 (1990). Soap in oil. Champaign, AOCS Press, 1p.

AOCS RECOMMENDED PRACTICE Ca 20-99 (1999). Analysis for phosphorus in oil by inductively coupled plasma optical emission spectroscopy. Champaign, AOCS Press, 3p.

AQUILANO, D. & SGUALDINO, G. (2001). Fundamental aspects of equilibrium and crystallization kinetics. In: Garti, N. & Sato, K. (eds.) Crystallization processes in fats and lipid systems. New York, Marcel Dekker Inc., 1-51.

ARRUDA, D.H. & DIMICK, P.S. (1991). Phospholipid composition of lipid seed crystal isolates from Ivory Coast cocoa butter. Journal of the American Oil Chemists' Society, 68, 385-390.

AVRAMI, M. (1939). Kinetics of phase change. I. General theory. Journal of Chemical Physics, 7, 1103-1112.

AVRAMI, M. (1940). Kinetics of phase change. II. Transformation-time relations for random distribution of nuclei. Journal of Chemical Physics, 8, 212-224.

BECKETT, S.T. (1994). Traditional chocolate making. In: Beckett, S.T. (ed.) Industrial chocolate manufacture and use. Glasgow, Chapman & Hall, 1-7.

BERG, T.G.O. & BRIMBERG, U.I. (1983). Über die Kinetik der Fettkristallisation. Fat Science Technology, 85, 142-149.

BOISTELLE, R. (1988). Fundamentals of nucleation and crystal growth. In: Garti, N. & Sato, K. (eds.) Crystallization and polymorphism of fats and fatty acids. Surfactant Science Series Volume 31. New York, Marcel Dekker Inc., 189-276.

BROSIO, E., CONTI, F., DI NOLA, A. & SYKORA, S. (1980). A pulsed low resolution NMR study on crystallization and melting processes of cocoa butter. Journal of the American Oil Chemists' Society, 57, 78-82.

CEBULA, D.J. & SMITH, K.W. (1992). Differential scanning calorimetry of confectionery fats: Part II: Effects of blends and minor components. Journal of the American Oil Chemists' Society, 69, 992-998.

CHAISERI, S. & DIMICK, P.S. (1989). Lipid and hardness characteristics of cocoa butters from different geographic regions. Journal of the American Oil Chemists' Society, 66, 1771-1776.

CHAISERI, S. & DIMICK, P.S. (1995a). Dynamic crystallization of cocoa butter. I.Characterization of simple lipids in rapid- and slow-nucleating cocoa butters and their seed crystals. Journal of the American Oil Chemists' Society, 72, 1491-1496.

CHAISERI, S. & DIMICK, P.S. (1995b). Dynamic crystallization of cocoa butter. II. Morphological, thermal and chemical characteristics during crystal growth. Journal of the American Oil Chemists' Society, 72, 1497-1504.

CHAPMAN, D. (1962). The polymorphism of glycerides. Chemical Reviews, 62, 433-456.

CHAPMAN, G.M., AKEHURST, E.E. & WRIGHT, W.B. (1971). Cocoa butter and confectionery fats. Studies using programmed temperature X-ray diffraction and differential scanning calorimetry. Journal of the American Oil Chemists' Society, 48, 824-830.

CHEN, C.W., LAI, O.M., GHAZALI, H.M. & CHONG, C.L. (2002). Isothermal crystallization kinetics of refined palm oil. Journal of the American Oil Chemists' Society, 79, 403-410.

CHRISTIE, W.W. (1982). Lipid analysis: isolation, separation, identification and structural analysis of lipids 2nd edition. Oxford, Pergamon Press, 207p.

COCOA BUTTER QUALITY (2002). http://www.britanniafood.com/invite_10.htm

CROS, E. & BIANCHI, J. (1998). Alcalinisation. In: Pontillon, J. (ed.) Cacao et chocolat: production, utilisation, caractéristiques. Paris, Lavoisier, 270-309.

DAVIS, T.R. & DIMICK, P.S. (1989). Lipid composition of high-melting seed crystals formed during cocoa butter solidification. Journal of the American Oil Chemists' Society, 66, 1494-1498.

DE GINESTEL, G. (1998a). Fabrication du chocolat. In: Pontillon, J. (ed.) Cacao et chocolat: production, utilisation, caractéristiques. Paris, Lavoisier, 397-412.

DE GINESTEL, G. (1998b). Les procédés du cacao. In: Pontillon, J. (ed.) Cacao et chocolat: production, utilisation, caractéristiques. Paris, Lavoisier, 208-237.

DE MEULENAER, B. & HUYGHEBAERT, A. (2002). Praktikum levensmiddelenchemie. Course, Ghent, Faculty of agricultural and applied biological sciences, 110p.

DIBILDOX-ALVARADO, E. & TORO-VAZQUEZ, J.F. (1997). Isothermal crystallization of tripalmitin in sesame oil. Journal of the American Oil Chemists' Society, 74, 69-76.

DI LORENZO, M.L. & SILVESTRE, C. (1999). Non-isothermal crystallization of polymers. Progress in Polymer Science, 24, 917-950.

DOCHAIN, D. & VANROLLEGHEM, P.A. (2001). Estimation of model parameters. In: Dochain, D. & Vanrolleghem, P.A. (eds.) Dynamical modelling and estimation in wastewater treatment processes. London, IWA Publishing, 1-83.

EG (2000). Richtlijn 2000/36/EG van het Europees Parlement en de Raad van 23 juni 2000 inzake cacao- en chocoladeproducten voor menselijke consumptie. Publicatieblad van de Europese Gemeenschappen L 197/19, 03.08.2000, 7p.

EVANS, U.R. (1945). The laws of expanding circles and spheres in relation to the lateral growth of surface films and the grain-size of metals. Transactions of the Faraday Society, 41, 365-374.

GARSIDE, J. (1987). General principles of crystallization. In: Blanshard, V.M.V. & Lillford, P. (eds.) Food structure and behaviour. London, Academic Press, 35-49.

GODERIS, B. & REYNAERS, H. (2002). Haal meer uit uw thermische analyse experimenten! Synchrotron WAXD en SAXS gecombineerd met DSC en met nog zoveel meer. Chemie Magazine, 2, 46-

GORDON, M.H. & RAHMAN, I.A. (1991). Effects of minor components on the crystallization of coconut oil. Journal of the American Oil Chemists' Society, 68, 577-579.

GUTSHALL-ZAKIS, A. & DIMICK, P.S. (1993). Influence of various refining treatments on the crystallization behaviour of hard and soft cocoa butters and formulated dark chocolate. The Manufacturing Confectioner, September 1993, 117-123.

HACHIYA, I., KOYANO, T. & SATO, K. (1989). Seeding effects on solidification behavior of cocoa butter and dark chocolate. I. Kinetics of solidification. Journal American Oil Chemists' Society, 66, 1757 – 1762.

HAGEMANN, J.W. (1988). Thermal behavior and polymorphism of acylglycerides. In: Garti, N. & Sato, K. (eds.) Crystallization and polymorphism of fats and fatty acids. Surfactant Science Series Volume 31. New York, Marcel Dekker Inc, 9-95.

HANCOCK, B.L. & FOWLER, M.S. (1994). Cocoa bean production and transport. In: Beckett, S.T. (ed.) Industrial chocolate manufacture and use. Glasgow, Chapman & Hall, 8-24.

HANNEMAN, E. (2000). The complex world of cocoa butter. The Manufacturing Confectioner, September 2000, 107-112.

HARTEL, R.W. (1992). Solid-liquid equilibrium: crystallization in foods. In: Schwartzberg, H.G. & Hartel, R.W. (eds.) Physical chemistry of foods. New York, Marcel Dekker Inc., 47-81.

HASHIM, L., HUDIYONO, S. & CHAVERON, H. (1997). Volatile compounds of oxidized cocoa butter. Food Research International, 30, 163-169.

HATAKEYAMA, T. & QUINN, F.X. (1994). Reaction rate kinetics. In: Thermal analysis: fundamentals and applications to polymer science. Chichester, John Wiley & Sons, 68-81.

HERNQVIST, L. (1990). Polymorphism of triacylglycerols a crystallographic review. Food Structure, 9, 39-44.

HERNQVIST, L. & LARSSON, K. (1982). On the crystal structure of the β' form of triacylglycerols and structural changes at the phase transitions LIQ → α → β' → β. Fat Science Technology, 84, 349-354.

HERRERA, M.L., DE LEON GATTI, M. & HARTEL, R.W. (1999a). A kinetic analysis of crystallization of a milk fat model system. Food Research International, 32, 289-298.

HERRERA, M.L., FALABELLA, C., MELGAREJO, M. & ANON, M.C. (1999b). Isothermal crystallization of hydrogenated sunflower oil: II. Growth and solid fat content. Journal of the American Oil Chemists' Society, 76, 1-6.

HINDLE, S.A., POVEY, M.J.W. & SMITH, K.W. (2002). Characterizing cocoa butter seed crystals by the oil-in-water emulsion crystallization method. Journal of the American Oil Chemists' Society, 79, 993-1002.

HOSKIN, J.C. & DIMICK, P.S. (1994). Chemistry of flavour development in chocolate. In: Beckett, S.T. (ed.) Industrial chocolate manufacture and use. Glasgow, Chapman & Hall, 102-116.

HUYGHEBAERT, A. & HENDRICKX, H. (1971). Polymorphism of cocoa butter, shown by differential scanning calorimetry. Lebensmittel-Wissenschaft und –Technologie, 4, 59-63.

ICCO (2000). Annual report of the ICCO for 1999/00. London, International Cocoa Organization, 28p.

ICCO (2002). Physical and chemical information on cocoa beans, butter, mass and powder. http://www.icco.org/questions/chemical.htm.

JACKSON, K. (1994). Recipes. In: Beckett, S.T. (ed.) Industrial chocolate manufacture and use. Glasgow, Chapman & Hall, 257-280.

JACOBSBERG, B. & OH CHUAN, H.O. (1976). Studies in palm oil crystallization. Journal of the American Oil Chemists' Society, 53, 609-617.

JINAP, S., THIEN, J. & YAP, T.N. (1994). Effect of drying on acidity and volatile fatty acids content of cocoa beans. Journal of the Science of Food and Agriculture, 65, 67-75.

KAWAMURA, K. (1979). The DSC thermal analysis of crystallization behavior in palm oil. Journal of the American Oil Chemists' Society, 56, 753-758.

KELLENS, M. (1991). Polymorphism of saturated monoacid triacylglycerols. PhD thesis, Leuven, Belgium, Katholieke Universiteit, 236p.

KERTI, K. (1998). Thermal analysis of cocoa butter and cocoa butter alternatives. Crystallisation using DSC Method. 2nd International workshop on control applications in post-harvest and processing technology, Budapest, Hungary, June 3-5, 1998, p.173-176.

KHANNA, Y.P. & TAYLOR, T.J. (1988). Comments and recommendation on the use of the Avrami equation for physico-chemical kinetics. Polymer Engineering and Science, 28, 1042-1045.

KLAGGE, P. & SEN GUPTA, A.K. (1990). Kakaobutter und ihre Alternativen für Schokoladenprodukte. Fat Science Technology, 92, 485-492.

KLEINERT, J. (1994). Cleaning, roasting and winnowing. In: Beckett, S.T. (ed.) Industrial chocolate manufacture and use. Glasgow, Chapman & Hall, 55-69.

KLOEK, W. (1998). Mechanical properties of fats in relation to their crystallization. PhD thesis, Wageningen, the Netherlands, Landbouwuniversiteit, 241p.

KLOEK, W., WALSTRA, P. & VAN VLIET, T. (2000). Crystallization kinetics of fully hydrogenated palm oil in sunflower oil mixtures. Journal of the American Oil Chemists' Society, 77, 389-398.

LADBROOKE, B.D. & CHAPMAN, D. (1969). Thermal analysis of lipids, proteins and biological membranes. A review and summary of some recent studies. Chemistry and Physics of Lipids, 3, 304-353.

LAMBRIGGER, M. (1996). Evaluation of data on the kinetics of isothermal polymer crystallization. Polymer Engineering and Science, 36(1), 98-99.

LARSSON, K. & DEJMEK, P. (1990). Crystal and liquid crystal structures of lipids. In: Larsson, K. & Friberg, S.E. (eds.) Food emulsions. New York, Marcel Dekker Inc., 97-125.

LE BOTLAN, D., OUGUERRAM, L., SMART, L. & PUGH, L. (1999). Characterization of a semi-solid state in milk fat through T2* resolved T1 distributions by time domain NMR. Journal American Oil Chemists' Society, 76, 1–6.

LEHRIAN, D.W., KEENEY, P.G. & BUTLER, D.R. (1980). Triacylglycerol characteristics of cocoa butter from cacao fruit matured in a microclimate of elevated temperature. Journal of the American Oil Chemists' Society, 57, 66-69.

LEY, D. (1994). Conching. In: Beckett, S.T. (ed.) Industrial chocolate manufacture and use. Glasgow, Chapman & Hall, 117-138.

LIPP, M. & ANKLAM, E. (1998). Review of cocoa butter and alternative fats for use in chocolate. Part A. Compositional data. Food Chemistry, 62(1), 73-97.

LITWENKO, J.W., ROJAS, A.M., GERSCHENSON, L.N. & MARANGONI, A.G. (2002). Relationship between crystallization behavior, microstructure, and mechanical properties in a palm oil-based shortening. Journal of the American Oil Chemists' Society, 79, 647-654.

LOISEL, C. (1996). Physico-chimie du chocolat: cristallisation du beurre de cacao et propriétés structurales. PhD thesis, Paris, France, Ecole Nationale Superieure des Industries Agricoles et Alimentaires (E.N.S.I.A.), 195p.

LOISEL, C., KELLER, G., LECQ, G., BOURGAUX, C. & OLLIVON, M. (1998a). Phase transitions and polymorphism of cocoa butter. Journal of the American Oil Chemists' Society, 75, 425-439.

LOISEL, C., LECQ, G., KELLER, G. & OLLIVON, M. (1998b). Dynamic crystallization of dark chocolate as affected by temperature and lipid additives. Journal of Food Science, 63 73-79.

LONG, Y., SHANKS, R.A. & STACHURSKI, Z.B. (1995). Kinetics of polymer crystallisation. Progress in Polymer Science, 20, 651-701.

LOPEZ, M., BONNARD, H. & PONTILLON, J. (1998). Travail du chocolat. In: Pontillon, J. (ed.) Cacao et chocolat: production, utilisation, caractéristiques. Paris, Lavoisier, 413-446.

MA, C.-Y. & HARWALKAR, V.R. (1991). Thermal analysis of food proteins. Advances in Food and Nutrition Research, 35, 317-366.

MARANGONI, A.G. (1998). On the use and misuse of the Avrami equation in characterization of the kinetics of fat crystallization. Journal of the American Oil Chemists' Society, 75, 1465-1467.

MARANGONI, A.G. & McGAULEY, S.E. (2003). Relationship between crystallization behavior and structure in cocoa butter. Crystal Growth and Design, 3, 95-108.

MARTINI, S., HERRERA, M.L. & HARTEL, R.W. (2001). Effect of cooling rate on nucleation behavior of milk fat – sunflower oil blends. Journal of Agricultural and Food Chemistry, 49, 3223-3229.

MATERIALS RESEARCH LABORATORY (2003). Introduction to X-ray diffraction. http://www.nrl.ucsb.edu/mrl/centralfacilities/xray/xray-basics/Xray-basics.html.

MERKEN, G.V. & VAECK, S.V. (1980). Etude du polymorphisme du beurre de cacao par calorimétrie DSC. Lebensmittel-Wissenschaft und –Technologie, 13, 314-317.

METIN, S. & HARTEL, R.W. (1998). Thermal analysis of isothermal crystallization kinetics in blends of cocoa butter with milk fat or milk fat fractions. Journal of the American Oil Chemists' Society, 75, 1617-1624.

MEURSING, E.H. (1994). Cocoa mass, cocoa butter, cocoa powder. In: Beckett, S.T. (ed.) Industrial chocolate manufacture and use. Glasgow, Chapman & Hall, 70-82.

NARINE, S.S. & MARANGONI, A.G. (1999). Relating structure of fat crystal networks to mechanical properties: a review. Food Research International, 32, 227-248.

NAWAR, W.W. (1996). Lipids. In: Fennema, O.R. (ed.) Food chemistry. New York, Marcel Dekker Inc., 239-319.

NELDER, J.A. & MEAD, R. (1965). A simplex method for function minimization. Computer Journal, 7, 308-313.

NELSON, R.B. (1994). Enrobers, moulding equipment, coolers and panning. In: Beckett, S.T. (ed.) Industrial chocolate manufacture and use. Glasgow, Chapman & Hall, 211-241.

NG, W.L. (1975). Thermal decomposition in the solid state. Australian Journal of Chemistry, 28, 1169-1178.

NG, W.L. (1990). A study of the kinetics of nucleation in a palm oil melt. Journal of the American Oil Chemists' Society, 67, 879-882.

NG, W.L. & OH, C.H. (1994). A kinetic study on isothermal crystallization of palm oil by solid fat content measurements. Journal of the American Oil Chemists' Society, 71, 1135-1139.

NICULA, R. (2002). Introduction to differential scanning calorimetry. Course, Rostock University, Physics Department, 17p.

PARSONS, J.G., KEENEY, P.G. & PATTON, S. (1969). Identification and quantitative analysis of phospholipids in cocoa beans. Journal of Food Science, 34, 497-499.

PONTILLON, J. (1998a). Le beurre de cacao et les matières grasses en chocolaterie. In: Pontillon, J. (ed.) Cacao et chocolat: production, utilisation, caractéristiques. Paris, Lavoisier, 326-393.

PONTILLON, J. (1998b). Utilisation des semi-produits du cacao. In: Pontillon, J. (ed.) Cacao et chocolat: production, utilisation, caractéristiques. Paris, Lavoisier, 309-314.

PONTILLON, J. & CROS, E. (1998). Méthodes analytiques pour le cacao et produits dérivés. In: Pontillon, J. (ed.) Cacao et chocolat: production, utilisation, caractéristiques. Paris, Lavoisier, 448-543.

RIINER, Ü (1970). Investigation of the polymorphism of fats and oils by temperature programmed X-ray diffraction. Lebensmittel-Wissenschaft und –Technologie, 3, 101-106.

ROSSI, M., SCHIRALDI, A., ARNOLDI, C. & SALVIONI, G. (1994). Characterization of cocoa extracts obtained with supercritical carbon-dioxide. Industrie Alimentari, Suppl. 4, 38-42.

ROUSSET, P. (1997). Etude expérimentale et modélisation de la cristallisation de triacylglycérols et du beurre de cacao. PhD thesis, Lausanne, Switzerland, Ecole Polytechnique Fédérale, 175p.

SAMBUC, E., DIRIK, Z., REYMOND, G. & NAUDET, M. (1980). Etude de la cristallisation de corps gras plastiques. VI. Influence des glycérides partiels et des phosphatides en absence et présence d'eau. A. Cas des monoglycérides stéaropalmitiques. Revue Française des Corps Gras, 27, 505-512.

SATO, K. (1987). Physical and molecular properties of lipid polymorphs. Food Microstructure, 6, 151-159.

SATO, K. & KURODA, T. (1987). Kinetics of melt crystallization and transformation of tripalmitin polymorphs. Journal of the American Oil Chemists' Society, 64, 124-127.

SATO, K., UENO, S. & YANO, J. (1999). Molecular interactions and kinetic properties of fats. Progress in Lipid Research, 38, 91-116.

SAVAGE, C.M. & DIMICK, P.S. (1995). Influence of phospholipids during crystallization of hard and soft cocoa butters. The Manufacturing Confectioner, May 1995, 127-132.

SCHLICHTER-ARONHIME, J. & GARTI, N. (1988a). Solidification and polymorphism in cocoa butter and the blooming problems. In: Garti, N. & Sato, K. (eds.) Crystallization and polymorphism of fats and fatty acids. Surfactant Science Series Volume 31. New York, Marcel Dekker Inc, 363-393.

SCHLICHTER-ARONHIME, J., SARIG, S. & GARTI, N. (1988b). Reconsideration of polymorphic transformations in cocoa butter using the DSC. Journal of the American Oil Chemist's Society, 65, 1140-1143.

SHUKLA, V.K.S. (1995). Cocoa butter properties and quality. Lipid Technology, 7(3), 54-57.

SIEW, W.L. & NG, W.L. (1996). Effect of diacylglycerols on the crystallization of palm oleins. Journal of the Science of Food and Agriculture, 71, 496-500.

SIMON, K. & SÜVERKRUP, R. (1995). Comparison of recent techniques to characterize the crystallization behaviour of fatty suppository bases. Thermochimica Acta, 248, 271-287.

SMITH, P.R. (2000). The effects of phospholipids on crystallization and crystal habit in triacylglycerols. European Journal Lipid Science Technology, 2, 122-127.

SMITH, P.R., CEBULA, D.J. & POVEY, M.J.W. (1994). The effect of lauric-based molecules on trilaurin crystallization. Journal of the American Oil Chemists' Society, 71, 1367-1372.

SMITH, P.R., HAGHSHENAS, N. & BERGENSTAHL, B. (2001). Development and use of a novel technique to measure exchange between lipid crystals and oils. In: Widlak, N., Hartel, R. & Narine, S. (eds.) Crystallization and solidification properties of lipids. Champaign, AOCS Press, 160-167.

SMITH, P.R. & POVEY, M.J.W. (1997). The effect of partial glycerides on trilaurin crystallization. Journal of the American Oil Chemists' Society, 74, 169-171.

STORGAARD, S. (2000). New vegetable fats. Sweetec, 4, 5p.

SUPAPHOL, P. & SPRUIELL, J.E. (2001). Isothermal melt- and cold-crystallization kinetics and subsequent melting behavior in syndiotactic polypropylene: a differential scanning calorimetry study. Polymer, 42, 699-712.

TALBOT, G. (1994a). Chocolate temper. In: Beckett, S.T. (ed.) Industrial chocolate manufacture and use. Glasgow, Chapman & Hall, 156-166.

TALBOT, G. (1994b). Vegetable fats. In: Beckett, S.T. (ed.) Industrial chocolate manufacture and use. Glasgow, Chapman & Hall, 242-257.

TEN GROTENHUIS, E., VAN AKEN, G.A., VAN MALSSEN, K.F. & SCHENK, H. (1999). Polymorphism of milk fat studied by differential scanning calorimetry and real-time X-ray powder diffraction. Journal of the American Oil Chemists' Society, 76, 1031-1039.

TIMMS, R.E. (1984). Phase behaviour of fats and their mixtures. Progress in Lipid Research, 23, 1-38.

TORO-VAZQUEZ, J.F., BRICENO-MONTELONGO, M., DIBILDOX-ALVARADO, E., CHARO-ALONSO, M. & REYES-HERNANDEZ, J. (2000). Crystallization kinetics of palm stearin in blends with sesame seed oil. Journal of the American Oil Chemists' Society, 77, 297-310.

TORO-VAZQUEZ, J.F. & DIBILDOX-ALVARADO, E. (1997). Parameters that determine tripalmitin crystallization in sesame oil. Journal of Food Lipids, 4, 269-282.

TORO-VAZQUEZ, J.F., DIBILDOX-ALVARADO, E. & CHARO-ALONSO, M. (2001). In: Widlak, N., Hartel, R. & Narine, S. (eds.) Crystallization and solidification properties of lipids. Champaign, AOCS Press, 53-78.

TORO-VAZQUEZ, J.F., HERRERA-CORONADO, V., DIBILDOX-ALVARADO, E., CHARO-ALONSO, M. & GOMEZ-ALDAPA, C. (2002). Induction time of crystallization in vegetable oils, comparative measurements by differential scanning calorimetry and diffusive light scattering. Journal of Food Science, 67, 1057-1062.

TZERO^{TM} DSC TECHNOLOGY (2001). Seminar, Breda, November 22, 2001.

VANHOUTTE, B. (2002). Milk fat crystallisation: fractionation and texturisation. PhD thesis, Gent, Belgium, Ghent University, 365p.

VAN LANGEVELDE, A., VAN MALSSEN, K., PESCHAR, R. & SCHENK, H. (2001). Effect of temperature on recrystallization behavior of cocoa butter. Journal of the American Oil Chemists' Society, 78, 919-925.

VAN MALSSEN, K., PESCHAR, R., BRITO, C. & SCHENK, H. (1996). Real-time X-ray powder diffraction investigations on cocoa butter III. Direct ß-crystallization of cocoa butter: occurrence of a memory effect. Journal of the American Oil and Chemists' Society, 72, 1225-1230.

VAN MALSSEN, K., VAN LANGEVELDE, A., PESCHAR, R. & SCHENK, H. (1999). Phase behavior and extended phase scheme of static cocoa butter investigated with real-time X-ray powder diffraction. Journal of the American Oil Chemists' Society, 76, 669-676.

VANROLLEGHEM, P.A. & DOCHAIN, D. (1998). Bioprocess model identification. In: Van Impe, J., Vanrolleghem, P.A. & Iserentant, D. (eds.) Advanced instrumentation, data interpretation and control of biotechnological processes. Dordrecht, Kluwer Academic Publishers, 251-318.

VERDONCK, E., SCHAAP, K. & THOMAS, L.C. (1999). A discussion of the principles and applications of Modulated Temperature DSC (MTDSC). International Journal of Pharmaceutics, 192, 3-20.

WAHNELT, S., MEUSEL, D. & TULSNER, M. (1991). Der Einfluβ isomerer Diacylglycerol auf Phasenumwandlungen von Kakaobutter – Untersuchungen mittels isothermer DSC. Fat Science Technology, 93, 174-178.

WALSTRA, P. (1987). Fat crystallization. In: Blanshard, V.M.V. & Lillford, P. (eds.) Food structure and behaviour. London, Academic Press, 67-85.

WILLE, R.L. & LUTTON, E.S. (1966). Polymorphism of cocoa butter. Journal of the American Oil Chemists' Society, 43, 491-496.

WRIGHT, A.J., HARTEL, R.W., NARINE, S.S. & MARANGONI, A.G. (2000). The effect of minor components on milk fat crystallization. Journal of the American Oil Chemists' Society, 77, 463-475.

WRIGHT, A.J. & MARANGONI, A.G. (2002). Effect of DAG on milk fat TAG crystallization. Journal of the American Oil Chemists' Society, 79, 395-402.

WRIGHT, A.J., NARINE, S.S. & MARANGONI, A.G. (2001). Comparison of experimental techniques used in lipid crystallization studies. In: Widlak, N., Hartel, R. & Narine, S. (eds.) Crystallization and solidification properties of lipids. Champaign, AOCS Press, 120-131.

WÜNDERLICH, B. (1990). Thermal analysis. New York, Academic Press, 450p.

ZIEGLEDER, G. (1988). Kristallisation von Kakaobutter unter statischen und dynamischen Bedingungen (DSC, Rheometer). Suesswaren, 12, 487-493.

ZIEGLEDER, G. (1990). DSC-Thermoanalyse und Kinetik der Kristallisation von Kakaobutter. Fat Science Technology, 92, 481-485.

ZWIETERING, M.H., JONGENBURGER, I., ROMBOUTS, F.M. & VAN 'T RIET, K. (1990). Modeling of the bacterial growth curve. Applied and Environmental Microbiology, 56, 1875-1881.

I EXPLANATION OF SYMBOLS USED

a_A maximum amount of crystallization in the Avrami model [% solid fat or J g^{-1}] depending on the measuring technique

a_P maximum amount of crystallization in the proposed model [% solid fat or J g^{-1}] depending on the measuring technique

a_G maximum amount of crystallization in the Gompertz model [% solid fat or J g^{-1}] depending on the measuring technique

$asym$ asymmetry of a curve [-]

A parameter of the unmodified Gompertz model [-]

A_J global kinetic coefficient [s^{-1} m^{-3}]

A_1, A_2 surface between nucleus and mother phase and between nucleus and foreign surface respectively in the calculation of ΔG_{het} [m^2]

AC auto-correlation value

B parameter of the unmodified Gompertz model [-]

C concentration [m^{-3} or equivalent]

C_0 initial value of C [m^{-3}]

C_p heat capacity [J g^{-1} K^{-1}]

C_s concentration at saturation [m^{-3} or equivalent]

d distance between reflecting entities [Å]

D parameter of the unmodified Gompertz model [s^{-1}]

e Euler number = 2.718281… [-]

f absolute amount of crystallization [% solid fat or J g^{-1}] depending on measuring technique

$f(0)$ absolute amount of crystallization at time zero [% solid fat or J g^{-1}] depending on measuring technique

F	relative amount of crystallized material, also used in the definition of t_ind_F and $t_{F\%}$ [-]
F_w	test statistic of F-test [-]
G	Gibbs free energy [J]
$\Delta G*$	critical activation free energy for nucleation [J]
$\Delta G*_{het}$	critical activation free energy for heterogeneous nucleation [J]
$\Delta G*_{vd}$	critical activation free energy for volume diffusion [J]
ΔG_{het}	Gibbs free energy change for heterogeneous nucleation [J]
ΔG_s	surface Gibbs free energy change [J]
ΔG_v	volume Gibbs free energy change [J]
h	relative amount of remaining crystallizable fat [-]
$h(0)$	relative amount of remaining crystallizable fat at time zero [-]
ΔH	(total) heat of crystallization [J g^{-1}]
ΔH_{ts-t}	heat of crystallization at a given time t [J g^{-1}]
ΔH_m	molar transition enthalpy [J $mole^{-1}$]
j_j	number of sign change [-]
J	nucleation rate [s^{-1} m^{-3}]
k	rate constant in Avrami model [s^{-m}]
k'	rate constant in modified Avrami model [s]
k_B	Boltzmann constant [1.380 10^{-23} J K^{-1}]
k_i	rate constants of the aggregation and flocculation model
K_1	rate constant of the first order forward reaction in the proposed model
K_n	rate constant of the reverse reaction of order n in the proposed model
ΔK_1	difference between K_1 and K_n in the reparameterized version of the 5-parameter differential equation form of the proposed model [h^{-1}]

m	Avrami exponent [-]
m'	exponent in the modified Avrami model [-]
M	mass of the blank in the determination of the amount of unsaponifiable matter [g]
n	order of the reverse reaction in the proposed model [-]
n_j	number of repetitions in group j [-]
n_p	number of parameters [-]
N	number of germ nuclei per unit nucleation region [m^{-3}]
N_d	number of data points [-]
$\bar{N}_0$	initial number of germ nuclei per unit nucleation region [m^{-3}]
N_m	number of molecules per m^3 [m^{-3}]
O	mass of the residue in the determination of the amount of unsaponifiable matter [g]
p	probability of occurrence of transformation germ nucleus – growth nucleus per unit time [s^{-1}]
P	mass of the fatty acids in the determination of the amount of unsaponifiable matter [g]
$\frac{dQ}{dt}$	heat flow as determined by DSC [W g^{-1}]
$\frac{dQ}{dt_f}$	last available heat flow value in the calculation algorithm for determination of the integration limits [W g^{-1}]
r	radius [m]
r^*	critical radius [m]
R	direction averaged rate of growth of r [m s^{-1}]
R_g	universal gas constant [8.314 J $mole^{-1}$ K^{-1}]
s	reciprocal distance [$Å^{-1}$]

s_{ji}^2	estimator of the variance $VAR(\omega_{ji})$ of $\hat{\omega}_{ji}$
s_j^2	sample variance
SSR	sum of squared residuals [(dependent variable)^2]
t	time [s]
t_e	end point of crystallisation
t_i	time at inflection point of curve [s]
t_0	initial value of t [s]
t_s	starting-point of crystallization
t_w	test statistic of the adapted t-test
$t_{F\%}$	time needed to reach $F\%$ crystallization [h]
t_ind_A	induction time of the Avrami model with induction time [h]
t_ind_F	induction time of the proposed model, time needed to reach $F\%$ of crystallization [h]
T	temperature [°C]
T_K	absolute temperature [K]
T_{K_m}	absolute melting temperature [K]
Tr	transmittance at time t [-]
Tr_f	minimum transmittance obtained during the crystallization process [-]
Tr_i	transmittance of the oil solution at time zero [-]
ΔT	supercooling [K] (= $T_{K\,m} - T_K$)
$v(\tau, z)$	volume at rescaled time τ of a grain which began growth from a nucleus at rescaled time z [m^3]
v_{ext}	extended volume of a grain [m^3]
V	volume of crystalline phase per unit volume of space [-]

V_{ext} total extended volume per unit volume of space [-]

V_m molar volume [m^3 $mole^{-1}$]

w help variable used in solving the differential equation of proposed model [-]

x length of the period for which the slope is determined in the calculation algorithm for determination of the integration limits [min]

y number of sign change after peak maximum taken as t_e in the calculation algorithm for determination of the integration limits [-]

Y logarithm of the relative population size [-]

z number of data points used to calculate the regression [-]

Z' equals 1-h, in the differential equation version of proposed model, used to facilitate parameter estimation [-]

Z'' equals log ($f(0)$) in the proposed model, used to facilitate parameter estimation [-]

α significance level in statistical test, chance of a type I error [-]

β $\frac{6\chi R^3 \bar{N}_0}{p^3}$ [s^{-3}]

χ shape factor [-]

δ angle of tilt [°]

ε residual (measured value – predicted value) [same as measured value]

φ lag in the auto-correlation calculation

γ surface free energy per unit surface area [J m^{-2}]

λ wavelength [Å]

λ_G lag time (Gompertz model) [s]

$\Delta\mu$ chemical potential [J $mole^{-1}$]

μ_G maximum specific growth rate (Gompertz model) [% solid fat s^{-1} or J g^{-1} s^{-1}] depending on measuring technique

θ scattering angle [°]

σ supersaturation ratio [-] (= C/C_s)

σ_n noise on the baseline in the calculation algorithm for determination of integration limits

σ_r relative supersaturation [-] (= $\frac{C - C_s}{C_s}$)

$\ln(\sigma)$ supersaturation [-] (= $\ln(C/C_s)$)

τ rescaled time [-]

ω contact angle [°]

$\hat{\omega}_{ji}$ estimator of parameter ω_{ji} (expectation ω_{ji} and variance $VAR(\omega_{ji})$)

ω_{ji} parameter with expectation ω_j and variance $VAR(\omega_j)$

$\overline{\omega}_{(j)}$ unbiased estimator of ω_j

II EXPLANATION OF ABBREVIATIONS USED

A	arachidic acid
AIC	Akaike's Information Criterion
BIC	Bayesian Information Criterion
CB	cocoa butter
CBA	cocoa butter alternative
CBE	cocoa butter equivalent
CBI	cocoa butter improver
CBR	cocoa butter replacer
CBS	cocoa butter substitute
DSC	differential scanning calorimetry
F face	flat face
FPE	final prediction error
K face	kinked face
L	linoleic acid
MF	milk fat
MSR	mean sum of squared residuals
O	oleic acid
P	palmitic acid
PCA	principal component analysis
PLM	polarized light microscopy
pNMR	pulsed nuclear magnetic resonance
PRESS	predicted residual error sum of squares
S	stearic acid
SAXS	short angle X-ray scattering
SDLS	scanning diffusive light scattering

S face	stepped face
SFC	solid fat content
SSR	sum of squared residuals
WAXD	wide angle X-ray diffraction
XRD	X-ray diffraction

III DETAILS ON PARAMETER ESTIMATION

III.1 Linearization of the Avrami equation to estimate model parameters (Dochain and Vanrolleghem, 2001)

It is common practice to transform a model that is non-linear in its parameters (equation [1.35]) into a model that is linear in its parameters (equation [1.56]). The rationale for pursuing this type of transformation is that the methods of non-linear regression are much less known with modellers than the generally known linear regression methods. Unfortunately, the ease of linear regression analysis is accompanied by fundamental drawbacks:

(i) When data are transformed (V into ln (-ln(1-V))), measurement errors are transformed as well. More particularly, although the measurement errors of the actually measured variable (V) may be independent and identically distributed normally, the transformed variable will typically not be. The important result is that a wrong assumption is made on the error characteristics, which may lead to biased parameter estimates. Indeed many authors found that different linearized forms of the same non-linear model yield different estimates of the same parameters.

(ii) Difficulties arise when trying to obtain confidence information on the estimated parameters. The actually estimated parameters are not the desired parameters, but a transformation or combination of parameters. In the linearized Avrami equation the estimated parameter is $\ln(k)$. It is not that easy at all to accurately calculate the confidence information on k from confidence information on $\ln(k)$.

(iii) The spacing of the data points becomes important. When the linearized Avrami equation is applied, many data points are located at high values of the variable $\ln(t)$ and only a few are found at small values of $\ln(t)$. This leads to a very high sensitivity of the parameters to the latter.

To illustrate the influence linearization has on the parameter estimates, Table III.1 gives the 95% confidence intervals of the Avrami parameters k and m obtained with non-linear regression and with linear regression using all data, the data between 10 and 90 % crystallization and the data between 25 and 75% crystallization, as suggested by different authors (see section 1.4.5).

Table III.1 Influence of parameter estimation procedure on 95% confidence interval for *k* and *m*

Parameter estimation procedure	95% confidence interval for k [h^{-m}]	95% confidence interval for m [-]
Non-linear regression	$[2.1 < k < 3.3]$	$[3.1 < m < 4.3]$
Linear regression using all data	$[1.07 < k < 2.04]$	$[2.9 < m < 4.5]$
Linear regression using data between 10 and 90% crystallization	$[1.86 < k < 2.45]$	$[2.7 < m < 3.5]$
Linear regression using data between 25 and 75% crystallization	$[2.09 < k < 4.4]$	$[3.0 < m < 4.6]$

III.2 Subsampling to eliminate auto-correlated residuals

(Dochain and Vanrolleghem, 2003)

Originally the absolute amount of crystallization f was calculated each minute. After parameter estimation, however, it appeared that using this sampling frequency, the residuals (predicted minus measured value) of the proposed model were auto-correlated. This means that more than 5% of the auto-correlations are higher than the threshold (in this study the auto-correlation was calculated for 20 lags and thus one auto-correlation was allowed above the threshold) (see section 4.3.5.3 for the theory on auto-correlation analysis). Auto-correlated residuals lead to underestimated errors on the parameter estimates.

A solution to this auto-correlation problem was to subsample the data series, i.e. to use only one data point each three or five minutes. The effect of subsampling on the auto-correlation of the residuals, on the quality of fit and on the errors on the parameter estimates was studied using different data series randomly selected from the ones obtained in chapter 4.

When one data point was taken each three minutes instead of each minute, the amount of auto-correlations above the threshold already decreased drastically: from between 5 and 12 to between 1 and 4. This means, however, that when using one data point each three minutes the residuals are still auto-correlated for most of the samples studied. When one data point was taken each five minutes, the residuals were not auto-correlated anymore. For all the samples, at the most one of the auto-correlations was found to be above the threshold.

The effect of subsampling on the quality of fit was studied using the mean sum of squared residuals (MSR). The conclusion is that the MSR value increases by about 15% when changing the sampling frequency from one each minute to one each five minutes. This slight decrease of the quality of fit was, however, expected.

The errors on the parameter estimates are two to three times higher when one data point each five minutes is used instead of one data point each minute. This proves that the errors on the parameter estimates are indeed underestimated when the residuals are auto-correlated.

The residuals of the Avrami and Gompertz models are also auto-correlated when one data point each minute is used. After subsampling to one data point each five minutes the amount of auto-correlations above the threshold decreases, as for the proposed model. However some samples not satisfying the assumption of independent residuals remain (see also section 4.4.2.1). The quality of fit after subsampling also decreases for these models and thus subsampling does not have any effect on the comparison of the different models.

III.3 Parameter estimation of the differential equation form of the proposed model using WEST

The Simplex algorithm (Nelder & Mead, 1964) was used to perform all parameter estimations in WEST (Hemmis N.V., Kortrijk, Belgium).

III.3.1 **Original 5-parameter model** (equation [4.11])

When no restriction for K_1 and K_n was inserted in the WEST code, nonsense results (decreasing crystallization curves) were sometimes obtained when simulations were performed with the model using particular parameter values. This is because an increasing amount of crystallization is only obtained for negative values of *dh/dt*. Taking this into account the following restriction for the two rate constants had to be inserted in the WEST code:

$$K_1 \geq K_n \qquad \textbf{[III.1]}$$

This was done by writing K_1 as $K_n + \Delta K_1$ leading to the following differential equation:

$$\frac{dh}{dt} = K_n \times h^n - (K_n + \Delta K_1) \times h$$

$$h(0) = \frac{a_P - f(0)}{a_P} \qquad \textbf{[III.2]}$$

Parameter estimation using equation [III.2] was tried. a_P, K_n, ΔK_1 and n were programmed as parameters and the initial value $h(0)$ was also estimated to get the best fit. Error messages related to the covariance calculation were obtained. Lowering the perturbation factor did not resolve this problem, which is probably due to the fact that *SSR* can change rather dramatically for very small variations in $h(0)$, and that the values for $h(0)$ are always very close to one (typically 0.99999). The optimization algorithm probably suffers from numerical problems because the first significant number is typically only around the fifth digit after the decimal point.

The introduction of a variable Z' equal to 1-h (equal to f/a, the relative amount of crystallization) was evaluated as a possible solution. Typical values for $Z'(0)$ are then around 1.10^{-5}, which is easier for the optimization algorithm to deal with, than 0.99999. The differential equation written in Z' is given in equation [III.3].

$$\frac{dZ'}{dt} = (K_n + \Delta K_1) \times (1 - Z') - K_n (1 - Z')^n$$

$$Z'(0) = \frac{f(0)}{a_P} \qquad \textbf{[III.3]}$$

By using this transformed version of the differential equation, the numerical problem during the calculation of the covariance of the parameters could be solved.

III.3.2 Simplified 4-parameter model (equation [4.13])

The same transformation to Z' was performed for parameter estimation of the simplified model.

III.3.3 Model with variable order of the forward reaction

To be able to perform parameter estimations with equation [4.14], it had to be rewritten taking account of the restriction on the values of n and n_2. This restriction arose again because dh/dt has to be negative. This led to:

$$n > n_2 \qquad \textbf{[III.4]}$$

and thus equation [4.14] was rewritten as:

$$\frac{dh}{dt} = K \times (h^{n_2+\Delta n} - h^{n_2}) \quad \textbf{[III.5]}$$

To eliminate problems with the covariance calculation, also equation [III.5] had to be transformed to *Z'*.

III.3.4 Model with induction time as parameter

To be able to estimate t_ind_F as one of the parameters of the differential equation [4.13], *h(0)* was written as function of t_ind_F (with *F* equal to 0.01):

$$h(0) = \left[1 + \frac{0.99^{1-n} - 1}{e^{(n-1)\times K \times t\_ind_{0.01}}}\right]^{\frac{1}{1-n}} \quad \textbf{[III.6]}$$

This expression was then used as the initial value in the WEST code.

III.4 Parameter estimation of the algebraic version of the proposed model using Sigmaplot

Sigmaplot uses the Levenberg-Marquardt algorithm to perform parameter estimations.

The first parameter estimations were performed on a variant of equation [4.19]: instead of transforming *h* and *h(0)* into *f* and *f(0)*, only *h* was transformed into *f* and *h(0)* was used as the fourth parameter (apart from a_P, *K* and *n*). Equation [III.7] was thus used for parameter estimation.

$$f(t) = a \times \left[1 - \left[1 + \left(h(0)^{1-n} - 1\right) \times e^{-(1-n)\times K \times t}\right]^{\frac{1}{1-n}}\right] \quad \textbf{[III.7]}$$

However, this equation caused problems since it was found that the obtained parameter estimates were dependent on the initial values indicating local minima in the optimisation problem. Changing the values for tolerance, step size and number of iterations did not solve the problem. The same problem persisted using different data series.

The reason for this problem is probably that for very small variations in *h(0)* (4^{th} or 5^{th} digit after the decimal point), the sum of squared residuals and thus the quality of the fit changes a lot. This problem also arose when parameter estimations with the differential equation were performed (see section III.3).

It was then decided to replace *h(0)* by *f(0)* and use equation [4.19] for parameter estimation. This solved the problem of the dependency on the initial values, but another problem rose: the obtained errors on the estimates of parameter *f(0)* were very large for some data series. Two examples are given. For sample CB N/19 an estimate of $6.15.10^{-7}$ J g^{-1} for parameter *f(0)* and an error of $7.23.10^{-7}$ J g^{-1} (or 117%) on this estimate were obtained. This led to a 95% confidence interval of [$-8.31.10^{-7}$ J $g^{-1} < f(0) < 2.06.10^{-6}$ J g^{-1}]. For sample CB N/21 an estimate of $7.08.10^{-4}$ J g^{-1} for parameter *f(0)* and an error of $1.19.10^{-4}$ J g^{-1} (or 17%) on this estimate were obtained. This led to a 95% confidence interval of [$4.70.10^{-4}$ J $g^{-1} < f(0) < 9.46.10^{-4}$ J g^{-1}].

To try to solve this problem, *f(0)* in equation [4.19] was replaced by $10^{Z''}$. The same parameter estimates for a_P, *K* and *n* were obtained when this reparameterized version of the model was used. When the estimate for *Z''* was retransformed into *f(0)*, the same estimate for *f(0)* was obtained as for the parameter estimation using the original model. The errors on the *Z''* estimates were, however, much smaller. For example, for sample CB N/19 an estimate for *Z''* of –6.21 and an error of 0.53 (or 8.5%) were obtained. For sample CB N/21 an estimate for *Z''* of –3.15 and an error of 0.07 (or 2.3%) were obtained. Apart from the estimate, also the error on the estimate needs to be retransformed from *Z''* into *f(0)*. This was done by first calculating a 95% confidence interval for *Z''* and then transforming the lower and the upper limit from *Z''* to *f(0)*. For the above examples, this led to the following 95% confidence intervals for *f(0)*: [$5.37.10^{-8}$ J $g^{-1} < f(0) < 7.07.10^{-6}$] for sample CB N/19 and [$5.06.10^{-4}$ J $g^{-1} < f(0) < 9.9.10^{-4}$ J g^{-1}] for sample CB N/21. It became apparent that the nonsense negative value had disappeared from the confidence interval of the first sample but that the broadness of the confidence intervals had not decreased.

V FATTY ACID AND TRIACYLGLYCEROL PROFILE OF STUDIED COCOA BUTTERS

V.1 Fatty acid profile

Sample	Palmitic acid [%]	Stearic acid [%]	Oleic acid [%]	Linoleic acid [%]	Arachidic acid [%]
A	26.2 ± 0.2	36.6 ± 0.1	33.6 ± 0.2	2.74 ± 0.18	0.895 ± 0.049
B	25.6 ± 0.1	36.5 ± 0.1	34.1 ± 0.0	2.77 ± 0.12	1.04 ± 0.04
C	26.5 ± 0.0	37.1 ± 0.2	33.1 ± 0.1	2.25 ± 0.05	1.03 ± 0.06
D	26.4 ± 0.4	36.5 ± 0.3	33.5 ± 0.1	2.70 ± 0.01	0.985 ± 0.035
E	26.1 ± 0.6	37.3 ± 0.3	33.3 ± 0.2	2.40 ± 0.11	0.990 ± 0.028
F	25.7 ± 0.1	37.1 ± 0.0	33.7 ± 0.1	2.41 ± 0.05	1.08 ± 0.01
G	26.9 ± 0.1	34.4 ± 0.1	34.8 ± 0.1	2.93 ± 0.04	1.00 ± 0.08
H	27.1 ± 0.0	35.4 ± 0.1	33.7 ± 0.2	2.62 ± 0.01	1.08 ± 0.03
I	25.1 ± 0.8	34.3 ± 0.4	36.4 ± 0.3	3.37 ± 0.13	0.910 ± 0.014
J	27.1 ± 0.3	36.3 ± 0.1	33.1 ± 0.2	2.67 ± 0.14	0.825 ± 0.205
K	25.8 ± 0.0	36.9 ± 0.2	33.5 ± 0.1	2.81 ± 0.14	0.995 ± 0.120
L	26.1 ± 0.1	36.4 ± 0.1	33.9 ± 0.0	2.61 ± 0.07	1.01 ± 0.00
M	27.6 ± 1.2	36.3 ± 0.9	32.7 ± 0.6	2.26 ± 0.08	1.07 ± 0.01
N	25.0 ± 0.2	37.7 ± 0.2	33.6 ± 0.0	2.72 ± 0.01	1.01 ± 0.06
O	26.0 ± 0.5	36.0 ± 0.1	34.2 ± 0.1	2.87 ± 0.11	0.960 ± 0.127
P	24.9 ± 0.3	32.9 ± 0.1	37.6 ± 0.1	3.71 ± 0.01	0.930 ± 0.028
Q	26.2 ± 0.2	37.0 ± 0.1	33.3 ± 0.2	2.61 ± 0.08	0.990 ± 0.014
R	26.0 ± 0.1	37.1 ± 0.0	33.5 ± 0.2	2.41 ± 0.06	0.980 ± 0.057
S	26.7 ± 0.8	36.5 ± 0.4	33.4 ± 0.1	2.37 ± 0.13	0.995 ± 0.205
T	26.4 ± 0.1	36.3 ± 0.1	33.8 ± 0.1	2.55 ± 0.05	0.980 ± 0.042

Mean and standard deviation of two repetitions are reported.

V.2 Triacylglycerol profile

Sample	PPP [%[	MOP [%]	PPS [%]	POP [%]	PLP [%]	PSS [%]	POS [%]	POO [%]	PLS [%]	PLO [%]	SSS [%]	SOS [%]	SOO [%]	SLS+OOO [%]	SOA [%]
A	0.222	0.232	0.889	17.7	1.61	0.646	41.3	2.29	2.86	0.434	0.777	25.5	3.01	1.33	1.21
B	0.385	0.253	0.688	18.3	1.79	0.334	41.7	2.40	2.88	0.364	0.223	25.2	2.86	1.40	1.21
C	0.514	0.262	0.836	18.3	1.36	0.464	43.0	1.80	2.51	0.322	0.282	25.7	2.09	1.27	1.33
D	0.383	0.252	0.726	18.1	1.69	0.564	41.9	2.35	2.90	0.433	0.252	25.1	2.73	1.28	1.24
E	0.333	0.232	0.717	17.5	1.79	0.485	41.8	2.37	2.81	0.465	0.293	25.8	2.75	1.28	1.31
F	0.221	0.201	0.844	17.8	1.84	1.03	40.7	2.38	2.67	0.493	0.563	25.9	2.82	1.29	1.32
G	0.364	0.233	0.577	19.4	1.91	0.263	41.4	3.08	3.00	0.435	0.182	23.2	3.54	1.35	1.13
H	0.383	0.302	0.948	18.9	1.55	0.696	41.0	2.36	2.46	0.383	0.615	25.2	2.86	1.04	1.27
I	0.256	0.205	0.583	17.0	2.18	0.317	38.7	5.02	2.97	0.337	0.235	23.8	5.96	1.38	1.10
J	0.231	0.211	0.934	17.8	1.70	1.46	40.4	2.47	2.79	0.512	0.824	25.4	2.86	1.23	1.15
K	0.222	0.212	0.829	17.8	1.75	0.566	40.7	2.28	2.87	0.222	0.617	26.1	3.06	1.59	1.22
L	0.201	0.211	0.715	18.3	1.61	0.866	41.4	2.54	2.91	0.362	0.362	25.0	3.02	1.36	1.22
M	0.344	0.253	0.740	17.6	1.54	0.40	41.1	2.44	2.76	0.456	0.588	25.9	3.23	1.37	1.34
N	0.192	0.222	0.656	18.4	1.82	0.525	41.1	2.53	3.01	0.424	0.252	25.0	3.17	1.51	1.21
O	0.213	0.192	0.729	17.6	1.86	0.435	40.9	3.18	2.98	0.405	0.324	24.9	3.69	1.35	1.20
P	0.307	0.184	0.368	16.6	1.74	0.194	38.6	5.96	3.10	0.317	0.205	23.1	7.00	1.33	1.05
Q	0.404	0.272	0.768	17.4	1.51	0.839	41.4	2.53	2.72	0.404	0.717	25.2	3.14	1.39	1.25
R	0.423	0.282	0.907	17.8	1.62	0.474	41.5	2.36	2.75	0.454	0.262	25.9	2.76	1.23	1.32
S	0.415	0.273	0.961	17.4	1.69	0.648	40.1	2.45	2.72	0.466	0.668	26.3	3.13	1.47	1.31
T	0.354	0.273	0.830	18.3	1.71	0.486	40.7	2.46	2.71	0.445	0.668	25.3	3.07	1.43	1.25

SAMENVATTING

Veel levensmiddelen bestaan voor een belangrijk gedeelte uit vet, waarvan een substantieel gedeelte in gekristalliseerde vorm voorkomt. De chemische samenstelling en de procescondities beïnvloeden het primair kristallisatiegedrag van een vet. Dit gedrag omvat niet enkel wanneer en in welke mate het vet uitkristalliseert, maar ook het polymorfisme (het bestaan van verschillende kristallijne fasen met dezelfde chemische samenstelling die van elkaar verschillen in structuur maar dezelfde vloeibare fase opleveren na afsmelten) en de morfologie van de kristallen en de mogelijke polymorfe transities. De procescondities beïnvloeden ook de verdere aggregatie van de primaire kristallen tot clusters en verder tot een driedimensionaal netwerk. Elk van deze structuurniveaus bepaalt de macroscopische eigenschappen van het levensmiddel. Dit onderzoek behandelde het primair kristallisatiegedrag van cacaoboter. Het kristallisatiegedrag van dit geel vet, dat geëxtraheerd wordt uit cacaobonen, is van uitzonderlijk belang voor de chocoladeindustrie.

De literatuurstudie over vetkristallisatie (hoofdstuk 1) behandelde enerzijds de basisbeginselen van nucleatie en kristalgroei en anderzijds het polymorfisme van vetten. De meeste aandacht werd echter besteed aan het modelleren van de kristallisatiekinetiek van vetten. Een overzicht werd gegeven van de verschillende experimentele technieken die gebruikt worden om kristallisatiedata te verzamelen en van de verschillende modellen die gebruikt worden om de kristallisatiekinetiek te beschrijven. Het Avrami model en in mindere mate het Gompertz model bleken de meest gebruikte. Het Avrami model heeft zijn theoretische basis als voordeel maar er werd aangetoond dat de fit verre van perfect is. Dit is mogelijk het gevolg van de veronderstellingen die gemaakt werden om de theorie te ontwikkelen, en waaraan in het geval van vetkristallisatie niet noodzakelijkerwijze voldaan is. Er werd aangetoond dat het Gompertz model reeds een betere fit toelaat dan het Avrami model maar dat ook die nog niet toereikend is. Een voordeel van het Gompertz model is de heldere fysische interpretatie van de parameters, een nadeel is zijn zwakke theoretische achtergrond. Deze literatuurstudie leidde bijgevolg tot de conclusie dat er nog ruimte is voor een ander model dat de kristallisatiekinetiek van vetten beter kan beschrijven.

De literatuurstudie over cacaoboter (hoofdstuk 2) toonde aan dat cacaoboter voor het belangrijkste gedeelte uit triacylglycerolen bestaat. Minorcomponenten zijn echter ook

aanwezig. De chemische samenstelling van cacaoboter kan lichtjes variëren afhankelijk van enerzijds de groeiomstandigheden en de ouderdom van de boom, en anderzijds van het productieproces uit de cacaobonen en de eventuele opzuivering van de cacaoboter. Deze kleine verschillen in chemische samenstelling brengen ook kleine verschillen in de fysische eigenschappen, zoals de kristallisatiekinetiek, met zich.

Het experimentele gedeelte van deze studie begon met de ontwikkeling van een verbeterde methode om de isotherme cacaoboterkristallisatie te volgen met behulp van differentiële scanning calorimetrie (hoofdstuk 3). De invloed op de isotherme kristallisatiekinetiek van cacaoboter van de staalnameprocedure, het protocol om de stalen af te smelten voorafgaand aan de kristallisatie, en de koelsnelheid naar de kristallisatietemperatuur werden onderzocht. Een smeltprotocol van 65°C gedurende 15 minuten en een koelsnelheid van 8°C min^{-1} werden gekozen voor gebruik in de verdere experimenten. Er werd eveneens aangetoond dat een wijziging in de staalnameprocedure de kristallisatie kan beïnvloeden. Speciale aandacht ging uit naar de integratie van de bekomen kristallisatiepieken. Deze integratie is noodzakelijk om een (in de meeste gevallen sigmoïdale) kristallisatiecurve te bekomen die de hoeveelheid vrijgestelde kristallisatiewarmte als functie van de tijd weergeeft. Er werd aangetoond dat wanneer de integratielimieten visueel bepaald worden, het resultaat in sterke mate afhangt van de uitvoerder en bovendien verschilt wanneer dezelfde uitvoerder de integratie verscheidene malen herhaalt. Om de hierdoor veroorzaakte hoge variabiliteit te elimineren, werd een objectief berekeningsalgoritme ontwikkeld om de integratiegrenzen vast te leggen.

In het tweede gedeelte van dit onderzoek werd een nieuw model ontwikkeld om de kristallisatiekinetiek van vetten te beschrijven (hoofdstuk 4). Dit model beschrijft het kristallisatieproces als een eerste orde voorwaartse reactie en een terugwaartse reactie met orde *n*. Deze terugwaartse reactie wordt mogelijk veroorzaakt door een lokaal herafsmelten en / of een heroplossen van kristallen. Er werd aangetoond dat het voorgestelde model steeds een betere fit vertoont dan het Avrami model en ook beter presteert dan het Gompertz model, voor de beschrijving van de meerderheid van de datasets. Bij de resterende datasets presteert het voorgestelde model slechts iets slechter dan het Gompertz model. Een belangrijke eigenschap van het voorgestelde model in vergelijking met het Gompertz model is de mogelijkheid om kristallisatiecurves met een verschillende graad van asymmetrie te beschrijven. De universaliteit van het voorgestelde model werd aangetoond door het te fitten aan datasets die de kristallisatie

beschrijven van twee totaal verschillende vetten (cacaoboter en melkvet) bij verschillende temperaturen en gemeten met behulp van verschillende experimentele technieken. Een belangrijk voordeel van het voorgestelde model is zijn ontwikkeling in de vorm van een differentiaalvergelijking. Dit laat toe om het model ook te gebruiken onder tijdsafhankelijke omstandigheden, zoals bijvoorbeeld bij niet-isotherme kristallisatie. Om de parameterschatting te vereenvoudigen werd eveneens de algebraïsche oplossing onder isotherme omstandigheden bepaald.

In het derde gedeelte van dit onderzoek (hoofdstuk 5) werden verschillende analysetechnieken (differentiële scanning calorimetrie, puls nucleair magnetische resonantie, microscopie met behulp van gepolariseerd licht en tijdsopgeloste X-stralen diffractie gebruik makend van synchrotronstraling) gebruikt om de isotherme cacaoboterkristallisatie te bestuderen bij temperaturen tussen 17°C en 23°C. Er werd aangetoond dat de kristallisatie binnen dit temperatuursbereik een tweestapsproces is. Een mechanisme voor de twee stappen werd voorgesteld. In de eerste stap kristalliseert een gedeelte van de smelt in de α polymorf, terwijl de tweede stap α gemedieerde β' kristallisatie omvat. Dit laatste betekent dat de reeds gevormde α kristallen omkristalliseren naar β' wat aanleiding geeft tot kristallisatie van bijkomende α kristallen, die dan op hun beurt omkristalliseren naar β'. Dit zou betekenen dat er geen β' kristallen rechtstreeks uit de smelt gevormd worden. In de laatste fase van de tweede kristallisatiestap vindt enkel een omkristallisatie van α naar β' plaats, wat aanleiding geeft tot de aanwezigheid van een isosbestisch punt in de X-stralendiffractiepatronen opgemeten bij kleine hoeken.

Het volgende gedeelte van dit onderzoek (hoofdstuk 6) bestudeerde de invloed van de temperatuur (19°C – 23°C) op de isotherme cacaoboterkristallisatie. De inductietijd van de eerste kristallisatiestap, namelijk de kristallisatie van een gedeelte van de smelt in de α polymorf, werd gemeten met behulp van een lichtverstrooiingstechniek. In het bestudeerde temperatuursbereik bleek het mogelijk de Turnbull-Fisher vergelijking aan deze data te fitten. Met differentiële scanning calorimetrie en puls nucleair magnetische resonantie werd verder aangetoond dat de hoeveelheid vast vet, afkomstig van de α kristallisatie in de eerste kristallisatiestap, daalt als functie van de temperatuur. De hoeveelheid warmte die vrijgesteld wordt in de tweede kristallisatiestap, begint echter slechts te dalen bij hogere temperaturen. De inductietijd van de tweede kristallisatiestap, dus de inductietijd voor de omkristallisatie van α naar β', neemt toe bij toenemende

temperatuur. Het is echter mogelijk dat de inductietijd van de tweede kristallisatiestap ook beïnvloed wordt door de snelheid van kristalgroei. De snelheidsconstante *K* daalt als functie van de temperatuur en dit vooral bij hogere temperaturen. De orde van de terugwaartse reactie daalt tot een bepaalde temperatuur en blijft dan constant.

De invloed van de chemische samenstelling op de isotherme cacaoboterkristallisatie werd bestudeerd in het laatste gedeelte van dit onderzoek (hoofdstuk 7). Naast het vetzuur- en triacylglycerolprofiel werd ook de hoeveelheid van een aantal minorcomponenten (diacylglycerolen, vrije vetzuren, fosfolipiden, zeep, onverzeepbare stoffen, ijzer en primaire oxidatieproducten) bepaald. Er werd aangetoond dat er significante verschillen zijn in de chemische karakteristieken en in de kristallisatieparameters tussen de bestudeerde cacaoboters. Met behulp van voorwaartse meervoudige lineaire regressie werd nagegaan welke chemische karakteristieken de kristallisatieparameters beïnvloeden. De verhouding van de verzadigde tot de onverzadigde vetzuren en de mono-onverzadigde tot de di-onverzadigde triacylglycerolen heeft de belangrijkste invloed op de hoeveelheid kristallisatie, de inductietijd van de tweede kristallisatiestap en de orde van de terugwaartse reactie. De hoeveelheid diacylglycerolen heeft de belangrijkste invloed op de snelheidsconstante. Andere minorcomponenten met een aanzienlijke impact op verschillende kristallisatieparameters zijn vrije vetzuren, fosfolipiden en zepen.

V FATTY ACID AND TRIACYLGLYCEROL PROFILE OF STUDIED COCOA BUTTERS

V.1 Fatty acid profile

Sample	Palmitic acid [%]	Stearic acid [%]	Oleic acid [%]	Linoleic acid [%]	Arachidic acid [%]
A	26.2 ± 0.2	36.6 ± 0.1	33.6 ± 0.2	2.74 ± 0.18	0.895 ± 0.049
B	25.6 ± 0.1	36.5 ± 0.1	34.1 ± 0.0	2.77 ± 0.12	1.04 ± 0.04
C	26.5 ± 0.0	37.1 ± 0.2	33.1 ± 0.1	2.25 ± 0.05	1.03 ± 0.06
D	26.4 ± 0.4	36.5 ± 0.3	33.5 ± 0.1	2.70 ± 0.01	0.985 ± 0.035
E	26.1 ± 0.6	37.3 ± 0.3	33.3 ± 0.2	2.40 ± 0.11	0.990 ± 0.028
F	25.7 ± 0.1	37.1 ± 0.0	33.7 ± 0.1	2.41 ± 0.05	1.08 ± 0.01
G	26.9 ± 0.1	34.4 ± 0.1	34.8 ± 0.1	2.93 ± 0.04	1.00 ± 0.08
H	27.1 ± 0.0	35.4 ± 0.1	33.7 ± 0.2	2.62 ± 0.01	1.08 ± 0.03
I	25.1 ± 0.8	34.3 ± 0.4	36.4 ± 0.3	3.37 ± 0.13	0.910 ± 0.014
J	27.1 ± 0.3	36.3 ± 0.1	33.1 ± 0.2	2.67 ± 0.14	0.825 ± 0.205
K	25.8 ± 0.0	36.9 ± 0.2	33.5 ± 0.1	2.81 ± 0.14	0.995 ± 0.120
L	26.1 ± 0.1	36.4 ± 0.1	33.9 ± 0.0	2.61 ± 0.07	1.01 ± 0.00
M	27.6 ± 1.2	36.3 ± 0.9	32.7 ± 0.6	2.26 ± 0.08	1.07 ± 0.01
N	25.0 ± 0.2	37.7 ± 0.2	33.6 ± 0.0	2.72 ± 0.01	1.01 ± 0.06
O	26.0 ± 0.5	36.0 ± 0.1	34.2 ± 0.1	2.87 ± 0.11	0.960 ± 0.127
P	24.9 ± 0.3	32.9 ± 0.1	37.6 ± 0.1	3.71 ± 0.01	0.930 ± 0.028
Q	26.2 ± 0.2	37.0 ± 0.1	33.3 ± 0.2	2.61 ± 0.08	0.990 ± 0.014
R	26.0 ± 0.1	37.1 ± 0.0	33.5 ± 0.2	2.41 ± 0.06	0.980 ± 0.057
S	26.7 ± 0.8	36.5 ± 0.4	33.4 ± 0.1	2.37 ± 0.13	0.995 ± 0.205
T	26.4 ± 0.1	36.3 ± 0.1	33.8 ± 0.1	2.55 ± 0.05	0.980 ± 0.042

Mean and standard deviation of two repetitions are reported.

V.2 Triacylglycerol profile

Sample	PPP [%[	MOP [%]	PPS [%]	POP [%]	PLP [%]	PSS [%]	POS [%]	POO [%]	PLS [%]	PLO [%]	SSS [%]	SOS [%]	SOO [%]	SLS+OOO [%]	SOA [%]
A	0.222	0.232	0.889	17.7	1.61	0.646	41.3	2.29	2.86	0.434	0.777	25.5	3.01	1.33	1.21
B	0.385	0.253	0.688	18.3	1.79	0.334	41.7	2.40	2.88	0.364	0.223	25.2	2.86	1.40	1.21
C	0.514	0.262	0.836	18.3	1.36	0.464	43.0	1.80	2.51	0.322	0.282	25.7	2.09	1.27	1.33
D	0.383	0.252	0.726	18.1	1.69	0.564	41.9	2.35	2.90	0.433	0.252	25.1	2.73	1.28	1.24
E	0.333	0.232	0.717	17.5	1.79	0.485	41.8	2.37	2.81	0.465	0.293	25.8	2.75	1.28	1.31
F	0.221	0.201	0.844	17.8	1.84	1.03	40.7	2.38	2.67	0.493	0.563	25.9	2.82	1.29	1.32
G	0.364	0.233	0.577	19.4	1.91	0.263	41.4	3.08	3.00	0.435	0.182	23.2	3.54	1.35	1.13
H	0.383	0.302	0.948	18.9	1.55	0.696	41.0	2.36	2.46	0.383	0.615	25.2	2.86	1.04	1.27
I	0.256	0.205	0.583	17.0	2.18	0.317	38.7	5.02	2.97	0.337	0.235	23.8	5.96	1.38	1.10
J	0.231	0.211	0.934	17.8	1.70	1.46	40.4	2.47	2.79	0.512	0.824	25.4	2.86	1.23	1.15
K	0.222	0.212	0.829	17.8	1.75	0.566	40.7	2.28	2.87	0.222	0.617	26.1	3.06	1.59	1.22
L	0.201	0.211	0.715	18.3	1.61	0.866	41.4	2.54	2.91	0.362	0.362	25.0	3.02	1.36	1.22
M	0.344	0.253	0.740	17.6	1.54	0.40	41.1	2.44	2.76	0.456	0.588	25.9	3.23	1.37	1.34
N	0.192	0.222	0.656	18.4	1.82	0.525	41.1	2.53	3.01	0.424	0.252	25.0	3.17	1.51	1.21
O	0.213	0.192	0.729	17.6	1.86	0.435	40.9	3.18	2.98	0.405	0.324	24.9	3.69	1.35	1.20
P	0.307	0.184	0.368	16.6	1.74	0.194	38.6	5.96	3.10	0.317	0.205	23.1	7.00	1.33	1.05
Q	0.404	0.272	0.768	17.4	1.51	0.839	41.4	2.53	2.72	0.404	0.717	25.2	3.14	1.39	1.25
R	0.423	0.282	0.907	17.8	1.62	0.474	41.5	2.36	2.75	0.454	0.262	25.9	2.76	1.23	1.32
S	0.415	0.273	0.961	17.4	1.69	0.648	40.1	2.45	2.72	0.466	0.668	26.3	3.13	1.47	1.31
T	0.354	0.273	0.830	18.3	1.71	0.486	40.7	2.46	2.71	0.445	0.668	25.3	3.07	1.43	1.25

CURRICULUM VITAE

PERSONALIA

Imogen Foubert
Geboren op 9 november 1976 te Duffel
Gehuwd met Aldo Peeters (31/03/2001)
Adres: Zwaanaardestraat 30, 9112 Sinaai
Telefoon: 03/5692970 (privé)
Telefoon: 09/2646168 (werk)
E-mail: imogen.foubert@rug.ac.be

STUDIES

Humaniora:
Koninklijk Atheneum Sint-Niklaas, Latijn – Wiskunde, afgestudeerd in 1994

Universitaire studies:
RUCA Antwerpen, kandidaat bio-ingenieur (1996), grote onderscheiding
Universiteit Gent, bio-ingenieur scheikunde (1999), grootste onderscheiding
Scriptie: Proteolyse gedurende de rijping van hogedrukbehandelde kazen, Promotor: Prof. dr. ir. A. Huyghebaert

Doctoraatsopleiding landbouwkundige en toegepaste biologische wetenschappen, Universiteit Gent, 2002

LOOPBAAN

Oktober 1999 – heden: aspirant van het Fonds voor Wetenschappelijk Onderzoek – Vlaanderen aan de Vakgroep Levensmiddelentechnologie en Voeding, Universiteit Gent, promotoren: Prof. dr. ir. K. Dewettinck en Prof. dr. ir. A. Huyghebaert

WETENSCHAPPELIJKE PUBLICATIES

Artikels in tijdschriften met referee-systeem en met internationale verspreiding

Messens, W., Foubert, I., Dewettinck, K. & Huyghebaert, A. (2000). Proteolysis of a high-pressure –treated smear-ripened cheese. Milchwissenschaft, 55, 328-332.

Messens, W., Foubert, I., Dewettinck, K. & Huyghebaert, A. (2001) Proteolysis of a high-pressure-treated mould-ripened cheese. Milchwissenschaft, 56, 201-204.

Foubert, I., Vanrolleghem, P.A., Vanhoutte, B. & Dewettinck, K. (2002). Dynamic mathematical model of the crystallization kinetics of fats. Food Research International, 35, 945-956.

Vanhoutte, B., Dewettinck, K., Foubert, I., Vanlerberghe, B. & Huyghebaert, A. (2002). The effect of phospholipids and water on isothermal crystallization of milk fat. European Journal of Lipid Science and Technology, 104, 490-495.

Vanhoutte, B., Foubert, I., Duplacie, F., Huyghebaert, A. & Dewettinck, K. (2002). Effect of phospholipids on isothermal crystallisation and fractionation of milk fat. European Journal of Lipid Science and Technology, 104, 738-744.

Foubert, I., Vanrolleghem, P. & Dewettinck, K. (2003). A differential scanning calorimetry method to determine the isothermal crystallization kinetics of cocoa butter. Thermochimica acta, 400, 131-142.

Foubert, I., Dewettinck, K. & Vanrolleghem, P. (2003). Modelling of the crystallization kinetics of fats. Trends in Food Science and Technology, 14, 79-92.

Andere artikels

Foubert, I., Van Cauteren, I., Dewettinck, K. & Huyghebaert, A. (2001). Differential scanning calorimetry as a means of predicting chocolate fat blooming. In: Crystallization and solidification properties of lipids, N. Widlak, R. Hartel & S. Narine (Eds.), Champaign, AOCS Press, p. 79-86.

Foubert, I., Vanrolleghem, P., Vanhoutte, B., Keersebilck, T., Huyghebaert, A. & Dewettinck, K. (2001). Modeling of the crystallization kinetics of cocoa butter. Med. Fac. Landbouww. Univ. Gent, 66/4, 263-267.

Vanhoutte, B., Foubert, I., Huyghebaert, A. & Dewettinck, K. (2001). The effect of phospholipids and water on the isothermal crystallisation behaviour of milk fat. Med. Fac. Landbouww. Univ. Gent, 66/4, 269-273.

DEELNAME AAN CONGRESSEN

American Oil Chemists' Society Conference on Crystallization and Solidification Properties of Lipids. Toronto, Canada, 1-4 oktober 2000. Presentatie: Foubert, I., Van Cauteren, I., Dewettinck, K. & Huyghebaert, A. Differential scanning calorimetry as a means of predicting chocolate fat blooming.

International Symposium on Materials Characterisation and Technology. Brussel, België, 5-7 september 2001. Presentatie: Foubert, I., Van Cauteren, I., Dewettinck, K. & Huyghebaert, A. Differential scanning calorimetry as a means of predicting chocolate fat blooming.

PhD Symposium. Gent, België, 10 oktober 2001.
Posters:
Foubert, I., Vanrolleghem, P., Vanhoutte, B., Keersebilck, T., Huyghebaert, A. & Dewettinck, K. Modeling of the crystallization kinetics of cocoa butter.
Vanhoutte, B., Foubert, I., Huyghebaert, A. & Dewettinck, K. The effect of phospholipids and water on the isothermal crystallisation behaviour of milk fat.

Annual Meeting of the American Oil Chemists' Society, Montreal, Canada, 5-8 mei 2002.
Presentatie: Vanrolleghem, P., Foubert, I. & Dewettinck, K. Mathematical modelling of the crystallization kinetics of fats: a methodological view.
Posters:

Foubert, I., Vanrolleghem, P., Keersebilck, T. & Dewettinck, K. Differential scanning calorimetry to measure the isothermal crystallization kinetics of cocoa butter.
Foubert, I., Vanrolleghem, P., Vanhoutte,B., Keersebilck, T. & Dewettinck, K. A new dynamic model to describe the crystallization kinetics of fats.
Foubert, I., Vanhoutte, B., Keersebilck, T., Vanrolleghem, P. & Dewettinck, K. Isothermal crystallization kinetics of cocoa butter.
Vanhoutte, B., Foubert, I., Huyghebaert, A. & Dewettinck, K. Multistep crystallization of fats.

Lipid Structural Properties Symposium, Northampton, VK, 15-17 oktober 2002.
Presentatie: Foubert, I., Vanrolleghem, P.A., Vanhoutte, B. & Dewettinck, K. Modelling of crystallisation kinetics of cocoa butter and milk fat.
Poster: Foubert, I., Vanrolleghem, P., Keersebilck, T. & Dewettinck, K. Differential scanning calorimetry to measure the isothermal crystallization kinetics of cocoa butter.

Annual Meeting of the American Oil Chemists' Society, Kansas City, VSA, 4-7 mei 2003.
Presentatie: Foubert, I., Vanrolleghem, P.A. & Dewettinck, K. A new mathematical model to describe the crystallization kinetics of fats: temperature dependence of the model parameters.

WETENSCHAPPELIJKE ONDERSCHEIDINGEN

2003 American Oil Chemists' Society Honoured Student Award

2003 Manuchehr Eijadi Award (American Oil Chemists' Society)